

**AWARD NUMBER:** W81XWH-20-1-0417

**TITLE:** Innovative Approaches to Enhance Chimeric Antigen Receptor (CAR) T-Cell Potency Using Quiescent T Cells

**PRINCIPAL INVESTIGATOR:** Saba Ghassemi

**CONTRACTING ORGANIZATION:** University of Pennsylvania, Philadelphia, PA

**REPORT DATE:** July 2022

**TYPE OF REPORT:** Annual

**PREPARED FOR:** U.S. Army Medical Research and Development Command  
Fort Detrick, Maryland 21702-5012

**DISTRIBUTION STATEMENT:** Approved for Public Release; Distribution Unlimited

The views, opinions and/or findings contained in this report are those of the author(s) and should not be construed as an official Department of the Army position, policy or decision unless so designated by other documentation.

<b>REPORT DOCUMENTATION PAGE</b>			<i>Form Approved</i> <i>OMB No. 0704-0188</i>		
Public reporting burden for this collection of information is estimated to average 1 hour per response, including the time for reviewing instructions, searching existing data sources, gathering and maintaining the data needed, and completing and reviewing this collection of information. Send comments regarding this burden estimate or any other aspect of this collection of information, including suggestions for reducing this burden to Department of Defense, Washington Headquarters Services, Directorate for Information Operations and Reports (0704-0188), 1215 Jefferson Davis Highway, Suite 1204, Arlington, VA 22202-4302. Respondents should be aware that notwithstanding any other provision of law, no person shall be subject to any penalty for failing to comply with a collection of information if it does not display a currently valid OMB control number. <b>PLEASE DO NOT RETURN YOUR FORM TO THE ABOVE ADDRESS.</b>					
<b>1. REPORT DATE</b> July 2022		<b>2. REPORT TYPE</b> Annual		<b>3. DATES COVERED</b> 01Jul2021-30Jun2022	
<b>4. TITLE AND SUBTITLE</b>  Innovative Approaches to Enhance Chimeric Antigen Receptor (CAR) T-Cell Potency Using Quiescent T Cells			<b>5a. CONTRACT NUMBER</b> W81XWH-20-1-0417		
			<b>5b. GRANT NUMBER</b>		
			<b>5c. PROGRAM ELEMENT NUMBER</b>		
<b>6. AUTHOR(S)</b>  Saba Ghassemi, PhD  E-Mail: ghassemi@penndmedicine.upenn.edu			<b>5d. PROJECT NUMBER</b>		
			<b>5e. TASK NUMBER</b>		
			<b>5f. WORK UNIT NUMBER</b>		
<b>7. PERFORMING ORGANIZATION NAME(S) AND ADDRESS(ES)</b>  University of Pennsylvania Philadelphia, PA 19104			<b>8. PERFORMING ORGANIZATION REPORT NUMBER</b>		
<b>9. SPONSORING / MONITORING AGENCY NAME(S) AND ADDRESS(ES)</b> U.S. Army Medical Research and Development Command Fort Detrick, Maryland 21702-5012			<b>10. SPONSOR/MONITOR'S ACRONYM(S)</b>		
			<b>11. SPONSOR/MONITOR'S REPORT NUMBER(S)</b>		
<b>12. DISTRIBUTION / AVAILABILITY STATEMENT</b> Approved for Public Release; Distribution Unlimited					
<b>13. SUPPLEMENTARY NOTES</b>					
<b>14. ABSTRACT</b>  My research focuses on developing Chimeric Antigen Receptor (CAR) T cells for adoptive immunotherapy. The goal of the research is to enhance the efficacy of CAR T therapy by developing potent CAR T cells. Another goal of this research is to shorten the CAR T manufacturing period to increase the availability of this therapy in resource constraint health care settings, as well those patients with rapidly progressive disease. CAR T cells are generated by transducing activated T cells with lentiviral vectors and expanding their progeny over 9-14 days. T cells progressively differentiate over time. Transducing non-activated T cells with CAR will preserve the intrinsic stem-like properties of naïve and memory T cells. This approach will yield CAR T cells with enhanced replicative capacity, engraftment, and in vivo activity. The purpose of this work is to determine the optimal T cell subset and corresponding optimal costimulatory domain for CAR when it is expressed in quiescent T cells. The scope of this research is that CAR T cells generated by transducing quiescent T cells will preserve the intrinsic stem-like properties of naïve and memory T cells. We found that spare respiratory capacity, SRC, is replenished in ICOSZ as well as BBZ CAR T cells. We also demonstrated that naïve T cell subsets have increased persistence with decreased tumor burden when BBZ CAR T cells is used.					
<b>15. SUBJECT TERMS</b> None listed.					
<b>16. SECURITY CLASSIFICATION OF:</b>			<b>17. LIMITATION OF ABSTRACT</b>	<b>18. NUMBER OF PAGES</b>	<b>19a. NAME OF RESPONSIBLE PERSON</b>
<b>a. REPORT</b>	<b>b. ABSTRACT</b>	<b>c. THIS PAGE</b>			<b>19b. TELEPHONE NUMBER</b> (include area code)
U	U	U	UU	94	USAMRDC

## TABLE OF CONTENTS

	<u>Page</u>
1. Introduction	4
2. Keywords	4
3. Accomplishments	4
4. Impact	8
5. Changes/Problems	10
6. Products	11
7. Participants & Other Collaborating Organizations	13
8. Special Reporting Requirements	16
9. Appendices	16

## 1. INTRODUCTION:

My research focuses on developing Chimeric Antigen Receptor (CAR) T cells for adoptive immunotherapy. The goal of the research is to enhance the efficacy of CAR T therapy by developing potent CAR T cells. Another goal of this research is to shorten the CAR T manufacturing period to increase the availability of this therapy in resource constraint health care settings, as well those patients with rapidly progressive disease. CAR T cells are generated by transducing activated T cells with lentiviral vectors and expanding their progeny over 9-14 days. T cells progressively differentiate over time. Transducing quiescent T cells with CAR will preserve the intrinsic stem-like properties of naïve and memory T cells. This approach will yield CAR T cells with enhanced replicative capacity, engraftment, and in vivo activity. The purpose of this work is to determine the optimal T cell subset and corresponding optimal costimulatory domain for CAR when it is expressed in quiescent T cells. The scope of this research is that CAR T cells generated by transducing quiescent T cells will preserve the intrinsic stem-like properties of naïve and memory T cells.

## 2. KEYWORDS:

CAR T cells, adoptive immunotherapy, CART19 (CD19-specific CAR), non-activated CAR T cells

## 3. ACCOMPLISHMENTS:

### What were the major goals of the project?

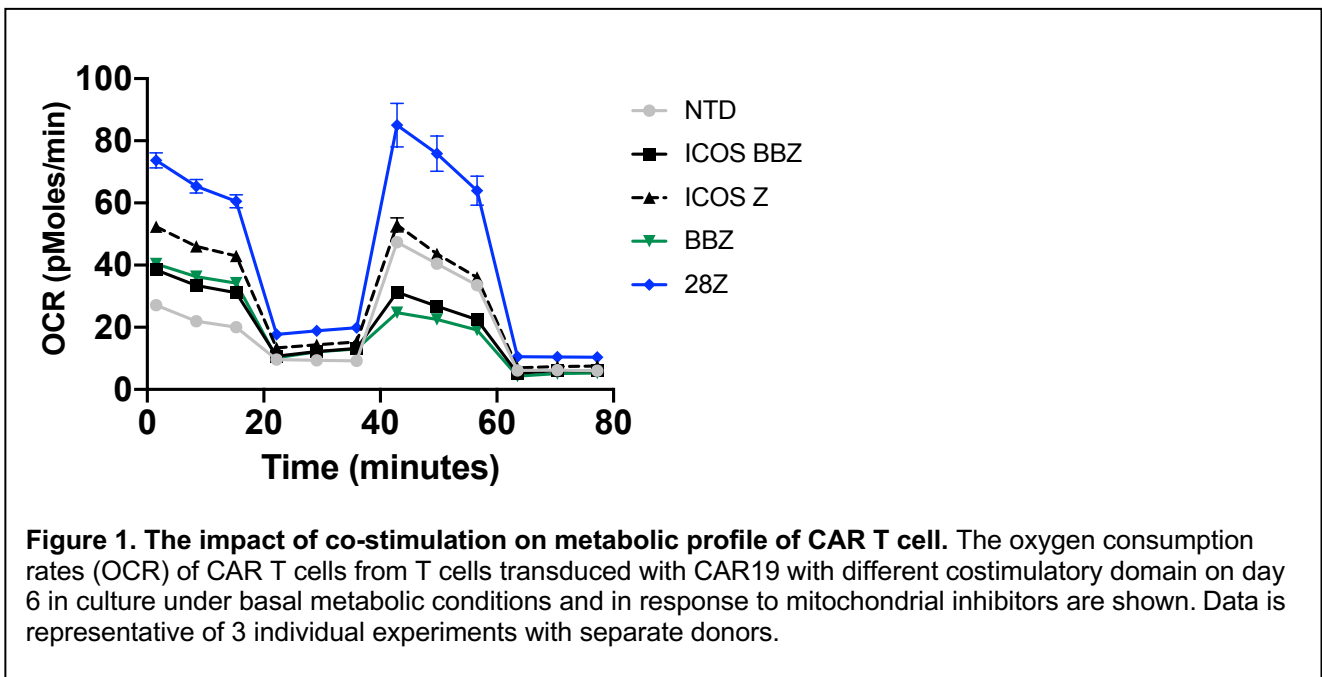
1. CAR Lentivirus production
2. Comparing the proliferation, differentiation, metabolism, and cytolytic effector function of quiescent CD19-specific CAR T cells in vitro.
3. Identifying which costimulatory domain, is most effective in xenograft models of ALL.
4. Comparing the effects of varying CAR design in different T cell subsets
5. Identifying which quiescent CAR T cell subset, with corresponding optimal costimulatory domain, is most effective in xenograft models of ALL

### What was accomplished under these goals?

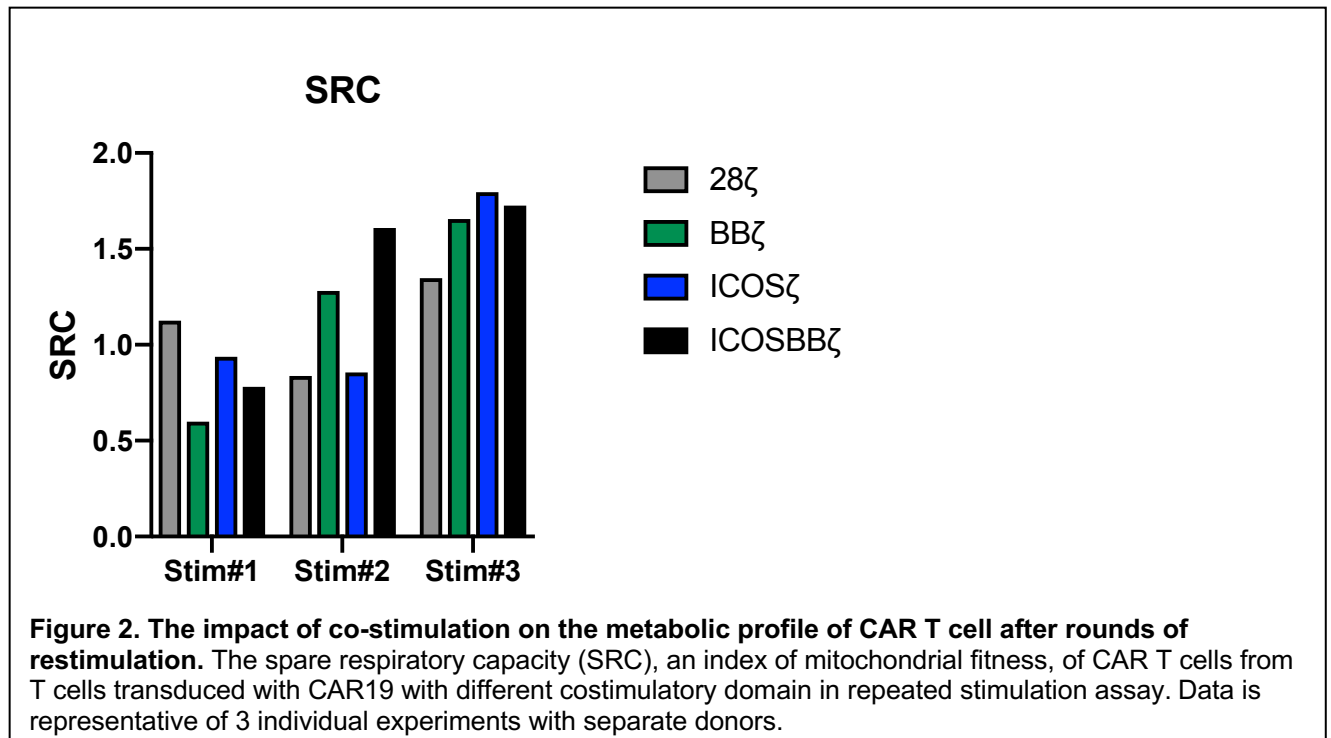
**Aim 1: To determine how CAR co-stimulation influences quiescent T cell potency**

**Major task 2: Comparing the proliferation, differentiation, metabolism, and cytolytic effector function of quiescent CD19-specific CAR T cells in vitro.**

In this aim, I evaluated the effect of CAR design on proliferation and metabolism of CD19 specific CAR T cells (CART19). Using a panel of CARs that we cloned previously, freshly isolated T cells were transduced with CAR19 with different costimulatory domain (bbz, 28z, ICOS Z and ICOS bbz). Following transduction, T cells were cultured for 5 days in IL-7 and IL-15 to permit CAR expression and support cell viability. T cells were then stimulated microbeads (Dynal) coated with anti-idiotype -Fc to the FMC63 scFv present within the corresponding CD19 specific CAR. Six days following activation, the metabolic properties of each group were assessed via seahorse assay (Fig. 1).



I also developed a repeated antigen stimulation model to assay mitochondrial fitness, as measured by spare respiratory capacity (SRC), over time. Freshly isolated T cells were expanded for 9 days. Following the rest-down, these cells were restimulated with irradiated K562-CD19 target cells for 5 days. To mimic repeated antigen encounter, the cells underwent 3 cycles of these restimulations. In each round, their metabolic properties were assessed by Seahorse Assay (Fig. 2).



### Significant results for Aim 2:

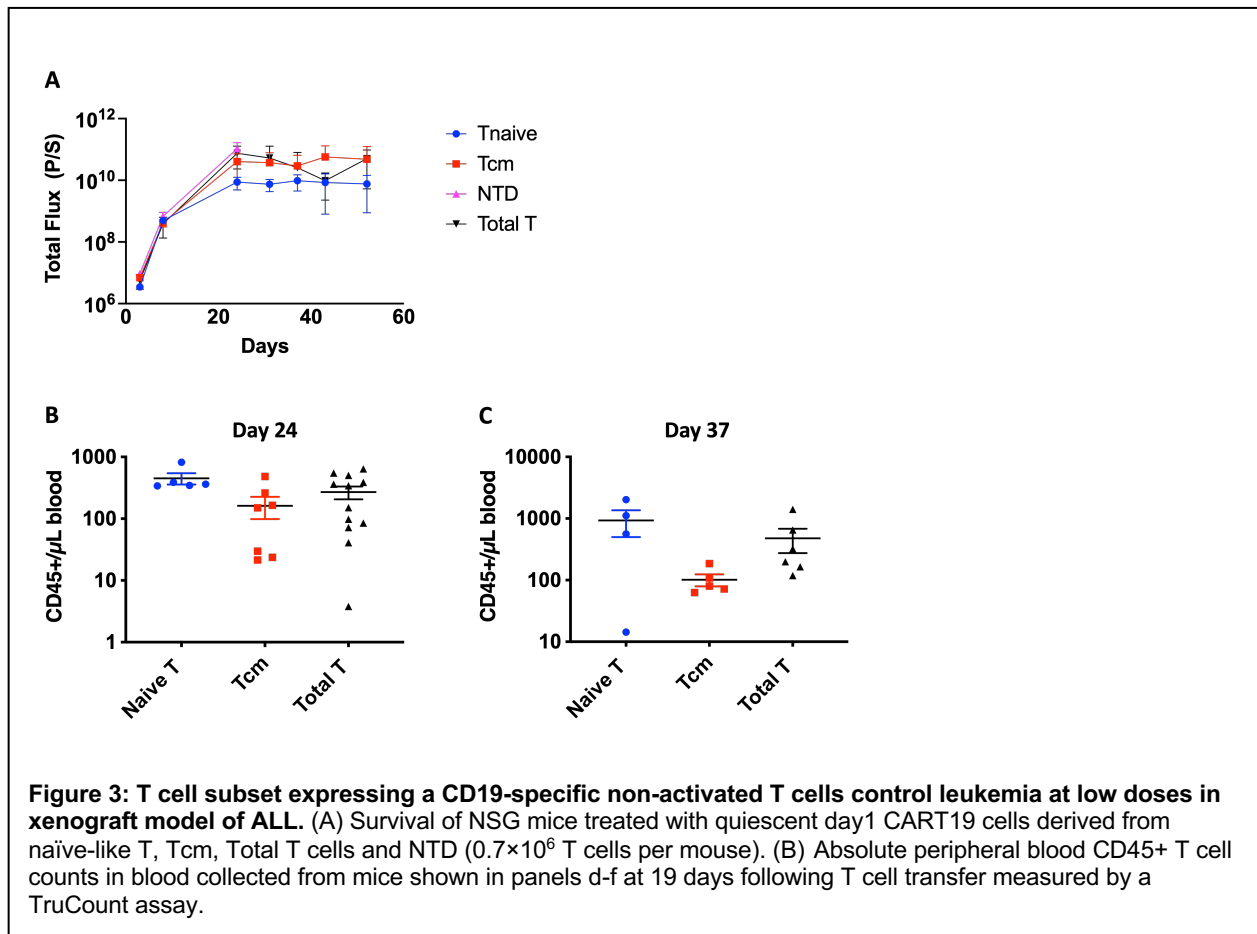
As shown in **Figure 1**, 28z cells had the highest oxidative response (Fig 1) following initial stimulation. This has limited insights for metabolic fitness in the context of persisting antigen. To this end, spare respiratory capacity, SRC, is sustained/replenished in ICOSZ as well as BBZ CAR T cells. This correlates with a contingency energy reserve that cells can access in order to survive the energy cost of the hostile tumor environment (**Figure 2**).

### Aim 3: Identifying which quiescent CAR T cell subset, with corresponding optimal costimulatory domain, is most effective in xenograft models of ALL.

In this aim, I evaluated the anti-tumor potency of different T cell subsets (Naïve like T cells, Tcm) when quiescent CAR-T cells are used. To evaluate the potency of these cells in vivo, I sorted T cells into different T cell subsets. Each subset was transduced separately with a CD19-specific CAR with 4-1BB co-stimulatory domain, for 24 hours. I then transferred  $2 \times 10^6$  of each subset into NSG mice bearing pre-established Nalm6 xenografts. Bulk quiescent T cells (unsorted) were used as a control as well as  $2 \times 10^6$  mock transduced quiescent T cells.

### Significant results for Aim 2:

As shown in **Figure 3**, all CAR T cell subsets show comparable ability to control tumor burden over an extended duration (60 days). However, tumor persists showing that CARTs cannot completely tumor cells; a feature often associated with a lack of CAR T cell number. However, naïve subsets have increased circulating numbers coinciding with decreased tumor burden (Fig 3A-B). These findings are compelling and we will repeat this study to 1) optimize the dose to completely eliminate tumor burden, and 2) show reproducibility in our findings.



**What opportunities for training and professional development has the project provided?**

My trainees had several opportunities to present their findings on this project at intramural conferences within the Penn Medicine Department. This facilitates valuable skill development in presenting data and obtaining feedback. In National and International presentations, I was responsible for presenting the findings. These talks are listed below.

## How were the results disseminated to communities of interest?

### Invited talk:

Engineering Next Generation CAR T cells with Enhanced Potency, The New York Academy of Sciences, Sep 2021

Engineering next generation CAR T cells with enhanced potency. ACC/IFI Cancer Retreat, Philadelphia, PA, Dec 2021

Rapid manufacturing of non-activated potent CAR T cells, Orion Corporation, Apr 2022

Engineering best-in-class CAR T cells with enhanced potency, Janssen Pharmaceutical, May 2022

## What do you plan to do during the next reporting period to accomplish the goals?

**Future plan of aim 2:** In the next step, I will determine what how the optimal costimulatory domain impacts cytolytic activity using our state-of-the-art eSIGHT RTCA impedance and imaging-based technology. We will sort T cells and each T cell subset (naïve, central memory, effector memory) will be transduced CD19-specific CARs containing either 4-1BB or CD28 co-stimulatory domain. The cytolytic function of each subset with specific CAR design will be evaluated as described using this innovative advance.

**Future plan of aim 3:** I have already performed a repeated in vivo experiment under condition above. This will provide results from a separate donor. This experiment is ongoing. In the next step, I will determine what is the optimal costimulatory domain for each individual subset. I will sort T cells and each T cell subset (naïve, central memory, effector memory) will be transduced CD19-specific CARs containing either 4-1BB or CD28 co-stimulatory domain. The potency of each subset with specific CAR design will be evaluated in vivo by injecting limiting doses of each subsets into the Nalm6 leukemia model.

## 4. IMPACT:

### What was the impact on the development of the principal discipline(s) of the project?

My work is amenable to the development of a micro-fluidic device that optimizes CAR gene delivery into quiescent T cells. We are engaged in collaborations with the Singh Center for Nanotechnology at Penn to generate such a device.

### **What was the impact on other disciplines?**

Stem cell therapies for tissue repair and regeneration face the same barriers as adoptively transferred T cells—poor survival and engraftment. My work highlights the therapeutic potential of maintaining quiescence during ex-vivo culture. My data suggests it preserves resilience and potency.

### **What was the impact on technology transfer?**

**Streamlining the process from 14 days to 24 hr will facilitate a breakthrough such that manufacturing hubs are no longer needed to manufacture CAR T cells. This versatile platform** is amenable to the widespread application of CAR T cells at point-of-care facilities including all hospital location. Decentralizing the entire system through the development of nonactivated rapid manufactured CAR T cells will decrease the cost burden and increased accessibility, and have inherent advances for patients with advanced disease. These next generation CARTs will be transformative for all T cell therapies against cancer and auto-immunity.

*Describe how results from the project made an impact, or are likely to make an impact, beyond the bounds of science, engineering, and the academic world on areas such as:*

My findings have particular translational relevance for extending the use of CAR T cells from large pharmaceutical Centers to point-of-care hospital facilities, thereby improving access for all.

**5. CHANGES/PROBLEMS:**

**Changes in approach and reasons for change**

Nothing to Report

**Actual or anticipated problems or delays and actions or plans to resolve them**

**Changes that had a significant impact on expenditures**

Unfortunately, with the advent of cell and gene therapies in Philadelphia, there has been an influx of companies (Cellican Valley), that recruit talent trained at Penn. This has led to high staff turnover and competition for talent as a valuable resource.  
I lost valuable lab members and am still trying to find suitable replacements.

**Significant changes in use or care of human subjects, vertebrate animals, biohazards, and/or select agents**

**Significant changes in use or care of human subjects**

Nothing to Report

## Significant changes in use or care of vertebrate animals

Nothing to Report

## Significant changes in use of biohazards and/or select agents

Nothing to Report

## 6. PRODUCTS:

- **Publications, conference papers, and presentations**

### **Journal publications.**

1. Garcia-Canaveras JC, Heo D, Trefely S, Leferovich J, Xu C, Philipson BI, **Ghassemi S**, Milone MC, Moon EK, Snyder NW, June CH, Rabinowitz JD, O'Connor RS. CAR T-Cells Depend on the Coupling of NADH Oxidation with ATP Production. *Cells*. 2021 Sep 6;10(9):2334.
2. Akbari B, Ghahri-Saremi N, Soltantoyeh T, Hadjati J, **Ghassemi S**, Mirzaei HR. Epigenetic strategies to boost CAR T cell therapy. *Mol Ther*. 2021 Sep 1;29(9):2640-2659.
3. Ghahri-Saremi N, Akbari B, Soltantoyeh T, Hadjati J, **Ghassemi S**, Mirzaei HR Genetic Modification of Cytokine Signaling to Enhance Efficacy of CAR T Cell Therapy in Solid Tumors. *Front Immunol*. 2021 Oct 14;12:738456.
4. Durgin JS, Thokala R, Johnson L, Song E, Leferovich J, Bhoj V, **Ghassemi S**, Milone M, Binder Z, O'Rourke DM, O'Connor RS., Enhancing CAR T function with the engineered secretion of *C. perfringens* neuraminidase, *Mol Ther*, 2022 Mar 2;30(3):1201-1214
5. **Ghassemi S**, Durgin JS, Nunez-Cruz S, Patel J, Leferovich J, Pinzone M, Shen F, Cummins KD, Plesa G, Cantu VA, Reddy S, Bushman FD, Gill SI, O'Doherty U, O'Connor RS, Milone MC. Rapid manufacturing of non-activated potent CAR T cells. *Nat Biomed Eng*. 2022 Feb;6(2):118-128.

**Books or other non-periodical, one-time publications.**

Nothing to Report

**Other publications, conference papers and presentations**

Reported above.

- **Website(s) or other Internet site(s)**

**News report:**

<https://www.pennmedicine.org/news/news-releases/2022/march/penn-researchers-shorten-manufacturing-time-for-car-t-cell-therapy>

<https://endpts.com/a-team-at-penn-says-it-has-slashed-car-t-cell-therapy-manufacturing-timeframe-to-just-24-hours/>

<https://www.cellandgene.com/doc/innovation-in-car-t-cell-therapy-manufacturing-0001>

- **Technologies or techniques**

Development of non-activated CAR T cells in the most rapid time done to-date.

- **Inventions, patent applications, and/or licenses**

Patent number: PCT/US2020/027734

- **Other Products**

Nothing to Report

## **7. PARTICIPANTS & OTHER COLLABORATING ORGANIZATIONS**

**What individuals have worked on the project?**

*Name:* Saba Ghassemi  
*Project Role:* PI  
*Researcher Identifier (e.g. ORCID ID):* 0000-0002-2415-3576

*Nearest person month worked:* 4.2

*Contribution to Project:* Dr. Ghassemi supervised the technician in carrying out the project aims, and she write the results and progress reports.

*Funding Support:* Current DOD Career Development Award

*Name:* Xiaoling Jin  
*Project Role:* Research Specialist

*Researcher Identifier (e.g. ORCID ID):*

*Nearest person month worked:* 12

*Contribution to Project:* Xiaoling performed the experiments mentioned in the project aims. He analyzed results and reported to the PI

*Funding Support:* Current DOD Career Development Award

**Has there been a change in the active other support of the PD/PI(s) or senior/key personnel since the last reporting period?**

Nothing to report

**What other organizations were involved as partners?**

Nothing to report

**8. SPECIAL REPORTING REQUIREMENTS**

**COLLABORATIVE AWARDS:**

**QUAD CHARTS:**

**9. APPENDICES:**



# Rapid manufacturing of non-activated potent CAR T cells

Saba Ghassemi<sup>1,2</sup>  , Joseph S. Durgin<sup>1</sup>, Selene Nunez-Cruz<sup>1,2</sup>, Jai Patel<sup>1</sup>, John Leferovich<sup>1,2</sup>, Marilia Pinzone<sup>2</sup>, Feng Shen<sup>1</sup>, Katherine D. Cummins<sup>1</sup> , Gabriela Plesa<sup>1</sup> , Vito Adrian Cantu<sup>3</sup>, Shantan Reddy<sup>3</sup>, Frederic D. Bushman<sup>3</sup>, Saar I. Gill<sup>1,4</sup>, Una O'Doherty<sup>2</sup>, Roddy S. O'Connor<sup>1,2</sup>  and Michael C. Milone<sup>1,2</sup>  

**Chimaeric antigen receptor (CAR) T cells can generate durable clinical responses in B-cell haematologic malignancies. The manufacturing of these T cells typically involves their activation, followed by viral transduction and expansion ex vivo for at least 6 days. However, the activation and expansion of CAR T cells leads to their progressive differentiation and the associated loss of anti-leukaemic activity. Here we show that functional CAR T cells can be generated within 24 hours from T cells derived from peripheral blood without the need for T-cell activation or ex vivo expansion, and that the efficiency of viral transduction in this process is substantially influenced by the formulation of the medium and the surface area-to-volume ratio of the culture vessel. In mouse xenograft models of human leukaemias, the rapidly generated non-activated CAR T cells exhibited higher anti-leukaemic in vivo activity per cell than the corresponding activated CAR T cells produced using the standard protocol. The rapid manufacturing of CAR T cells may reduce production costs and broaden their applicability.**

Adoptive cellular immunotherapy using T cells that are genetically modified to express a chimaeric antigen receptor (CAR) or cloned T cell receptor (TCR) yield durable clinical responses in patients with cancer<sup>1–6</sup>. The effectiveness of adoptive cellular immunotherapy led to the regulatory approval of several CD19-specific CAR T (CART19) cell therapies, including tisagenlecleucel and axicabtagene ciloleucel. Both these therapies involve the isolation of mononuclear cells containing T cells from the peripheral blood of the patient, followed by T-cell activation through their endogenous T cell receptor–CD3 complex, genetic modification using a viral vector and expansion ex vivo before re-infusion. We recently showed that activated T cells undergoing rapid proliferation ex vivo differentiate towards effector cells with a loss of anti-leukaemic potency<sup>7</sup>. The ability of T cells to engraft following adoptive transfer is related to their state of differentiation with less-differentiated naive-like and central memory cells showing the greatest potency in several preclinical studies<sup>8–11</sup>. A number of interventions have been reported to limit the differentiation of T cells and enhance the potency of ex vivo-expanded T cells, such as blockade of Fas–FasL interactions<sup>12</sup>, inhibition of Akt signalling<sup>13,14</sup> or activation of Wnt signalling<sup>15–17</sup>. However, elimination of the activation step and corresponding proliferative phase of T cells ex vivo offers a far simpler and more cost-effective approach provided the barriers to gene transfer into quiescent T cells can be overcome.

Natural human immunodeficiency virus (HIV) has the ability to infect quiescent T cells in the G0 stage of the cell cycle<sup>18–20</sup>. Unlike gammaretroviruses, HIV-based lentiviral vectors can infect both dividing and non-dividing cells. However, the transduction efficiencies in quiescent T cells are typically lower than their activated counterparts. Lentiviral infection is a multi-step process involving binding of the viral particle to the plasma membrane of a T cell and

endocytosis, followed by envelope fusion, reverse transcription to form a pre-integrated DNA provirus and finally integration into the host T-cell genome. Lentiviral particles that are pseudotyped with the vesicular stomatitis virus g-glycoprotein (VSV-G) to broaden the viral tropism depend on the low-density lipoprotein receptor (LDL-R), which is ubiquitously expressed on the surface of various cells, including lymphocytes, for entry<sup>21,22</sup>. Limitations to efficient lentiviral transduction of quiescent T cells occur at each stage of infection. The fusion of lentiviral particles with quiescent T cells is inefficient<sup>23,24</sup>. Conditioning the cell culture medium with recombinant interleukin (IL)-7 and IL-15 cytokines can overcome this limitation<sup>25</sup> and increase the transduction efficiencies as well as cell survival in quiescent T cells<sup>26,27</sup>. Engineering viral particles to express an IL-7 fusion protein increases quiescent T-cell lentiviral transduction<sup>28</sup>. Post entry, low concentrations of nucleotides and the presence of additional restriction factors such as SAMHD1 limit the rate of reverse transcription in quiescent T cells<sup>29–31</sup>. Collectively, these factors make lentiviral transduction of non-activated T cells inefficient.

Having previously shown that shortening the ex vivo culture of CAR T cells yields a cellular product with less-differentiated T cells and significantly enhanced effector function, we hypothesized that elimination of the CD3 and CD28 (CD3/CD28) activation step could yield a T-cell product with high functional potency. Reducing the culture duration could also substantially reduce the vein-to-vein time and substantially improve the logistics required to make CAR T-cell products. Here we have overcome some of the barriers to lentiviral transduction of non-activated T cells with a CAR by modifying the ex vivo manufacturing protocol. This technical advance resulted in CAR T cells with potent antitumor function that were available within 24 h of mononuclear-cell collection compared with

<sup>1</sup>Center for Cellular Immunotherapies, Perelman School of Medicine, University of Pennsylvania, Philadelphia, PA, USA. <sup>2</sup>Department of Pathology and Laboratory Medicine, Perelman School of Medicine, University of Pennsylvania, Philadelphia, PA, USA. <sup>3</sup>Department of Microbiology, Perelman School of Medicine, University of Pennsylvania, Philadelphia, PA, USA. <sup>4</sup>Division of Hematology–Oncology, Department of Medicine, Perelman School of Medicine, University of Pennsylvania, Philadelphia, PA, USA. ✉e-mail: [ghassemi@penmedicine.upenn.edu](mailto:ghassemi@penmedicine.upenn.edu); [milone@penmedicine.upenn.edu](mailto:milone@penmedicine.upenn.edu)

the 9d process currently used by tisagenlecleucel. These results demonstrate the potential for a vast reduction in the time, materials and labour required to generate CAR T cells, which could be especially beneficial in patients with rapidly progressive disease and in resource-poor healthcare environments.

## Results

**Transduction of non-activated T cells by lentiviral vectors.** We confirmed the previously reported low transduction efficiency of freshly isolated quiescent T cells with VSV-G-pseudotyped lentivirus vector. Primary human T cells obtained from healthy donors were mixed with an infrared red fluorescent protein (iRFP)-encoding lentiviral vector under conditions identical to activated T cells and followed for 96h to assess the efficiency and kinetics of transduction (Fig. 1a). In comparison to lentiviral transduction of T cells activated 24h previously with anti-CD3/CD28 microbeads at a multiplicity of infection (MOI) of five, which yields >85% transduction at 48h, the efficiency (Fig. 1a) and kinetics (Fig. 1b,c) of lentiviral transduction in non-activated T cells was substantially slower, requiring at least 72h to achieve detectable expression of an *iRFP* transgene and with a transduction efficiency that was about 11-fold lower at 96h than activated T cells (Fig. 1a). The slower kinetics of this process is consistent with the previous observation of inefficient transduction efficiency of VSV-G-pseudotyped lentivirus vector<sup>23</sup> and the decreased rate of reverse transcription reported for natural HIV in quiescent T cells compared with activated T cells<sup>32</sup>. Transduction was observed in both memory and naive subsets of CD4<sup>+</sup> and CD8<sup>+</sup> T cells, with the highest efficiency observed in CD8<sup>+</sup> cells with a memory phenotype (Fig. 1d,e).

We repeated the same studies using a third-generation lentiviral vector encoding a CD19-specific CAR (CAR19), which in contrast to the cytoplasmic nature of iRFP is a cell membrane-expressed protein. The levels of CAR expression were measured by immunostaining with a monoclonal antibody recognizing the idiotype of the single-chain variable fragment<sup>33</sup>. In a similar kinetic analysis to that performed with the iRFP-encoding lentiviral vector, we observed that non-activated T cells acquired CAR expression as early as 12h after the addition of the CAR lentiviral vector, with a steady increase to >80% of T cells transduced by 96h (Fig. 2a). To determine whether the CARs were stably expressed, the T cells were treated with either a reverse transcriptase (RT) or integrase inhibitor during the lentiviral transduction process. As shown in Fig. 2b,c, CAR expression in non-activated T cells was unaffected by either compound, whereas both RT and integrase inhibition completely abrogated CAR expression in activated T cells. This pseudotransduction observed in non-activated T cells is probably due to the transfer of CAR protein from the lentiviral vector envelope by viral fusion to the T cell, as it is well-known that membrane proteins expressed in the packaging cells are incorporated into the HIV envelope<sup>34</sup>. The absence of apparent pseudotransduction with a vector that encodes iRFP, a cytoplasmic protein, provides support for this envelope-mediated transfer mechanism (Fig. 2d). Notably, the observed pseudotransduction was not exclusive to non-activated T cells. However, greater rates of pinocytosis in activated T cells may increase cell-membrane turnover and hence clearance of passively transferred proteins contributing to pseudotransduction. Importantly, CART19 cells generated by lentiviral transduction of non-activated T cells in the presence of RT and integrase inhibitors showed no specific cytolytic activity and cytokine production against CD19-expressing target cells (Supplementary Fig. 1a,b). Based on these data, we conclude that long-term persistence of CAR expression in T cells will require vector integration, which occurs at a substantially lower frequency in non-activated T cells compared with activated T cells.

Although functional CAR expression could not be assessed post transduction due to the substantial pseudotransduction, we

hypothesized that the transduction process would probably continue following adoptive transfer in vivo, giving rise to functional CART19 cells. We therefore performed an in vivo experiment to evaluate non-activated CART19 cells transduced for 24h (day 1, d1) as in Fig. 1 using a well-established Nalm6 B-cell acute lymphoblastic leukaemia (ALL) mouse model<sup>35</sup>. As shown in Fig. 3, a dose of  $3 \times 10^6$  non-activated CART19 cells (d1) washed and infused within 24h of collection was compared with a dose of  $3 \times 10^6$  CAR<sup>+</sup> CD3/CD28-activated CAR T cells that were expanded ex vivo for 9d before injection, a research process comparable to that used to manufacture tisagenlecleucel, as shown schematically in Fig. 3a,b. Although non-activated CAR T cells were unable to induce a complete regression of leukaemia, they controlled leukaemia for an extended duration of 60d. As a comparison, we show the effectiveness of d9 CAR T cells is highly variable across donors (Fig. 3d,e). Typically, d9 cells exit their logarithmic growth phase and are resting down. However, some donors can maintain high metabolic activity and function at this time point. This contributes to donor-to-donor variability in antitumour responses. Given the persistence of T cells in the peripheral blood of mice (Fig. 3f,g), our findings suggest that non-activated CAR T cells retain replicative capacity to maintain function under continuous antigenic stimulation (Fig. 3d). This contributed to a significant increase in the overall survival of the leukaemia-bearing mice (Fig. 3h). These results support the functional nature of non-activated CART19 cells, and they encouraged the optimization of the transduction process to further enhance non-activated CART19 activity.

**Modification of the culture conditions to enhance non-activated T-cell transduction.** Numerous mechanisms restrict quiescent T-cell infection by natural HIV. Viral attachment and entry represent a critical initial phase of the transduction process, during which the RNA genome of the lentiviral vector is inserted into the cytoplasm of the host T cell. Although natural HIV uses both chemokine receptors and CD4 for attachment and entry<sup>36</sup>, VSV-G-pseudotyped lentiviral vectors use the LDL-R as their primary receptor<sup>22</sup>. The low transduction efficiency of non-activated T cells has been attributed to low expression of LDL-R<sup>21</sup>. As the abundance of LDL-R is linked to the metabolic state of the cell and LDL uptake can be enhanced by cholesterol restriction<sup>37</sup>, we evaluated whether a brief serum starvation before lentiviral-vector transduction increases the lentiviral-vector transduction of non-activated T cells. Brief (3–6h) serum starvation increased iRFP expression by an average of two-fold in non-activated T cells (Fig. 4a and Supplementary Fig. 1). The slow kinetics of reverse transcription in non-activated T cells by both natural HIV and lentiviral vectors also contribute to the reduced transduction efficiency. Completion of reverse transcription during natural HIV infection is enhanced by high concentrations of deoxynucleosides (dNs)<sup>19</sup>. Supplementation of the culture medium with 50  $\mu$ M dNs also increased the lentiviral transduction of non-activated T cells by two- to threefold (Fig. 4b). Finally, the limited diffusibility of lentivirus in large culture vessels is another major barrier limiting the transduction efficiency in T cells<sup>38</sup>. To evaluate this, we adjusted the geometric conditions to enhance the colocalization of vector particles with T cells. By increasing the surface area-to-volume ratio of the culture vessel, while keeping the volume constant, we increased the transduction of non-activated T cells by at least twofold (Fig. 4c). Furthermore, we show that the transduction efficiencies can be enhanced by 2–12-fold in non-activated T cells by combining these approaches (Fig. 4d).

Given that pseudotransduction with CAR19 interferes with the ability to estimate the transduction efficiency (Fig. 2) and vector integration is likely to be ongoing at the time of infusion, we estimated the efficiency of the optimized transduction process by adoptively transferring the transduced T cells into non-leukaemia-bearing NSG mice, which permits an estima-

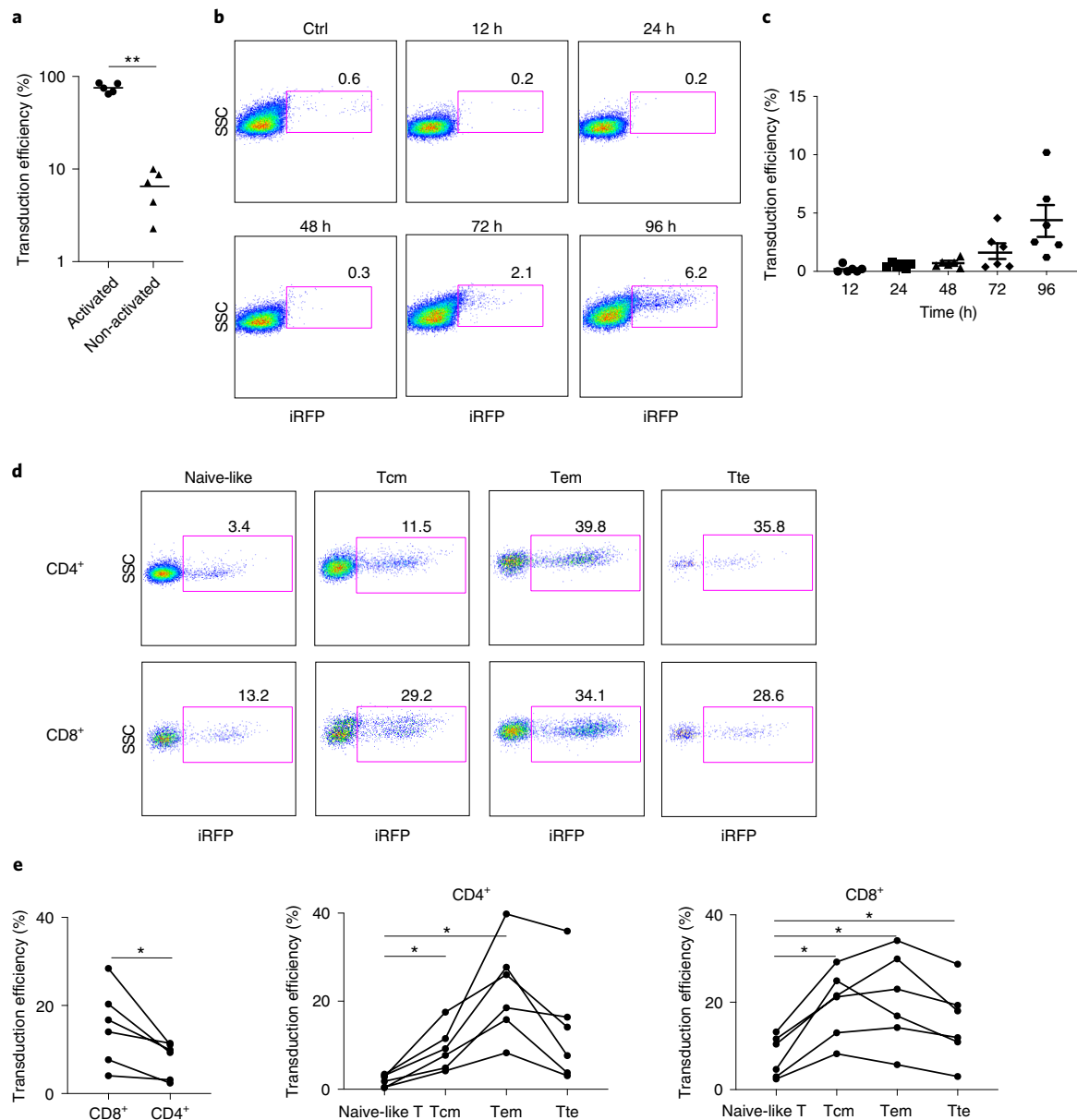


**Fig. 1 | Lentiviral vectors transduce non-activated T-cell subsets with a preference for memory subsets.** **a**, Transduction efficiency of freshly isolated human T cells that were either cultured in IL-7 ( $10 \text{ ng ml}^{-1}$ ) and IL-15 ( $10 \text{ ng ml}^{-1}$ ) or activated with beads coated with anti-CD3/CD28 and transduced with lentiviral vector encoding iRFP for 5 d. The mean of each group is indicated by the solid black line. The two groups were compared using a two-tailed unpaired Mann-Whitney test;  $P = 0.0079$ . **b,c**, Freshly isolated human T cells were cultured in IL-7 and IL-15, and transduced with lentiviral vector encoding iRFP for the indicated time periods. **b**, iRFP<sup>+</sup> cells were quantified by flow cytometry. Ctrl, control. **c**, Similar transduction efficiencies were obtained in an independent experiment from six different donors. Data are the mean  $\pm$  s.e.m. **d**, Representative flow cytometric analysis of non-activated T cells transduced as in **a**. Naive, central memory (Tcm), effector memory (Tem) and total effector (Tte) T-cell subsets were identified following gating on live singlets of CD3<sup>+</sup>CD4<sup>+</sup> (top) and CD3<sup>+</sup>CD8<sup>+</sup> (bottom) T cells using CD45RO and CCR7 expression. **b,d**, The percentages of transduced cells (pink boxes) are indicated. **e**, Similar transduction efficiencies were obtained in an independent experiment from six different donors. CD4<sup>+</sup> versus CD8<sup>+</sup> cells,  $P = 0.0308$ ; two-tailed paired *t*-test (left). CD8<sup>+</sup> naive-like T cells versus Tcm, Tem and Tte cells,  $P = 0.0133$ ,  $0.0204$  and  $0.0427$ , respectively (right); and CD4<sup>+</sup> naive-like T cells versus Tcm and Tem cells,  $P = 0.0423$  and  $0.0208$ , respectively (middle); paired one-way analysis of variance. \* $P < 0.05$ ; \*\* $P < 0.01$ .

tion of the frequency of integrated vector in the absence of CAR stimulation by antigen-expressing tumour cells that would normally stimulate and enrich for CAR T cells. CART19 cells were generated from freshly isolated peripheral blood T cells by serum starving the T cells for 3 h, followed by transduction in a minimal volume of lentiviral vector encoding CAR19 (MOI of five) for 20 h in the presence of dNs ( $50 \mu\text{M}$ ), and IL-7 and IL-15 ( $10 \text{ ng ml}^{-1}$  each; Fig. 4e). When we evaluated three CART19 products produced from three separate donors, we observed a mean trans-

duction frequency of 8% (range of 6–16%) based on analysis performed 3 weeks following the adoptive transfer (Fig. 4f), which is within the lower end of the range of CART19 products using a 9 d manufacturing process<sup>39</sup>. This was confirmed by quantitative PCR (qPCR) analysis of the integration of lentivirus vector in non-activated T cells over time (Table 1). Thus, our data are consistent with the integration of the lentiviral vector in the non-activated T cells occurring over several days after infusion of the non-activated CART19 cells.

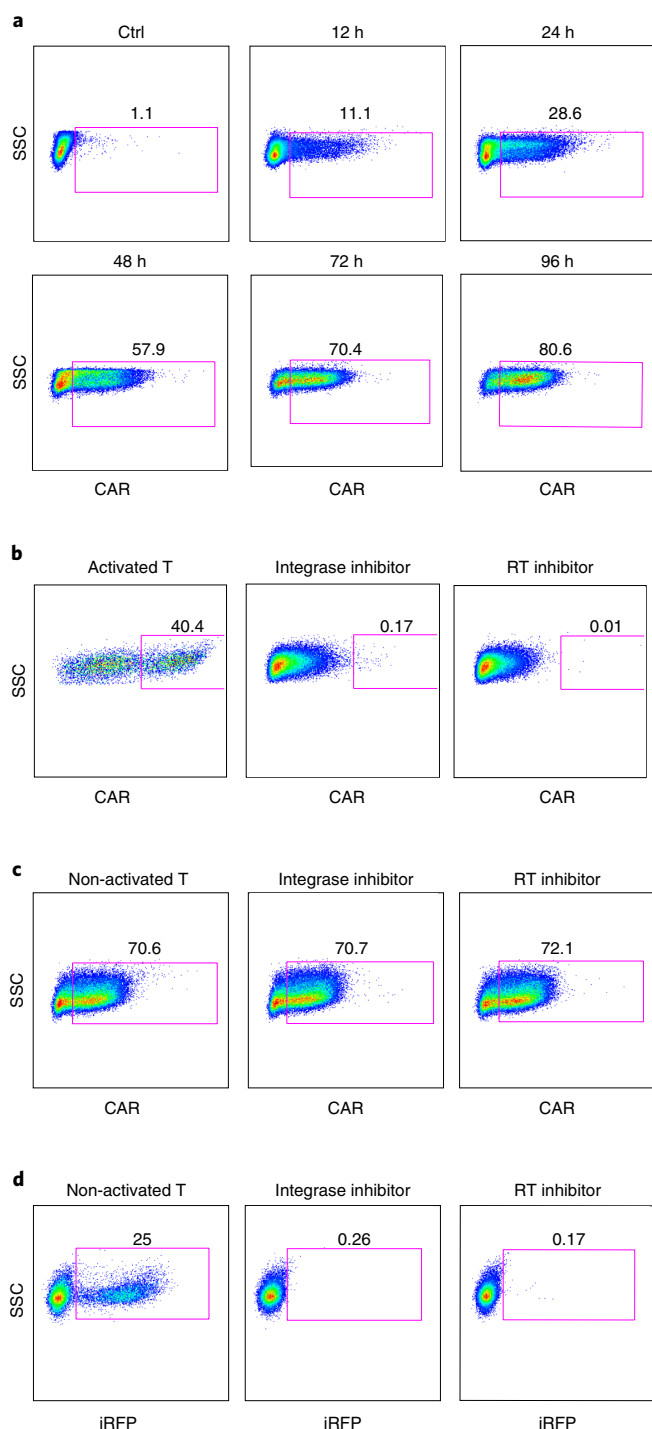


**Fig. 2 | CAR lentivirus mediates pseudotransduction in non-activated T cells.** **a**, Freshly isolated human T cells were cultured in IL-7 and IL-15, and transduced with lentiviral vector encoding CAR19. The gene transduction efficiency was measured after immunostaining with an anti-idiotypic antibody for the indicated time periods. Representative flow cytometry plots of CAR expression from six separate experiments with independent donors are shown. **b,c**, T cells that had been previously stimulated with anti-CD3/CD28 microbeads (**b**) as well as non-activated T cells (**c**) were transduced with CAR lentivirus and co-cultured with integrase (middle) or RT (right) inhibitor for 4 d. The CAR<sup>+</sup> cells were quantified by flow cytometry. **a–c**, The percentages of transduced cells (pink boxes) are indicated. **d**, Non-activated T cells were transduced with iRFP lentivirus and co-cultured with integrase (middle) or RT (right) inhibitor as in **b,c**. iRFP<sup>+</sup> cells were quantified by flow cytometry.

**Table 1 | Integrated lentiviral vector analysis using repetitive sample *Alu-gag* qPCR**

Sample	RU5 copies per cell	Proviral HIV copies per cell
12 h	0.19	0.01
24 h	0.16	0.09
48 h	0.55	0.23
72 h	0.69	0.60
12 h (RT and integrase inhibitor)	0.15	<LOD
24 h (RT and integrase inhibitor)	0.12	<LOD
48 h (RT and integrase inhibitor)	0.07	<LOD
72 h (RT and integrase inhibitor)	0.05	<LOD

<LOD, below the limit of detection; RU5, long-terminal repeat (LTR) primer only for total vector (integrated + non-integrated). Comparison of integrated vector (number of proviral HIV copies per cell) with the total vector copies (number of RU5 copies per cell, detected total integrated + non-integrated vector) with or without RT and integrase inhibitors.

**In vivo functional assessment of optimally transduced CART19 cells.** We hypothesized that a non-activated CAR T-cell product preserves the intrinsic stem-like properties of naive and memory T cells, culminating in enhanced persistence following infusion. To evaluate this hypothesis, we performed an in vivo functional ‘CAR stress test’ using limited numbers of CAR T cells in the Nalm6 leukaemia model. Total non-activated T cells ( $2 \times 10^6$ ,  $7 \times 10^5$  or  $2 \times 10^5$ ) transduced using our optimized process were adoptively transferred into NSG mice bearing pre-established Nalm6 xenografts. Activated CART19 cells ( $3 \times 10^6$ ) prepared by anti-CD3/CD28 bead stimulation, followed by 9 d of ex vivo expansion were used as a control in addition to  $3 \times 10^6$  mock-transduced non-activated T cells (Fig. 5). As shown in Fig. 5b–d, complete regression of Nalm6 leukaemia to a bioluminescence flux (BLI) of less than  $1 \times 10^6$  photons per second was observed in all groups treated with non-activated CART19 cells. The kinetics of the anti-leukaemic response for the non-activated CART19 cells was dose dependent; the lowest dose group cleared the tumour by d18, whereas the highest dose group achieved tumour regression by d11 (Fig. 5e). The CD3/CD28-stimulated and expanded CART19 cells were the quickest to clear leukaemia (Fig. 5d). However, the depth and durability of the response for this donor was limited, with all mice relapsing by d17. In contrast, the non-activated CART19 cells controlled leukaemia for the duration of the experiment in all mice at the highest dose and in most mice at the lower doses (Fig. 5c). This durability was associated with an increased persistence of T cells. As seen in Fig. 5f–h, the absolute counts of CART19 cells were significantly increased in the peripheral blood of the mice treated with non-activated CART19 cells—which was proportional to the dose infused—compared with treatment with activated CART19 cells. These cells were mostly effector memory cells (Supplementary Fig. 3). To demonstrate the broader applicability of our approach, we also evaluated the antitumour function of CD33-specific CAR T cells generated from non-activated T cells in a xenograft model of acute myeloid leukaemia (AML). As seen in Extended Data Fig. 1, non-activated CAR T cells demonstrated an anti-leukaemic function that was similar to CAR T cells generated from CD3/CD28-activated T cells and expanded over 9 d. Unfortunately, the durability of the response could not be assessed in this model due to an allogeneic response that was evident with non-transduced (NTD) cells 2 weeks after the CAR T-cell infusion.

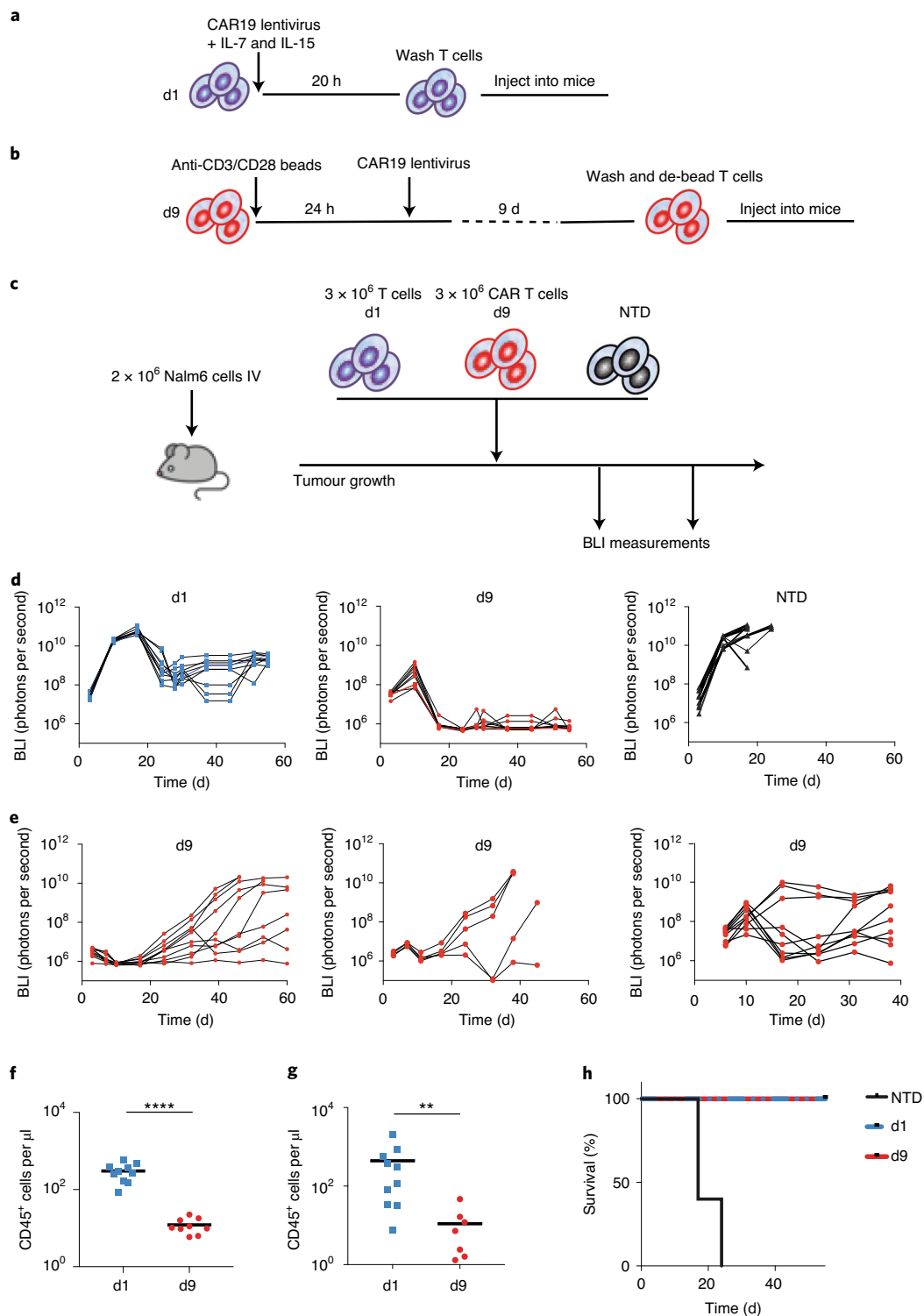


**Fig. 3 | Non-activated T cells expressing CAR19 control leukaemia in xenograft models of ALL.** **a**, Schematic of the generation of non-activated CART19 cells in less than 24 h. Freshly isolated human T cells were transduced with CAR19 lentiviral vector for 20 h in the presence of IL-7 and IL-15. The cells were then washed and injected into mice. **b**, Schematic showing how CART19 cells are generated using standard approaches. After overnight stimulation with anti-CD3/CD28 beads, T cells are transduced with CAR19 lentiviral vector and expanded for 9 d. The cells are then washed, de-beaded and injected into mice. **c**, Schematic of the xenograft model with CART19 cell treatment in NSG mice. IV, intravenously. **d**, Total BLI in mice treated with  $3 \times 10^6$  non-activated T cells transduced as in **a** (d1; left) and mice treated with  $3 \times 10^6$  CAR<sup>+</sup> T cells previously stimulated with anti-CD3/CD28 microbeads and expanded over 9 d as in **b** (d9; middle) and NTD (right) control non-activated T cells ( $3 \times 10^6$  cells per treatment;  $n = 10$  mice per group). **e**, Representative BLI in mice treated with  $3 \times 10^6$  CAR T cells stimulated with anti-CD3/CD28 microbeads and expanded over 9 d from three additional donors. **f, g**, Absolute CD45<sup>+</sup> T-cell counts, measured using a TruCount assay, of peripheral blood collected from the mice in **d** on d27 (**f**) and d55 (**g**) following T-cell transfer. The mean of each group is indicated by the solid black line. Groups were compared using a two-tailed unpaired Mann–Whitney test; \*\* $P = 0.02$ ; \*\*\*\* $P < 0.0001$ . **h**, Overall survival of the mice in each group.  $P < 0.0001$  for d1 versus NTD and d9 versus NTD; two-sided log-rank test.

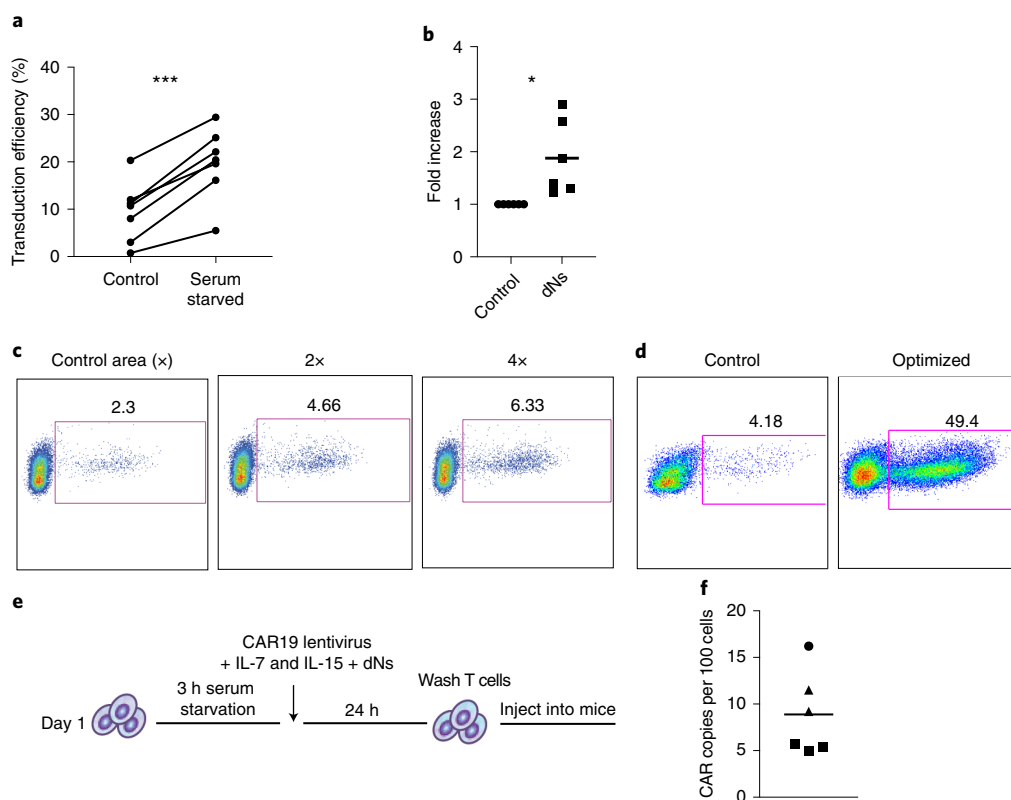


**Fig. 4 | The transducing conditions can enhance the transduction efficiency in non-activated T cells.** **a**, Freshly isolated human T cells were either serum starved by washing and resuspending in serum-free medium or maintained in complete medium for 3–6 h. The cells were then transduced with a lentiviral vector encoding iRFP for 24 h in the presence of IL-7 and IL-15 in complete medium and maintained in culture for 5 d before determining the iRFP<sup>+</sup> cell frequency. Each dot represents the transduction frequency, determined by flow cytometry, from an independent experiment using six different donors. \*\*\* $P=0.0002$ . **b**, Relative fold change in transduction of iRFP<sup>+</sup> cells transduced in the presence of 50  $\mu\text{M}$  dNs normalized to iRFP<sup>+</sup> cells transduced in complete medium without dNs. Data are the mean  $\pm$  s.d. of six experiments performed with different donors. \* $P=0.0312$ . In **a** and **b**, a two-tailed paired  $t$ -test was used. **c**, T-cells transduction with iRFP lentiviral vector was performed in one (control; left), two (middle) or four (right) wells, with the total culture volume kept constant. The cells were then maintained in culture for 5 d in IL-7 and IL-15-containing medium before determining the iRFP<sup>+</sup> cell frequency by flow cytometry. Results are representative of three independent experiments using three different donors. **d**, Freshly isolated human T cells were transduced with a lentiviral vector encoding iRFP in optimized conditions as described in **a–c** (serum starvation, dNs and optimized geometry). The T cells were then maintained in culture for 5 d, followed by flow cytometric analysis for iRFP expression. Results are representative of the best transduction achieved using this process. **c,d**, The percentages of transduced cells (pink boxes) are indicated. **e**, Schematic of the generation of non-activated CART19 cells in 24 h. **f**, Frequency of CAR T cells, estimated by qPCR analysis of the vector copy number, in peripheral blood collected 3 weeks following the adoptive transfer of T cells. The results are expressed as a percentage of human cells by normalization to the *CDKN1A* gene, which has two copies in the human diploid genome. Each symbol represents a separate donor.

In summary, these findings demonstrate that as few as an estimated 12,000–32,000 non-activated CAR T cells, based on the range of transduction efficiency generated with the optimized transduction process (Fig. 3e), within 24 h from collection could eradicate leukaemia. The long-term engraftment of non-activated CAR T cells probably occurs due to their enhanced replicative capacity compared with activated CAR T cells.

**Feasibility and functionality of non-activated CAR T cells using patient samples.** After showing that non-activated CAR T cells can be generated from healthy donor lymphocytes, we extended our observations to T cells isolated from patients undergoing cancer treatment. Immunosuppressive factors in the tumour environment may impede the ability to generate functional CAR T cells using our approach. We therefore evaluated the anti-leukaemic activity of non-activated CAR T cells generated using apheresis-collected mononuclear cells derived from an individual with diffuse large B-cell lymphoma who was treated in one of our CART19 cell clinical trials (ClinicalTrials.gov number [NCT02030834](https://clinicaltrials.gov/ct2/show/study/NCT02030834)). Given that

apheresis-collected mononuclear cells comprise numerous cell types in addition to T cells, we employed a CD4<sup>+</sup> and CD8<sup>+</sup> T-cell positive selection strategy using current good manufacturing practice (cGMP)-compliant anti-CD4 and anti-CD8 magnetic microbeads (Supplementary Fig. 4a). Following selection, the enriched T cells were lentivirally transduced with CAR19 in medium conditioned with 50  $\mu\text{M}$  dNs and 10 ng ml<sup>-1</sup> IL-7 and IL-15 for 24 h as in the previous studies with healthy donor T cells. CART19 cells manufactured at the University of Pennsylvania's Cell and Vaccine Production Facility using a cGMP-compliant 9 d process were used as a control.  $3 \times 10^6$  total non-activated T cells (d1) versus  $3 \times 10^6$  CAR T cells (d9) were adoptively transferred to NSG mice bearing pre-established Nalm6 xenografts. To control for CD19-specific cytolytic activity,  $3 \times 10^6$  mock-transduced non-activated T cells were included as an additional control. To estimate the transduction efficiency of the non-activated CAR T cells,  $3 \times 10^6$  transduced T cells were infused into NSG mice without leukaemia (Fig. 4e). The lentiviral infection efficiency was estimated to be 32%, as assessed by integration analysis performed 7 weeks following the adoptive

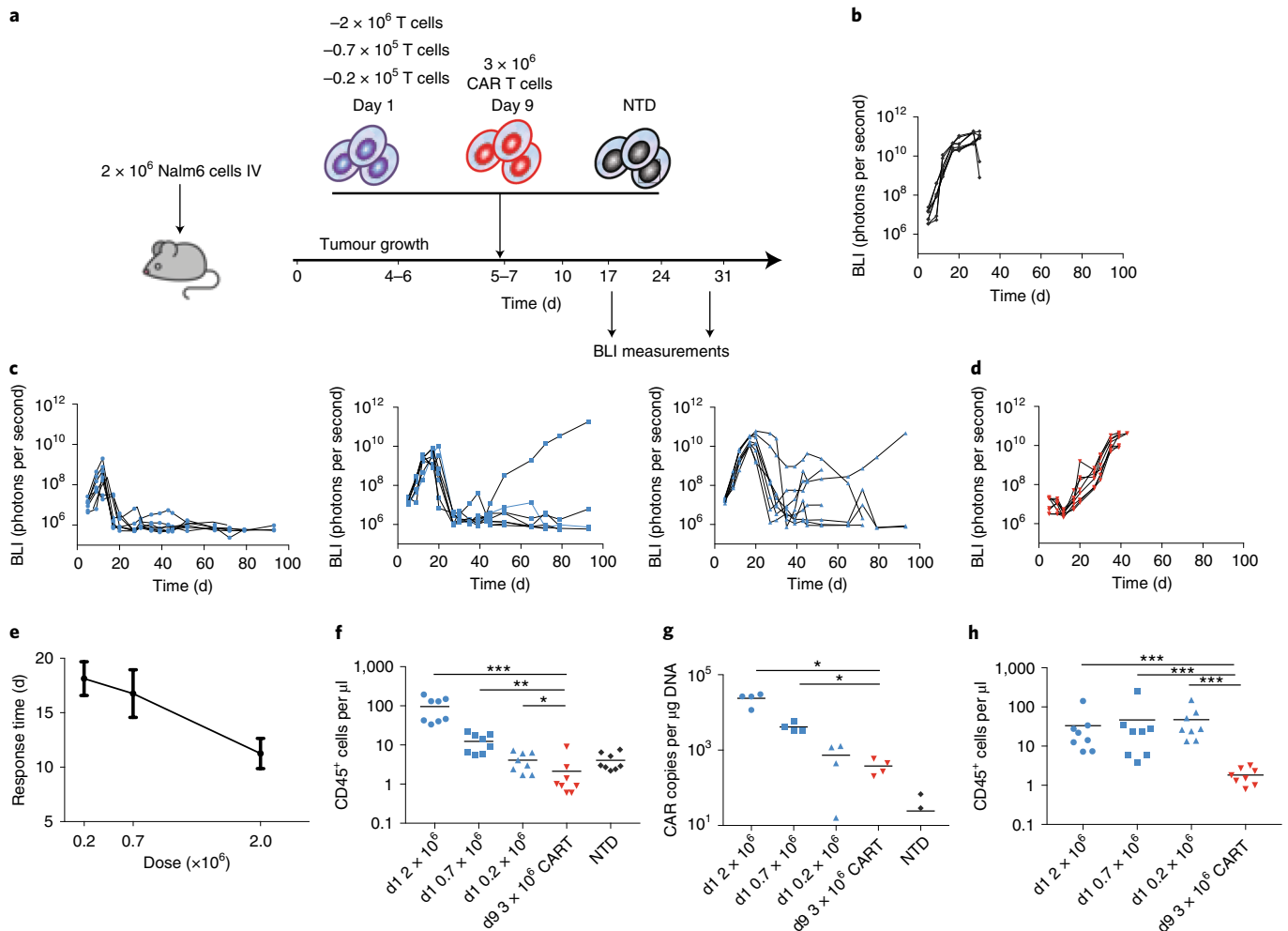


**Fig. 5 | Non-activated CART19 cells induce potent and durable remission of ALL at low doses.** **a**, Schematic of the xenograft model and CART19 cell treatment in NSG mice. **b–d**, Serial quantification of disease burden by bioluminescence imaging. **b**, Total BLI in mice treated with NTD control non-activated T cells. **c**, Total BLI in mice treated with a single high ( $2 \times 10^6$ ; left), medium ( $0.7 \times 10^6$ ; middle) or low ( $0.2 \times 10^6$ ; right) dose of non-activated T cells (d1) transduced as in Fig. 4e. **d**, Total BLI in mice treated with  $3 \times 10^6$  CAR T cells stimulated with anti-CD3/CD28 microbeads and expanded over 9 d. For **b–d**, there were eight mice in each group. **e**, Time to initial anti-leukaemic response (that is, first reduction in bioluminescence) after infusion of non-activated CART19 cells relative to the T-cell dose. Data are mean  $\pm$  s.d. **f**, Absolute CD45<sup>+</sup> T-cell counts, measured using a TruCount assay, of peripheral blood collected from the mice in **b–d** on d10 following the T-cell transfer. \* $P=0.0255$ ; \*\* $P=0.0011$ ; \*\*\* $P=0.0002$ . **g**, Vector copy number, measured by qPCR and normalized to the DNA concentration, in peripheral blood collected on d10 following the T-cell transfer. \* $P=0.0286$ . **h**, Absolute CD45<sup>+</sup> T-cell counts, measured using a TruCount assay, of peripheral blood collected from the mice shown in **b–d** on d30 following the T cell transfer measured by a TruCount assay. \*\*\* $P=0.0002$ . **f–h**, The mean of each group is indicated by the solid black line. Groups were compared using a two-tailed unpaired Mann-Whitney test.

transfer. These data were corroborated by flow cytometric analysis (Supplementary Fig. 4b). As shown in Fig. 6a,b, the d9 CART19 cells exhibited complete regression of Nalm6 leukaemia. However, all mice relapsed by d20, consistent with the progressive loss of function and low replicative capacity of CAR T cells in this model. In contrast, non-activated CART19 cells provided sustained leukaemia control in half of the mice (three of six) for the duration of the experiment. The enhanced durability of the anti-leukaemic activity in the mice treated with non-activated CAR T cells, demonstrated by a lower bioluminescence signal on d49 (Fig. 6e), was associated with an improved persistence of T cells in the peripheral blood (Fig. 6f–h). In summary, these results demonstrate the feasibility of generating CAR T cells from patient-derived non-activated T cells using a process that can be imported into a cGMP environment and further demonstrated that rapidly produced non-activated CAR T cells exhibit a more durable anti-leukaemic function compared

with CAR T cells manufactured using a 9 d ex vivo expansion process following CD3/CD28 activation.

**Distribution of vector integration sites in non-activated CAR T cells.** To assess whether the different methods of cell preparation affected the distribution of the vector integration sites, samples were analysed by ligation-mediated PCR<sup>40–42</sup> and compared with historical CAR T-cell products<sup>43</sup> (Supplementary Report). Experimental infections were carried out in non-activated and activated cells, and their DNA was purified. The DNA was sheared by sonication, DNA adaptors were ligated onto the free DNA ends and the region between the adaptor and the edge of the integrated vector was PCR amplified. The PCR products were then subjected to sequencing, the DNA sequences were mapped to the human genome and the distributions of the vector integration sites were compared. We also compared a set of pre-infusion samples from CAR T-cell products

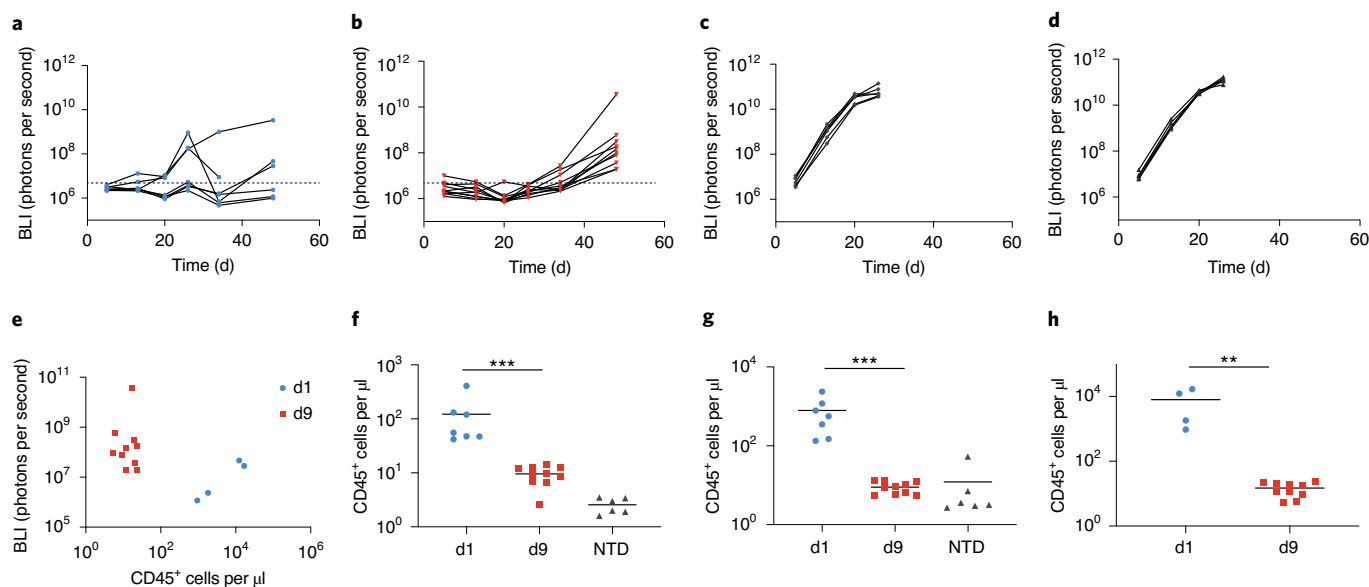


**Fig. 6 | Non-activated CAR T cells generated from patient samples show potent efficacy in vivo. a–d**, Serial quantification of disease burden by bioluminescence imaging. Total BLI in mice treated with  $3 \times 10^6$  non-activated T cells (d1) transduced as in Fig. 4e (a;  $n = 7$ ), CAR T cells stimulated with anti-CD3/CD28 microbeads and expanded over 9 d (d9; b;  $n = 10$ ) or NTD control non-activated T cells (c;  $n = 10$ ) as well as the total BLI of untreated mice (tumour only; d). In a and b, the dashed line is the baseline BLI. e, BLI measurement of the disease burden of the mice from the d1 and d9 groups (from a and b) in relation to the absolute CD45<sup>+</sup> T-cell counts in their peripheral blood on d49. f–h, Absolute CD45<sup>+</sup> T-cell counts, measured using a TruCount assay, of peripheral blood collected from the mice in a–c on d16 (f), d23 (g) and d49 (h) following the T-cell transfer. The mean of each group is indicated by the solid black line. Groups were compared using a two-tailed unpaired Mann–Whitney test. \*\*\* $P = 0.0001$ ; \*\* $P = 0.002$ .

where aliquots were later infused into human study participants and for which no vector-associated adverse events were noted<sup>43</sup>.

Integration in both the resting and activated cell samples was favoured in active transcription units and the associated genomic annotation, as has been seen in many studies<sup>44–46</sup>. No expanded clones were observed. The integration frequency near annotated cancer-associated genes was comparable for the non-activated and activated CAR T cells and not obviously different from the CAR T-cell pre-infusion comparison set. Thus, we conclude that there were no obvious differences in integration-site distributions that might raise safety concerns. These findings correlate with studies of HIV integration-site distributions in resting and activated T cells, where at most modest differences were detected<sup>47</sup>.

## Discussion

This study presents an approach to rapidly generate highly functional CAR T cells for adoptive immunotherapy. This approach capitalizes on the unique ability of lentiviral vectors to transduce non-activated quiescent T cells. Ex vivo cell culture following T-cell activation is an essential part of the manufacturing of CAR T-cell therapies. Because T-cell-receptor activation and clonal expansion promote irreversible differentiation of T cells as well as potentially other detrimental changes to the T cells through processes such as oxidative stress<sup>48,49</sup>, the potency of CAR T cells may be compromised during their manufacturing process. Although interventions such as the provision of different costimulatory receptor signals<sup>50</sup> and cytokines<sup>51</sup>, or other alterations to the culture conditions (for example, Akt inhibition)<sup>52</sup> help to limit this cellular differentiation, stable expression of a CAR in a non-activated T cell provides a far simpler approach to limiting differentiation. Our results demonstrate that functional transduction of non-activated T cells, including memory subsets, can be achieved within less than 24 h of the T-cell collection. Moreover, non-activated T cells transduced with CAR19 exhibit potent

in vivo anti-leukaemic efficacy at cell doses well below those effective for activated T cells<sup>7</sup>.

To show the potential benefit of our approach beyond CART19 in models of ALL, we confirmed the antitumour potency of unstimulated CAR T cells redirected against CD33. These findings broaden the impact of our approach to other blood-based leukaemias, including AML. We found that NTD cells controlled the tumour burden 2 weeks following infusion in our xenograft model of AML. High levels of antigen presentation specific to AML may create an allogeneic immune pressure that stimulates the ‘graft versus leukaemia effect’ in donor T cells. This is an expected response as bone-marrow transplantation works to treat patients with leukaemia.

Importantly, we established that our overall process was technically feasible in line with current manufacturing procedures, facilitating a rapid transition into the clinical sector. Using patient apheresis material, we demonstrated that T cells can be isolated using cGMP-grade antibodies and standard column-based purification methods. These cells retain maximal functional competence using our method of CAR gene delivery and preparatory phase, which eliminates activation. Our approach is poised for a rapid implementation to Clinimax-based systems that are currently used in our manufacturing division at the University of Pennsylvania as well as other facilities.

The approach used for the transduction of non-activated T cells in our studies has only been partially optimized and it is probable that the efficiency of the transduction process can be further enhanced. A recent study demonstrated that the use of a microfluidic chamber for transduction could significantly increase both the efficiency and kinetics of the transduction process by overcoming the diffusion barriers inherent to static cultures<sup>38,53</sup>. Interference with SAMHD1, a deoxynucleoside triphosphate triphosphohydrolase that restricts HIV-1 infection in quiescent T cells, is another potential strategy to enhance non-activated T-cell transduction<sup>31,54</sup>.

Mechanistically, SAMHD1 hinders lentivirus infection by impeding the rate of reverse transcription. Loss-of-function approaches show that SAMHD1 elimination leads to increased infection efficiencies in non-activated T cells<sup>54</sup>. Small molecules that inhibit SAMHD1 are under development and may have applications here<sup>55</sup>. In addition to the post-entry restrictions, substitution of the VSV-G envelope protein with alternative glycoproteins such as the coxal virus envelope may also enhance the lentiviral entry step into quiescent T cells, as this envelope protein has yielded superior transduction efficiencies in haematopoietic stem cells and activated T cells<sup>56</sup>.

In addition to optimizing the transduction process, the optimal composition of non-activated T cells for adoptive immunotherapy is largely unknown. Various syngeneic murine models show that memory T-cell subsets have a superior antitumour function following adoptive transfer<sup>8,11,16,57</sup>. In the CD8<sup>+</sup> T-cell compartment, the transduction efficiencies were highest in the memory T-cell subsets (Fig. 1e). It cannot be assumed that the T-cell subsets found to be optimal for activated T cells will be the same when using non-activated T cells in adoptive immunotherapy. Cells with effector differentiation and function may be needed in addition to memory cells for replenishment of the tumour-specific T-cell pool when starting with quiescent T cells. The optimal CAR design for non-activated T cells has also not been defined. Our study used a second-generation CAR incorporating the 4-1BB cytoplasmic domain; however, this design was previously selected for its function in activated T cells, in which natural 4-1BB is typically expressed<sup>58</sup>. Alternate CAR designs may be required for optimal function in quiescent T cells. Combining T-cell subsets with their preferred costimulatory domain may be the most beneficial approach for immediate effector function and long-lasting engraftment.

Intriguingly, quiescent memory T cells seem to be more susceptible to lentiviral transduction than their naive counterparts. These findings suggest that previous activation supports lentiviral transduction, even when the T cells are in a quiescent state at the time of transduction. It is possible that epigenetic alterations underlying the commitment to memory render the cells more susceptible to infection at a later date. In support of this hypothesis, H3K36me3 histone modifications promote viral integration in actively transcribed regions in non-dividing cells<sup>59</sup>. In addition to the unique epigenetic landscape of memory cells, transcriptional complexes are redistributed to the nuclear pore in non-dividing cells<sup>60</sup>. Proteins assembled at the nuclear pore may enhance HIV-1 nuclear entry in memory T cells through unknown mechanisms.

The slow kinetics of lentiviral transduction observed in our study complement the delay in reverse transcription and integration observed in natural HIV infection of non-activated CD4<sup>+</sup> T cells<sup>18–20</sup>. It is probable that the majority of T cells used in our in vivo studies lacked integrated proviral DNA at the time of adoptive transfer and the processes of reverse transcription and integration instead probably continue post infusion. This introduces challenges for the assessment of the quality of the CAR T cells. Transduction efficiency, typically measured by CAR expression at the cell surface and/or vector integration, is routinely used as a surrogate measure of product potency as well as CAR T-cell dose. Translation of a rapid manufacturing approach using non-activated T cells will therefore require the development of alternative methods to evaluate the transduction process, such as quantitation of the reverse transcription intermediates.

There are inherent regulatory challenges to conforming to the current Food and Drug Administration guidelines, which were largely developed for small-molecule drugs and simpler biologics like protein therapeutics to highly complex, living therapeutics such as CAR-modified T cells. In the case of the rapid manufacturing process described here, one of the most important challenges is that the ‘manufacturing’ process is to some extent still ongoing at the time of the CAR T-cell harvest. Limiting the ex vivo transduction process

to 24 h means that a number of vector particles will still be undergoing reverse transcription and integration post infusion as these processes are significantly slower in non-activated T cells. As we have shown, quantitative measures of the active reverse transcription and integration process, such as the *Alu* repeat-based qPCR, may be the most direct methods for assessing the quality of the transduction process in lieu of directly measuring CAR protein expression, as traditionally done with activated CAR T-cell products; however, this needs to be rigorously evaluated in future studies.

In summary, the ability to generate highly functional CAR T cells within a day has important implications for improving CAR T-cell therapies. Lentiviral vectors provide a highly efficient method to produce CAR T-cell products with durable engraftment and function by leveraging the unique ability of these vectors to enter and integrate into the genome of non-dividing cells. Extended ex vivo culture of T cells is unnecessary to produce CAR T cells for therapeutic purposes. Minimizing ex vivo manipulation, in addition to reducing costs, conserves limited resources, such as human serum and manufacturing space, as T-cell clonal expansion occurs entirely in vivo. If the process can be reduced to a few simple steps, it also has the potential to decentralize CAR T-cell manufacturing to local hospital laboratories. This will avoid many of the logistical challenges. The generation of engineered T-cell products within a shorter interval between apheresis collection and the re-infusion of CAR T cells could also be of particular benefit to patients with rapidly progressive disease, who may otherwise be unable to receive the therapy<sup>61</sup>.

## Methods

**Generation of lentiviral vectors.** Replication-defective lentivirus was produced by standard methods using a third-generation lentiviral vector transfer plasmid encoding iRFP, an anti-CD19-BB $\zeta$  CAR<sup>33</sup> or anti-CD33-BB $\zeta$  CAR<sup>38</sup> mixed with three packaging plasmids encoding VSV-G (pMDG.1), gag/pol (pMDLg/pRRE) and rev (pRSV-rev), and transfected into HEK293T cells using Lipofectamine 2000 (Invitrogen).

**Cells.** Peripheral blood leukocytes from healthy donors were obtained from the Human Immunology Core of the University of Pennsylvania. Informed consent was obtained from all participants before collection. All methods and experimental procedures were approved by the University of Pennsylvania Institutional Review Board. Healthy donor T cells were purified at the Human Immunology Core by negative selection using a RosetteSep T cell enrichment cocktail (Stem Cell Technologies). Patient-derived T cells were isolated by positive selection using CD4- and CD8-specific microbeads (Miltenyi Biotec) according to the manufacturer's protocols.

All cell lines (Nalm6, MOLM14 and HEK293T) were originally obtained from the American Type Culture Collection. Cells were expanded in RPMI medium containing 10% fetal bovine serum, penicillin and streptomycin at a low passage and tested for mycoplasma contamination. The culture medium was adjusted to pH 7.4. Cell-line authentication was performed by the University of Arizona Genetics Core based on criteria established by the International Cell Line Authentication Committee. Short-tandem-repeat profiling revealed that these cell lines were above the 80% match threshold. All cells were cultured in standard conditions using a humidified incubator with set-points at 5% CO<sub>2</sub>, 20% O<sub>2</sub> and 37 °C.

**Transduction of T cells.** For activated T cells, T cells were resuspended ( $1 \times 10^6$  cells per ml) in X-VIVO 15 medium (Cambrex) supplemented with 5% human AB serum (Valley Biomedical), 2 mM L-glutamine (Cambrex), 20 mM HEPES (Cambrex), and IL-7 and IL-15 (10 ng ml<sup>-1</sup> each, Miltenyi Biotec). Dynabeads human T-activator CD3/CD28 beads (Thermo Fisher) were added to a final ratio of three beads to one cell. After 24 h, lentiviral vector supernatant was added at the indicated MOI. The cells were maintained in culture at a concentration of  $0.5 \times 10^6$  cells per ml by adjusting the concentration every other day based on counting by flow cytometry using CountBright beads (BD Bioscience) and monoclonal antibodies to human CD4 and CD8 (ref. 62). The cell volume was also measured using a Multisizer III particle counter (Beckman-Coulter) every other day. For non-activated T cells, T cells were resuspended ( $1 \times 10^6$  cells per ml) in RPMI medium containing penicillin and streptomycin as well as 20 mM HEPES for 3–6 h. The T cells were then resuspended ( $1 \times 10^7$  cells per ml) in X-VIVO 15 medium supplemented with 5% human AB serum, 2 mM L-glutamine, 20 mM HEPES, IL-7 and IL-15 (10 ng ml<sup>-1</sup> each), and lentiviral vector supernatant to achieve the desired MOI, as indicated. Integrase (Raltegravir, 1  $\mu$ M) and RT (Saquinavir, 1  $\mu$ M; Cayman Chemical) inhibitors, and dNPs (50  $\mu$ M; Sigma) were also added to the medium in some experiments, as indicated.

**Flow cytometry.** T-cell differentiation was assessed using the following antibodies: anti-CCR7-FITC clone 150503 (BD Pharmingen); anti-CD45RO-PE clone UCHL1 and anti-CD8-H7APC clone SK1 (BD Biosciences); and anti-CD4-BV510 clone OKT4, anti-CD3-BV605 clone OKT3, anti-CD14-Pacific Blue clone HCD14 and anti-CD19-Pacific Blue clone H1B19 (BioLegend). The anti-CAR19 idiotype for surface expression of CAR19 was provided by Novartis. Cells were washed with PBS, incubated with LIVE/DEAD fixable violet (Molecular Probes) for 15 min and resuspended in fluorescence activated cell sorting buffer consisting of PBS, 1% BSA and 5 mM EDTA. The cells were then incubated with antibodies for 1 h at 4°C. Positively stained cells were differentiated from the background using fluorescence-minus-one controls. A representative gating strategy to identify T-cell subsets is shown in Supplementary Fig. 5. Flow cytometry was performed on a BD LSR Fortessa system. Analysis was performed using the FlowJo software (Tree Star Inc. version 10.1).

**qPCR analysis.** Genomic DNA was isolated using a QIAamp DNA micro kit (Qiagen). Using 200 ng genomic DNA, qPCR analysis was performed to detect the integrated BB $\zeta$  CAR transgene sequence using ABI Taqman technology as previously described<sup>6,33</sup>. To determine the number of transgene copies in the genomic DNA (copies per  $\mu$ g DNA), an eight-point standard curve was generated consisting of  $5 \times 10^6$ – $1 \times 10^6$  copies of the BB $\zeta$  lentivirus plasmid spiked into 100 ng non-transduced control genomic DNA. A primer–probe set specific for the *CDKN1A* gene, a single-copy gene in the human haploid genome, was used as a normalization control to estimate the number of vector copies per cell. The levels of total and integrated DNA were measured by PCR as previously described<sup>6,34</sup>. Briefly, for total lentiviral levels, primers against the LTR (LTR F, 5'-TTAAGCCTCAATAAAGCTTGCC-3' and LTR R, 5'-GTTCCGGCGCCACTGCTAGA-3') were used. Integrated DNA was measured using primers against the human *Alu* element (Alu F, 5'-GCTCCCAAGTGCTGGGATTACAG-3') and the lentiviral *gag* gene (gag R, 5'-GCTCTCGCACCCATCTCTCC-3'). Notably, a small amount of *gag* was retained in the lentiviral vector. For both reactions, a nested approach was utilized. For the LTR PCR, the PCR conditions for the first round were: 95°C for 2 min; followed by 12 cycles of 95°C for 15 s, 64°C for 45 s and 72°C for 1 min; and then 72°C for 10 min. For the *Alu*-*gag* PCR, the following PCR conditions were used: 95°C for 2 min; followed by 40 cycles of 95°C for 15 s, 56°C for 45 s and 72°C for 3.5 min; and then 72°C for 10 min. Aliquots of the first-round PCR reactions (15  $\mu$ l) were run on the qPCR instrument using the LTR F and LTR R primers and the probe 5'-CCAGAGTACACAACAGACGGGCACA-3'. The PCR conditions were: 95°C for 15 s; followed by 40 cycles of 95°C for 10 s and 60°C for 20 s. For the *Alu*-*gag* PCR, genomic DNA was diluted to target 30–80% positive wells at two dilutions to minimize variance. The percentage of positive wells was used to estimate the lentiviral levels using a binomial distribution.

**Sequencing sites of vector integration.** The integration-site sequences were acquired using ligation-mediated PCR as described<sup>40–42</sup>. Bioinformatic analysis of the distribution of the integration sites, described in Supplementary Report, was carried out as previously described<sup>40–42</sup>. All primer and adaptor sequences were as previously described<sup>41</sup>.

**Cytokine secretion.** T cells were incubated with irradiated target cells at a ratio of 1:1 ( $1 \times 10^6$  cells per ml each) in cytokine-free medium. Supernatants were collected after 24 h to assess the cytokine production. The cytokine measurements were performed using a Luminex bead array platform (Life Technologies) according to the manufacturer's instructions<sup>39</sup>.

**Cytotoxicity assays.** Cytotoxicity assays were performed using a <sup>51</sup>Cr release-assay as previously described<sup>7</sup>. Briefly, Na<sub>2</sub><sup>51</sup>CrO<sub>4</sub>-labelled target cells were incubated with CAR T cells for 20 h at various effector:target ratios and placed into 96-well Lumaplates (PerkinElmer). The amount of <sup>51</sup>Cr released from the labelled target cells was measured on a liquid scintillation counter (MicroBeta trilux, PerkinElmer). Target cells incubated in medium alone or with 1% SDS were used to determine the spontaneous or maximum <sup>51</sup>Cr release. The percentage of specific lysis was calculated as follows:  $100 \times (\text{experimental release c.p.m.} - \text{spontaneous release c.p.m.}) / (\text{maximum release c.p.m.} - \text{spontaneous release c.p.m.})$ .

**In vivo models.** Xenograft models of leukaemia were used as previously reported<sup>43,65</sup>. Briefly, 6–10-week-old NOD-SCID  $\gamma$ c<sup>-/-</sup> (NSG) mice, which lack an adaptive immune system, were obtained from Jackson Laboratories or bred in-house under a protocol approved by the Institutional Animal Care and Use Committees (IACUC) of the University of Pennsylvania. In all experiments, the animals were assigned to treatment/control groups using a randomized approach. The animals were injected via the tail vein with  $2 \times 10^6$  Nalm6 or  $1 \times 10^6$  MOLM14 cells expressing click beetle green luciferase and enhanced green fluorescent protein (eGFP) in 0.1 ml sterile PBS. CAR T cells or NTD human T cells were injected via the tail vein at the indicated dose in a volume of 100  $\mu$ l 4 d after the injection with leukaemic cells. Given the inherent limitations of comparing cells that were frozen before adoptive transfer (d1) and directly infused cells (d9), the d1 and d9 cells were manufactured from different donors. The mice were given an intraperitoneal injection of 150 mg kg<sup>-1</sup> D-luciferin (Caliper Life Sciences).

Anaesthetized mice were imaged using a Xenogen IVIS Spectrum system (Caliper Life Science). The total flux was quantified using Living Image 4.4 (PerkinElmer). T-cell engraftment was defined as >1% human CD45<sup>+</sup> cells in peripheral blood by flow cytometry. The animals were euthanized at the end of the experiment or when they met pre-specified end points according to the protocols, except for the AML model experiment, which was terminated due to a Coronavirus Disease 2019-related shutdown of research.

**Reporting Summary.** Further information on research design is available in the Nature Research Reporting Summary linked to this article.

## Data availability

The main data supporting the findings of this study are available within the article and its Supplementary Information. All raw data generated during the study are available from the corresponding authors on reasonable request. Source data are provided with this paper.

Received: 10 April 2021; Accepted: 17 December 2021;

Published online: 21 February 2022

## References

- Salter, A. I., Pont, M. J. & Riddell, S. R. Chimeric antigen receptor-modified T cells: CD19 and the road beyond. *Blood* **131**, 2621–2629 (2018).
- Bruđno, J. N. et al. T cells genetically modified to express an anti-B-cell maturation antigen chimeric antigen receptor cause remissions of poor-prognosis relapsed multiple myeloma. *J. Clin. Oncol.* **36**, 2267–2280 (2018).
- Cohen, A. D. et al. B cell maturation antigen-specific CAR T cells are clinically active in multiple myeloma. *J. Clin. Invest.* **129**, 2210–2221 (2019).
- D'Angelo, S. P. et al. Antitumor activity associated with prolonged persistence of adoptively transferred NY-ESO-1 (c259)T cells in synovial sarcoma. *Cancer Discov.* **8**, 944–957 (2018).
- Raje, N. et al. Anti-BCMA CAR T-cell therapy bb2121 in relapsed or refractory multiple myeloma. *N. Engl. J. Med.* **380**, 1726–1737 (2019).
- Kalos, M. et al. T cells with chimeric antigen receptors have potent antitumor effects and can establish memory in patients with advanced leukemia. *Sci. Transl. Med.* **3**, 95ra73 (2011).
- Ghassemi, S. et al. Reducing ex vivo culture improves the antileukemic activity of chimeric antigen receptor (CAR) T cells. *Cancer Immunol. Res.* **6**, 1100–1109 (2018).
- Berger, C. et al. Adoptive transfer of effector CD8<sup>+</sup> T cells derived from central memory cells establishes persistent T cell memory in primates. *J. Clin. Invest.* **118**, 294–305 (2008).
- Graef, P. et al. Serial transfer of single-cell-derived immunocompetence reveals stemness of CD8<sup>+</sup> central memory T cells. *Immunity* **41**, 116–126 (2014).
- Hinrichs, C. S. et al. Adoptively transferred effector cells derived from naive rather than central memory CD8<sup>+</sup> T cells mediate superior antitumor immunity. *Proc. Natl Acad. Sci. USA* **106**, 17469–17474 (2009).
- Hinrichs, C. S. et al. Human effector CD8<sup>+</sup> T cells derived from naive rather than memory subsets possess superior traits for adoptive immunotherapy. *Blood* **117**, 808–814 (2011).
- Klebanoff, C. A. et al. Memory T cell-driven differentiation of naive cells impairs adoptive immunotherapy. *J. Clin. Invest.* **126**, 318–334 (2016).
- Crompton, J. G. et al. Akt inhibition enhances expansion of potent tumor-specific lymphocytes with memory cell characteristics. *Cancer Res.* **75**, 296–305 (2015).
- van der Waart, A. B. et al. Inhibition of Akt signaling promotes the generation of superior tumor-reactive T cells for adoptive immunotherapy. *Blood* **124**, 3490–3500 (2014).
- Gattinoni, L. et al. Wnt signaling arrests effector T cell differentiation and generates CD8<sup>+</sup> memory stem cells. *Nat. Med.* **15**, 808–813 (2009).
- Gattinoni, L. et al. A human memory T cell subset with stem cell-like properties. *Nat. Med.* **17**, 1290–1297 (2011).
- Muralidharan, S. et al. Activation of Wnt signaling arrests effector differentiation in human peripheral and cord blood-derived T lymphocytes. *J. Immunol.* **187**, 5221–5232 (2011).
- Naldini, L. et al. In vivo gene delivery and stable transduction of nondividing cells by a lentiviral vector. *Science* **272**, 263–267 (1996).
- Plesa, G. et al. Addition of deoxynucleosides enhances human immunodeficiency virus type 1 integration and 2LTR formation in resting CD4<sup>+</sup> T cells. *J. Virol.* **81**, 13938–13942 (2007).
- Swiggard, W. J. et al. Human immunodeficiency virus type 1 can establish latent infection in resting CD4<sup>+</sup> T cells in the absence of activating stimuli. *J. Virol.* **79**, 14179–14188 (2005).
- Amirache, F. et al. Mystery solved: VSV-G-LVs do not allow efficient gene transfer into unstimulated T cells, B cells, and HSCs because they lack the LDL receptor. *Blood* **123**, 1422–1424 (2014).

22. Finkelshtein, D., Werman, A., Novick, D., Barak, S. & Rubinstein, M. LDL receptor and its family members serve as the cellular receptors for vesicular stomatitis virus. *Proc. Natl Acad. Sci. USA* **110**, 7306–7311 (2013).
23. Agosto, L. M. et al. The CXCR4-tropic human immunodeficiency virus envelope promotes more-efficient gene delivery to resting CD4<sup>+</sup> T cells than the vesicular stomatitis virus glycoprotein G envelope. *J. Virol.* **83**, 8153–8162 (2009).
24. Pace, M. J., Agosto, L. & O'Doherty, U. R5 HIV env and vesicular stomatitis virus G protein cooperate to mediate fusion to naive CD4<sup>+</sup> T cells. *J. Virol.* **85**, 644–648 (2011).
25. Unutmaz, D., KewalRamani, V. N., Marmon, S. & Littman, D. R. Cytokine signals are sufficient for HIV-1 infection of resting human T lymphocytes. *J. Exp. Med.* **189**, 1735–1746 (1999).
26. Cavallieri, S. et al. Human T lymphocytes transduced by lentiviral vectors in the absence of TCR activation maintain an intact immune competence. *Blood* **102**, 497–505 (2003).
27. Trinite, B., Chan, C. N., Lee, C. S. & Levy, D. N. HIV-1 Vpr- and reverse transcription-induced apoptosis in resting peripheral blood CD4 T cells and protection by common gamma-chain cytokines. *J. Virol.* **90**, 904–916 (2016).
28. Verhoeven, E. et al. IL-7 surface-engineered lentiviral vectors promote survival and efficient gene transfer in resting primary T lymphocytes. *Blood* **101**, 2167–2174 (2003).
29. Korin, Y. D. & Zack, J. A. Nonproductive human immunodeficiency virus type 1 infection in nucleoside-treated G0 lymphocytes. *J. Virol.* **73**, 6526–6532 (1999).
30. Rausell, A. et al. Innate immune defects in HIV permissive cell lines. *Retrovirology* **13**, 43 (2016).
31. Descours, B. et al. SAMHD1 restricts HIV-1 reverse transcription in quiescent CD4<sup>+</sup> T-cells. *Retrovirology* **9**, 87 (2012).
32. Pierson, T. C. et al. Molecular characterization of preintegration latency in human immunodeficiency virus type 1 infection. *J. Virol.* **76**, 8518–8531 (2002).
33. Milone, M. C. et al. Chimeric receptors containing CD137 signal transduction domains mediate enhanced survival of T cells and increased antileukemic efficacy in vivo. *Mol. Ther.* **17**, 1453–1464 (2009).
34. Burnie, J. & Guzzo, C. The incorporation of host proteins into the external HIV-1 envelope. *Viruses* **11**, 85 (2019).
35. Eyquem, J. et al. Targeting a CAR to the TRAC locus with CRISPR/Cas9 enhances tumour rejection. *Nature* **543**, 113–117 (2017).
36. Wilen, C. B., Tilton, J. C. & Doms, R. W. HIV: cell binding and entry. *Cold Spring Harb. Perspect. Med.* **2**, a006866 (2012).
37. Brown, M. S. & Goldstein, J. L. A receptor-mediated pathway for cholesterol homeostasis. *Science* **232**, 34–47 (1986).
38. Tran, R. et al. Microfluidic transduction harnesses mass transport principles to enhance gene transfer efficiency. *Mol. Ther.* **25**, 2372–2382 (2017).
39. Maude, S. L. et al. Chimeric antigen receptor T cells for sustained remissions in leukemia. *N. Engl. J. Med.* **371**, 1507–1517 (2014).
40. Berry, C. C. et al. INSPIRED: quantification and visualization tools for analyzing integration site distributions. *Mol. Ther. Methods Clin. Dev.* **4**, 17–26 (2017).
41. Sherman, E. et al. INSPIRED: a pipeline for quantitative analysis of sites of new DNA integration in cellular genomes. *Mol. Ther. Methods Clin. Dev.* **4**, 39–49 (2017).
42. Berry, C. C. et al. Estimating abundances of retroviral insertion sites from DNA fragment length data. *Bioinformatics* **28**, 755–762 (2012).
43. Nobles, C. L. et al. CD19-targeting CAR T cell immunotherapy outcomes correlate with genomic modification by vector integration. *J. Clin. Invest.* **130**, 673–685 (2019).
44. Schroder, A. R. et al. HIV-1 integration in the human genome favors active genes and local hotspots. *Cell* **110**, 521–529 (2002).
45. Mitchell, R. S. et al. Retroviral DNA integration: ASLV, HIV, and MLV show distinct target site preferences. *PLoS Biol.* **2**, E234 (2004).
46. Wang, G. P., Ciuffi, A., Leipzig, J., Berry, C. C. & Bushman, F. D. HIV integration site selection: analysis by massively parallel pyrosequencing reveals association with epigenetic modifications. *Genome Res.* **17**, 1186–1194 (2007).
47. Brady, T. et al. HIV integration site distributions in resting and activated CD4<sup>+</sup> T cells infected in culture. *AIDS* **23**, 1461–1471 (2009).
48. Haining, W. N. et al. Antigen-specific T-cell memory is preserved in children treated for acute lymphoblastic leukemia. *Blood* **106**, 1749–1754 (2005).
49. Halliwell, B. Cell culture, oxidative stress, and antioxidants: avoiding pitfalls. *Biomed. J.* **37**, 99–105 (2014).
50. Zhang, H. et al. 4-1BB is superior to CD28 costimulation for generating CD8<sup>+</sup> cytotoxic lymphocytes for adoptive immunotherapy. *J. Immunol.* **179**, 4910–4918 (2007).
51. Klebanoff, C. A. et al. Determinants of successful CD8<sup>+</sup> T-cell adoptive immunotherapy for large established tumors in mice. *Clin. Cancer Res.* **17**, 5343–5352 (2011).
52. Klebanoff, C. A. et al. Inhibition of AKT signaling uncouples T cell differentiation from expansion for receptor-engineered adoptive immunotherapy. *JCI Insight* **2**, e95103 (2017).
53. O'Doherty, U., Swiggard, W. J. & Malim, M. H. Human immunodeficiency virus type 1 spinoculation enhances infection through virus binding. *J. Virol.* **74**, 10074–10080 (2000).
54. Baldauf, H. M. et al. SAMHD1 restricts HIV-1 infection in resting CD4<sup>+</sup> T cells. *Nat. Med.* **18**, 1682–1687 (2012).
55. Mauney, C. H., Perrino, F. W. & Hollis, T. Identification of inhibitors of the dNTP triphosphohydrolase SAMHD1 using a novel and direct high-throughput assay. *Biochemistry* **57**, 6624–6636 (2018).
56. Trobridge, G. D. et al. Cocal-pseudotyped lentiviral vectors resist inactivation by human serum and efficiently transduce primate hematopoietic repopulating cells. *Mol. Ther.* **18**, 725–733 (2010).
57. Klebanoff, C. A. et al. Central memory self/tumor-reactive CD8<sup>+</sup> T cells confer superior antitumor immunity compared with effector memory T cells. *Proc. Natl Acad. Sci. USA* **102**, 9571–9576 (2005).
58. Pollok, K. E., Kim, S. H. & Kwon, B. S. Regulation of 4-1BB expression by cell–cell interactions and the cytokines, interleukin-2 and interleukin-4. *Eur. J. Immunol.* **25**, 488–494 (1995).
59. Lelek, M. et al. Chromatin organization at the nuclear pore favours HIV replication. *Nat. Commun.* **6**, 6483 (2015).
60. Wong, R. W., Mamede, J. I. & Hope, T. J. Impact of nucleoporin-mediated chromatin localization and nuclear architecture on HIV integration site selection. *J. Virol.* **89**, 9702–9705 (2015).
61. Couzin-Frankel, J. Supply of promising T cell therapy is strained. *Science* **356**, 1112–1113 (2017).
62. O'Connor, R. S. et al. Substrate rigidity regulates human T cell activation and proliferation. *J. Immunol.* **189**, 1330–1339 (2012).
63. De Spiegelaere, W. et al. Quantification of integrated HIV DNA by repetitive-sampling *Alu*-HIV PCR on the basis of poisson statistics. *Clin. Chem.* **60**, 886–895 (2014).
64. Liszewski, M. K., Yu, J. J. & O'Doherty, U. Detecting HIV-1 integration by repetitive-sampling *Alu*-gag PCR. *Methods* **47**, 254–260 (2009).
65. Kenderian, S. S. et al. CD33-specific chimeric antigen receptor T cells exhibit potent preclinical activity against human acute myeloid leukemia. *Leukemia* **29**, 1637–1647 (2015).

## Acknowledgements

We thank the University of Pennsylvania Cell and Vaccine Production Facility for technical support as well as the University of Pennsylvania Stem Cell and Xenograft Core and University of Pennsylvania Flow Cytometry Core and Human Immunology Core, which is supported by NIH grants nos AI045008 and CA016520, for providing de-identified human T cells. We thank J. K. Everett and A. M. Roche for their technical expertise. This work was supported in part through funding provided by Novartis Pharmaceuticals through a research alliance with the University of Pennsylvania (M.C.M.) as well as a St. Baldrick's Foundation Scholar Award (S.G.), a National Blood Foundation Scientific Research Grant Award (S.G.), the Office of the Assistant Secretary of Defense for Health Affairs through the Peer Reviewed Cancer Research Program under award nos W81XWH-20-1-0417 (S.G.) and RO1CA226983 (R.S.O'C.).

## Author contributions

S.G. and M.C.M. designed the study. S.G., M.C.M., J.S.D., R.S.O'C., U.O'D., F.D.B. and S.I.G. provided conceptual guidance. S.G., J.S.D., R.S.O'C., S.N.-C., J.P., K.D.C., E.S., M.P., G.P., V.A.C., S.R. and J.L. performed the experiments. S.G. and M.C.M. analysed the data. S.G. and M.C.M. wrote the manuscript. R.S.O'C. and J.S.D. read and made comments on the manuscript.

## Competing interests

M.C.M. is an inventor on patent applications related to CAR technology (US patents 9,481,728 and 9,499,629 B2) and has received licencing royalties from the Novartis corporation. S.G. and M.C.M. are inventors on a patent application related to methods of manufacturing non-activated CAR T cells (provisional patent PCT/US2020/027734). The other authors declare no competing interests.

## Additional information

**Extended data** is available for this paper at <https://doi.org/10.1038/s41551-021-00842-6>.

**Supplementary information** The online version contains supplementary material available at <https://doi.org/10.1038/s41551-021-00842-6>.

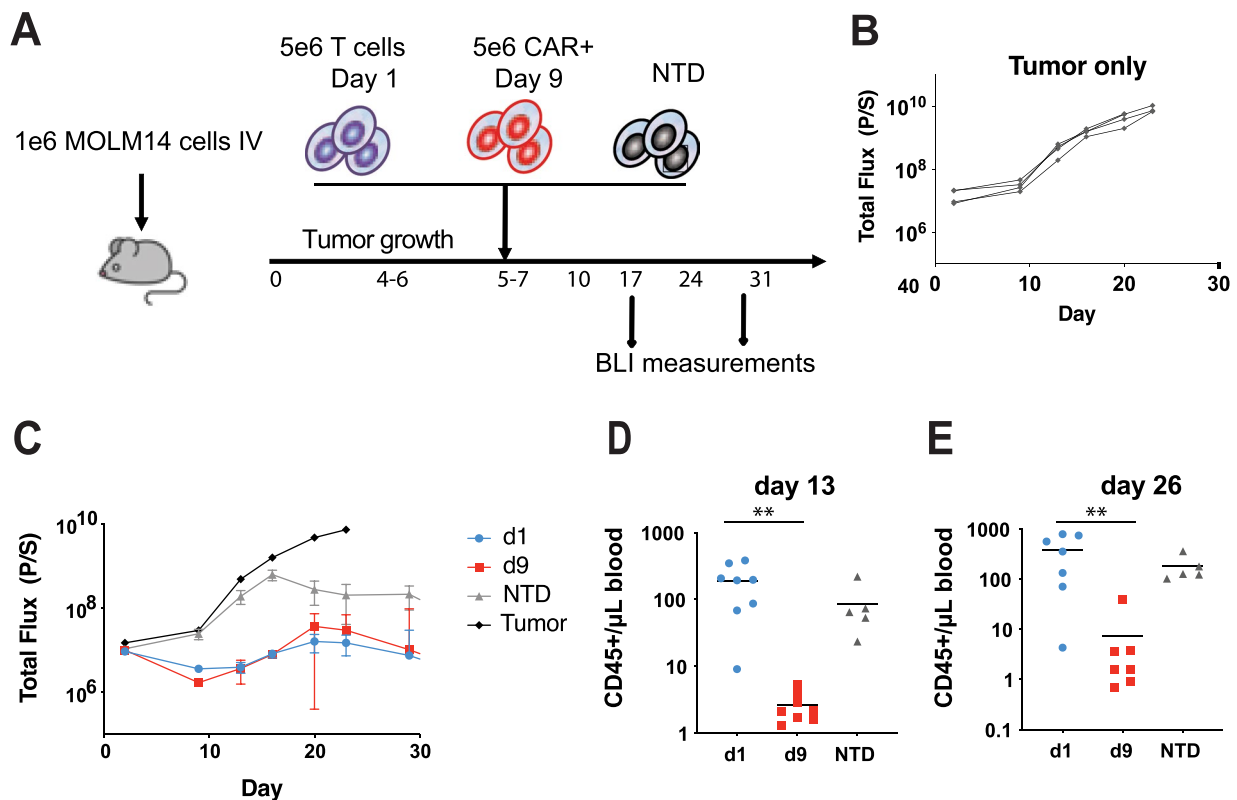
**Correspondence and requests for materials** should be addressed to Saba Ghassemi or Michael C. Milone.

**Peer review information** *Nature Biomedical Engineering* thanks Bryon Johnson and the other, anonymous, reviewer(s) for their contribution to the peer review of this work.

**Reprints and permissions information** is available at [www.nature.com/reprints](http://www.nature.com/reprints).

**Publisher's note** Springer Nature remains neutral with regard to jurisdictional claims in published maps and institutional affiliations.

© The Author(s), under exclusive licence to Springer Nature Limited 2022



**Extended Data Fig. 1 | Non-activated T cells expressing a CD33-specific CAR exhibit an antileukemic effect in vivo in the Aml xenograft model.**

**a**, Schematic of the xenograft model and CART33 cell treatment in NSG mice. **b, c**, Serial quantification of disease burden by bioluminescence imaging. **b**, Total bioluminescence flux in mice with no treatment. **c**, Total bioluminescence flux in mice treated with  $5 \times 10^6$  non-activated T cells transduced as in panel **(a)** (d1),  $5 \times 10^6$  CAR+ T cells stimulated with anti- CD3/CD28 microbeads and expanded over 9 days (d9), and  $5 \times 10^6$  non-transduced (NTD) control non-activated T cells ( $n=10$  per group). **d, e**, Absolute peripheral blood CD45<sup>+</sup> T cell counts in blood collected from mice shown in panels **(c)** at **d**, 13 days ( $P=0.0065$ ), and **e**, 26 days ( $P=0.0012$ ) following T cell transfer measured by a TruCount assay. The mean of each group is indicated by the solid black line. Groups were compared using the two-tailed, unpaired Mann-Whitney test.

## Reporting Summary

Nature Portfolio wishes to improve the reproducibility of the work that we publish. This form provides structure for consistency and transparency in reporting. For further information on Nature Portfolio policies, see our [Editorial Policies](#) and the [Editorial Policy Checklist](#).

### Statistics

For all statistical analyses, confirm that the following items are present in the figure legend, table legend, main text, or Methods section.

n/a Confirmed

- |                                     |                                     |  |
|-------------------------------------|-------------------------------------|--|
| <input type="checkbox"/>            | <input checked="" type="checkbox"/> | The exact sample size ( $n$ ) for each experimental group/condition, given as a discrete number and unit of measurement  |
| <input type="checkbox"/>            | <input checked="" type="checkbox"/> | A statement on whether measurements were taken from distinct samples or whether the same sample was measured repeatedly  |
| <input type="checkbox"/>            | <input checked="" type="checkbox"/> | The statistical test(s) used AND whether they are one- or two-sided<br><i>Only common tests should be described solely by name; describe more complex techniques in the Methods section.</i>   |
| <input checked="" type="checkbox"/> | <input type="checkbox"/>            | A description of all covariates tested   |
| <input checked="" type="checkbox"/> | <input type="checkbox"/>            | A description of any assumptions or corrections, such as tests of normality and adjustment for multiple comparisons  |
| <input type="checkbox"/>            | <input checked="" type="checkbox"/> | A full description of the statistical parameters including central tendency (e.g. means) or other basic estimates (e.g. regression coefficient) AND variation (e.g. standard deviation) or associated estimates of uncertainty (e.g. confidence intervals) |
| <input type="checkbox"/>            | <input checked="" type="checkbox"/> | For null hypothesis testing, the test statistic (e.g. $F$ , $t$ , $r$ ) with confidence intervals, effect sizes, degrees of freedom and $P$ value noted<br><i>Give <math>P</math> values as exact values whenever suitable.</i>                            |
| <input checked="" type="checkbox"/> | <input type="checkbox"/>            | For Bayesian analysis, information on the choice of priors and Markov chain Monte Carlo settings   |
| <input checked="" type="checkbox"/> | <input type="checkbox"/>            | For hierarchical and complex designs, identification of the appropriate level for tests and full reporting of outcomes   |
| <input checked="" type="checkbox"/> | <input type="checkbox"/>            | Estimates of effect sizes (e.g. Cohen's $d$ , Pearson's $r$ ), indicating how they were calculated   |

*Our web collection on [statistics for biologists](#) contains articles on many of the points above.*

### Software and code

Policy information about [availability of computer code](#)

Data collection Flow-cytometry data were collected on BD LSR Fortessa. Cytokine measurements were performed with a Luminex bead array platform (Life Technologies). Mice were imaged using a Xenogen IVIS Spectrum system (Caliper Life Science).

Data analysis Flow-cytometry analysis was performed using Flowjo software (Tree Star Inc. version 10.1). Total bioluminescence flux in mice was quantified using Living Image 4.4 (PerkinElmer). The amount of  $^{51}\text{Cr}$  released from the labelled target cells was measured on a liquid scintillation counter (MicroBeta trilux, Perkin Elmer).

For manuscripts utilizing custom algorithms or software that are central to the research but not yet described in published literature, software must be made available to editors and reviewers. We strongly encourage code deposition in a community repository (e.g. GitHub). See the Nature Portfolio [guidelines for submitting code & software](#) for further information.

### Data

Policy information about [availability of data](#)

All manuscripts must include a [data availability statement](#). This statement should provide the following information, where applicable:

- Accession codes, unique identifiers, or web links for publicly available datasets
- A description of any restrictions on data availability
- For clinical datasets or third party data, please ensure that the statement adheres to our [policy](#)

The main data supporting the findings of this study are available within the Article and its Supplementary Information. Source data for the tumour-growth experiments are provided with this paper. All raw data generated during the study are available from the corresponding authors on reasonable request.

## Field-specific reporting

Please select the one below that is the best fit for your research. If you are not sure, read the appropriate sections before making your selection.

Life sciences  Behavioural & social sciences  Ecological, evolutionary & environmental sciences

For a reference copy of the document with all sections, see [nature.com/documents/nr-reporting-summary-flat.pdf](https://www.nature.com/documents/nr-reporting-summary-flat.pdf)

## Life sciences study design

All studies must disclose on these points even when the disclosure is negative.

Sample size	We selected sample sizes to make the statistical power greater than 0.8.
Data exclusions	No data were excluded from the experiments.
Replication	All experimental findings were reliably reproduced. Data from each figure have been repeated in independent experiments using different donors.
Randomization	Animals were assigned in all experiments to the treatment and control groups using a randomized approach.
Blinding	The investigators were not blinded. Blinding is unnecessary for the type of assays used, as a uniform gating strategy was used for all samples.

## Reporting for specific materials, systems and methods

We require information from authors about some types of materials, experimental systems and methods used in many studies. Here, indicate whether each material, system or method listed is relevant to your study. If you are not sure if a list item applies to your research, read the appropriate section before selecting a response.

### Materials & experimental systems

n/a	Involved in the study
<input type="checkbox"/>	<input checked="" type="checkbox"/> Antibodies
<input type="checkbox"/>	<input checked="" type="checkbox"/> Eukaryotic cell lines
<input checked="" type="checkbox"/>	<input type="checkbox"/> Palaeontology and archaeology
<input type="checkbox"/>	<input checked="" type="checkbox"/> Animals and other organisms
<input checked="" type="checkbox"/>	<input type="checkbox"/> Human research participants
<input checked="" type="checkbox"/>	<input type="checkbox"/> Clinical data
<input checked="" type="checkbox"/>	<input type="checkbox"/> Dual use research of concern

### Methods

n/a	Involved in the study
<input checked="" type="checkbox"/>	<input type="checkbox"/> ChIP-seq
<input type="checkbox"/>	<input checked="" type="checkbox"/> Flow cytometry
<input checked="" type="checkbox"/>	<input type="checkbox"/> MRI-based neuroimaging

## Antibodies

Antibodies used	anti-CCR7-FITC clone 150503, Cat. No. 561271 (BD Pharmingen); anti-CD45RO-PE clone UCHL1, Cat. No. 304206, anti-CD8-H7APC clone SK1, Cat. No. 560179 (BD Biosciences); anti-CD4-BV510 clone OKT4, Cat. No. 317444, anti-CD3-BV605 clone OKT3, Cat. No. 317322, anti-CD14-Pacific Blue (PB) clone HCD14, Cat. No. 325616, anti-CD19-PB clone H1B19, Cat. No. 302232 (BioLegend). The anti-CAR19 idiotype for surface expression of CAR19 was provided by Novartis (Basel, Switzerland).
Validation	Validation of each antibody was done under standard information offered by the supplier.

## Eukaryotic cell lines

Policy information about [cell lines](#)

Cell line source(s)	All cell lines (NALM-6, MOLM14 and HEK293T) were originally obtained from the American Type Culture Collection (ATCC).
Authentication	Cell-line authentication was performed by the University of Arizona Genetics Core, based on criteria established by the International Cell Line Authentication Committee. Short-tandem-repeat profiling revealed that these cell lines were above the 80% match threshold.
Mycoplasma contamination	Cells were tested for mycoplasma using the MycoAlert detection Kit according to the manufacturer's instructions (Lonza).
Commonly misidentified lines (See <a href="#">ICLAC</a> register)	No commonly misidentified cell lines were used.

## Animals and other organisms

Policy information about [studies involving animals](#); [ARRIVE guidelines](#) recommended for reporting animal research

Laboratory animals	Male and female 6-to-10-week-old NOD-SCID $\gamma c^{-/-}$ (NSG) mice, which lack an adaptive immune system, were obtained from Jackson Laboratories.
Wild animals	The study did not involve wild animals.
Field-collected samples	The study did not involve samples collected from the field.
Ethics oversight	All experimental protocols were approved by the Institutional Animal Care and Use Committees (IACUC) of the University of Pennsylvania.

Note that full information on the approval of the study protocol must also be provided in the manuscript.

## Flow Cytometry

### Plots

Confirm that:

- The axis labels state the marker and fluorochrome used (e.g. CD4-FITC).
- The axis scales are clearly visible. Include numbers along axes only for bottom left plot of group (a 'group' is an analysis of identical markers).
- All plots are contour plots with outliers or pseudocolor plots.
- A numerical value for number of cells or percentage (with statistics) is provided.

### Methodology

Sample preparation	Cells were washed with phosphate-buffered saline (PBS), incubated with LIVE/DEAD Fixable Violet (Molecular Probes) for 15 minutes, and resuspended in fluorescence activated cell sorting (FACS) buffer consisting of PBS, 1% BSA, and 5 mM EDTA. Cells were then incubated with antibodies for 1 hour at 4°C.
Instrument	Flow cytometry was performed on BD LSR Fortessa.
Software	Analysis was performed using Flowjo software (Tree Star Inc. version 10.1).
Cell population abundance	The purity of samples after sorting was confirmed by flow cytometry.
Gating strategy	Positively stained cells were differentiated from background using fluorescence-minus-one (FMO) controls.

Tick this box to confirm that a figure exemplifying the gating strategy is provided in the Supplementary Information.



# Genetic Modification of Cytokine Signaling to Enhance Efficacy of CAR T Cell Therapy in Solid Tumors

Navid Ghahri-Saremi<sup>1</sup>, Behnia Akbari<sup>1</sup>, Tahereh Soltantoyeh<sup>1</sup>, Jamshid Hadjati<sup>1</sup>, Saba Ghassemi<sup>2\*</sup> and Hamid Reza Mirzaei<sup>1\*</sup>

<sup>1</sup> Department of Medical Immunology, School of Medicine, Tehran University of Medical Sciences, Tehran, Iran, <sup>2</sup> Center for Cellular Immunotherapies, Perelman School of Medicine, University of Pennsylvania, Philadelphia, PA, United States

## OPEN ACCESS

### Edited by:

Michal Amit Rahat,  
Technion-Israel Institute of  
Technology, Israel

### Reviewed by:

Saad Kenderian,  
Mayo Clinic, United States  
Jason Lohmueller,  
University of Pittsburgh Cancer  
Institute, United States

### \*Correspondence:

Hamid Reza Mirzaei  
h-mirzaei@tums.ac.ir  
Saba Ghassemi  
ghassemi@penmedicine.upenn.edu

### Specialty section:

This article was submitted to  
Cancer Immunity  
and Immunotherapy,  
a section of the journal  
Frontiers in Immunology

**Received:** 08 July 2021

**Accepted:** 28 September 2021

**Published:** 14 October 2021

### Citation:

Ghahri-Saremi N, Akbari B,  
Soltantoyeh T, Hadjati J, Ghassemi S  
and Mirzaei HR (2021) Genetic  
Modification of Cytokine Signaling to  
Enhance Efficacy of CAR T Cell  
Therapy in Solid Tumors.  
*Front. Immunol.* 12:738456.  
doi: 10.3389/fimmu.2021.738456

Chimeric antigen receptor (CAR) T cell therapy has shown unprecedented success in treating advanced hematological malignancies. Its effectiveness in solid tumors has been limited due to heterogeneous antigen expression, a suppressive tumor microenvironment, suboptimal trafficking to the tumor site and poor CAR T cell persistence. Several approaches have been developed to overcome these obstacles through various strategies including the genetic engineering of CAR T cells to blunt the signaling of immune inhibitory receptors as well as to modulate signaling of cytokine/chemokine molecules and their receptors. In this review we offer our perspective on how genetically modifying cytokine/chemokine molecules and their receptors can improve CAR T cell qualities such as functionality, persistence (e.g. resistance to pro-apoptotic signals) and infiltration into tumor sites. Understanding how such modifications can overcome barriers to CAR T cell effectiveness will undoubtedly enhance the potential of CAR T cells against solid tumors.

**Keywords:** cytokines, chemokines, genetic modification, CAR T cell, immunotherapy, solid tumors

## INTRODUCTION

Surgery, chemotherapy and radiation therapy have been the principal cornerstones of cancer treatment since the middle of the last century. The development of novel molecular targeted therapies and immunotherapies such as immune checkpoint inhibitors and CAR T cells, among others, have led to a paradigm shift in the treatment of cancer patients (1, 2). Exciting progress with CD19-CAR T cells for the treatment of certain pediatric and young adult patients with B cell acute lymphoblastic leukemia has led to the successful approval by the US Food and Drug Administration (FDA) in August 2017 (3, 4). Despite the advancement in the treatment of blood cancers with CAR T cells, treating solid tumors has been challenging in part due to heterogeneous tumor antigen expression, the presence of immunosuppressive and hostile tumor microenvironment (TME) that exacerbates CAR T cell exhaustion and apoptosis, and insufficient infiltration into the tumor sites (5–7).

It is well-recognized that cytokines, chemokines and their receptors play pivotal roles in regulating the functional and phenotypic features of CAR T cells; influencing parameters such as persistence, trafficking, memory cell formation and proliferation. All of which are essential determinants of an effective therapy (8, 9). Cytokines and chemoattractant cytokines (also known

as chemokines) are small glycoproteins that regulate immune cell activation, differentiation, growth and trafficking. Moreover, these small glycoproteins not only have critical roles in shaping of immune responses against different types of pathogens and tumor antigens but also determine which type of immune responses (e.g. cell-mediated vs. humoral immunity) should be developed to effectively eliminate their targets. Each cytokine has different functions and can provoke different responses depending on the target, cellular source and different phase of immune response. These small glycoproteins can have proinflammatory and anti-inflammatory properties which partly depend on the nature of target antigen and the context that an immune response initiated (10). Although systemic or local administration of cytokines in combination with CAR T cells improved antitumoral efficacy of these cells, some adverse effects including toxicity or even death, have been considered as significant barriers for systemic application of cytokines (11, 12).

Considering the importance of cytokines, chemokines and their receptors in the biology and immunology of CAR T cells, several investigators have tried to modulate the profile of cytokines and chemokines in CAR T cells or equip them with cytokines, chemokines or their receptors aiming to alleviate CAR T cell overactivation (i.e. cytokine release syndrome(CRS)) and/or overcome barriers (e.g. harsh immunosuppressive tumor microenvironment, suboptimal trafficking of CAR T cells to tumor site and activation-induced cell death) to their effectiveness. There are various strategies to genetically manipulate CAR T cells to enhance the overall functionality of these engineered cells against various types of tumors. For example, one of these strategies is the use of CRISPR-based gene editing technology to blunt the expression of cytokine genes responsible for CAR T cell dysfunction or CAR T cell-related toxicity (e.g. CRS). In this system, a single guide RNA (sgRNA) directs CAS9 endonuclease to the target gene. Binding of sgRNA to targeted gene activates CAS9 endonuclease which then leads to cleavage and knocking out of the target gene (13, 14). Another example is incorporation of truncated cytokine receptors into CAR T cells (through viral transduction) which lack a specific intracellular domain. These receptors block signal transduction of inhibitory cytokines and therefore enhance the persistence and effector function of CAR T cells (15, 16). Another approach is the co-expression of CAR construct with desirable cytokine through the 2A linker system or two vector systems. 2As are viral oligopeptides that can mediate cleavage of translated construct which leads to co-expression of both cytokine and CAR on T cells at the same time and expression level (17, 18). SynNotch receptor system and inducible promoter systems are examples of inducible expression of cytokines (19, 20). In the SynNotch receptor system, the recognition of specific antigen, mediates transcriptional activation of a specific cytokine gene in CAR T cells (21). Also, there are other strategies such as inverted cytokine receptors (ICRs) in which ectodomain of inhibitory cytokine is fused with endodomain of immunostimulatory cytokines (22), and membrane tethered cytokines that can be transferred *via* viral transduction or sleeping beauty (SB) system (excision and insertion of SB transposon into TA dinucleotide

repeat of target-cell genome) (Table 1) (34, 46). In this review we discuss how employing various genetic strategies like incorporating dominant negative receptors, inverted cytokine receptors and immunostimulatory cytokines not only can diminish and/or reverse negative CAR T cell regulators in the tumor microenvironment but also can augment positive regulators of CAR T cells (e.g. proliferation and persistence) in solid tumors.

## IMPROVING CAR T CELL PERSISTENCE

It is well-known that persistence of CAR T cells is directly correlated with durable clinical remissions in patients with cancers (47, 48). In fact, poor persistence potentially hinders the long-term therapeutic effects of CAR T cell *in vivo*. It has been shown that several parameters can affect the survival of adoptively transferred CAR T cells (49). In the two following sections, we discuss how genetic modification of CAR T cells to overexpress cytokines or their receptors makes prolong their survival.

### Production of Less Differentiated CAR T Cells

It is well-documented that the differentiation status of CAR T cells plays a prominent role in therapeutic success. It seems this successful therapeutic outcome is largely depend on the fact that less differentiated CAR T cells (e.g. naïve T cells (TN), stem cell memory (TSCM) and central memory (TCM)) are correlated with improved expansion, prolonged *in vivo* persistence, and long-term anti-tumor control (50).

As a result, many studies have focused on the production of CAR T cells with a less differentiated phenotype through employing different pharmacological and genetic mechanisms. For instance, less differentiated CAR T cells have been generated through inclusion of cytokine genes (e.g. IL-9, IL-7, IL-15 and IL-21) in the CAR gene construct (51, 52) and incorporation of cytokine-induced JAK/STAT signaling domains in the CAR gene construct (53–55). Using a hepatocellular carcinoma model, it has been revealed that co-incorporation of IL-15 and IL-21 genes into the anti-GPC3 CAR construct, leads to greater proliferation capacity, enhanced persistence and survival and elevated proportion of stem cell memory CAR T cell subpopulation (23). Adachi and colleagues also showed that IL-7 and CCL19 co-expressing CAR-T cells become differentiated into central memory CAR T cells with superior tumor-infiltrating capacity and higher persistence rate in a P815-hCD20 (mastocytoma) mouse model (24). Incorporation of IL-15 into CAR construct could also enhance stem-cell like memory CAR T cell portion with superior tumor killing ability and reduced expression of PD-1 receptor in neuroblastoma-bearing mice compared to conventional CAR T cells (25).

Using JAK/STAT signaling domains downstream of cytokine receptors is also another tactic for blunting CAR T cells differentiation towards terminally differentiated phenotype. The  $\gamma$ c-family cytokine-stimulated JAK/STAT signaling pathway is shown to dampen CAR T cells phenotype into terminally-

**TABLE 1 |** Novel genetic modifications in cytokine, chemokine and their receptors to enhance the efficacy of CAR T cell therapy.

Strategies	Cytokines & Chemo-kines	Genetic modification	Reference
Improving persistence	IL-15 & IL-21	Overexpression	(23)
	IL-7 & CCL9	Overexpression	(24)
	IL-15	Overexpression	(25, 26)
	TGF $\beta$	CRISPR-mediated knockout	(27)
	IL-7	ICR	(28)
Converting immuno-suppressive to immuno-promoting signals	IL-4R/IL-7R	ICR	(29)
	IL-4R/IL-21R	ICR	(22)
	TGF $\beta$ /IL-7R	ICR	(30)
	GM-CSF/IL-18R	ICR	(31)
Overcoming Exhaustion	TGF $\beta$ RII	Truncated	(15)
		CRISPR-mediated knockout	(27)
	aPD1/TGF $\beta$ trap	Overexpression	(32)
	IL-18	Inducible expression	[20]
	IL-7	Overexpression	(33)
	IL-15	Membrane tethered	(34)
	IL-7	ICR	(28)
AICD prevention	IL-15	Membrane tethered	(34)
Improving infiltration	CCR6	Overexpression	(35)
	CCR2b	Overexpression	(18, 36)
	CCR4	Overexpression	(37)
	CXCR2	Overexpression	(38)
CRS and neurotoxicity inhibition	IL-6	shRNA-mediated Knockdown	(39)
	mbalL-6	Truncated	(40)
	GM-CSF	CRISPR-mediated knockout	(41)
	GM-CSF & aIL-6/IL-1RA	CRISPR-mediated knockout & secreting neutralizing antibody & antagonist	(14)
Endogenous immune system activation	IL-7 & CCL19	Overexpression	(24)
	IL-18	Overexpression	(42)
	IL-12	Overexpression	(43, 44)
	IL-36 $\gamma$	Overexpression	(45)

ICR: inverted cytokine receptor; CRS: cytokine release syndrome; mbalL6: membrane-bound IL-6 receptor; aIL-6R: anti-IL-6 receptor antibody; IL-1RA: IL-1 receptor antagonist.

differentiated CAR T cells. Using a CAR construct encoding a truncated cytoplasmic domain from IL-2R $\beta$  and a STAT3-binding tyrosine-X-X-glutamine (YXXQ) motif, together with the CD3z and CD28 domains [also referred to as 28- $\Delta$ IL2RB-z (YXXQ)], it has been exhibited that the 28- $\Delta$ IL2RB-z(YXXQ) CAR T cells are highly proliferative and are not vulnerable to the acquisition of terminally-differentiated phenotype in a B-ALL experimental model. Compared to CAR T cells without STAT3 motif, 28- $\Delta$ IL2RB-z(YXXQ) CAR T cells maintained proliferation, IL-2 secretion, cytokine polyfunctionality. These results suggest a key role of STAT3 in suppressing terminal differentiation of T cells, which is consistent with recent human and mouse studies (54, 55). Modified CAR T cells also expressed markers related to stem cell like memory phenotype (such as, CD27, CD28 and CD95) (53). These characteristics have been also described in less differentiated memory T cells (56, 57). Currently, a phase 1 clinical trial is being planned to investigate the effect of IL-15 and IL-21 armored Glypican-3-specific CAR T cells for pediatric solid tumors (NCT04715191).

## Production of CAR T Cells Resistant to Pro-Apoptotic Signaling Cues

Overexpression of proapoptotic proteins such as Bid, Bim and FasL has been related to progressive T cell differentiation and loss of self-renewal capacity (58). Resistance to pro-apoptotic signals and/or augmentation of anti-apoptotic signaling pathway are

supposed to be an alternative option for promoting CAR T cell survival and persistence (49). TGF- $\beta$  as a potent immunosuppressant of TME is produced by different cell types such as cancer associated fibroblasts, mesenchymal stem cells, lymphatic epithelial cells and blood endothelial cells (59). It is generally accepted that TGF- $\beta$  inhibit T cell activation and proliferation likely due to induction of T cell apoptosis *via* either proapoptotic-dependent (e.g. BIM) or independent pathways (60–62). To blunt its suppressive effects on CAR T cells and to enhance the overall antitumor function of CAR T cells, CRISPR-mediated TGF $\beta$ 2-knockout CART cells (TGF $\beta$ 2.KO CART cells) have been developed. TGF $\beta$ 2.KO CART cells displayed higher survival and proliferation rates and were more resistant to exhaustion in the pancreatic carcinoma-bearing mice (27). IL-15 is known as a general inhibitor of apoptosis, which possesses potential therapeutic properties. Overexpression of murine IL-15 in CAR T cells has led to generation of CAR T cells with enhanced persistence, lower level of PD-1 expression, being more resistant to proapoptotic signals (probably due to augmentation of BCL-2 level) and improved antitumor immune response in a B16 melanoma model *in vivo* compared to conventional 2nd generation CAR T cells (26). In addition, IL-7 signaling through STAT5 has shown to be in favor of CAR T cell resistance to proapoptotic signals. In a study, Shum and colleagues have shown that constitutive signaling downstream of IL-7 receptor, through

using CD34 ectodomain and endodomain of IL-7R $\alpha$  (C7R), leads to upregulation of anti-apoptotic protein BCL2 and downregulation of proapoptotic protein CASP8 (Caspase-8) in an orthotopic glioblastoma mouse model (28). Altogether, these findings indicate that genetic modification of cytokines and their receptors might make CAR T cells more resistant to negative regulators of persistence through reprogramming of CAR T cell differentiation and abrogation of proapoptotic signaling.

## CONVERTING IMMUNOSUPPRESSIVE SIGNALS TO IMMUNOPROMOTING SIGNALS

Immunosuppressive cytokines including IL-10, TGF $\beta$  and IL-4, are one of the key components of TME contributing to CAR T cell dysfunction. These cytokines induce immunosuppression *via* several mechanisms such as recruitment and activation of regulatory T cells (Tregs), myeloid-derived suppressor cells (MDSCs), inhibition of the effector function of CAR T cells. In addition, they can inhibit the activity of several endogenous antitumor immune cells like T cells, NK cells, dendritic cells, and M1 macrophages. Immunosuppressive cytokines such as TGF $\beta$  can also disrupt the balance between TH1 and TH2 cells toward TH2 cells which leads to induction of other suppressive cytokines (e.g. IL-4) (63). To overcome cytokine-induced immunosuppression in the CAR T cells, Mohammed and colleagues have developed an inverted cytokine receptor IL-4R/IL-7R [i.e. 4/7 ICR, consisted of an IL-4R exodomain fused to an IL-7R endodomain]. Upon ligation to immunosuppressive cytokine IL-4, this chimeric switch receptor not only could significantly restrict the immunosuppressive effects of IL-4 but also could successfully convert inhibitory signals to IL-7 immunostimulatory signals. This immunostimulatory downstream signaling could prevent and/or restore CAR T cell exhaustion and dysfunction as well as could improve CAR T cell survival in a harsh TME of pancreatic cancer experimental model (29). In another study, Wang et al., have showed that overexpression of IL-4R/IL-21R inverted cytokine receptor (4/21 ICR) in CAR T cells could promote TH17-like polarization and enhance tumor specific cytotoxicity of 4/21 ICR-engineered CAR T cells in an IL-4-enriched hepatoma tumor milieu *via* activation of STAT3 pathway. Also, these cells were characterized by enhanced persistence and could successfully control established IL-4-secreting tumors *in vivo* (22). Weimin et al., have also reported that equipment of CAR T cells with chimeric cytokine switch receptor TGF $\beta$ /IL-7 not only could enhance their cytotoxic activity, cytokine production ability (e.g. IFN $\gamma$  and TNF $\alpha$ ) and proliferation capacity but also could reduce the expression of inhibitory receptors (e.g. PD-1 and LAG-3) in a prostate cancer model (30). Chimeric cytokine switch receptor GM-CSF/IL-18R (GM18) overexpressed in CAR T cells could also confer a higher rate of cellular expansion, cytokine production and sustain cytotoxic activity in a chronic antigen-stimulated condition of various preclinical EPHA2 or HER2 positive solid tumor models, compared to unmodified CAR T cells (31). In aggregate, it seems converting immunosuppressive cytokine signals to immunopromoting signals may be a promising strategy for improving CAR T cell functionality and longevity.

## OVERCOMING CAR T CELL EXHAUSTION

CAR T cell exhaustion represents a substantial barrier to the eradication of tumors and is associated with poor clinical outcome. Exhaustion is a common feature of tumor-infiltrating CAR T cells. Immunological exhaustion is characterized by progressive loss of T cell effector functions and proliferative capacity, sustained expression of inhibitory receptors (e.g. PD-1), increased susceptibility to apoptosis and activation of a transcriptional state distinct from that of functional effector or memory T cells (64). Tumor cells, and their surrounding immunosuppressive cells and cytokines are supposed to contribute to this exhausted T cell phenotype (65). As exhausted CAR T cells showed impaired effector function and failed to eradicate tumors (66), thus reversing this state can potentiate/restore the function of exhausted CAR T cells and thereby restore a robust antitumor response.

It has been shown that genetic modification of CAR T cells in this particular case-cytokine overexpression (e.g. IL-18, IL-15 and IL-7) or repression/abrogation (e.g. TGF $\beta$ R) can be a powerful approach for reverting CAR T cell exhaustion. TGF $\beta$  is a well-known immunosuppressive cytokine. This cytokine can induce T cell exhaustion through downstream signaling molecules (e.g. SMAD2 and SMAD3) of its receptor (e.g. TGF $\beta$ RII). Therefore, genetic modification of TGF $\beta$ R signal transduction can be an efficient method for the prevention of CAR T cell exhaustion. One of the examples is generation of dominant negative TGF $\beta$ RII CAR T cells which have truncated TGF $\beta$ RII that lack an intracellular signaling domain. This method makes CAR T cells resistant to exhaustion, enhances their proliferation and cytokine production abilities and confers long-term persistence with effective antitumor response against PSMA positive prostate cancer cells (15). In another study using CRL5826 positive melanoma cells, Tang and colleagues have demonstrated that knocking out the endogenous TGF $\beta$ RII in CAR T cells with CRISPR/Cas9 technology could reduce the induced Treg conversion and prevent the exhaustion of CAR T cells (27). Secretion of bispecific protein of anti-PD-1 fused with TGF- $\beta$  trap has also shown to enhance antitumor efficacy of CAR T cells through attenuating inhibitory T cell signaling, enhancing T cell persistence and expansion, and improving effector function and resistance to exhaustion in a prostate cancer xenograft mouse model (32). It has been well-documented that overexpression of cytokines (e.g. IL-18, IL-7 and IL-15) can prevent/revert CAR T cell exhaustion. Chmielewski and colleagues have revealed that CAR T cells engineered with inducible IL-18 release, as a potent immune modifier, can prevent CAR T cell exhaustion in large pancreatic and lung tumor models (20). Previous studies have also suggested an anti-exhaustive role for IL-7 (67). IL-7 secreting CAR T cells were also shown to express lower levels of exhaustion markers (e.g. PD-1 and LAG3) and higher levels of anti-transcription factor TCF-1, a transcription factor that is supposed to counteract exhaustion programs, in a gastric cancer experimental model (33, 68, 69). IL-15 has also proven beneficial in antagonizing CAR T cell exhaustion (70, 71). In agreement with these reports, Singh and colleagues have demonstrated that CAR T cells expressing a membrane-bound chimeric IL-15 (mbIL15) are not only characterized by long-term persistence with a memory stem-cell phenotype but also express lower levels of exhaustion

markers and higher expression level of anti-exhaustive transcription factor TCF-1 in a xenograft mouse model of leukemia (34). Furthermore, Narayan et al. have conducted a phase 1 clinical trial for dominant negative TGF $\beta$ R CAR T cell (PSMA-directed/TGF $\beta$ -insensitive CAR T cells) against metastatic castration-resistant prostate cancer (CRPC). Cohorts 1 and 2 have been done without observed dose-limiting toxicity (DLT). Intriguingly, a cytokine release syndrome has been observed that is reversible and responsive to tocilizumab (72).

## OVERCOMING ACTIVATION-INDUCED CELL DEATH (AICD)

Activation-induced cell death (AICD) is a major mechanism of T cell homeostasis and acts to prevent excessive T cell responses towards possible subsequential autoimmunity (73). Induced by repeated antigen stimulation under particular conditions, T cells undergo apoptosis in a controlled manner through the engagement of death receptors (e.g. Fas) and activation of specific caspases (e.g. caspase-8). Although AICD is generally considered as a T cell regulatory mechanism in the physiological conditions, this process is also triggered in the TME following chronic activation of tumor-infiltrating T cells (e.g. adoptively transferred CAR T cells), leading to apoptosis of tumor-redirected CAR T lymphocytes, thereby, hampering their full therapeutic potential (74).

Several efforts have been made over the years to overcome this barrier aiming to preserve CAR T cell efficacy and improve their survival and persistence in the TME. It has been shown that various cytokines are involved in either induction (e.g. TNF $\alpha$  and IL-2) or prevention (e.g. IL-7 and IL-15) of AICD. As mentioned above, Shum et al., have exhibited that CAR T cells supporting constitutive signaling downstream of IL-7 receptor have lower levels of Fas and proapoptotic protein CASP8 (Caspase-8), two major proteins that are involved in AICD (28). These findings highlight the role of IL-7 and its related signaling pathways in the inhibition of AICD. IL-15 is another potential cytokine for antagonizing AICD. The role of IL-15 in preventing AICD has been very well established (75). For instance, it has been shown that engineering of CAR T cells with membraned-bound IL-15 makes them more resistant to AICD (34). In other hand, it has been reported that cytokines like IL-2, IL-4, TNF $\alpha$  and IFN $\gamma$  are in favor of AICD induction (76). Therefore, it seems that genetic abrogation of these cytokines may alleviate the role of these cytokines in the induction of AICD in CAR T cells, however, it is remained to be further studied in future (76). In conclusion, these findings indicate that genetic modification and/or targeting of specific cytokine genes and/or their receptors may be a good option for overcoming activation-induced cell death in the CAR T cells, thereby, improving the efficacy of CAR T cell therapy.

## IMPROVING CAR T CELL INFILTRATION INTO TUMOR SITE

Suboptimal trafficking of CAR T cells to the tumor sites represents another hurdle to CAR T cell therapy. Several

reports have demonstrated that enhanced trafficking of adoptively transferred-CAR T cells to tumor sites is correlated to their therapeutic efficacy and clinical outcome in the cancer patients (77–79).

Various barriers that hinder optimal trafficking of CAR T cells to the tumor sites have been described. These barriers include: i) chemokine/receptor mismatch between the CAR T cell chemokine receptors and the chemokines secreted by tumors (e.g. such as CXCL1, CXCL5 and CXCL12), ii) low levels of tumor-derived chemokines for which effector CAR T cells lack receptors, iii) abnormal tumor vascularity and iv) physical (e.g. extracellular matrix (ECM]) and cellular barriers (e.g. cancer associated-fibroblasts [CAFs]) (80, 81). Although various strategies such as local delivery of CAR T cells, targeting tumor-related cellular and physical barriers (e.g. generation of anti-FAP CAR T cells targeting CAFs and CAR T cells to overexpress heparanase, an ECM-degrading enzyme) and targeting abnormal tumor vascularity (e.g. generation of CAR T cells targeting VEGFR2 expressed tumor-associated blood vessels) have been employed to overcome CAR T cell infiltration, genetic modification of chemokine receptors, among the others, has been the most common strategy to improve CAR T cell infiltration into the tumor bed (82–84). Genetic modifications of these molecules have widely been used as a novel strategy for conferring new migratory capacity to administrated CAR T cells. Jin et al. showed that anti-EGFR CAR T cell migration to lung cancer site was enhanced by overexpression of CCR6, which recognizes lung cancer-produced CCL20, a chemokine that is highly expressed by lung adenocarcinoma cells. The authors also found that overexpression of CCR6 has no negative effects on the CAR T cell effector functions and their phenotype. In addition, mice receiving CCR6-overexpressing CAR T cells showed enhanced survival and an improved antitumor activity compared to mice receiving conventional unmodified CAR T cells (35). AS chemokine CCL20 is also overexpressed in various types of cancer like colon adenocarcinoma (COAD), rectum adenocarcinoma (READ) and stomach adenocarcinoma (STAD), therefore, overexpression of CCR6 in CAR T cells might be an effective strategy to overcome insufficient infiltration of CAR T cells into CCL20-expressing tumor sites. CCR2b is a chemokine receptor that poorly expressed in all resting and activated peripheral blood T cells and IL-2 activated malignant pleural mesothelioma (MPM)-infiltrating lymphocytes. To promote infiltration of CAR T cells into MPM-bearing sites, Moon et al., generated an anti-mesoCAR T cells overexpressing CCR2b (i.e. CCR2b-mesoCAR T cells). Their data showed that overexpression of CCR2b in mesoCAR T cells can significantly increase their migration to mesothelin+ MPM sites *in vivo*, leading to enhanced antitumor effects (18). A separate report showed that expression of CCR2b on GD2-CAR T cells significantly increase migration of CAR T cells toward CCL2 secreting neuroblastoma cells (36). Di Stasi et al., have reported that overexpression of CCR4 on anti-CD30 CAR T cells improved the trafficking of these engineered T cells toward CCL17-Hodgkin lymphoma cells (37). Another report also proved that overexpression of CXCR2 on CAR T cells increase homing capability of CXCR2-expressing CAR T cells toward hepatocellular carcinoma cells-producing CXCL1, CXCL2,

CXCL3, CXCL5, CXCL6, and CXCL8 (38). In aggregate, these data indicate that genetic modification of chemokine receptors in CAR T cells may be a novel strategy to improve the efficacy and homing capabilities of adoptively transferred CAR T cells.

## MODULATING CYTOKINE RELEASE SYNDROME AND NEUROTOXICITY FOLLOWING CAR T CELL THERAPY

Systemic cytokine release [also known as cytokine release syndrome (CRS)] is a common but potentially fatal adverse event following CAR T cell therapy (85). Following the administration of CAR T cells, an exaggerated systemic immune response mediated by activated CAR T cells and various endogenous immune system components (e.g. monocytes/macrophages) is initiated. This acute systemic inflammatory response is mainly triggered by the release of a large amount of inflammatory mediators such as cytokines (e.g. IL-6, IL-1, IFN- $\gamma$  and GM-CSF) and chemokines [e.g. MCP-1 and MIP-1 $\alpha$ ] (86). This acute inflammatory response also induce endothelial and organ injury, which leads to microvascular leakage, heart failure and even death (85). Therefore, timely and properly interventional strategies that control CRS symptoms better or even to prevent CRS and neurotoxicity associated with CAR T cell therapy while preserving the efficacy CAR T cell treatment is of great importance and are urgently needed. Unlike hematological malignancies, the data on CRS incidence in solid tumors is limited probably due to the existence of immunosuppressive TME and insufficient infiltration of CAR T cells to tumor site (87–90). Thus, in this section will discuss different strategies that have been employed to overcome CRS in both hematological and non-hematological cancers.

Since it has been shown that IL-6 is the key molecule of CRS, many studies have recently focused to reduce and/or overcome IL-6-mediated CRS (91, 92). To do so, two independent studies have knocked down IL-6 gene in anti-CD19 CAR T cells *via* incorporation of short hairpin RNA (shRNA) into CAR construct (termed ssCART-19) (39, 92). Their data revealed that IL-6 released from CAR T cells not only cause CRS but also induces secretion of proinflammatory cytokines in the monocytes which altogether participate in the incidence and exacerbation of CRS. The authors also found that ssCART-19 cells produce lower levels of IL-6 and significantly reduce IL-6 secretion by monocytes in xenograft mouse model of leukemia. No significant difference in CAR T cell functionality in terms of proliferation and cytotoxicity was observed in both ssCART-19 cells and regular CART-19 cells. Reduced production of IL-6 by both CAR T cells and monocytes might lead to a significant reduction in the CRS incidence in the patients receiving CAR T cell therapy (39, 92).

In another study, Tan et al., have engineered anti-CD19 CAR T cells to express a non-signaling membrane bound IL-6 receptor (mbaIL6). *In vitro* testing of mbaIL6-expressing CAR T cells (termed mbaIL6CAR T cells) revealed similar cytotoxic and proliferative abilities compared to conventional CAR T cells.

Moreover, mbaIL6CAR T cells were able to neutralize macrophage-derived IL-6 while preserving their powerful antitumor activity *in vitro*. *In vivo* studies using CD19+ ALL cell line Nalm-6 also showed that anti-CD19CAR T cells were effective in targeting of CD19+ tumor cells regardless of mbaIL6 expression. However, level of human IL-6 in mice was significantly diminished in the mbaIL6CAR T-treated tumor-bearing mice compared to unmodified anti-19CAR T cells (40). GM-CSF has been also identified as a crucial cytokine in the development of neurotoxicity and CRS. Elevated levels of GM-CSF promote secretion of IL-6, IL-8 and MCP-1, as other important CRS biomarkers, from monocytes (41). To prevent or reduce the risk of CRS and neuroinflammation mediated by GM-CSF following CAR T cell therapy, Sterner and colleagues have utilized lenzilumab, a GM-CSF neutralizing antibody, in combination with anti-CD19CAR T cells. Their data showed that blocking GM-CSF leads to enhanced CART cells proliferation and efficacy. They found that blocking of GM-CSF has no significant effect on the tumor killing capacity of CAR T cells in the presence of monocytes *in vitro*. In line with their *in vitro* findings, *in vivo* studies also revealed that lenzilumab not only inhibits GM-CSF effector functions, but also preserves anti-leukemia activity. *In vivo* studies also proved that CAR T 19 cells in combination with GM-CSF neutralizing antibody could significantly reduce neuroinflammation and prevent of CRS. To rule out any critical role for GM-CSF in CAR T cell function, the authors also generated GM-CSF knockout anti-CD19 CAR T cells (termed GM-CSFK.O CAR T 19 cells) using CRISPR/Cas9 gene editing technology. Their findings revealed that GM-CSFK.O CART19 cells could significantly reduce GM-CSF production compared to conventional CART19 cells. In addition, gene-editing strategy had no interventional effect on the production of other effector cytokines (e.g. IFN $\gamma$  and IL-2) in the gene-edited anti-CD19 CAR T cells *in vitro*. While GM-CSFK.O CAR T19 cells were not able to produce GM-CSF, they could control leukemia growth *in vivo* (41). Another example is production of CRISPR-edited GM-CSF knockout CAR T cells secreting anti-IL-6 scFv and IL1RA with TCR knockout (CART-aIL6/IL1RA with GM-CSF/TCR KO). Compared to GM-CSF wild type counterparts, CART-aIL6/IL1RA with GM-CSF/TCR KO showed similar cytotoxicity and reduced GM-CSF production against CD19+ Nalm6 leukemia cells. Also, a pilot study of three patients, one with refractory Non-Hodgkin lymphoma (NHL) and two with multiple myelomas (MMs) with CART-aIL6/IL1RA with GM-CSF/TCR KO showed 3/3 complete response, 2/3 with no CRS incidence, one with grade 2 CRS incidence and no neurotoxicity which proved safety and efficacy of CART-aIL6/IL1RA with GM-CSF/TCR KO. In addition, cytokine analysis revealed a low level of GM-CSF, IL-6 and IL-1 $\beta$  and elevated level of IL1RA in the treated patients (14). It was also reported that genetic disruption of GM-CSF in the CAR T cells can abolish macrophage-dependent secretion of CRS mediators, including IL-6, IL-8 and MCP-1 (93). Furthermore, Kang et al. have conducted a clinical trial to evaluate safety and efficacy of ssCART-19 in patients with acute lymphoblastic leukemia (ALL). Their data exhibited a

significant reduction of severe CRS incidence in patients receiving ssCART-19 compared to those who received regular CART-19 (39). Neurotoxicity, also referred to as immune effector cell-associated neurotoxicity syndrome (ICANS), is another CAR T cell-related toxicity which often occurs and correlates with CRS, but it has also been sometimes reported to occur independently from CRS. The data obtained from preclinical studies revealed that monocyte-derived IL-1 appeared to mediate neurotoxicity and CRS (94). Stimulation of monocytes by GM-CSF following CART cell therapy was shown to be related to neuroinflammation in tumor-bearing mice (41). High levels of IL-6 and GM-CSF was detected in the cerebrospinal fluid (CSF) of non-human primate models of neurotoxicity following CART cell therapy (95). After CAR T cell therapy, cytokines, especially IL-1 and IL-6 and GM-CSF, have been demonstrated to promote systemic inflammation which associates with the development of severe neurotoxicity (96). GM-CSF has been also described as the cytokine most significantly correlated to the development of neurotoxicity following CART cell therapy in the ZUMA-1 clinical trial (97). These findings not only describe the crucial role of cytokines in pathogenesis of neurotoxicity but also highlight how genetic modification of cytokines by various strategies like shRNA-mediated knocking down of cytokine genes, design of nonsignaling membrane bound cytokine receptors and knocking out of cytokine genes in CAR T cells may significantly prevent and/or alleviate the post-CAR T cell therapy-related neurotoxicity.

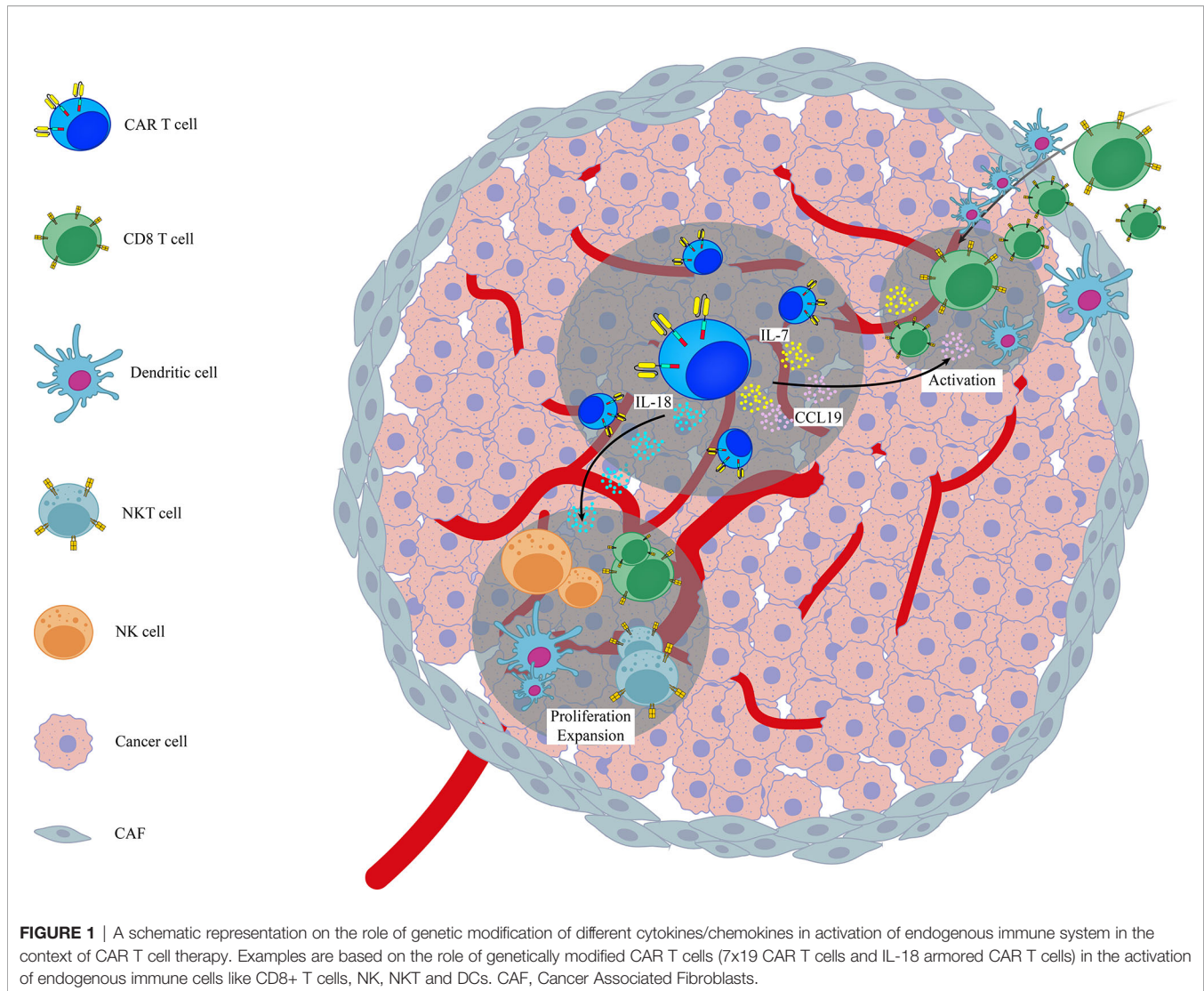
In the case of solid tumors, although rare, but CRS incidence can occur much like happen in B-NHL as characterized by local CRS (L-CRS or compartmental-CRS) followed by systemic CRS (S-CRS). It seems immunosuppressive TME and suboptimal trafficking of CAR T cells to tumor bed prevent optimal tumor antigen recognition and therefore limit full activation of CAR T cells and subsequent cytokine release and CRS incidence (87). There are a few reports on the incidence of compartmental CRS in a patient with recurrent ovarian cancer after treatment with anti-mesothelin CAR T cell (98) or the occurrence of severe CRS in a 45-year-old patient with malignant mesothelioma after the treatment with anti-EpCAM CAR T cells (87). Altogether, these data suggest that genetic modification of cytokines and receptors in CAR T cells would be an appealing strategy to prevent CRS and neurotoxicity or reduce its severity without affecting the antitumor potential of CAR T cell therapy.

## ACTIVATION OF ENDOGENOUS IMMUNE SYSTEM

Although genetically-modified CAR T cells have shown promising results compared to conventional CAR T cells, yet converting the CAR T cell response to a stronger and more continual one remains to be an important issue. CAR T cells are programmed to recognize one to three specific antigens utmost, but due to the pressure of immune selection and tumor antigen heterogeneity, some antigen-

negative tumor variants can outgrowth and outperform the a successful antitumor function of administrated CAR T cells. One overcoming solution would be the induction of epitope spreading towards antigens beyond those recognized by adoptively transferred CAR T cells. Epitope spreading is characterized by the enhancement and diversification of the endogenous T-cell-mediated immune response against non-CAR antigenic epitopes (99, 100). Based on this strategy, stimulation of endogenous immune cells along with CAR T cells can collaboratively target tumor cells (**Figure 1**). It seems that the inflammatory environment made by engineered CAR T cells can result in priming of endogenous immune cells against additional target antigens that is beyond the CAR target and are present on tumor cells.

Various studies have shown that infiltration of endogenous immune cells (in particular T lymphocytes) into the tumor sites can expand the efficacy of CAR T cell therapy (87, 101). In line with this notion, Adachi et al., reported that overexpression of IL-7 and CCL19, as two essential cytokines for generation of less-differentiated, long-lived non-exhausted (CAR) T cells and recruitment of endogenous DCs and T cells, in CAR T cells (termed 7x19 CAR T cells) increased infiltration of DCs and T cells into tumor sites following  $7 \times 19$  CAR T cell therapy. They also found that depletion of recipient T cells before  $7 \times 19$  CAR T cell therapy diminished the therapeutic efficacy of these genetically-modified CAR T cells, indicating that CAR T cells and endogenous immune cells collaboratively exert antitumor activity (24). Avanzi and colleagues also demonstrated that IL-18 armored CAR T cells, unlike unmodified CAR T cells, were able to activate and recruit endogenous antitumor immune effector cells such as CD8 T cells, DCs, NK cells and NKT cells into B-ALL tumor sites and metastatic ovarian tumor sites broadening the antitumor response beyond the CAR target (42). Arming CAR T cells with IL-12, a potent immunostimulatory cytokine that activates the innate and adaptive cellular immune system, was also shown to enhance antitumor efficacy through TME reprogramming and activation of endogenous immune system with antitumor function in both lymphoma and ovarian tumor models (43, 44). However, it should be noted that in study conducted by the Koneru et al, the total concentration of serum IL-12 was consisted of both endogenous and exogenous IL-12, and was not a reflection of IL-12 solely produced by IL-12 armored-CAR T cells (102). In another independent study, Kueberuwa et al. have exhibited that IL-12-expressing anti-CD19CAR T cells not only directly kill lymphoma cells, but also recruit host antitumor immune effector cells to an anti-cancer immune response in the lymphoreplete mice (103). CAR T cells secreting IL-36 $\gamma$  have also shown higher expansion rate with superior antitumor function compared with unmodified CAR T cells. Their data also revealed that IL-36 $\gamma$  armored CAR T cells activate endogenous antigen-presenting cells (APCs) and T cells through promotion of a secondary antitumor response and delayed the progression of antigen-negative tumor challenge in an experimental model of B-cell lymphoma (45). A separate study has also reported that effective CAR T cell antitumor activity of IL13Ra2-CAR T cells against mouse syngeneic glioblastoma (GBM) is significantly dependent on the activation of patient-derived endogenous T cells and monocyte/



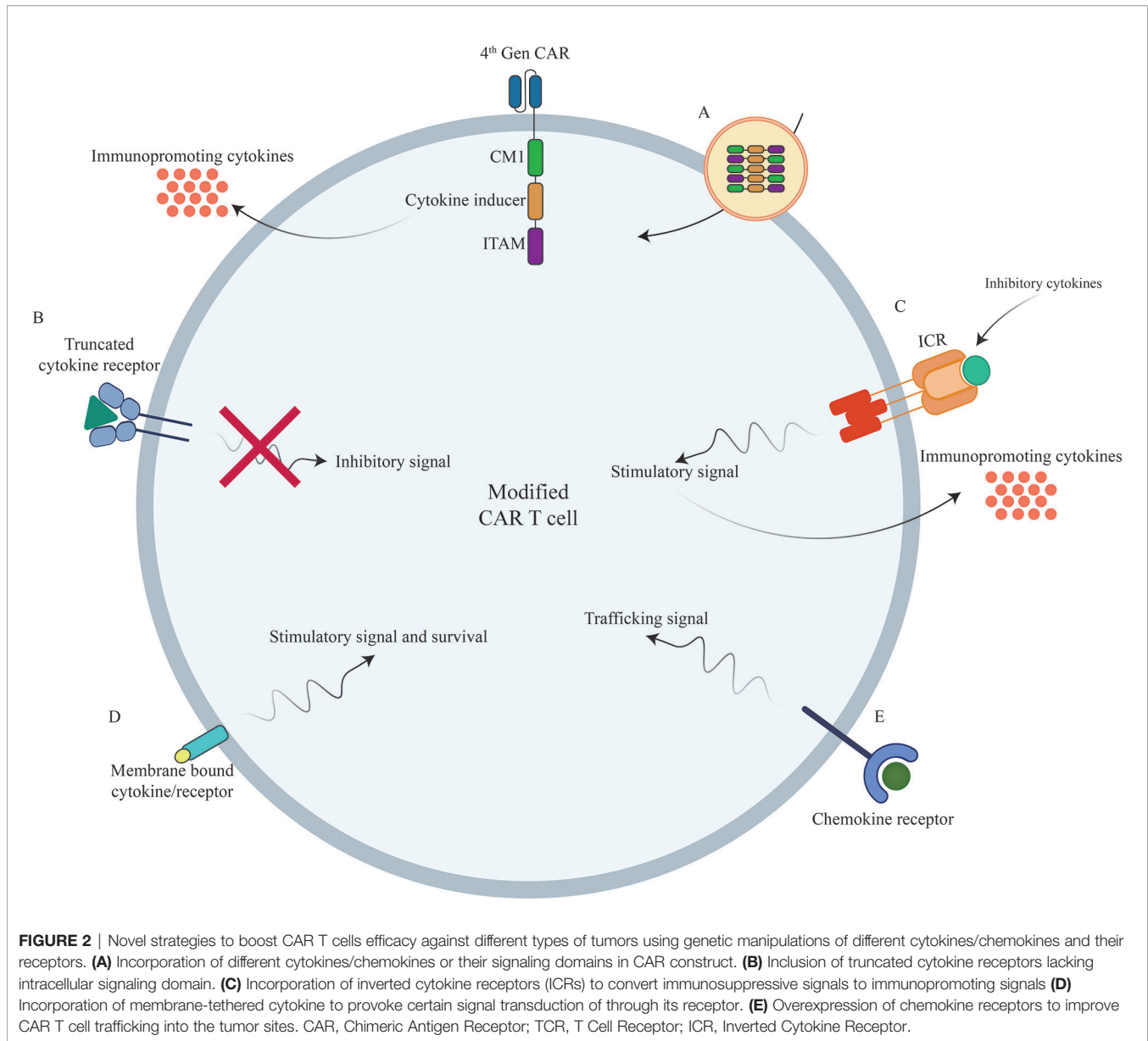
macrophages at the tumor site in an IFN $\gamma$ -dependent manner (101). Currently, a phase 2 clinical trial for IL-7 and CCL-19 expressing CAR T cells against Refractory/Relapsed B Cell Lymphoma is in recruiting status (NCT03929107). Altogether, these findings highlight the importance of activation of endogenous immune system in the context of CAR T cell therapy. It seems CAR T cells act as immunomodulatory adjuvant for the activation of host immune cells. This insight strongly supports the need to consider targeting/engaging host immunity to improve the efficacy of CAR T cell therapy. Moreover, activation of endogenous immune system can additionally prevent or delay the progression of antigen-negative tumor variants.

## CONCLUDING REMARKS

Although CAR T cell therapy has made great strides in the treatment of patients with advanced blood cancers; their success

in solid tumors has been limited partly due to the cellular, molecular and physical barriers of the TME. Developing innovative approaches including arming CARTs with cytokine signaling modalities to overcome these barriers has important translational relevance. In this review, we outline several strategies to enhance the effectiveness of CAR T cells emphasizing roles for several cytokines, chemokines and their signaling pathways to overcome and/or prevent CAR T cell dysfunction or hyperactivation (**Figure 2**).

Genetically modifying cytokine/chemokine signaling pathways is an appealing approach to enhance the therapeutic properties of CAR T cell therapy for solid tumors. It is anticipated that new generations of cytokine/chemokine-gene-modified CAR T cells could effectively target/engage endogenous immune system to synergistically improve overall antitumor immunity and additionally prevent the appearance of antigen-negative tumor variants, and thereby, tumor relapse in the context of CAR T cell therapy. However, CRS and ICANS incidences remain main safety concerns as CRS and ICANS



are potentially fatal adverse effect of CAR T cell therapy and genetic modifications of cytokines/chemokines that enhance CAR T cell function could exacerbate CRS and ICANS. To date, nearly all of studies have only investigated constitutive expression of single chemokine/cytokine. Thus, generation of CAR T cells engineered with an inducible chemokine/cytokine platform not only can increase efficacy but also guarantee safety of CAR T cell therapy.

Due to the fact that cytokine/chemokine gene expression profile can be various between different individuals or even at different stages of same tumor in an individual, hence; analysis of cytokine/chemokine gene expression signature in TME before CAR T cell therapy could aid scientists to individualize cytokine engineered-based CAR T cell therapy. Although genetic modification of

cytokine signaling in CAR T cells have shown promising clinical results in both hematologic and non-hematologic cancers (**Table 2**), it seems combination of different genetic modification approaches could be beneficial as some of cytokines are immunoinhibitory and others are immuno-stimulatory. Thus, modification of immunoinhibitory pathways using gene editing technologies (e.g. CRISPR/Cas9) or use of truncated cytokine receptors or cytokine traps alongside with overexpression of immunostimulatory cytokines may reprogram TME and significantly improve the efficacy of CAR T cell therapy.

Finally, it seems that a more comprehensive understanding of the relevant cellular and molecular adaptations to tumor cells and immunological processes in their surrounding microenvironment will help us develop new generations of cytokine/chemokine-gene-

**TABLE 2** | Selected clinical trials with cytokine/chemokine genetically-modified CAR T cells.

Clinical trial ID	Status	Cytokine/Chemokine Genetic Modification	CAR	Condition or disease	Phase
NCT04099797	Recruiting	C7R <sup>1</sup>	GD2-CAR	High Grade Glioma/Diffuse Intrinsic Pontine Glioma/Medulloblastoma	Phase 1
NCT03635632	Recruiting	C7R	GD2-CAR	Relapsed/Refractory Neuroblastoma	Phase 1
NCT03198546	Recruiting	IL-7 and CCL19	GPC3-CAR	Hepatocellular Carcinoma or Squamous Cell Lung Cancer	Phase 1
NCT03929107	Recruiting	IL-7 and CCL19	CD19-CAR	Refractory/Relapsed B Cell Lymphoma	Phase 2
NCT04381741	Recruiting	IL-7 and CCL19	CD19-CAR	Relapsed/Refractory Diffuse Large B Cell Lymphoma	Phase 1
NCT03778346	Recruiting	IL-7 and CCL19	BCMA-CAR, CD138-CAR, CD38-CAR, Integrin $\beta$ 7-CAR, CS1-CAR	Relapsed/Refractory Multiple Myeloma	Phase 1
NCT03932565	Recruiting	IL-7 and CCL19, or IL-12	Nectin4/FAP-CAR	Solid Tumors	Phase 1
NCT03721068	Recruiting	IL-15	GD2-CAR	Relapsed/Refractory Neuroblastoma or Relapsed/Refractory Osteosarcoma	Phase 1
NCT04377932	Recruiting	IL-15	GPC3-CAR	Pediatric Solid Tumors	Phase 1
NCT03579888	Terminated	mbIL-15 <sup>2</sup>	CD19-CAR	B Cell Lymphoma and Leukemia	Phase 1
NCT04715191	Not yet recruiting	IL-15 and IL-21	GPC3-CAR	Pediatric Solid Tumors	Phase 1
NCT02498912	Active, not recruiting	IL-12	4H11-CAR	MUC16ecto <sup>+</sup> Solid Tumors	Phase 1
NCT03542799	Unknown	IL-12	EGFR-CAR	Metastatic Colorectal Cancer	Phase 1 and 2
NCT01818323	Recruiting	IL-4R $\alpha$ and IL-2R $\beta$ (4 $\alpha$ $\beta$ )	T1E-CAR	Head and Neck Squamous Cell Carcinoma	Phase 1
NCT04153799	Recruiting	CXCR5	EGFR-CAR	Non-Small Cell Lung Cancer	Phase 1

modified CAR T cells that are more potent in overcoming the challenges of solid tumors.

## AUTHOR CONTRIBUTIONS

NG-S, SG, and HM conceived the idea of the manuscript. NG-S, BA, and TS performed the bibliographic research, wrote the original draft and drew the figures. HM, SG, and JH edited and critically revised the manuscript. All authors contributed to the article and approved the submitted version.

## REFERENCES

- Miliotou AN, Papadopoulou LC. CAR T-Cell Therapy: A New Era in Cancer Immunotherapy. *Curr Pharm Biotechnol* (2018) 19:5–18. doi: 10.2174/1389201019666180418095526
- Ramalingam SS, Owonikoko TK, Khuri FR. Lung Cancer: New Biological Insights and Recent Therapeutic Advances. *CA: Cancer J Clin* (2011) 61:91–112. doi: 10.3322/caac.20102
- Cummins KD, Gill S. Anti-CD123 Chimeric Antigen Receptor T-Cells (CART): An Evolving Treatment Strategy for Hematological Malignancies, and a Potential Ace-in-the-Hole Against Antigen-Negative Relapse. *Leuk Lymphoma* (2018) 59:1539–53. doi: 10.1080/10428194.2017.1375107
- Brudno JN, Kochenderfer JN. Recent Advances in CAR T-Cell Toxicity: Mechanisms, Manifestations and Management. *Blood Rev* (2019) 34:45–55. doi: 10.1016/j.blre.2018.11.002
- Mirzaei HR, Rodriguez A, Shepphird J, Brown CE, Badie B. Chimeric Antigen Receptors T Cell Therapy in Solid Tumor: Challenges and Clinical Applications. *Front Immunol* (2017) 8:1850. doi: 10.3389/fimmu.2017.01850
- Rodriguez-Garcia A, Palazon A, Noguera-Ortega E, Powell DJ Jr., Guedan S. CAR-T Cells Hit the Tumor Microenvironment: Strategies to Overcome Tumor Escape. *Front Immunol* (2020) 11:1109. doi: 10.3389/fimmu.2020.01109
- Slaney CY, Kershaw MH, Darcy PK. Trafficking of T Cells Into Tumors. *Cancer Res* (2014) 74:7168–74. doi: 10.1158/0008-5472.CAN-14-2458
- Jin J, Cheng J, Huang M, Luo H, Zhou J. Fueling Chimeric Antigen Receptor T Cells With Cytokines. *Am J Cancer Res* (2020) 10:4038–55.
- Zhou J, Jin L, Wang F, Zhang Y, Liu B, Zhao T. Chimeric Antigen Receptor T (CAR-T) Cells Expanded With IL-7/IL-15 Mediate Superior Antitumor Effects. *Protein Cell* (2019) 10:764–9. doi: 10.1007/s13238-019-0643-y
- Borish LC, Steinke JW. 2. Cytokines and Chemokines. *J Allergy Clin Immunol* (2003) 111:S460–475. doi: 10.1067/mai.2003.108
- Yeku OO, Purdon TJ, Koneru M, Spriggs D, Brentjens RJ. Armored CAR T Cells Enhance Antitumor Efficacy and Overcome the Tumor Microenvironment. *Sci Rep* (2017) 7:10541. doi: 10.1038/s41598-017-10940-8
- Hawkins ER, D'Souza RR, Klampatsa A. Armored CAR T-Cells: The Next Chapter in T-Cell Cancer Immunotherapy. *Biol Targets Ther* (2021) 15:95–105. doi: 10.2147/BTT.S291768
- Bak RO, Gomez-Ospina N, Porteus MH. Gene Editing on Center Stage. *Trends Genet TIG* (2018) 34:600–11. doi: 10.1016/j.tig.2018.05.004
- Yi Y, Chai X, Zheng L, Zhang Y, Shen J, Hu B, et al. CRISPR-Edited CART With GM-CSF Knockout and Auto Secretion of IL6 and IL1 Blockers in Patients With Hematologic Malignancy. *Cell Discovery* (2021) 7:27. doi: 10.1038/s41421-021-00255-4
- Kloss CC, Lee J, Zhang A, Chen F, Melenhorst JJ, Lacey SF, et al. Dominant-Negative TGF- $\beta$  Receptor Enhances PSMA-Targeted Human CAR T Cell Proliferation And Augments Prostate Cancer Eradication. *Mol Ther* (2018) 26:1855–66. doi: 10.1016/j.ymthe.2018.05.003

## FUNDING

This work was supported in part through funding provided by Tehran University of Medical Sciences (grants numbers 50756 and 50760, awarded to HM), St. Baldrick's Foundation Scholar Award (SG), National Blood Foundation Scientific Research Grant Award (SG), as well as Office of the Assistant Secretary of Defense for Health Affairs through the Peer Reviewed Cancer Research Program under Award No. W81XWH-20-1-0417 (SG).

16. Wieser R, Attisano L, Wrana JL, Massagué J. Signaling Activity of Transforming Growth Factor Beta Type II Receptors Lacking Specific Domains in the Cytoplasmic Region. *Mol Cell Biol* (1993) 13:7239–47. doi: 10.1128/MCB.13.12.7239
17. Liu Z, Chen O, Wall JBJ, Zheng M, Zhou Y, Wang L, et al. Systematic Comparison of 2A Peptides for Cloning Multi-Genes in a Polycistronic Vector. *Sci Rep* (2017) 7:2193. doi: 10.1038/s41598-017-02460-2
18. Moon EK, Carpenito C, Sun J, Wang LC, Kapoor V, Predina J, et al. Expression of a Functional CCR2 Receptor Enhances Tumor Localization and Tumor Eradication by Retargeted Human T Cells Expressing a Mesothelin-Specific Chimeric Antibody Receptor. *Clin Cancer Res* (2011) 17:4719–30. doi: 10.1158/1078-0432.CCR-11-0351
19. Luo H, Wu X, Sun R, Su J, Wang Y, Dong Y, et al. Target-Dependent Expression of IL12 by Synnotch Receptor-Engineered NK92 Cells Increases the Antitumor Activities of CAR-T Cells. *Front Oncol* (2019) 9:1448. doi: 10.3389/fonc.2019.01448
20. Chmielewski M, Abken H. CAR T Cells Releasing IL-18 Convert to T-Bet (high) FoxO1(low) Effectors That Exhibit Augmented Activity Against Advanced Solid Tumors. *Cell Rep* (2017) 21:3205–19. doi: 10.1016/j.celrep.2017.11.063
21. Roybal KT, Williams JZ, Morsut L, Rupp LJ, Kolinko I, Choe JH, et al. Engineering T Cells With Customized Therapeutic Response Programs Using Synthetic Notch Receptors. *Cell* (2016) 167:419–32.e416. doi: 10.1016/j.cell.2016.09.011
22. Wang Y, Jiang H, Luo H, Sun Y, Shi B, Sun R, et al. An IL-4/21 Inverted Cytokine Receptor Improving CAR-T Cell Potency in Immunosuppressive Solid-Tumor Microenvironment. *Front Immunol* (2019) 10:1691. doi: 10.3389/fimmu.2019.01691
23. Batra SA, Rathi P, Guo L, Courtney AN, Fleurence J, Balzeau J, et al. Glypican-3-Specific CAR T Cells Coexpressing IL15 and IL21 Have Superior Expansion and Antitumor Activity Against Hepatocellular Carcinoma. *Cancer Immunol Res* (2020) 8:309–20. doi: 10.1158/2326-6066.CIR-19-0293
24. Adachi K, Kano Y, Nagai T, Okuyama N, Sakoda Y, Tamada K. IL-7 and CCL19 Expression in CAR-T Cells Improves Immune Cell Infiltration and CAR-T Cell Survival in the Tumor. *Nat Biotechnol* (2018) 36:346–51. doi: 10.1038/nbt.4086
25. Chen Y, Sun C, Landoni E, Metelitsa L, Dotti G, Savoldo B. Eradication of Neuroblastoma by T Cells Redirected With an Optimized GD2-Specific Chimeric Antigen Receptor and Interleukin-15. *Clin Cancer Res* (2019) 25:2915–24. doi: 10.1158/1078-0432.CCR-18-1811
26. Lanitis E, Rota G, Kosti P, Ronet C, Spill A, Seijo B, et al. Optimized Gene Engineering of Murine CAR-T Cells Reveals the Beneficial Effects of IL-15 Coexpression. *J Exp Med* (2021) 218:1–19. doi: 10.1084/jem.20192203
27. Tang N, Cheng C, Zhang X, Qiao M, Li N, Mu W, et al. TGF- $\beta$  Inhibition via CRISPR Promotes the Long-Term Efficacy of CAR T Cells Against Solid Tumors. *JCI Insight* (2020) 5:1–17. doi: 10.1172/jci.insight.133977
28. Shum T, Omer B, Tashiro H, Kruse RL, Wagner DL, Parikh K, et al. Constitutive Signaling From an Engineered IL7 Receptor Promotes Durable Tumor Elimination by Tumor-Redirected T Cells. *Cancer Discovery* (2017) 7:1238–47. doi: 10.1158/2159-8290.CD-17-0538
29. Mohammed S, Sukumaran S, Bajgain P, Watanabe N, Heslop HE, Rooney CM, et al. Improving Chimeric Antigen Receptor-Modified T Cell Function by Reversing the Immunosuppressive Tumor Microenvironment of Pancreatic Cancer. *Mol Ther* (2017) 25:249–58. doi: 10.1016/j.mth.2016.10.016
30. Weimin S, Abula A, Qianghong D, Wenguang W. Chimeric Cytokine Receptor Enhancing PSMA-CAR-T Cell-Mediated Prostate Cancer Regression. *Cancer Biol Ther* (2020) 21:570–80. doi: 10.1080/15384047.2020.1739952
31. Lange S, Sand LG, Bell M, Patil SL, Langfitt D, Gottschalk S. A Chimeric GM-CSF/IL18 Receptor to Sustain CAR T-Cell Function. *Cancer Discovery* (2021) 7:1661–71. doi: 10.1158/2159-8290.CD-20-0896
32. Chen X, Yang S, Li S, Qu Y, Wang HY, Liu J, et al. Secretion of Bispecific Protein of Anti-PD-1 Fused With TGF- $\beta$  Trap Enhances Antitumor Efficacy of CAR-T Cell Therapy. *Mol Ther Oncol* (2021) 21:144–57. doi: 10.1016/j.omto.2021.03.014
33. Luo H, Su J, Sun R, Sun Y, Wang Y, Dong Y, et al. Coexpression of IL7 and CCL21 Increases Efficacy of CAR-T Cells in Solid Tumors Without Requiring Preconditioned Lymphodepletion. *Clin Cancer Res* (2020) 26:5494–505. doi: 10.1158/1078-0432.CCR-20-0777
34. Hurton LV, Singh H, Najjar AM, Switzer KC, Mi T, Maiti S, et al. Tethered IL-15 Augments Antitumor Activity and Promotes a Stem-Cell Memory Subset in Tumor-Specific T Cells. *Proc Natl Acad Sci* (2016) 113:E7788–97. doi: 10.1073/pnas.1610544113
35. Jin L, Cao L, Zhu Y, Cao J, Li X, Zhou J, et al. Enhance Anti-Lung Tumor Efficacy of Chimeric Antigen Receptor-T Cells by Ectopic Expression of C-C Motif Chemokine Receptor 6. *Sci Bull* (2020) 8:803–12. doi: 10.1016/j.scib.2020.12.027
36. Craddock JA, Lu A, Bear A, Pule M, Brenner MK, Rooney CM, et al. Enhanced Tumor Trafficking of GD2 Chimeric Antigen Receptor T Cells by Expression of the Chemokine Receptor CCR2b. *J Immunother (Hagerstown Md. 1997)* (2010) 33:780–8. doi: 10.1097/CJI.0b013e3181ee6675
37. Di Stasi A, De Angelis B, Rooney CM, Zhang L, Mahendravada A, Foster AE, et al. T Lymphocytes Coexpressing CCR4 and a Chimeric Antigen Receptor Targeting CD30 Have Improved Homing and Antitumor Activity in a Hodgkin Tumor Model. *Blood* (2009) 113:6392–402. doi: 10.1182/blood-2009-03-209650
38. Liu G, Rui W, Zheng H, Huang D, Yu F, Zhang Y, et al. CXCR2-Modified CAR-T Cells Have Enhanced Trafficking Ability That Improves Treatment of Hepatocellular Carcinoma. *Eur J Immunol* (2020) 50:712–24. doi: 10.1002/eji.201948457
39. Kang L, Tang X, Xu N, Li M, Tan J, Qi W, et al. shRNA-Interleukin-6 Modified CD19-Specific Chimeric Antigen Receptor T Cell Significantly Improves the Safety in Acute Lymphoblastic Leukemia. *Blood* (2019) 134:2621–1. doi: 10.1182/blood-2019-132067
40. Tan AHJ, Vivanica N, Campana D. Chimeric Antigen Receptor-T Cells With Cytokine Neutralizing Capacity. *Blood Adv* (2020) 4:1419–31. doi: 10.1182/bloodadvances.2019001287
41. Sterner RM, Sakemura R, Cox MJ, Yang N, Khadka RH, Forsman CL, et al. GM-CSF Inhibition Reduces Cytokine Release Syndrome and Neuroinflammation But Enhances CAR-T Cell Function in Xenografts. *Blood* (2019) 133:697–709. doi: 10.1182/blood-2018-10-881722
42. Avanzi MP, Yeku O, Li X, Wijewarnasuriya DP, van Leeuwen DG, Cheung K, et al. Engineered Tumor-Targeted T Cells Mediate Enhanced Anti-Tumor Efficacy Both Directly and Through Activation of the Endogenous Immune System. *Cell Rep* (2018) 23:2130–41. doi: 10.1016/j.celrep.2018.04.051
43. Pegram HJ, Lee JC, Hayman EG, Imperato GH, Tedder TF, Sadelain M, et al. Tumor-Targeted T Cells Modified to Secrete IL-12 Eradicate Systemic Tumors Without Need for Prior Conditioning. *Blood* (2012) 119:4133–41. doi: 10.1182/blood-2011-12-400044
44. Koneru M, Purdon TJ, Spriggs D, Koneru S, Brentjens RJ. IL-12 Secreting Tumor-Targeted Chimeric Antigen Receptor T Cells Eradicate Ovarian Tumors *In Vivo*. *Oncoimmunology* (2015) 4:e994446. doi: 10.4161/2162402X.2014.994446
45. Li X, Daniyan AF, Lopez AV, Purdon TJ, Brentjens RJ. Cytokine IL-36 $\gamma$  Improves CAR T-Cell Functionality and Induces Endogenous Antitumor Response. *Leukemia* (2021) 35:506–21. doi: 10.1038/s41375-020-0874-1
46. Singh H, Figliola MJ, Dawson MJ, Olivares S, Zhang L, Yang G, et al. Manufacture of Clinical-Grade CD19-Specific T Cells Stably Expressing Chimeric Antigen Receptor Using Sleeping Beauty System and Artificial Antigen Presenting Cells. *PLoS One* (2013) 8:e64138. doi: 10.1371/journal.pone.0064138
47. Louis CU, Savoldo B, Dotti G, Pule M, Yvon E, Myers GD, et al. Antitumor Activity and Long-Term Fate of Chimeric Antigen Receptor-Positive T Cells in Patients With Neuroblastoma. *Blood J Am Soc Hematol* (2011) 118:6050–6. doi: 10.1182/blood-2011-05-354449
48. Maude SL, Frey N, Shaw PA, Aplenc R, Barrett DM, Bunin NJ, et al. Chimeric Antigen Receptor T Cells for Sustained Remissions in Leukemia. *N Engl J Med* (2014) 371:1507–17. doi: 10.1056/NEJMoa1407222
49. Jafarzadeh L, Masoumi E, Fallah-Mehrjardi K, Mirzaei HR, Hadjati J. Prolonged Persistence of Chimeric Antigen Receptor (CAR) T Cell in Adoptive Cancer Immunotherapy: Challenges and Ways Forward. *Front Immunol* (2020) 11:702. doi: 10.3389/fimmu.2020.00702
50. Stock S, Schmitt M, Sellner L. Optimizing Manufacturing Protocols of Chimeric Antigen Receptor T Cells for Improved Anticancer Immunotherapy. *Int J Mol Sci* (2019) 20:1–21. doi: 10.3390/ijms20246223

51. McLellan AD, Ali Hosseini Rad SM. Chimeric Antigen Receptor T Cell Persistence and Memory Cell Formation. *Immunol Cell Biol* (2019) 97:664–74. doi: 10.1111/imcb.12254
52. Liu L, Bi E, Ma X, Xiong W, Qian J, Ye L, et al. Enhanced CAR-T Activity Against Established Tumors by Polarizing Human T Cells to Secrete Interleukin-9. *Nat Commun* (2020) 11:5902. doi: 10.1038/s41467-020-19672-2
53. Kagoya Y, Tanaka S, Guo T, Anczurowski M, Wang CH, Saso K, et al. A Novel Chimeric Antigen Receptor Containing a JAK-STAT Signaling Domain Mediates Superior Antitumor Effects. *Nat Med* (2018) 24:352–9. doi: 10.1038/nm.4478
54. Siegel AM, Heimall J, Freeman AF, Hsu AP, Brittain E, Brenchley JM, et al. A Critical Role for STAT3 Transcription Factor Signaling in the Development and Maintenance of Human T Cell Memory. *Immunity* (2011) 35:806–18. doi: 10.1016/j.immuni.2011.09.016
55. Cui W, Liu Y, Weinstein JS, Craft J, Kaech SM. An Interleukin-21-Interleukin-10-STAT3 Pathway is Critical for Functional Maturation of Memory CD8+ T Cells. *Immunity* (2011) 35:792–805. doi: 10.1016/j.immuni.2011.09.017
56. Sabatino M, Hu J, Sommariva M, Gautam S, Fellowes V, Hocker JD, et al. Generation of Clinical-Grade CD19-Specific CAR-Modified CD8+ Memory Stem Cells for the Treatment of Human B-Cell Malignancies. *Blood* (2016) 128:519–28. doi: 10.1182/blood-2015-11-683847
57. Cieri N, Camisa B, Cocchiarella F, Forcato I, Oliveira G, Provasi E, et al. IL-7 and IL-15 Instruct the Generation of Human Memory Stem T Cells From Naive Precursors. *Blood* (2013) 121:573–84. doi: 10.1182/blood-2012-05-431718
58. Ghosh A, Smith M, James SE, Davila ML, Velardi E, Argyropoulos KV, et al. Donor CD19 CAR T Cells Exert Potent Graft-Versus-Lymphoma Activity With Diminished Graft-Versus-Host Activity. *Nat Med* (2017) 23:242–9. doi: 10.1038/nm.4258
59. Turley SJ, Cremasco V, Astarita JL. Immunological Hallmarks of Stromal Cells in the Tumour Microenvironment, Nature Reviews. *Immunology* (2015) 15:669–82. doi: 10.1038/nri3902
60. Principe DR, Doll JA, Bauer J, Jung B, Munshi HG, Bartholin L, et al. TGF- $\beta$ : Duality of Function Between Tumor Prevention and Carcinogenesis. *J Natl Cancer Inst* (2014) 106:djt369. doi: 10.1093/jnci/djt369
61. Ramesh S, Wildev GM, Howe PH. Transforming Growth Factor Beta (TGFbeta)-Induced Apoptosis: The Rise & Fall of Bim. *Cell Cycle (Georgetown Tex.)* (2009) 8:11–7. doi: 10.4161/cc.8.1.7291
62. Weller M, Constam DB, Malipiero U, Fontana A. Transforming Growth Factor-Beta 2 Induces Apoptosis of Murine T Cell Clones Without Down-Regulating Bcl-2 mRNA Expression. *Eur J Immunol* (1994) 24:1293–300. doi: 10.1002/eji.1830240608
63. Belli C, Trapani D, Viale G, D'Amico P, Duso BA, Della Vigna P, et al. Targeting the Microenvironment in Solid Tumors. *Cancer Treat Rev* (2018) 65:22–32. doi: 10.1016/j.ctrv.2018.02.004
64. Wherry EJ, Kurachi M. Molecular and Cellular Insights Into T Cell Exhaustion. *Nat Rev Immunol* (2015) 15:486–99. doi: 10.1038/nri3862
65. Davoodzadeh Gholami M, Kardar GA, Saeedi Y, Heydari S, Garsen J, Falak R. Exhaustion of T Lymphocytes in the Tumor Microenvironment: Significance and Effective Mechanisms. *Cell Immunol* (2017) 322:1–14. doi: 10.1016/j.cellimm.2017.10.002
66. Jiang Y, Li Y, Zhu B. T-Cell Exhaustion in the Tumor Microenvironment. *Cell Death Dis* (2015) 6:e1792. doi: 10.1038/cddis.2015.162
67. Pellegrini M, Calzascia T, Elford AR, Shahinian A, Lin AE, Dissanayake D, et al. Adjuvant IL-7 Antagonizes Multiple Cellular and Molecular Inhibitory Networks to Enhance Immunotherapies. *Nat Med* (2009) 15:528–36. doi: 10.1038/nm.1953
68. Wu T, Ji Y, Moseman EA, Xu HC, Manglani M, Kirby M, et al. The TCF1-Bcl6 Axis Counteracts Type I Interferon to Repress Exhaustion and Maintain T Cell Stemness. *Sci Immunol* (2016) 1:1–27. doi: 10.1126/sciimmunol.aai8593
69. Chen Z, Ji Z, Ngjow SF, Manne S, Cai Z, Huang AC, et al. TCF-1-Centered Transcriptional Network Drives an Effector Versus Exhausted CD8 T Cell-Fate Decision. *Immunity* (2019) 51:840–855.e845. doi: 10.1016/j.immuni.2019.09.013
70. Alizadeh D, Wong RA, Yang X, Wang D, Pecoraro JR, Kuo C-F, et al. IL-15-Mediated Reduction of Mtorc1 Activity Preserves the Stem Cell Memory Phenotype of CAR-T Cells and Confers Superior Antitumor Activity. *Cancer Immunol Res* (2019) 5:759–72. doi: 10.1158/2326-6066.CIR-18-0466
71. Giuffrida L, Sek K, Henderson MA, House IG, Lai J, Chen AX, et al. IL-15 Preconditioning Augments CAR T Cell Responses to Checkpoint Blockade for Improved Treatment of Solid Tumors. *Mol Ther* (2020) 28:2379–93. doi: 10.1016/j.yimthe.2020.07.018
72. Narayan V, Barber-Rotenberg J, Fraietta J, Hwang W-T, Lacey SF, Plesa G, et al. A Phase I Clinical Trial of PSMA-Directed/Tgfb-Insensitive CAR-T Cells in Metastatic Castration-Resistant Prostate Cancer. *J Clin Oncol* (2021) 39:125–5. doi: 10.1200/JCO.2021.39.6\_suppl.125
73. Green DR, Droin N, Pinkoski M. Activation-Induced Cell Death in T Cells. *Immunol Rev* (2003) 193:70–81. doi: 10.1034/j.1600-065X.2003.00051.x
74. Otano I, Alvarez M, Minute L, Ochoa MC, Migueliz I, Molina C, et al. Human CD8 T Cells are Susceptible to TNF-Mediated Activation-Induced Cell Death. *Theranostics* (2020) 10:4481–9. doi: 10.7150/tno.41646
75. Marks-Konczalik J, Dubois S, Losi JM, Sabzevari H, Yamada N, Feigenbaum L, et al. IL-2-Induced Activation-Induced Cell Death is Inhibited in IL-15 Transgenic Mice. *Proc Natl Acad Sci USA* (2000) 97:11445–50. doi: 10.1073/pnas.200363097
76. Arakaki R, Yamada A, Kudo Y, Hayashi Y, Ishimaru N. Mechanism of Activation-Induced Cell Death of T Cells and Regulation of FasL Expression. *Crit Rev Immunol* (2014) 34:301–14. doi: 10.1615/CritRevImmunol.2014009988
77. Brown CE, Vishwanath RP, Aguilar B, Starr R, Najbauer J, Aboody KS, et al. Tumor-Derived Chemokine MCP-1/CCL2 is Sufficient for Mediating Tumor Tropism of Adoptively Transferred T Cells. *J Immunol* (2007) 179:3332–41. doi: 10.4049/jimmunol.179.5.3332
78. Galon J, Costes A, Sanchez-Cabo F, Kirilovsky A, Mlecnik B, Lagorce-Pagès C, et al. Type, Density, and Location of Immune Cells Within Human Colorectal Tumors Predict Clinical Outcome. *Science* (2006) 313:1960–4. doi: 10.1126/science.1129139
79. Kmiecik J, Poli A, Brons NH, Waha A, Eide GE, Enger PØ, et al. Elevated CD3+ and CD8+ Tumor-Infiltrating Immune Cells Correlate With Prolonged Survival in Glioblastoma Patients Despite Integrated Immunosuppressive Mechanisms in the Tumor Microenvironment and at the Systemic Level. *J Neuroimmunol* (2013) 264:71–83. doi: 10.1016/j.jneuroim.2013.08.013
80. Ma S, Li X, Wang X, Cheng L, Li Z, Zhang C, et al. Current Progress in CAR-T Cell Therapy for Solid Tumors. *Int J Biol Sci* (2019) 15:2548–60. doi: 10.7150/ijbs.34213
81. Martinez M, Moon EK. CAR T Cells for Solid Tumors: New Strategies for Finding, Infiltrating, and Surviving in the Tumor Microenvironment. *Front Immunol* (2019) 10. doi: 10.3389/fimmu.2019.00128
82. Caruana I, Savoldo B, Hoyos V, Weber G, Liu H, Kim ES, et al. Heparanase Promotes Tumor Infiltration and Antitumor Activity of CAR-Redirected T Lymphocytes. *Nat Med* (2015) 21:524–9. doi: 10.1038/nm.3833
83. Wang L-CS, Lo A, Scholler J, Sun J, Majumdar RS, Kapoor V, et al. Targeting Fibroblast Activation Protein in Tumor Stroma With Chimeric Antigen Receptor T Cells can Inhibit Tumor Growth and Augment Host Immunity Without Severe Toxicity. *Cancer Immunol Res* (2014) 2:154–66. doi: 10.1158/2326-6066.CIR-13-0027
84. Kanagawa N, Yanagawa T, Nakagawa T, Okada N, Nakagawa S. Tumor Vessel-Injuring Ability Improves Antitumor Effect of Cytotoxic T Lymphocytes in Adoptive Immunotherapy. *Cancer Gene Ther* (2013) 20:57–64. doi: 10.1038/cgt.2012.85
85. Maude SL, Barrett D, Teachey DT, Grupp SA. Managing Cytokine Release Syndrome Associated With Novel T Cell-Engaging Therapies. *Cancer J (Sudbury Mass.)* (2014) 20:119. doi: 10.1097/PPO.0000000000000035
86. Chen H, Wang F, Zhang P, Zhang Y, Chen Y, Fan X, et al. Management of Cytokine Release Syndrome Related to CAR-T Cell Therapy. *Front Med* (2019) 13:610–7. doi: 10.1007/s11684-019-0714-8
87. Wei J, Liu Y, Wang C, Zhang Y, Tong C, Dai G, et al. The Model of Cytokine Release Syndrome in CAR T-Cell Treatment for B-Cell non-Hodgkin Lymphoma. *Signal Transduct Targeted Ther* (2020) 5:134. doi: 10.1038/s41392-020-00256-x
88. Lee DW, Kochenderfer JN, Stetler-Stevenson M, Cui YK, Delbrook C, Feldman SA, et al. T Cells Expressing CD19 Chimeric Antigen Receptors for Acute Lymphoblastic Leukemia in Children and Young Adults: A Phase I Dose-Escalation Trial. *Lancet (Lond Engl)* (2015) 385:517–28. doi: 10.1016/S0140-6736(14)61403-3
89. Wang Y, Zhang WY, Han QW, Liu Y, Dai HR, Guo YL, et al. Effective Response and Delayed Toxicities of Refractory Advanced Diffuse Large B-

- Cell Lymphoma Treated by CD20-Directed Chimeric Antigen Receptor-Modified T Cells. *Clin Immunol (Orlando Fla.)* (2014) 155:160–75. doi: 10.1016/j.clim.2014.10.002
90. Fried S, Avigdor A, Bielorai B, Meir A, Besser MJ, Schachter J, et al. Early and Late Hematologic Toxicity Following CD19 CAR-T Cells. *Bone Marrow Transplant* (2019) 54:1643–50. doi: 10.1038/s41409-019-0487-3
  91. Bonifant CL, Jackson HJ, Brentjens RJ, Curran KJ. Toxicity and Management in CAR T-Cell Therapy. *Mol Ther Oncol* (2016) 3:16011. doi: 10.1038/mto.2016.11
  92. Kang L, Tang X, Zhang J, Li M, Xu N, Qi W, et al. Interleukin-6-Knockdown of Chimeric Antigen Receptor-Modified T Cells Significantly Reduces IL-6 Release From Monocytes. *Exp Hematol Oncol* (2020) 9:11. doi: 10.1186/s40164-020-00166-2
  93. Sachdeva M, Aranda-Orgilles B, Duchateau P, Poirot L, Valton J. Abstract A60: GM-CSF Modulation Restricts the Secretion of Main Cytokines Associated With CAR T-Cell Induced Cytokine Release Syndrome. *Cancer Immunol Res* (2020) 8:A60–0. doi: 10.1158/2326-6074.TUMIMM19-A60
  94. Norelli M, Camisa B, Barbiera G, Falcone L, Purevdorj A, Genua M, et al. Monocyte-Derived IL-1 and IL-6 are Differentially Required for Cytokine-Release Syndrome and Neurotoxicity Due to CAR T Cells. *Nat Med* (2018) 24:739–48. doi: 10.1038/s41591-018-0036-4
  95. Taraseviciute A, Tkachev V, Ponce R, Turtle CJ, Snyder JM, Liggitt HD, et al. Chimeric Antigen Receptor T Cell-Mediated Neurotoxicity in Nonhuman Primates. *Cancer Discov* (2018) 8:750–63. doi: 10.1158/2159-8290.CD-17-1368
  96. Gust J, Hay KA, Hanafi LA, Li D, Myerson D, Gonzalez-Cuyar LF, et al. Endothelial Activation and Blood-Brain Barrier Disruption in Neurotoxicity After Adoptive Immunotherapy With CD19 CAR-T Cells. *Cancer Discov* (2017) 7:1404–19. doi: 10.1158/2159-8290.CD-17-0698
  97. Neelapu SS, Locke FL, Bartlett NL, Lekakis LJ, Miklos DB, Jacobson CA, et al. Axicabtagene Ciloleucel CAR T-Cell Therapy in Refractory Large B-Cell Lymphoma. *N Engl J Med* (2017) 377:2531–44. doi: 10.1056/NEJMoa1707447
  98. Tanyi JL, Stashwick C, Plesa G, Morgan MA, Porter D, Maus MV, et al. Possible Compartmental Cytokine Release Syndrome in a Patient With Recurrent Ovarian Cancer After Treatment With Mesothelin-Targeted CAR-T Cells. *J Immunother (Hagerstown Md. 1997)* (2017) 40:104–7. doi: 10.1097/CJI.0000000000000160
  99. Brossart P. The Role of Antigen Spreading in the Efficacy of Immunotherapies. *Clin Cancer Res* (2020) 26:4442–7. doi: 10.1158/1078-0432.CCR-20-0305
  100. Schneider D, Xiong Y. Trispecific CD19-CD20-CD22-Targeting duoCAR-T Cells Eliminate Antigen-Heterogeneous B Cell Tumors in Preclinical Models. *Sci Transl Med* (2021) 13:586. doi: 10.1126/scitranslmed.abc6401
  101. Alizadeh D, Wong RA, Gholamin S, Maker M, Aftabizadeh M, Yang X, et al. IFN $\gamma$  Is Critical for CAR T Cell Mediated Myeloid Activation and Induction of Endogenous Immunity. *Cancer Discov* (2021) 9:2248–65. doi: 10.1158/2159-8290.CD-20-1661
  102. Mirzaei HR, Hadjati J. Commentary: IL-12-Secreting Tumor-Targeted Chimeric Antigen Receptor T Cells: An Unaddressed Concern on Koneru Et al. (2015). *Oncoimmunology* (2016) 5:e1100792. doi: 10.1080/2162402X.2015.1100792
  103. Kueberuwa G, Kalaitidou M, Cheadle E, Hawkins RE, Gilham DE. CD19 CAR T Cells Expressing IL-12 Eradicate Lymphoma in Fully Lymphoreplete Mice Through Induction of Host Immunity. *Mol Ther Oncol* (2018) 8:41–51. doi: 10.1016/j.omto.2017.12.003
- Conflict of Interest:** The authors declare that the research was conducted in the absence of any commercial or financial relationships that could be construed as a potential conflict of interest.
- Publisher's Note:** All claims expressed in this article are solely those of the authors and do not necessarily represent those of their affiliated organizations, or those of the publisher, the editors and the reviewers. Any product that may be evaluated in this article, or claim that may be made by its manufacturer, is not guaranteed or endorsed by the publisher.
- Copyright © 2021 Ghahri-Saremi, Akbari, Soltantoyeh, Hadjati, Ghassemi and Mirzaei. This is an open-access article distributed under the terms of the Creative Commons Attribution License (CC BY). The use, distribution or reproduction in other forums is permitted, provided the original author(s) and the copyright owner(s) are credited and that the original publication in this journal is cited, in accordance with accepted academic practice. No use, distribution or reproduction is permitted which does not comply with these terms.

Article

# CAR T-Cells Depend on the Coupling of NADH Oxidation with ATP Production

Juan C. Garcia-Canaveras <sup>1,2</sup> , David Heo <sup>3,4</sup>, Sophie Trefely <sup>5</sup>, John Leferovich <sup>3,4</sup>, Chong Xu <sup>3,4,6</sup>, Benjamin I. Philipson <sup>3,4</sup>, Saba Ghassemi <sup>3,4</sup>, Michael C. Milone <sup>3,4</sup>, Edmund K. Moon <sup>7,8</sup>, Nathaniel W. Snyder <sup>5,9</sup>, Carl H. June <sup>3,4</sup>, Joshua D. Rabinowitz <sup>1,2,\*</sup> and Roddy S. O'Connor <sup>3,4,\*</sup>

- <sup>1</sup> Department of Chemistry, Princeton University, Princeton, NJ 08544, USA; juancarlos\_garcia@iislafe.es
- <sup>2</sup> Lewis-Singer Institute for Integrative Genomics, Princeton University, Princeton, NJ 08544, USA
- <sup>3</sup> Center for Cellular Immunotherapies, Perelman School of Medicine at the University of Pennsylvania, Philadelphia, PA 19104, USA; davidheo153@gmail.com (D.H.); jleferov@pennmedicine.upenn.edu (J.L.); chongxu@pennmedicine.upenn.edu (C.X.); bphili@pennmedicine.upenn.edu (B.I.P.); ghassemi@pennmedicine.upenn.edu (S.G.); michael.milone@pennmedicine.upenn.edu (M.C.M.); cjune@upenn.edu (C.H.J.)
- <sup>4</sup> Department of Pathology and Laboratory Medicine, Perelman School of Medicine of the University of Pennsylvania, Philadelphia, PA 19104, USA
- <sup>5</sup> A.J. Drexel Autism Institute, Drexel University, Philadelphia, PA 19140, USA; strefely@pennmedicine.upenn.edu (S.T.); natewsnyder@temple.edu (N.W.S.)
- <sup>6</sup> The Parker Institute for Cancer Immunotherapy, Perelman School of Medicine, University of Pennsylvania, Philadelphia, PA 19104, USA
- <sup>7</sup> Department of Medicine, Perelman School of Medicine, University of Pennsylvania, Philadelphia, PA 19140, USA; edmund.moon@pennmedicine.upenn.edu
- <sup>8</sup> Division of Pulmonary, Allergy, and Critical Care, Perelman School of Medicine at the University of Pennsylvania, Philadelphia, PA 19104, USA
- <sup>9</sup> Penn SRP center, Center of Excellence in Environmental Toxicology and Department of Systems Pharmacology and Translational Therapeutics at the University of Pennsylvania, Philadelphia, PA 19104, USA; edmund.moon@pennmedicine.upenn.edu
- \* Correspondence: josh@princeton.edu (J.D.R.); oconnorr@pennmedicine.upenn.edu (R.S.O.)



**Citation:** Garcia-Canaveras, J.C.; Heo, D.; Trefely, S.; Leferovich, J.; Xu, C.; Philipson, B.I.; Ghassemi, S.; Milone, M.C.; Moon, E.K.; Snyder, N.W.; et al. CAR T-Cells Depend on the Coupling of NADH Oxidation with ATP Production. *Cells* **2021**, *10*, 2334. <https://doi.org/10.3390/cells10092334>

Academic Editor: Sébastien Wälchli

Received: 21 July 2021

Accepted: 25 August 2021

Published: 6 September 2021

**Publisher's Note:** MDPI stays neutral with regard to jurisdictional claims in published maps and institutional affiliations.



**Copyright:** © 2021 by the authors. Licensee MDPI, Basel, Switzerland. This article is an open access article distributed under the terms and conditions of the Creative Commons Attribution (CC BY) license (<https://creativecommons.org/licenses/by/4.0/>).

**Abstract:** The metabolic milieu of solid tumors provides a barrier to chimeric antigen receptor (CAR) T-cell therapies. Excessive lactate or hypoxia suppresses T-cell growth, through mechanisms including NADH buildup and the depletion of oxidized metabolites. NADH is converted into NAD<sup>+</sup> by the enzyme *Lactobacillus brevis* NADH Oxidase (*LbNOX*), which mimics the oxidative function of the electron transport chain without generating ATP. Here we determine if *LbNOX* promotes human CAR T-cell metabolic activity and antitumor efficacy. CAR T-cells expressing *LbNOX* have enhanced oxygen as well as lactate consumption and increased pyruvate production. *LbNOX* renders CAR T-cells resilient to lactate dehydrogenase inhibition. But in vivo in a model of mesothelioma, CAR T-cell's expressing *LbNOX* showed no increased antitumor efficacy over control CAR T-cells. We hypothesize that T cells in hostile environments face dual metabolic stressors of excessive NADH and insufficient ATP production. Accordingly, futile T-cell NADH oxidation by *LbNOX* is insufficient to promote tumor clearance.

**Keywords:** armor CAR T-cells; *Lactobacillus brevis* NADH oxidase; LDHA

## 1. Introduction

The success of CAR T-cells in acute and chronic leukemia highlights their therapeutic promise against cancer. CARs are synthetic receptors that control antigen specificity, signal transduction, and effector function in a single polypeptide. Previously, we showed that CAR design has a profound influence on cellular metabolism; CARs expressing CD28 signaling domains yield glycolytic, effector T-cells whereas CARs expressing 4-1BB promote the development of mitochondrial-enriched, memory T cells [1]. Implicit in these earlier

discoveries is that T cell metabolism is not fixed and can be dynamically modified to suit the target environment.

Extending the therapeutic impact of CD28 or 4-1BB-based CAR T-cells to solid tumors is a significant priority for the clinical domain. Often T-cells can effectively penetrate solid tumors and undergo antigen-specific stimulation; however, their ability to form cytolytic effector cells is impaired [2,3]. Metabolic checkpoints including nutrient depletion and oxygen deprivation contribute to T-cell dysfunction in solid tumors. Functional competence is restored as T-cells evacuate tumor regions and colonize oxygen-rich, nutrient-rich environments, such as non-draining lymph nodes [4] or even standard tissue culture environments [2,5]. These findings underscore the need for novel strategies that sustain CAR T-cell metabolic function in harsh environments.

The exact mechanism(s) limiting T-cell metabolism in solid tumors is unknown. Mitochondrial function as measured by an ability to synthesize new mitochondria in response to extrinsic stimuli and undergo high rates of oxidative phosphorylation for energy production is severely impaired in T cells traversing hypoxic tumors [4]. Conditioning agents that support T-cell mitochondrial biogenesis [6], and small molecules that selectively impair oxidative phosphorylation in tumor cells [7] enhance the antitumor function of T-cells in melanoma. Reducing competition for glucose by genetically depleting tumor cell (but not T-cell) glucose transporter expression yielded less benefit. Thus, energy deficits from limited substrate availability may not always be the principal metabolic reason underlying T-cell hypofunction in cancer.

T-cell redox imbalances as measured by elevated NADH/NAD<sup>+</sup> ratios have also been observed in mouse models of melanoma [8]. All cells rely on the reducing power of NADH to support ATP synthesis in the electron transport chain (ETC). Reductive stress, as measured by excess NADH production, can occur when the ETC is impaired in high lactate environments and hypoxia. Reductive stress can also impact cytoplasmic metabolism, suppressing both glycolysis and serine production [9]. To date no study has addressed how reductive stress impacts antitumor function, particularly in activated CAR T-cells undergoing high rates of Warburg metabolism in hostile environments.

For these reasons, we devised an approach to “arm” T-cells with an enzyme that restores redox balance whilst simultaneously catalyzing the conversion of lactate to pyruvate. *Lactobacillus brevis* NADH oxidase (*LbNOX*) fulfills this dual role. The bacterial enzyme *LbNOX* was effectively repurposed as a genetic tool to regulate redox status in HeLa cells [10]. A mitochondrial form of *LbNOX* normalized NADH/NAD<sup>+</sup> ratios, decreased reductive stress, and rescued proliferative defects in fibroblasts treated with an inhibitor to complex 1 of the ETC [11]. A more recent study provided evidence that *LbNOX* restored redox balance in chronically stimulated mouse T-cells [8]. Collectively, these data support our hypothesis that heterologous *LbNOX* expression will restore functional competence to CAR T-cells traversing lactate-rich, hypoxic tumor environments.

Applying *LbNOX* to our cell culture and xenograft models allowed us to isolate the impact of lactate-induced reductive stress, independent of energy production, on the metabolic attributes and antitumor function of CAR T-cells. Understanding the relative importance of redox balance versus energy deficits is important to design metabolic strategies to advance CAR T-cell therapies against cancer. We found that *LbNOX*-expressing CAR T-cells have greater total oxygen consumption relative to control CAR T-cells, are strategically poised to oxidize lactate as a fuel in support of TCA cycle anaplerosis and withstand ETC inhibition. Despite these metabolic attributes, *LbNOX* expressing CAR T-cells displayed inferior tumor control in a xenograft model of mesothelioma, suggesting that T-cells depend on the coupling of NADH oxidation with ATP production by mitochondrial respiration.

## 2. Materials and Methods

### 2.1. Cell Culture

Primary human leukocytes (PBLs) from healthy male and female volunteers, averaging 34 years of age, were collected at the University of Pennsylvania's Apheresis Unit. Informed consent was obtained from all participants prior to collection. All methods and experimental procedures were approved by the University of Pennsylvania Institutional Review Board (Protocol #11705906). T-cells were purified at the University's Human Immunology Core by negative selection using the RosetteSep T-cell enrichment cocktail. Following isolation, T-cells were cultured in growth medium (GM) comprising RPMI 1640 (Lonza, Basel, Switzerland) supplemented with 10% FBS (Hyclone, Logan, UT, USA), 10 mM HEPES, 2 mM L-glutamine, 100 U/mL penicillin G, and 100 µg/mL streptomycin. For T-cell activation, 4.5 µm Dynabeads containing immobilized anti-human CD3 and anti-human CD28 (Life Technologies, Carlsbad, CA, USA) were used at a ratio of 3 beads to 1 cell. T cells were maintained in culture at a concentration of  $0.8\text{--}1.0 \times 10^6$  cells/mL through regular counting by flow cytometry using CountBright beads (BD Biosciences, Franklin Lakes, NJ, USA), a viability marker (Viaprobe) and mAbs to either human CD4 or CD8 as described O'Connor et al. [12]. Lymphocytes were cultured at 37 °C, 20% O<sub>2</sub>, and 95% humidity with 5% CO<sub>2</sub> unless otherwise stated.

A patient-derived human mesothelioma cell line (EM-meso), genetically engineered to stably express mesothelin and click beetle green (CBG) luciferase, has been previously described [2].

To isolate murine CD8+ T cells, spleens were harvested, and single-cell suspensions prepared by manual disruption and passage through a 70 mm cell strainer in PBS supplemented with 0.5% BSA and 2 mM EDTA. After red blood cell lysis, naive CD8+ T cells were purified by magnetic bead separation using commercially available kits following vendor instructions (Naive CD8a+T Cell Isolation Kit, mouse, Miltenyi Biotec Inc., Germany). Murine T-Cells were cultured in complete RPMI media (supplemented with 10% FBS, 100U/mL penicillin, 100 mg/mL streptomycin, and 50 mM 2-mercaptoethanol). For activation, T-cells were stimulated for 48 h with plate-bound anti-CD3 (10 mg/mL) and anti-CD28 (5 mg/mL) in complete media supplemented with recombinant IL-2 (100 U/mL). Cells were maintained in complete RPMI media supplemented with 100 U/mL recombinant IL-2. Metabolomics experiments were performed at day 4–5 post-activation.

### 2.2. *LbNOX* and *mitoLbNOX* Lentiviral Plasmid Construction

pTRPE is a bicistronic lentiviral vector containing a T2A ribosomal skipping sequence that separates two unique coding sequences that are co-translated as separate proteins. pTRPE\_eGFP contains the open reading frame for eGFP upstream of T2A permitting an accurate measurement of lentiviral-mediated gene delivery by flow cytometry. The second gene sequence is positioned within AVR11 and Sal1 restriction sites. Expression plasmids for *LbNOX* and *mito-LbNOX* that have been codon-optimized for mammalian cells were kindly provided by Dr. Vamsi Mootha. Using standard molecular biology techniques, a 1.417kb cDNA insert was PCR-amplified using PUC57-Lb LBNOX plasmid as a template with forward (5'-CGTCC**TAGG**ATGAAGGTCACCGTGGTCGGA-3') and reverse primers (5'-CGTGTCGAC**TTA**CTTGTCATCGTCATCC-3') containing built-in AVR11 (underlined) and Sal1 (underlined) restriction sites. The purified PCR product and pTRPE\_eGFP-T2A were digested with the relevant enzymes (NEB), gel purified, and ligated at a 3:1 insert:vector ratio using T4 DNA ligase to create a pTRPE\_eGFP-T2A\_*LbNOX* lentiviral plasmid. Similarly, a 1.484kb mitochondrial targeted LBNOX (*mitoLbNOX*) cDNA insert was PCR amplified using PUC57- *MitoLbNOX* as a template with forward (5'-AGCCTAGG**ATG**CTCGCTACAAGGGTCTTTA-3') and reverse primers (5'-CGTGTCGAC**TTA**CTTGTCATCGTCATCC-3') containing built-in Avr11 (underlined) and Sal1 (underlined) restriction sites. The purified PCR product and pTRPE\_eGFP-T2A were digested with the relevant enzymes (NEB), gel purified, and ligated at a 3:1 insert:vector ratio using T4 DNA ligase to create a pTRPE\_eGFP-T2A\_*mitoLbNOX* lentiviral

plasmid. In assessments of cell proliferation, enumeration was performed using bead-based counting methods following gating on GFP<sup>+</sup> cells.

### 2.3. Lentiviral Production

The lentiviral vector pTRPE encodes discrete gene products under the transcriptional control of EF-1  $\alpha$ . Lentiviral supernatants were generated by transient transfection of 293-T cells with pTRPE. Then, 293-T cells were initially seeded in T150 flasks and grown to 80% confluence in 25 mL of culture medium (RPMI1640), and 90  $\mu$ L Lipofectamine 2000 DNA transfection reagent was combined with 7  $\mu$ g pCL-VSVG, 18  $\mu$ g pRSV-REV, and 18  $\mu$ g of pGAG-POL (Nature Technology Corporation, Lincoln, NE, USA), as well as 15  $\mu$ g of pTRPE. This mixture was incubated at room temperature for 15 min. DNA-lipofectamine complexes were then added to the 293-T cells. After 24 h, infectious supernatants were sterile filtered through a 0.45- $\mu$ m syringe tip cellulose acetate filter and collected in a 50 mL conical tube. To pellet the lentivirus, the supernatant was spun in a Thermo Fisher Scientific Centrifuge (LYNX 4000) at 18,000 RCF, overnight, at 4 °C. The supernatant was removed, and the lentiviral pellet was resuspended in 1.6 mL of culture medium, aliquoted, and stored at –80 °C. The mesothelin-specific CAR lentiviral plasmid was previously described [5] and contains the SS1 scFv, CD8 $\alpha$  hinge, and CD8 $\alpha$  transmembrane domain linked to the CD28 costimulatory domain and the CD3 $\zeta$  signaling domain under the transcriptional control of an EF1 $\alpha$  promoter.

### 2.4. Lentiviral Infection

Primary human T-cells were activated with Dynabeads as described above. Furthermore, 24 h after activation, T cells were seeded at 100,000 cells/well at a concentration of  $1 \times 10^6$  cells/mL in a 96-well culture dish. Serial dilutions of lentiviral supernatant over a range of 1:3, 1:9, 1:27, 1:81, 1:243, and 1:729 were performed. Transduced T-cells were grown for 72 h to ensure optimal gene expression before comparing transduction efficiencies. The percentage of GFP<sup>+</sup> cells was determined by flow cytometry, and the corresponding titer was calculated as the number of transforming units/mL. The titers for pTRPE\_eGFP-T2A\_LbNOX and pTRPE\_eGFP-T2A\_MitoLbNOX viral supernatants were  $34.2 \times 10^6$  and  $35.5 \times 10^6$  TU/mL, respectively. T cells were infected with lentiviral vectors at multiplicities of infection from 3–5. Titers for the SS1 CAR lentivirus were  $58.3 \times 10^6$  TU/mL.

### 2.5. LDH Inhibition

LDH inhibitor NCGC00420737 was obtained from the NCI Experimental Therapeutics (NExT) Project team located in Bethesda, MD, USA [13]. A 10 mg aliquot of compound NCGC00420737 was added to 250  $\mu$ L of 0.1M NaOH. This solution was sonicated for 10 min. Then, 750  $\mu$ L of PBS was added and the solution was sonicated for an additional 10 min. Finally, the pH was adjusted to 7.5, and the solution was passed through a 0.2  $\mu$ m syringe filter.

### 2.6. Mitochondrial Respiratory Features as a Function of LbNOX Expression

Mitochondrial function was assessed using an extracellular flux analyzer (Agilent/Seahorse Bioscience, Santa Clara, CA, USA). Individual wells of an XF96 cell culture microplate were coated with CellTak in accordance with the manufacturer's instructions. The matrix was adsorped overnight at 37 °C, aspirated, air dried, and stored at 4 °C until use. Following overnight stimulation with Dynabeads, T-cells were LbNOX, and expanded for three days. To assay mitochondrial function, T cells were centrifuged at  $1200 \times g$  for 5 min. Cell pellets were re-suspended in XF assay medium (non-buffered RPMI 1640) containing 10 mM glucose, 2 mM L-glutamine, and 5 mM HEPES. T-cells were seeded at  $0.2 \times 10^6$  cell/well. During instrument calibration, the microplate was centrifuged at  $1000 \times g$  for 3 min and switched to a CO<sub>2</sub>-free, 37 °C incubator for 30 min. Cellular oxygen consumption rates (OCR) were measured under basal conditions and following

treatment with 20 mM sodium-L-lactate (MilliporeSigma St. Louis, MO, USA), 1.5  $\mu$ M fluoro-carbonyl cyanide phenylhydrazone (FCCP), and 500 nM rotenone/antimycin A.

### 2.7. Extracellular Acidification as a Function of LDHA Inhibition

To assess lactic acid production in EM-meso cancer cells,  $0.1 \times 10^6$  EM-meso cells were seeded onto uncoated XF96 microplates. The following day, the cells were washed in PBS, and the medium was switched to the customized XF assay medium described above. During instrument calibration, the microplate was switched to a CO<sub>2</sub>-free 37 °C incubator for 30 min. Extracellular acidification rates (ECAR) were measured under basal conditions and following treatment with 10m M glucose, 1.3  $\mu$ M oligomycin, varying concentrations of LDHi (5–50  $\mu$ M), and 20 mM 2-deoxyglucose (2-DG).

### 2.8. Anti-Mesothelin 28 $\zeta$ CAR T-Cell Cytolytic Function

T-cells were activated with Dynabeads as described above. Following overnight stimulation, activated T cells were co-infected with a 28 $\zeta$  CAR against mesothelin and either a eGFP control lentiviral vector or a vector expressing *LbNOX*. Mock infected (nontransduced) T-cells were used as a control. Activated T-cells were then expanded for 9 days until restdown (Cell size: 340–400 fL). EM-meso target cells were seeded at overnight in a U-bottom 96-well plate at 10,000 cells/well. The following day, CAR T-cells were added at established effector:target cell ratios of 3:1. CAR T-cell mediated killing, as measured by a decrease in the luciferase signal generated by live target cells, was assessed at 24 h. Briefly, Luciferin was added at a final concentration of 150  $\mu$ g/mL per well. Luminescence was measured after 10-min incubation using the Envision (PerkinElmer, Waltham, MA, USA) plate reader, and luciferase activity was expressed as relative luminescence units (RLUs). Note that target cells incubated in medium alone or treated with 1% SDS were used to calculate spontaneous cell death (RLU<sub>spont</sub>) or maximal cell death (RLU<sub>max</sub>), respectively. The percent specific lysis was calculated using the formula: % specific lysis =  $100 \times ([RLU_{spont} - RLU_{test}] / [RLU_{spont} - RLU_{max}])$ .

Mean luciferase activity (from at least 5 replicates) was calculated and compared across each treatment group. All data are presented as mean  $\pm$  SEM.

### 2.9. In Vivo Xenograft Studies

A xenograft model was used in this study as previously reported [5]. Briefly, 6–10-week-old NOD-SCID  $\gamma_c^{-/-}$  (NSG) mice, which lack an adaptive immune system, were obtained from Jackson Laboratories (Bar Harbor, ME, USA) or bred in-house under a protocol approved by the Institutional Animal Care and Use Committees of the University of Pennsylvania. Animals were assigned in all experiments to treatment/control groups using a randomized approach. Animals were injected subcutaneously with  $5 \times 10^6$  Em-meso tumor cells in 0.1 mL sterile PBS. After tumors reached  $>200 \mu\text{M}^2$ , mice were randomized to each treatment group. Anti-mesothelin CAR T-cells co-expressing either *LbNOX* or eGFP and non-transduced NTD human T-cells were injected I.V. at the indicated dose in 100  $\mu$ L of sterile PBS. Oral gavage (Ldhi vs. PBS vehicle) was performed (75 mg/kg twice weekly) and three times weekly (days 52–59) using an 18–20 G needle. Tumor size was measured biweekly using digital calipers.

### 2.10. Isotope Labeling

For lactate-labeled isotope experiments, T-cells were activated with Dynabeads as described above. Following overnight stimulation, the cells were expanded for 6 days with regular counting and feeding on alternate days. The medium was then switched to RPMI 1640, conditioned with 10% dialyzed FBS (Life Technologies, Carlsbad, CA, USA), and supplemented with 20 mM U-13C-Lactate (MilliporeSigma, MA, USA) for 1 h.

### 2.11. Short-Chain Acyl-CoA Extraction

Extractions were performed as described previously [14]. Briefly, lymphocytes were centrifuged at  $1200\times$  rcf for 5 min. Cell pellets were resuspended in 750  $\mu$ L of ice-cold 10% trichloroacetic acid and pulse-sonicated using a sonic dismembrator (Fisher Scientific, Hampton, NH, USA). The samples were centrifuged at  $15,000\times$  rcf for 15 min, and the supernatants were purified by solid phase extraction. Briefly, Oasis HLB 1-mL (30 mg) solid-phase extraction columns were conditioned with 1 mL methanol, followed by 1 mL of H<sub>2</sub>O. The supernatants were applied to the column and washed with 1 mL of H<sub>2</sub>O. The analytes were eluted in methanol containing 25 mM ammonium acetate. The eluates were dried overnight in N<sub>2</sub> gas and resuspended in 50  $\mu$ L of 5% 5-sulfosalicylic acid, and 10  $\mu$ L injections were applied in LC/ESI/MS/MS analysis.

### 2.12. Metabolite Extraction from Murine T-Cells

RPMI-1640 media without glucose and glutamine was supplemented with 10% dialyzed FBS, 100 U/mL penicillin, 100 mg/mL streptomycin, 50 mM 2-mercaptoethanol, and 100 U/mL recombinant IL-2. For <sup>13</sup>C-glucose incubation, it was supplemented with 11 mM U-<sup>13</sup>C-glucose and 2 mM glutamine; for <sup>13</sup>C-glutamine incubation, with 11 mM glucose and 2 mM U-<sup>13</sup>C-glutamine; and for <sup>13</sup>C-lactate incubation, with 11 mM glucose, 2 mM glutamine, and 20 mM U-<sup>13</sup>C-lactate.

Cells were seeded at 106 cells/mL and incubated for 24 h. They were then transferred to 1.5 mL Eppendorf tubes and pelleted (3 min,  $500\times$  g, RT). Media was removed by aspiration, and 500  $\mu$ L of PBS was added. Then, cells were pelleted (30 s,  $6000\times$  g, RT), PBS removed by aspiration, and metabolome extraction was performed by the addition of 100  $\mu$ L of cold methanol:water (80:20). The extract was incubated at  $-20$  °C for at least 30 min.

### 2.13. Analysis of Polar Metabolites in Murine T-Cells

After centrifugation (15 min, benchtop microfuge maximum speed, 4 °C), the clean supernatant was transferred to LC-MS vial for analysis. Samples were analyzed by reversed-phase ion-pairing chromatography coupled with negative-mode electrospray-ionization high-resolution MS on a stand-alone Orbitrap (ThermoFisher Exactive, Waltham, MA, USA) [15]. Data were analyzed using El-MAVEN software (Elucidata, Cambridge, MA, USA). Isotope labeling was corrected for natural <sup>13</sup>C abundance [16].

### 2.14. Analysis of Fatty Acids in Murine T-Cells

Cell extracts were saponified fatty acids extracted and analyzed by reversed-phase ion-pairing chromatography coupled with negative-mode electrospray-ionization high-resolution MS on a stand-alone Orbitrap (ThermoFisher Exactive, Waltham, MA, USA) [17]. Data were analyzed using El-MAVEN software (Elucidata, Cambridge, MA, USA). Isotope labeling was corrected for natural <sup>13</sup>C abundance (Su et al. [16]). Relative contribution of the various carbon sources to fatty acid synthesis was calculated using R by fitting the data into a zero truncated binomial distribution.

## 3. Results

NADH and its oxidized derivative NAD<sup>+</sup> support anabolic reactions in T-cells undergoing clonal expansion and differentiation. NAD<sup>+</sup>/NADH levels are highly regulated and exist in near-equilibrium with pyruvate and lactate. We used stable isotope labeling to trace the contribution of isotopically labeled (<sup>13</sup>C<sub>3</sub>) lactate to metabolic pathways in CAR T-cells. Activated T-cells were infected with a lentiviral CAR construct containing a mouse anti-human mesothelin scFv (SS1) linked to the human intracellular signaling domains CD28 and CD3 $\zeta$  (Figure S1A). As CAR signaling profoundly influences T-cell metabolic activities [1] and clinical efficacy [18], we included CARs engineered with 4-1BB signaling domains (Figure S1B) in our analyses. At day seven of stimulation, coinciding with the mid-phase of logarithmic growth, we transferred activated T-cells to a cell culture medium



### 3.1. Arming T-Cells with Exogenous, Futile NADH Oxidation Capacity

Given its central role in oxidation/reduction reactions, an increase in lactate metabolism can have important consequences on the intracellular redox state. Lactate can be immunosuppressive by potentiating reductive stress in hypoxic environments. We engineered CAR T-cells with a bacterial-derived NADH-dependent oxidase to support the use of lactate as a fuel and dissipate redox gradients causing stress. Our central hypothesis is shown in Figure 2A. Using NADH as a cofactor, *LbNOX* catalyzes the transfer of free electrons to oxygen. In cells engineered to overexpress *LbNOX*, the production of  $\text{NAD}^+$  will push the pyruvate/lactate equilibrium towards pyruvate production and NADH replenishment by mass action. *LbNOX* catalyzes the reaction  $\text{NADH} + \frac{1}{2} \text{O}_2 \rightarrow \text{NAD}^+ + \text{H}_2\text{O}$ . Coupled to lactate dehydrogenase, the net reaction is  $\text{lactate} + \frac{1}{2} \text{O}_2 \rightarrow \text{pyruvate} + \text{H}_2\text{O}$ . To study the potential benefit of *LbNOX* in primary human T-cells, we generated mitochondrial as well as cytoplasmic *LbNOX* lentiviral constructs (Figure 2B).

### 3.2. Cytoplasmic *LbNOX* Enhances T-Cell Oxidation

Previous studies showed that mitochondrial *LbNOX* improved oxidative function in fibroblasts [10]. To assess the impact of cytoplasmic versus mitochondrial *LbNOX* isoforms on T-cell redox status and substrate metabolism, we collected cellular supernatants from *LbNOX*-expressing T-cells undergoing log-phase expansion. *LbNOX* promotes NADH oxidation and can accordingly decrease the lactate/pyruvate ratio. Using LC-MS, we show that cytoplasmic *LbNOX* decreases the Lac/Pyr ratio by 63%, an effect largely driven by increased pyruvate, while mitochondrial *LbNOX* did not (Figure 2C). Consistent with these results, while both cytosolic and mitochondrial *LbNOX* increased oxygen consumption, cytosolic did so to a greater extent (Figure 2D).

We then measured the oxidative response to 20 mM lactate. Again, the respiratory response to lactate was accentuated in T-cells expressing the cytoplasmic rather than mitochondrial isoform of *LbNOX* (Figure 2E). Lactate increased OCR to 87, 141, and 278 pMoles  $\text{O}_2/\text{min}$  in GFP, mitoNOX, and *LbNOX*-expressing T cells, respectively (\*  $p < 0.05$  for mitoNOX versus GFP;  $p < 0.05$  for *LbNOX* relative to mitoNOX).

To simulate hypoxia, we measured the respiratory response to rotenone and antimycin A, inhibitors of the mitochondrial electron transport chain complex I and III, respectively. As seen in Figure 2D, *LbNOX*-expressing T-cells sustain higher rates of oxygen consumption (117% of their baseline OCR), whereas OCR levels in mitoNOX T-cells decreased to 70% of baseline, and OCR in control CAR T-cells diminished to 28% of baseline values. As the cytoplasmic isoform of *LbNOX* conferred superior metabolic attributes than its mitochondrial version, we pursued our studies with the cytoplasmic isoform only.

### 3.3. *LbNOX* Does Not Alter In Vitro CAR T-Cell Proliferation

In the clinical sector, CAR T-cells are propagated over several days to increase their quantity prior to adoptive cell transfer. We set out to compare proliferative rates in CAR T-cells infected with *LbNOX* or control lentiviral constructs. We first confirmed equivalent CAR expression across experimental groups. As seen in Figure 3A, 77% of T-cells were double positive for CAR as well as the eGFP control plasmid. Similarly, 75% of T-cells were double positive for CAR as well as *LbNOX*. In line with clinical manufacturing protocols, these cells were expanded for 10 days until restdown. The effect of *LbNOX* on CAR T-cell proliferation and survival was assessed by flow cytometry at regular intervals during their proliferative phase. *LbNOX* had no adverse effect on T-cell proliferation or survival (Figure 3B).

of lactate as a fuel and dissipate as redox gradients causing stress. Our central hypothesis is shown in Figure 2A. Using NADH as a cofactor, *LbNOX* catalyzes the transfer of free electrons to oxygen. In cells engineered to overexpress *LbNOX*, the production of  $\text{NAD}^+$  will push the pyruvate/lactate equilibrium towards pyruvate production and NADH replenishment by mass action. *LbNOX* catalyzes the reaction  $\text{NADH} + \frac{1}{2} \text{O}_2 \rightarrow \text{NAD}^+ + \text{H}_2\text{O}$ . Coupled to lactate dehydrogenase, the net reaction is  $\text{lactate} + \frac{1}{2} \text{O}_2 \rightarrow \text{pyruvate} + \text{H}_2\text{O}$ . To study the potential benefit of *LbNOX* in primary human T-cells, we generated mitochondrial as well as cytoplasmic *LbNOX* lentiviral constructs (Figure 2B).

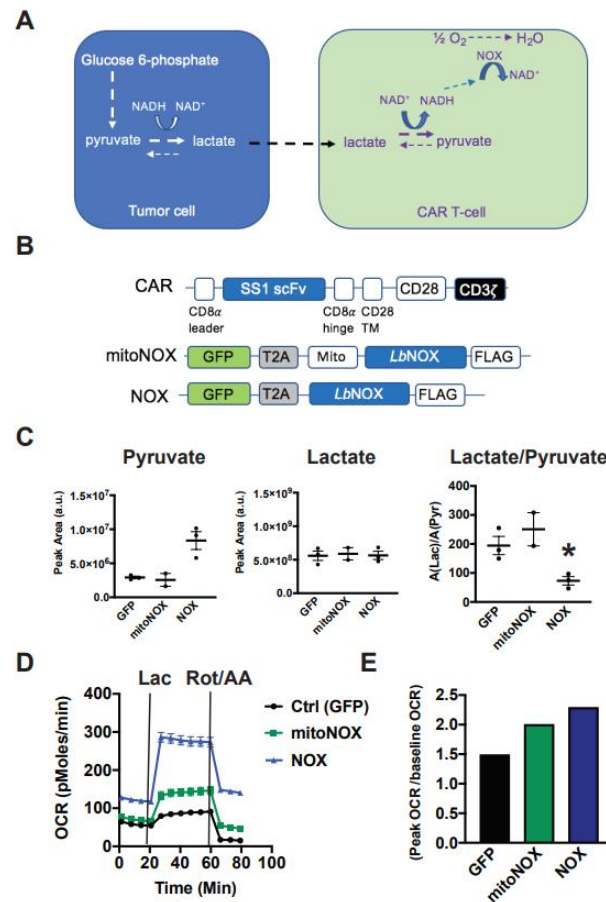


**Figure 2.** Cytoplasmic *Lactobacillus brevis* NADH Oxidase (*LbNOX*) reprograms T-cell metabolism towards lactate oxidation. **(A)** Our model proposing how *LbNOX* promotes lactate metabolism in CAR T-cells. Using NADH as a cofactor, *LbNOX* drives the vectorial flux of lactate to pyruvate in CAR T-cells. **(B)** Schematic representation of the mesothelin lentiviral CAR containing an SS1 single chain variable fragment (scFv), which is linked via a CD8 $\alpha$  hinge, as well as a CD28 TM to the CD28 and CD3 $\zeta$  intracellular signaling domains. TM, transmembrane. *LbNOX* is a bicistronic lentiviral construct containing the coding sequence for *LbNOX*, linked via T2A to the transduction marker GFP. A lentiviral construct encoding the mitochondrial (mito) NOX isoform is also shown. **(C)** After overnight stimulation with Dynabeads, activated T-cells were infected with either cytoplasmic or mito *LbNOX* lentivirus. Cellular supernatants were collected from NOX-expressing T-cells undergoing log-phase expansion. Lactate, as well as pyruvate levels, was compared by LC-MS. Mean values  $\pm$  S.E.M are plotted with the horizontal bars representing the mean and each symbol representing a separate donor from independent experiments. The lactate/pyruvate ratio was significantly decreased in *LbNOX* relative to GFP (\*  $p < 0.05$ ). Statistical comparisons were performed using an unpaired Student's  $t$  test. **(D)** After overnight stimulation with Dynabeads, activated T-cells were infected with either cytoplasmic or mito *LbNOX* lentiviral supernatants. These cells were expanded for 3 days and then transferred to bicarbonate-free XF assay medium. Metabolic parameters were measured by a Seahorse assay. Cellular oxygen consumption rates (OCR) were measured at baseline and following the serial addition of 20 mM lactate and 500 nM rotenone/antimycin A. Values are means  $\pm$  S.E.M. from 7–8 replicates. Values are representative of 2 independent experiments. Baseline OCR levels were significantly increased in mitoNOX relative to GFP ( $p < 0.05$ ); *LbNOX* relative to GFP ( $p < 0.05$ ); and *LbNOX* relative to mitoNOX ( $p < 0.05$ ). Lactate-stimulated OCR levels were significantly increased in mitoNOX relative to GFP ( $p < 0.05$ ); *LbNOX* relative to GFP ( $p < 0.05$ ); and *LbNOX* relative to mitoNOX ( $p < 0.05$ ). Data were analyzed by a one-way ANOVA using a Holm–Sidak multiple comparison post hoc test. **(E)** Energy reserve (peak OCR/baseline OCR) as a function of *LbNOX* is shown. Values are calculated from the data illustrated in panel D.

double positive for CAR as well as the eGFP control plasmid. Similarly, 75% of T-cells were double positive for CAR as well as *LbNOX*. In line with clinical manufacturing protocols, these cells were expanded for 10 days until restdown. The effect of *LbNOX* on CAR T-cell proliferation and survival was assessed by flow cytometry at regular intervals during their proliferative phase. *LbNOX* had no adverse effect on T-cell proliferation or survival (Figure 3B).

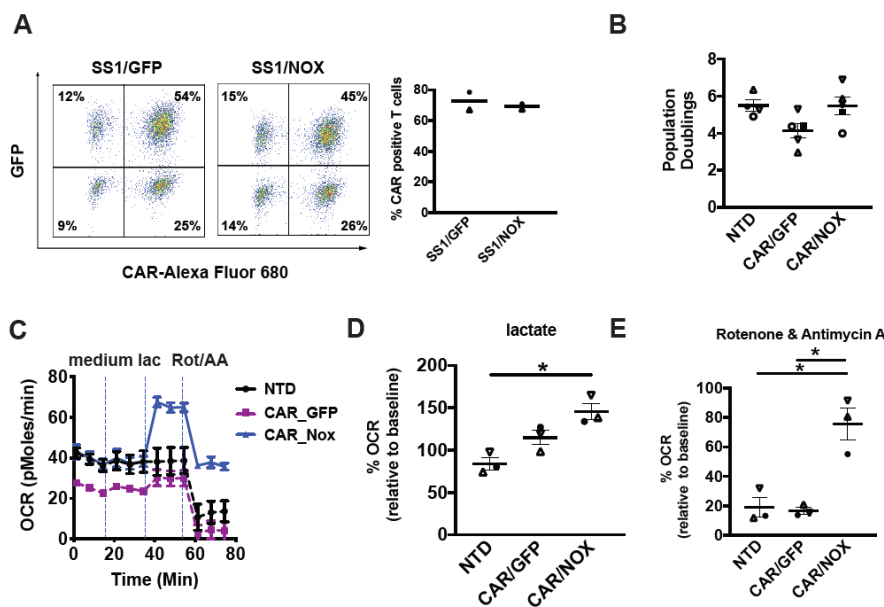


**Figure 3.** *Lactobacillus brevis* NADH Oxidase (*LbNOX*)-expressing CAR T-cells maintain high rates of oxygen consumption despite electron transport chain (ETC) inhibition. (A) After overnight stimulation with Dynabeads, T-cells were co-infected with a mesothelin-specific (SS1-28z) CAR and *LbNOX* lentiviral supernatants, or T-cells were co-infected with a mesothelin-specific (SS1-28z) CAR and GFP lentiviral supernatants. The expanded cells were cultured for 5 days. CAR expression was measured by staining as either by staining with anti-biotinylated GFP (left) or anti-CD28 (right) (SS1) and by staining with anti-Alexa Fluor 680 labeling CAR. Cells were gated for GFP expression. CAR+ T-cells were defined as double positive for *LbNOX* (Y-axis) and APC (X-axis). Representative flow plots and mean frequencies  $\pm$  SEM from two independent experiments with separate donors are shown (left and right panels, respectively). (B) After overnight stimulation with Dynabeads, activated T-cells were co-infected with a mesothelin-specific (SS1-28z) CAR and *LbNOX* lentiviral supernatants. Cell enumeration was performed every other day beginning on day 3 until the number of cells in the culture ceased increasing, and the number of cells was low (day 10). The maximum number of population doublings and the number of population doublings are plotted with the horizontal bars representing the mean and each symbol representing a separate donor. (C) *LbNOX*-expressing CAR T-cells were expanded for 5 days and then transferred to Seahorse medium containing 10 mM glucose and 2 mM glutamine and 2 mM glutamine. Metabolic parameters were measured with a Seahorse assay. Cellular oxygen consumption rates (OCR) were measured at baseline, and following the serial addition of XF assay medium, 20 mM lactate and 500 nM rotenone/antimycin A. Representative data from 3 independent experiments with separate donors are shown. Values are means  $\pm$  S.E.M from 6–8 replicates per assay. (D) OCR levels following lactate treatment are expressed as a percentage of baseline OCR. These are plotted with the horizontal bars representing the mean and each symbol representing a separate donor. (E) OCR levels following rotenone and antimycin A treatment are expressed as a percentage of baseline OCR. These are plotted with the horizontal bars representing the mean and each symbol representing a separate donor. \* p < 0.05 for CAR/NOX vs. NTD. (F) OCR levels following rotenone and antimycin A treatment are expressed as a percentage of baseline OCR. These are plotted with the horizontal bars representing the mean and each symbol representing a separate donor. \* p < 0.05 for CAR/NOX vs. NTD. (G) OCR levels following rotenone and antimycin A treatment are expressed as a percentage of baseline OCR. These are plotted with the horizontal bars representing the mean and each symbol representing a separate donor. \* p < 0.05 for CAR/NOX vs. NTD. All data were analyzed by ANOVA using a Holm–Sidak multiple comparison post hoc test.

**3.4. *LbNOX*-Expressing CAR-T Cells Sustain Oxidative Metabolism despite ETC Inhibition**  
 Given their individual impact on T-cell metabolic activity, we examined how *LbNOX* and CD28-CAR co-expression impacts metabolism. With respect to CAR design, the CD28 signaling domain was preferred to 4-1BB as it confers superior effector function in several CD28 signaling domain was preferred to 4-1BB as it confers superior effector function in several solid tumors tumor models including mesothelioma [5] and glioblastoma [19]. We co-infected activated T-cells with a mesothelin-specific 28zCAR lentivirus along with *LbNOX* or GFP control lentivirus. After several days of expansion, the metabolic properties of *LbNOX* expressing CAR T-cells were tested by Seahorse assay. As seen in Figure 3C, baseline levels of oxygen consumption are higher in *LbNOX*-expressing CAR T-cells rel-

ative to control (GFP-expressing CAR T-cells). Interestingly, constitutive expression of a 28 $\zeta$  CAR leads to lower baseline levels of oxidative metabolism relative to nontransduced controls. These findings corroborate our prior work demonstrating an increased emphasis of glycolysis over oxidative phosphorylation in 28 $\zeta$  CAR T-cells [1]. As oxygen consumption increases in line with substrate metabolism, we measured OCR in cells treated with medium alone or medium containing 20 mM lactate. We show that *LbNOX* enhanced lactate-induced oxygen consumption by 141% (Figure 3D). As oxygen is critically limiting in solid tumors, we tested the ability of *LbNOX* CAR T-cells to maintain oxidative function in hypoxia-like conditions. To simulate the disruptive effects of hypoxia on respiratory function and oxidative metabolism, we treated CAR T-cells with rotenone and antimycin A. As seen in Figure 3E, *LbNOX*-expressing CAR T-cells maintain 91% of their baseline OCR ( $36.5 \pm 0.6$  pMoles/min), whereas OCR in control CAR T-cells decreases to 15% of baseline values ( $3.8 \pm 0.4$  pMoles/min).

### 3.5. *LbNOX*-Expressing CAR T-Cells Are Resilient to LDH Inhibition

As *LbNOX* catalyzes the oxidation of NADH to NAD<sup>+</sup>, we tested its ability to rescue cytotoxicity in CAR T-cells treated with an LDH inhibitor. We reasoned that tumor cell glycolytic function could be selectively impaired by LDH inhibition if the corresponding CAR T-cells had a “built-in” mechanism to replenish NAD<sup>+</sup>. We used the LDH inhibitor NCGC00420737 to impair glycolytic function in EM-meso cells (Figure 4A,B). Inhibiting glycolysis with *Ldhi* significantly impeded tumor cell proliferation in vitro (Figure 4C). In cytotoxicity assays, *LbNOX*-expressing CAR T-cells retained complete functional competence despite LDH inhibition (Figure 4D).

We next evaluated the antitumor function of *LbNOX* expressing CAR T-cells, with/without *Ldhi* using our well-established human xenograft model of mesothelioma. EM-meso xenografts establish an immune-suppressive tumor environment enriched with immune and metabolic checkpoints. Infused CAR T-cells effectively traffic to EM-meso tumors. Despite undergoing robust proliferation, their antitumor function is severely limited [5]. The experimental layout for testing the efficacy of anti-mesothelin CAR T-cells in this model is illustrated in Figure 5A. *LbNOX*-expressing, anti-mesothelin 28 $\zeta$ CAR-T cells were expanded over 10 days until restdown. CARs were expressed in 90% of T-cells in the control group. In the *LbNOX* group, 87% of T-cells expressed CAR. As seen in Figure 5B, 60% of T-cells were double positive for CAR as well as the GFP control plasmid. In the other experimental group, 74% of T-cells were double positive for CAR as well as *LbNOX*. To establish mesothelin xenografts, immunodeficient mice were subcutaneously injected with  $5 \times 10^6$  EM-meso tumor cells. After tumors reached 200 mm<sup>3</sup>,  $5 \times 10^6$  GFP or *LbNOX*-expressing CAR T-cells were injected intravenously. Tumor growth was monitored regularly over the next 50 days. As expected, EM-meso xenografts grew exponentially over time. Control T-cells (no CAR) had minimal impact on tumor cell growth (Figure 5D). Overall tumor volume was significantly reduced in tumor-bearing mice infused with CAR transduced T-cells (\*  $p < 0.05$  for CAR/GFP vs. NTD). Tumor control was incomplete but sustained through day 48 in this group (Figure 5D,E). *LbNOX*-expressing CAR T-cells also demonstrated significant tumor clearance ( $p < 0.05$  for CAR/NOX vs. NTD); however, overall tumor burden remained higher than CAR T-cells alone (Figure 5D–F). Despite the potential for additive benefits from CAR T-directed cytotoxicity with *Ldhi*, we observed no additive benefit of *Ldhi* and CAR against tumor growth in our xenograft model of mesothelioma (Figure S3).

glycolytic function was selectively impaired by LDH inhibition in the context of CAR T-cells had a “built-in” mechanism to replenish NAD<sup>+</sup>. We used the LDH inhibitor NCGC00420737 to impair glycolytic function in EM-meso cells (Figure 4A,B). In glycolysis with Ldhi significantly impeded tumor cell proliferation in vitro (Figure 4C). In cytotoxicity assays, LbNOX-expressing CAR T-cells retained complete functional competence despite LDH inhibition (Figure 4D).

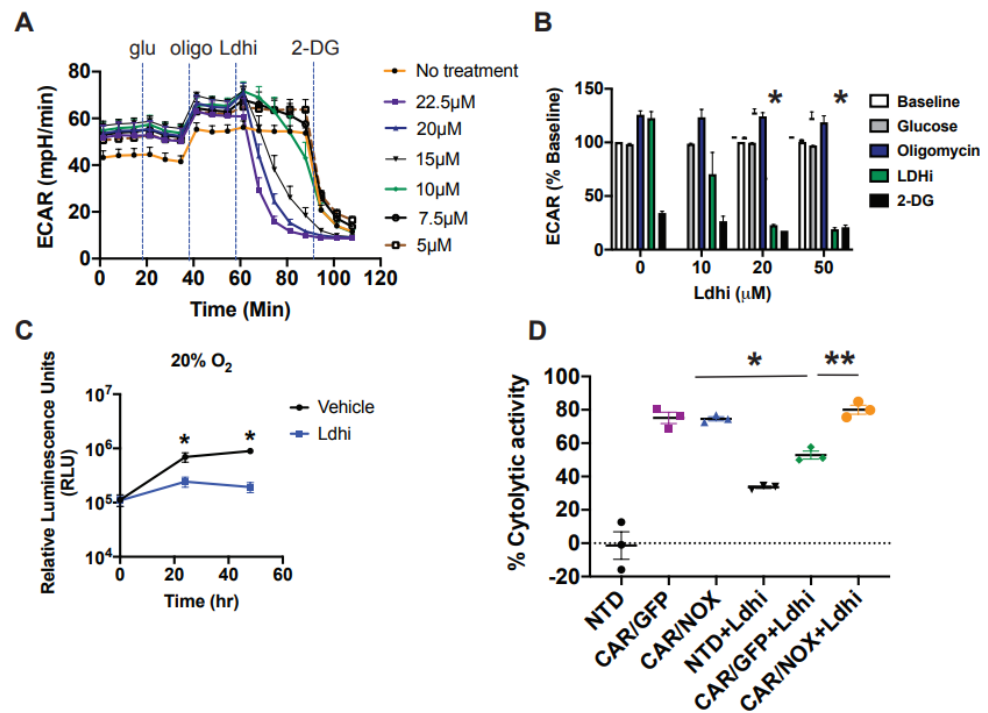


**Figure 4.** *Lactobacillus brevis* NADH:FMN oxidase (Ldhi) rescues CAR T-cell cytotoxicity in culture treated following Lactate Dehydrogenase (LDH) inhibition (A–B). The metabolic properties of EM-meso cells were measured by a Seahorse assay. Extracellular acidification rates (ECAR) following the serial addition of 20 mM glucose, 1.5 μM oligomycin, Ldhi, and 20 mM 2-DG are shown in a representative Seahorse plot (left panel). Inhibiting LDH (Ldhi) reduces EM-meso cell glycolytic activity in a dose-dependent manner. Mean ± SEM values from multiple independent experiments with separate donors ( $n = 2–3$ ) are shown (right panel). Ldhi ECAR values were measured 33 min following Ldhi injection and 20 μM Ldhi significantly reduced glycolytic activity relative to vehicle control ( $* p < 0.05$ ). Statistical comparisons were compared using an unpaired Student's  $t$  test.

(C) EM-meso-CBG cells were seeded in triplicate in 96-well plates and treated with either the vehicle or 20 μM Ldhi. Their growth was measured by a luminescent assay. The mean ± S.E.M. values of 3 independent experiments are shown.  $* p < 0.05$  for Ldhi vs. the vehicle at 24 h and 48 h. (D) The specific cytotoxicity of anti-mesothelin CAR T-cells was measured by luciferase-based killing assay. CAR T-cells were co-cultured with EM-meso cells at a 3:1 effector: target cell ratio for 22 h in medium conditioned with 20 μM Ldhi. The mean ± S.E.M. values of 3 independent experiments with separate donors are shown.  $* p < 0.05$  for CAR/GFP vs. CAR/GFP+Ldhi;  $** p < 0.05$  for CAR/GFP+Ldhi vs. CAR/NOX+Ldhi. Data were analyzed by a two-way ANOVA using a Newman–Keuls multiple comparison post hoc test.



Strategies to enhance T-cell metabolic fitness have shown promise in a number of preclinical models. Limiting Warburg metabolism by inhibiting hexokinase [20], LDH [21], P38MAPK [22], arginine conditioning [23], and glucose restriction [24] improves the metabolic, phenotypic, and functional features of cultured T-cells. An inherent limitation shared by these approaches is that they are confined to the ex vivo expansion phase prior to adoptive transfer. Developing approaches to overcome the metabolic nature of the TME requires a deeper understanding of the mechanisms limiting metabolic fitness in situ.

Intra-tumoral hypoxia correlates with T-cell hypofunction and poor response to PD-1 blockade in syngeneic models of melanoma [7]. Restoring access to oxygen rather than glucose enhanced T-cell antitumor function, implicating oxygen as a critical metabolite for tumor-infiltrating lymphocytes. Our data provide mechanistic insight into the oxygen requirements of T-cells traversing solid tumors: the benefits of oxygen may be inextricably tied to its role in ATP replenishment. Future studies may reveal how CAR design influences the effectiveness of *LbNOX* following adoptive transfer. While we focused our attention on CD28 costimulation, the inherent ability of 4-1BB or ICOS to sustain high rates of oxidative phosphorylation, along with their contingency energy reserve, would likely extend CAR T-cell persistence and survival in solid tumors. Alleviating reductive stress (*LbNOX*) in CAR T-cells geared for long-term immunosurveillance, with enhanced energy-generating capacity, may be a better strategy for success against solid tumors.

We show that  $^{13}\text{C}_3$  lactate supports TCA cycle anaplerosis and short chain CoA synthesis in CAR T-cells (Figure 1), challenging the widely-accepted belief that lactate is inherently immunosuppressive [25,26]. In vivo, tumor cells may co-opt select monocarboxylate transporters to restrict access to local lactate pools, sequestering it for their own benefit [27].

To effectively use lactate as fuel instead of glucose, cells require a functional electron transport chain to generate ATP from NADH. Expressing *LbNOX* constitutively may deplete NADH and thus aerobic ATP production. Elevated NAD may also drive enhanced rates of glycolysis during ex vivo expansion; committing CAR T-cells to an effector differentiated program prior to adoptive transfer. We previously showed that short-lived glycolytic effector CAR T-cells have limited therapeutic potential due to poor engraftment and impaired persistence following infusion [1]. By avoiding such in vitro reprogramming, the controlled induction of *LbNOX* after adoptive transfer may have benefits that are not captured in the present constitutive expression experiments.

Taken together, our findings highlight the challenges in developing strategies targeting individual aspects of metabolic dysfunction in solid tumors. The decoupling of NADH oxidation and ATP production was ineffective. Metabolic enhancements that maintain such coupling are future priorities.

**Supplementary Materials:** The following are available online at <https://www.mdpi.com/article/10.3390/cells10092334/s1>, Figure S1: CAR Design, Figure S2: Lactate supports long chain fatty acid synthesis in murine T cells, Figure S3: Nonadditive effect of Lactate Dehydrogenase inhibition (Ldhi) with CAR T-cells in vivo, Video S1: CAR T-cells depend on coupling of NADH oxidation with ATP production.

**Author Contributions:** J.D.R., R.S.O., J.C.G.-C. and C.H.J. designed the research. R.S.O., J.C.G.-C., D.H., C.X., S.T., J.L. and S.G. performed the experiments. R.S.O., J.C.G.-C., S.G., S.T., B.I.P., N.W.S., J.D.R., M.C.M. and E.K.M., analyzed the data. R.S.O., J.C.G.-C. and J.D.R. wrote the manuscript. NCGC00420737 was kindly provided by the NCI Experimental Therapeutics (NExT) LDHA project team. All authors have read and agreed to the published version of the manuscript.

**Funding:** R.S.O. is supported by an NIH grant RO1CA226983-04 awarded to C.H.J. This work was also supported by a St. Baldrick's Foundation Scholar Award (587296) and a National Blood Foundation (NBF) Early Career Scientific Research Grant to S.G.

**Institutional Review Board Statement:** The study was conducted according to the guidelines of the Declaration of Helsinki, and approved by the University of Pennsylvania Institutional Review Board (protocol code Protocol #11705906, which was last updated on 12 October 2020).

**Informed Consent Statement:** Informed consent was obtained from all subjects involved in the study as described in the Methods section.

**Data Availability Statement:** The data presented in this study are available on request from the corresponding author.

**Acknowledgments:** The authors thank Yinan Lu, Ai Wang, Andre Kelly, and Lili Guo for expert technical assistance. We thank Ulf Beier for helpful discussions.

**Conflicts of Interest:** R.S.O., S.G., M.C.M. and C.H.J. are inventors on several granted and pending patents related to CAR T cells and their use for cancer therapy.

## References

1. Kawalekar, O.U.; O'Connor, R.S.; Fraietta, J.A.; Guo, L.; McGettigan, S.E.; Posey, A.D., Jr.; Patel, P.R.; Guedan, S.; Scholler, J.; Keith, B.; et al. Distinct Signaling of Coreceptors Regulates Specific Metabolism Pathways and Impacts Memory Development in CAR T Cells. *Immunity* **2016**, *44*, 380–390. [[CrossRef](#)]
2. Moon, E.K.; Wang, L.-C.; Dolfi, D.V.; Wilson, C.B.; Ranganathan, R.; Sun, J.; Kapoor, V.; Scholler, J.; Puré, E.; Milone, M.C.; et al. Multifactorial T-cell Hypofunction That Is Reversible Can Limit the Efficacy of Chimeric Antigen Receptor–Transduced Human T cells in Solid Tumors. *Clin. Cancer Res.* **2014**, *20*, 4262–4273. [[CrossRef](#)]
3. Schietinger, A.; Delrow, J.J.; Basom, R.S.; Blattman, J.N.; Greenberg, P.D. Rescued Tolerant CD8 T Cells Are Preprogrammed to Reestablish the Tolerant State. *Science* **2012**, *335*, 723–727. [[CrossRef](#)]
4. Scharping, N.E.; Menk, A.V.; Moreci, R.S.; Whetstone, R.D.; Dadey, R.E.; Watkins, S.C.; Ferris, R.L.; Delgoffe, G.M. The Tumor Microenvironment Represses T Cell Mitochondrial Biogenesis to Drive Intratumoral T Cell Metabolic Insufficiency and Dysfunction. *Immunity* **2016**, *45*, 701–703. [[CrossRef](#)]
5. Wang, E.; Wang, L.-C.; Tsai, C.-Y.; Bhoj, V.; Gershenson, Z.; Moon, E.; Newick, K.; Sun, J.; Lo, A.; Baradet, T.; et al. Generation of Potent T-cell Immunotherapy for Cancer Using DAP12-Based, Multichain, Chimeric Immunoreceptors. *Cancer Immunol. Res.* **2015**, *3*, 815–826. [[CrossRef](#)]
6. Menk, A.V.; Scharping, N.E.; Rivadeneira, D.B.; Calderon, M.J.; Watson, M.J.; Dunstane, D.; Watkins, S.C.; Delgoffe, G.M. 4-1BB costimulation induces T cell mitochondrial function and biogenesis enabling cancer immunotherapeutic responses. *J. Exp. Med.* **2018**, *215*, 1091–1100. [[CrossRef](#)] [[PubMed](#)]
7. Scharping, N.E.; Menk, A.V.; Whetstone, R.D.; Zeng, X.; Delgoffe, G.M. Efficacy of PD-1 Blockade Is Potentiated by Metformin-Induced Reduction of Tumor Hypoxia. *Cancer Immunol. Res.* **2017**, *5*, 9–16. [[CrossRef](#)] [[PubMed](#)]
8. Vardhana, S.A.; Hwee, M.A.; Berisa, M.; Wells, D.K.; Yost, K.E.; King, B.; Smith, M.; Herrera, P.S.; Chang, H.Y.; Satpathy, A.T.; et al. Impaired mitochondrial oxidative phosphorylation limits the self-renewal of T cells exposed to persistent antigen. *Nat. Immunol.* **2020**, *21*, 1022–1033. [[CrossRef](#)]
9. Quinn, W.J., 3rd; Jiao, J.; TeSlaa, T.; Stadanlick, J.; Wang, Z.; Wang, L.; Akimova, T.; Angelin, A.; Schäfer, P.M.; Cully, M.D.; et al. Lactate Limits T Cell Proliferation via the NAD(H) Redox State. *Cell Rep.* **2020**, *33*, 108500. [[CrossRef](#)]
10. Titov, D.V.; Cracan, V.; Goodman, R.P.; Peng, J.; Grabarek, Z.; Mootha, V.K. Complementation of mitochondrial electron transport chain by manipulation of the NAD<sup>+</sup>/NADH ratio. *Science* **2016**, *352*, 231–235. [[CrossRef](#)] [[PubMed](#)]
11. Cracan, V.; Titov, D.V.; Shen, H.; Grabarek, Z.; Mootha, V.K. A genetically encoded tool for manipulation of NADP<sup>+</sup>/NADPH in living cells. *Nat. Chem. Biol.* **2017**, *13*, 1088–1095. [[CrossRef](#)]
12. O'Connor, R.S.; Hao, X.; Shen, K.; Bashour, K.; Akimova, T.; Hancock, W.W.; Kam, L.C.; Milone, M.C. Substrate rigidity regulates human T cell activation and proliferation. *J. Immunol.* **2012**, *189*, 1330–1339. [[CrossRef](#)] [[PubMed](#)]
13. Rai, G.; Urban, D.J.; Mott, B.T.; Hu, X.; Yang, S.-M.; Benavides, G.A.; Johnson, M.S.; Squadrito, G.L.; Brimacombe, K.R.; Lee, T.D.; et al. Pyrazole-Based Lactate Dehydrogenase Inhibitors with Optimized Cell Activity and Pharmacokinetic Properties. *J. Med. Chem.* **2020**, *63*, 10984–11011. [[CrossRef](#)] [[PubMed](#)]
14. Guo, L.; Shestov, A.A.; Worth, A.J.; Nath, K.; Nelson, D.S.; Leeper, D.B.; Glickson, J.D.; Blair, I.A. Inhibition of mitochondrial complex II by the anti-cancer agent lonidamine. *J. Biol. Chem.* **2016**, *291*, 42–57. [[CrossRef](#)] [[PubMed](#)]
15. Lu, W.; Clasquin, M.F.; Melamud, E.; Amador-Noguez, D.; Caudy, A.; Rabinowitz, J.D. Metabolomic Analysis via Reversed-Phase Ion-Pairing Liquid Chromatography Coupled to a Stand Alone Orbitrap Mass Spectrometer. *Anal. Chem.* **2010**, *82*, 3212–3221. [[CrossRef](#)]
16. Su, X.; Lu, W.; Rabinowitz, J.D. Metabolite Spectral Accuracy on Orbitraps. *Anal. Chem.* **2017**, *89*, 5940–5948. [[CrossRef](#)]
17. Kamphorst, J.J.; Fan, J.; Lu, W.; White, E.; Rabinowitz, J.D. Liquid Chromatography–High Resolution Mass Spectrometry Analysis of Fatty Acid Metabolism. *Anal. Chem.* **2011**, *83*, 9114–9122. [[CrossRef](#)] [[PubMed](#)]
18. June, C.H.; O'Connor, R.S.; Kawalekar, O.U.; Ghassemi, S.; Milone, M.C. CAR T cell immunotherapy for human cancer. *Science* **2018**, *359*, 1361–1365. [[CrossRef](#)]
19. Wang, D.; Starr, R.; Chang, W.-C.; Aguilar, B.; Alizadeh, D.; Wright, S.L.; Yang, X.; Brito, A.; Sarkissian, A.; Ostberg, J.R.; et al. Chlorotoxin-directed CAR T cells for specific and effective targeting of glioblastoma. *Sci. Transl. Med.* **2020**, *12*, eaaw2672. [[CrossRef](#)]

20. Fraietta, J.A.; Lacey, S.F.; Orlando, E.J.; Pruteanu-Malinici, I.; Gohil, M.; Lundh, S.; Boesteanu, A.C.; Wang, Y.; O'Connor, R.S.; Hwang, W.-T.; et al. Determinants of response and resistance to CD19 chimeric antigen receptor (CAR) T cell therapy of chronic lymphocytic leukemia. *Nat. Med.* **2018**, *24*, 563–571. [[CrossRef](#)]
21. Hermans, D.; Gautam, S.; García-Cañaveras, J.C.; Gromer, D.; Mitra, S.; Spolski, R.; Li, P.; Christensen, S.; Nguyen, R.; Lin, J.-X.; et al. Lactate dehydrogenase inhibition synergizes with IL-21 to promote CD8+T cell stemness and antitumor immunity. *Proc. Natl. Acad. Sci. USA* **2020**, *117*, 6047–6055. [[CrossRef](#)] [[PubMed](#)]
22. Gurusamy, D.; Henning, A.N.; Yamamoto, T.N.; Yu, Z.; Zacharakis, N.; Krishna, S.; Kishton, R.J.; Vodnala, S.K.; Eidizadeh, A.; Jia, L.; et al. Multi-phenotype CRISPR-Cas9 Screen Identifies p38 Kinase as a Target for Adoptive Immunotherapies. *Cancer Cell* **2020**, *37*, 818–833.e9. [[CrossRef](#)]
23. Geiger, R.; Rieckmann, J.C.; Wolf, T.; Basso, C.; Feng, Y.; Fuhrer, T.; Kogadeeva, M.; Picotti, P.; Meissner, F.; Mann, M.; et al. L-Arginine Modulates T Cell Metabolism and Enhances Survival and Anti-tumor Activity. *Cell* **2016**, *167*, 829–842.e13. [[CrossRef](#)]
24. Klein Geltink, R.I.; Edwards-Hicks, J.; Apostolova, P.; O'Sullivan, D.; Sanin, D.E.; Patterson, A.E.; Puleston, D.J.; Lighthart, N.A.M.; Buescher, J.M.; Grzes, K.M.; et al. Metabolic conditioning of CD8(+) effector T cells for adoptive cell therapy. *Nat. Metab.* **2020**, *2*, 703–716. [[CrossRef](#)] [[PubMed](#)]
25. Fischer, K.; Hoffmann, P.; Voelkl, S.; Meidenbauer, N.; Ammer, J.; Edinger, M.; Gottfried, E.; Schwarz, S.; Rothe, G.; Hoves, S.; et al. Inhibitory effect of tumor cell-derived lactic acid on human T cells. *Blood* **2007**, *109*, 3812–3819. [[CrossRef](#)] [[PubMed](#)]
26. Brand, A.; Singer, K.; Koehl, G.E.; Kolitzus, M.; Schoenhammer, G.; Thiel, A.; Matos, C.; Bruss, C.; Klobuch, S.; Peter, K.; et al. LDHA-Associated Lactic Acid Production Blunts Tumor Immunosurveillance by T and NK Cells. *Cell Metab.* **2016**, *24*, 657–671. [[CrossRef](#)] [[PubMed](#)]
27. García-Cañaveras, J.C.; Chen, L.; Rabinowitz, J.D. The Tumor Metabolic Microenvironment: Lessons from Lactate. *Cancer Res.* **2019**, *79*, 3155–3162. [[CrossRef](#)]

# Enhancing CAR T function with the engineered secretion of *C. perfringens* neuraminidase

Joseph S. Durgin,<sup>2,4</sup> Radhika Thokala,<sup>1,2</sup> Lexus Johnson,<sup>2,4</sup> Edward Song,<sup>2,4</sup> John Leferovich,<sup>2,4</sup> Vijay Bhoj,<sup>2,4</sup> Saba Ghassemi,<sup>2,4</sup> Michael Milone,<sup>2,4</sup> Zev Binder,<sup>1,3</sup> Donald M. O'Rourke,<sup>1,3</sup> and Roddy S. O'Connor<sup>2,4</sup>

<sup>1</sup>Glioblastoma Translational Center of Excellence, The Abramson Cancer Center, Perelman School of Medicine at the University of Pennsylvania, Philadelphia, PA, USA; <sup>2</sup>Center for Cellular Immunotherapies, Perelman School of Medicine at the University of Pennsylvania, 3400 Civic Center Boulevard, Building 421, SPE 8-105, Philadelphia, PA, USA; <sup>3</sup>Department of Neurosurgery, Perelman School of Medicine at the University of Pennsylvania, Philadelphia, PA, USA; <sup>4</sup>Department of Pathology & Laboratory Medicine, Perelman School of Medicine at the University of Pennsylvania, Philadelphia, PA, USA

**Prior to adoptive transfer, CAR T cells are activated, lentivirally infected with CAR transgenes, and expanded over 9 to 11 days. An unintended consequence of this process is the progressive differentiation of CAR T cells over time in culture. Differentiated T cells engraft poorly, which limits their ability to persist and provide sustained tumor control in hematologic as well as solid tumors. Solid tumors include other barriers to CAR T cell therapies, including immune and metabolic checkpoints that suppress effector function and durability. Sialic acids are ubiquitous surface molecules with known immune checkpoint functions. The enzyme *C. perfringens* neuraminidase (*CpNA*) removes sialic acid residues from target cells, with good activity at physiologic conditions. In combination with galactose oxidase (GO), NA has been found to stimulate T cell mitogenesis and cytotoxicity *in vitro*. Here we determine whether *CpNA* alone and in combination with GO promotes CAR T cell antitumor efficacy. We show that *CpNA* restrains CAR T cell differentiation during *ex vivo* culture, giving rise to progeny with enhanced therapeutic potential. CAR T cells expressing *CpNA* have superior effector function and cytotoxicity *in vitro*. In a Nalm-6 xenograft model of leukemia, CAR T cells expressing *CpNA* show enhanced antitumor efficacy. Arming CAR T cells with *CpNA* also enhanced tumor control in xenograft models of glioblastoma as well as a syngeneic model of melanoma. Given our findings, we hypothesize that charge repulsion via surface glycans is a regulatory parameter influencing differentiation. As T cells engage target cells within tumors and undergo constitutive activation through their CARs, critical thresholds of negative charge may impede cell-cell interactions underlying synapse formation and cytolysis. Removing the dense pool of negative cell-surface charge with *CpNA* is an effective approach to limit CAR T cell differentiation and enhance overall persistence and efficacy.**

## INTRODUCTION

Chimeric antigen receptor (CAR) T cells have become an important modality in cancer immunotherapy, producing a high rate of durable response for Food and Drug Administration-approved indications such as B cell acute lymphoblastic leukemia.<sup>1,2</sup> However, for solid ma-

lignancies, in which CAR T cells must contend with a complex, hostile, and often heterogeneous microenvironment, the results have been less encouraging. Most patients in clinical trials of CAR T for solid malignancies have had no objective response.<sup>2</sup> Moreover, even in relatively favorable indications such as hematologic malignancies, eventual disease progression is common. To overcome immunotherapy resistance, efforts have turned toward developing novel drugs and combination strategies to sensitize tumors to CAR T-mediated lysis. Among other approaches, the engineering of CAR T cells to produce effector proteins that block immune checkpoints, promote immune cell migration, and facilitate immune reactivity are exciting strategies on the frontier of immunotherapy research.<sup>2</sup>

The canonical immune checkpoints include inhibitory receptors such as CTLA4, PD1, and BTLA, which are expressed by T cells, and that serve to maintain peripheral tolerance and homeostatic contraction of T cell populations following immunologic stimulus.<sup>3</sup> However, following the discovery of immune checkpoint receptors, many other diverse mediators of peripheral tolerance have been discovered, including inhibitory cytokines, small molecule metabolites such as kynurenines, and cell-surface glycans.<sup>4</sup> For the latter category, the composition of glycans on mammalian cell surfaces has been shown to play a powerful role in modulating host-immune interactions. These discoveries have nominated promising therapeutic targets for enhancing immunotherapy. For example, glioblastoma cells were shown to overexpress truncated O-linked glycans that bind to the MGL receptor, which polarizes macrophages to an immunosuppressive phenotype.<sup>5</sup> Other glycan-binding receptors such as sialic acid-binding Ig-like lectins (siglecs) and dendritic cell (DC)-specific ICAM-3-grabbing nonintegrin 1 (DC-SIGN) have been shown to have roles in immune suppression.<sup>6,7</sup> Surface sialic acids, in particular, are appealing targets due to the manifold pathways in which

Received 16 April 2021; accepted 16 November 2021;  
<https://doi.org/10.1016/j.ymthe.2021.11.014>

**Correspondence:** Roddy S. O'Connor, PhD, Research Assistant Professor, Center for Cellular Immunotherapies, Perelman School of Medicine at the University of Pennsylvania, 3400 Civic Center Boulevard, Building 421, SPE 8-105, Philadelphia, PA 19104.

**E-mail:** [oconnorr@pennmedicine.upenn.edu](mailto:oconnorr@pennmedicine.upenn.edu)



they function as protective self-associated molecular patterns.<sup>8</sup> By binding to siglecs, sialoglycans trigger counterinflammatory cellular programs mediated by immunoglobulin receptor family tyrosine-based inhibitory motifs in the siglec cytoplasmic domains.<sup>5,6</sup> Siglec signaling on T cells can negatively modulate T cell receptor (TCR) signaling by reducing phosphorylation of Tyr<sup>319</sup> on ZAP-70, one of the critical downstream mediators of both TCR and CAR signaling.<sup>9</sup> Beyond binding to siglecs, sialoglycans also mediate immune inhibition by reducing cell-cell interactions through electrostatic repulsion, disabling the contents of T cell cytotoxic granules, and inhibiting complement activation.<sup>10–12</sup> Concordantly, diverse cancer types have been shown to highly express surface sialic acid, and this overexpression has been associated with worse clinical outcomes.<sup>8,10,13,14</sup>

The targeting of sialoglycans for cancer pharmacotherapy is a relatively old concept, predating our understanding of their mechanisms as immune checkpoint effectors. Treatment of tumor cells with sialic acid-cleaving neuraminidase enzymes was demonstrated in mouse and canine models to potentiate immune recognition of both treated and nontreated cells.<sup>15–17</sup> Neuraminidases (NAs) are produced by diverse species including *Vibrio cholerae*, *Clostridium perfringens*, influenza viruses, and mammals.<sup>18</sup> While the initial studies of NA-treated tumor cells were encouraging, a randomized, controlled trial in colorectal cancer published in 1989, using subcutaneous injection of *Vibrio cholerae* neuraminidase (VCN)-modified autologous tumor cells, found no benefit for progression-free or overall survival over 5 years, a setback in the nascent field of immunotherapy.<sup>19</sup>

However, as our understanding of sialoglycans as immune checkpoints has advanced, there is now renewed interest in targeting these structures in cancer therapy. Promising next generation strategies have included an engineered adenovirus expressing the hemagglutinin-NA of Newcastle Disease Virus, which reduced tumor sialic acid content and promoted disease regression *in vivo*.<sup>20</sup> More recently, a sialidase-conjugated antibody-like polymer targeting PD-L1 demonstrated both *in vitro* and *in vivo* efficacy against the MDA-MB-231 mammary adenocarcinoma.<sup>21</sup>

We hypothesized that CAR T cells engineered to express a highly active, secreted neuraminidase would be a more potent immunotherapeutic strategy than CAR T alone in solid tumors. We engineered epidermal growth factor receptor (EGFR) and CD19-directed CAR T cells to secrete functional *C. perfringens* NA. The *C. perfringens* NA was chosen due to having a pH optimum in the range of 6.5 to 7.2, closer to the physiological range of human extracellular fluid when compared with the NA of the enteric pathogen *Vibrio cholerae* (optimum pH of 5.5–6.0) or the human NAs that are optimized for acidic compartments (optima of 4.4–4.6 for lysosomal Neu1, 6.0–6.5 for the cytosolic Neu2, 4.6–4.8 for Neu3, and 3.5 for lysosomal Neu4).<sup>22–24</sup> The influenza NA was not suitable, as adults and the elderly often have high titers of anti-influenza NA antibodies due to past virus exposure.<sup>25</sup>

Interestingly, the work of Novogrodsky with NA also demonstrated that its combination with the enzyme galactose oxidase

(GO) can activate T cell mitogenesis and cytotoxicity more so than NA alone.<sup>26,27</sup> The enzyme GO oxidizes the galactose residues revealed by NA's uncapping of terminal sialic acids, creating reactive galactose aldehydes. These reactive groups have been hypothesized to account for the mitogenic effect of the NAGO combination by cross-linking cell-surface glycoproteins in a lectin-like manner.<sup>27</sup> The proinflammatory effect of the NAGO combination has made it an effective vaccine adjuvant in animal studies, promoting immunologic memory as measured by antiparasitic immunity and delayed hypersensitivity reactions to antigen reexposure.<sup>28</sup> While mitogen activation of T cells also risks overstimulation, inviting exhaustion and activation induced cell death, there has also been some evidence that stimulating T cell activation outside of the tumor microenvironment can promote immunotherapeutic response. For example, Reinhard et al. co-treated mice with large syngeneic LL/2-LLc1 or CT26 tumors using CAR T cells in combination with an RNA vaccine encoding the claudin target antigen.<sup>29</sup> By introducing target antigen outside of the tumor, this strategy allowed the CAR T product to establish a foothold in more permissive environments prior to engaging with the tumor microenvironment. It seemed reasonable to suppose that the combination of NA and GO might similarly augment tumor lysis beyond the antitumor effects of interfering with sialoglycan checkpoint pathways alone.

We explored the potential of *C. perfringens* NA-producing T cells, either alone or combined with GO, to promote CAR T mediated tumor lysis. The mechanisms of NA and GO stimulation of T cells, being previously poorly defined, were probed with CRISPR knockouts to reveal the importance of the CD2 adhesion and costimulatory receptor in this therapeutic approach. We demonstrate *in vivo* that CpNA secreting CAR T cells exert better control than conventional CAR T alone, but the addition of exogenous GO produces no further benefit despite its promise in *in vitro* assays. Secretion of CpNA led to enriched naïve-like differentiation of CAR T cells during *ex vivo* expansion, a phenotype that is associated with greater persistence and activity of the therapeutic product *in vivo*, suggesting that cleaving surface sialic acids influences T cell differentiation in addition to modulating checkpoint pathways.<sup>30–32</sup> In the design of novel immunotherapies, the targeting of tumor and immune cell-surface glycans to enhance immunogenicity, such as through the glyco-active enzyme NA, has the potential to enhance CAR T efficacy against solid tumors.

## RESULTS

### Engineered CAR T cells secrete functional CpNA in an antigen-responsive manner

To study the potential role of NA as a secreted factor that enhances CAR T cell antitumor function, we generated the lentiviral vector GFP\_T2A\_NA (GTN) by cloning the *C. perfringens* neuraminidase (CpNA) into a pTRPE plasmid backbone containing enhanced GFP (eGFP) and the T2A self-cleaving peptide (Figure 1A). After overnight stimulation with Dynabeads, activated T cells were co-transduced with GTN and either 806 (an EGFR-specific, 4-1BBZ CAR)

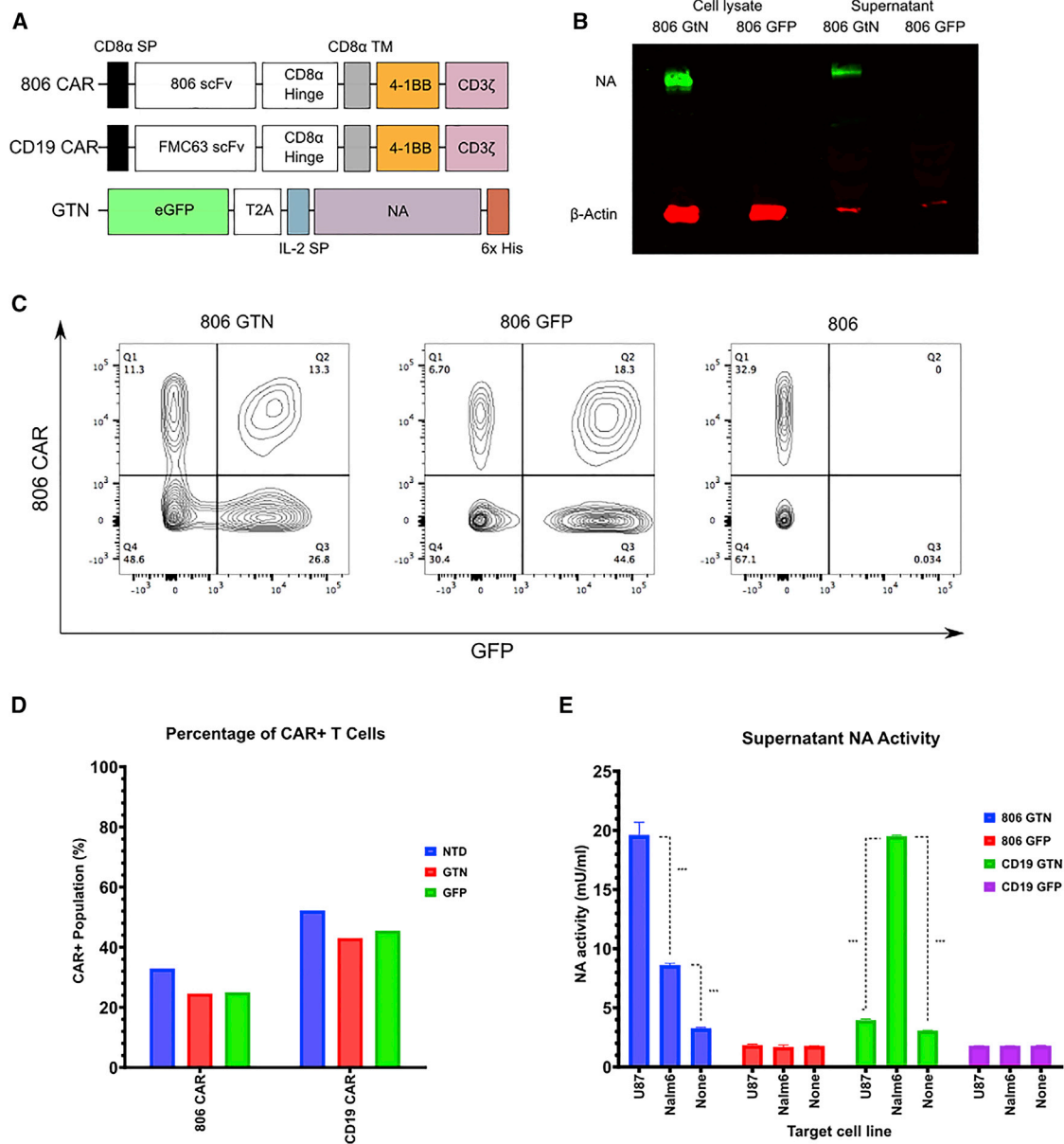


**Figure 1. Engineering CAR T cells to secrete functional *Clostridium perfringens* neuraminidase (CpNA)**

(A) Schematic representation of the hEGFR lentiviral CAR containing an 806 scFv, which is linked via a CD8α hinge as well as a CD8α TM to the 4-1BB and CD3zeta intracellular signaling domains. SP, signal peptide; TM, transmembrane. A lentiviral CAR construct against human CD19 containing the FMC63 scFv is also shown. GTN is a bicistronic lentiviral construct expressing *C. perfringens* neuraminidase (CpNA) in tandem with a C-terminal 6× Histidine tag (6× His) as well as the transduction marker GFP. (B) After overnight stimulation with Dynabeads, T cells were co-infected with an EGFR CAR and GTN lentiviral supernatants. These cells were expanded for 3 days. Cellular lysates and supernatants were collected and immunoblotted with anti-His antibody. Relative protein loading was determined by immunoblotting for B-Actin. Representative data from two independent experiments are shown. (C) CpNA-expressing CAR T cells were generated as in (B) Surface EGFR CAR expression was measured by staining with a recombinant EGFRVIII-Fc protein (H + L) followed by anti-Fc-APC labeling. GTN levels were simultaneously detected by GFP expression. CAR + cells were defined as double-positive for CpNA (x axis) and PE (y axis). Representative flow plots from three independent experiments are shown. (D) The percentage of T cells positive for CAR expression after preparation as in (C). Representative data from one of three donors are shown. (E) CAR T cells were co-cultured with either U87-MG or Nalm6 tumor cells at a 10:1 ratio for 24 h. Cellular supernatants were collected and NA enzymatic activity was detected as described in the materials and methods. The mean ± SEM values of three independent experiments with separate donors are shown. Data were analyzed with pairwise t tests corrected for multiple comparisons using the Holm-Sidak method. \*\*\*p < 0.001 for CAR T cells co-cultured with tumor cells expressing the CAR's target antigen versus control cells expressing an irrelevant antigen.

or CD19-specific, 4-1BBZ CAR lentivirus. As a control, T cells were transduced with eGFP lentivirus instead of GTN. After 3 days, cellular lysates and supernatants were collected and CpNA expression was confirmed by western blot with antibodies against the C-terminal 6× histidine tag (Figure 1B). The CpNA secreting CAR T cells expanded efficiently (25.4-fold, Figure S1A), although more slowly than GFP-transduced controls, with 45.3% fewer total T cells at the end of expansion (defined by median cell size <400 fL) across three donors ( $p = 0.016$ ). As sialic acids have been implicated in protecting immune effector cells from degranulation-associated self-killing,<sup>11</sup> we examined T cell viability at consecutive time points during expansion (Figure S1B). By live dead staining, there was a greater proportion of dead cells in the CpNA secreting condition versus the GFP control, with 20.7% versus 12.5% dead cells on day 3, 11.8% versus 4.2% on day 5, and 4.4% versus 1.4% on day 7, but these differences were not significant by paired t test statistics with three donors ( $p = 0.1172, 0.1147, \text{ and } 0.0858$  on days 3, 5, and 7, respectively).

To evaluate CpNA expression in CAR + subsets, we performed two-color flow cytometry with GFP positivity indicating transduction with the GTN construct. After dual transduction with CAR and GTN lentiviral preparations, we observed a mix of singly positive CAR, GTN, and CAR + GTN T cells (Figures 1C and 1D). The CAR + transduction efficiencies were comparable in the GTN (24.6%) and GFP (25%) populations and similar to the targeted CAR + percentage in clinical products.<sup>33</sup> To evaluate whether CpNA production confers a relative growth disadvantage to T cells producing it, we examined GFP positivity as a proxy for CpNA expression at serial time points during expansion (Figure S1C). By paired t testing across three donors, there was no significant decrease in GFP percent positivity between days 3 and 7 ( $p = 0.4755$ ) in the CpNA condition, suggesting that the decrease in *ex vivo* expansion related to NA is due to its effects on the population and not limited to cells expressing the enzyme.

To test how CpNA secretion responds to CAR stimulation, we selected target lines U87 and Nalm6 with EGFR and CD19 positivity, respectively. Activated T cells were co-infected with GTN and CAR, expanded for 10 days, and frozen before use. CAR T cells were then co-cultured with either U87 or Nalm-6 target cells for 24 h at a 10:1 effector to target cell (E:T) ratio.

Cellular supernatants were collected and CpNA activity was determined with a cleavage-activated fluorescent NA substrate. We show that CpNA activity is significantly induced following direct stimulation of the CAR with its corresponding ligand. As shown in Figure 1E, CpNA levels/activity significantly increased 2.3-fold from 8.62 to 19.63 mU/mL ( $p = 0.0001$ ) when GTN 806 CAR T cells were co-cultured with U87 versus Nalm6 cells, respectively. Similarly, CpNA functional activity increased 4.9-fold from 3.96 to 19.52 mU/mL ( $p < 0.0001$ ) when GTN CD19 CAR T cells were co-cultured with Nalm6 versus U87, demonstrating that enzyme secretion is enhanced after CAR-mediated T cell activation.

### CAR T-secreted CpNA enhances T cell-mediated tumor lysis *in vitro*

We hypothesized that CAR T cells secreting CpNA would have enhanced tumor lysis compared with CAR T cells alone. As Novogrodsky found that GO in the presence of NA induced T cell mitogenesis, we also hypothesized that adding GO to CpNA secreting CAR T cells would confer additional antitumor function.<sup>27</sup> To rule out direct toxic effect of the enzymes on tumor cell lines, we initially examined whether NA and GO inhibit the growth of U87 or Nalm6 cells in the absence of T cells. Using luciferase-expressing tumor cells, we showed that the addition of exogenous CpNA and GO, in the absence of T cells, did not inhibit growth of either tumor line (Figure 2A). To determine the effective range of GO doses that stimulate T cell-induced lysis in combination with CpNA secreting CAR T cells, we co-cultured GTN or GFP CD19 CAR T cells with U87 cells at a 1:1 ratio for 24 h. In the absence of CpNA, exogenous GO at higher doses (375 mU/mL) induced nonspecific lysis of U87 cells by GFP CD19 CAR T cells (Figure 2B). However, CpNA-expressing GTN CD19 CAR T cells produced significantly greater lysis of U87 cells compared with GFP-transduced CD19 CAR T cells after the addition of GO, with a 4.4-fold, 3.3-fold, and 1.6-fold increase in tumor cell lysis at GO doses of 3.75, 37.5, and 375 mU/mL, respectively (Figure 2B,  $p = 0.0053, <0.0001, \text{ and } 0.0001$ ).

To assess whether secreted CpNA, alone or in combination with GO, enhances the ability of CAR T cells to lyse their corresponding target cells, we co-cultured GTN and GFP CAR T cells with U87, U251, or Nalm6 target cells. CAR T cells were expanded for 10 days until rested, and then co-cultured with target cells at various effector to target (E:T) ratios for 24 h. In the absence of exogenous GO, the cytolytic activity of GTN and GFP CAR T cells against U87 cells is similar (Figures 2C and 2D). However, the addition of exogenous GO potentiated U87 cell lysis by CpNA-expressing CAR T cells, leading to a 2.47-fold increase in tumor lysis at the 1:3 ET ratio compared with CpNA secreting CAR T cells alone (Figure 2C,  $p = 0.0024$ ). For U251 and Nalm6 cells, the CpNA secreting CAR T cells alone outperformed control GFP-transduced CAR T cells. With U251 targets, CpNA secretion produced a 1.27- and 1.7-fold increase in lysis at ET ratios of 1:1 and 1:3, respectively (Figure S2A,  $p = 0.0035 \text{ and } 0.0347$ ). With Nalm6 targets, CpNA secretion by CD19-directed CAR T cells produced a 2.5- and -3.9-fold increase in lysis at ET ratios of 3:1 and 1:1, respectively (Figure S2D,  $p = 0.0006 \text{ and } 0.0053$ ). For both U251 and Nalm6 targets, the addition of GO further enhanced lysis compared with CpNA secreting CAR T cells alone, with 1.7- and 3.3-fold increases in tumor lysis, respectively, at an ET ratio of 1:3 (Figure S2,  $p = <0.0001 \text{ and } 0.0098$ ).

By ELISA assay, interferon (IFN)- $\gamma$  and interleukin (IL)-2 cytokine levels were significantly increased in the CAR T and tumor co-cultures in the presence of secreted CpNA and exogenous GO (Figures 2E and 2F), even with an irrelevant CD19-directed CAR, showing that CpNA secretion plus exogenous GO leads to antigen-independent T cell reactivity and TH1 cytokine production.

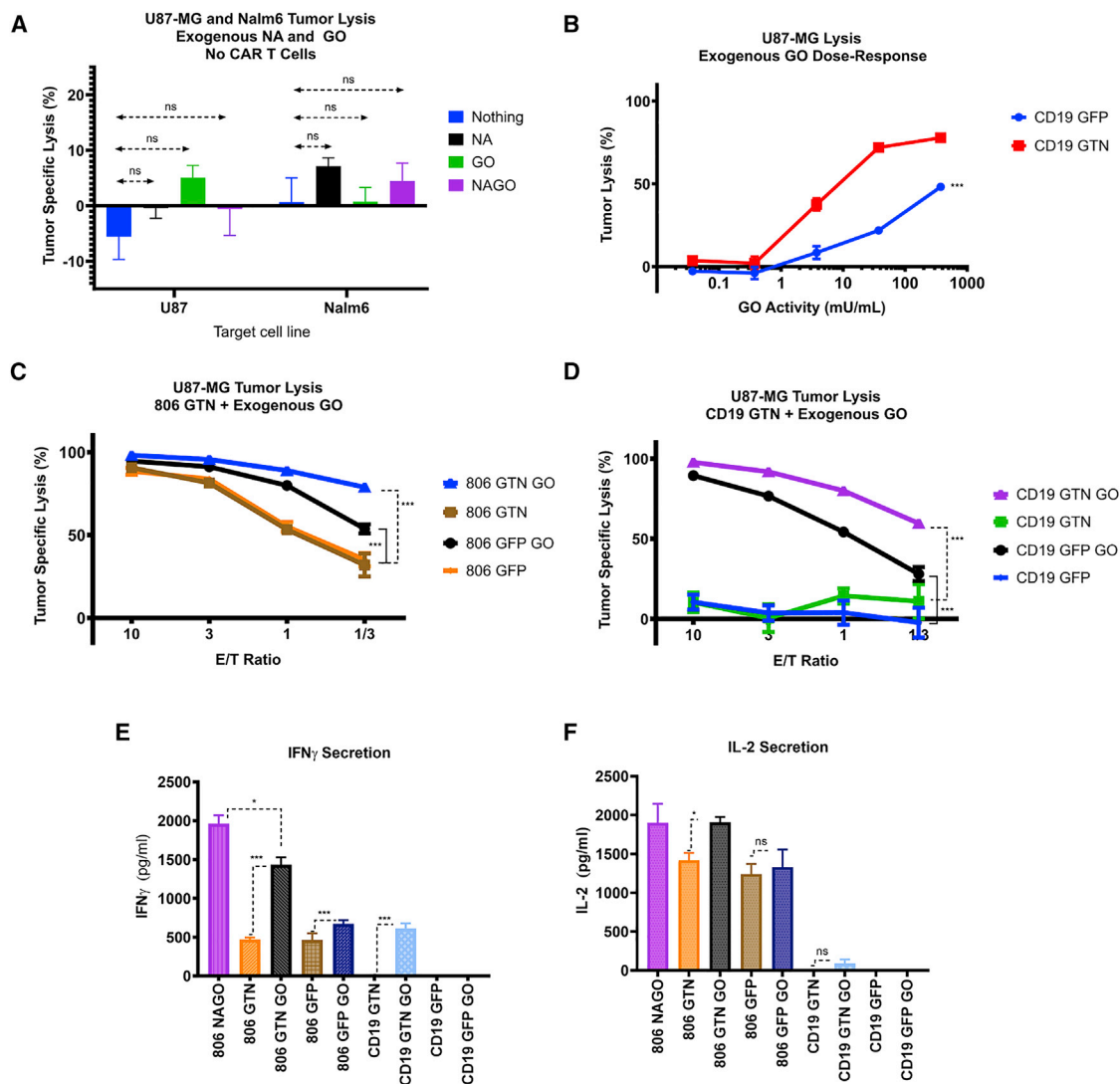


**Figure 2. The combination of CAR T-secreted CpNA and exogenous galactose oxidase (GO) enhances T cell-mediated tumor lysis of U87 cells**

(A) U87-MG as well as Nalm6 tumor cells were treated with exogenous CpNA and GO for 24 h. Tumor cell lysis was measured by luciferase assay.  $p = 0.31$  for enzyme effect on cell proliferation by a one-way ANOVA using a Tukey multiple comparison correction. (B) CD19-directed CAR T cells were co-cultured with U87 target cells. The media was conditioned with exogenous GO at various concentrations, and U87-MG tumor lysis was assessed via bioluminescence at 24 h. (C) T cells were co-infected with an EGFR-specific CAR and either GFP or CpNA lentiviral supernatants. The CAR T cells were co-cultured with luciferase-expressing U87-MG target cells, in medium conditioned with exogenous GO. After 24 h, cytotoxicity across a range of E:T ratios was measured by a luciferase-based killing assay. Values are mean  $\pm$  SEM. A representative experiment from three independent replicates with separate donors is shown. \*\*\* $p = 0.0002$  for 806 GTN GO versus 806 GTN at a 1:1 E:T ratio; \*\* $p = 0.0024$  for 806 GTN GO versus 806 GTN at a 1:3 E:T ratio. (D) Tumor cell lysis was measured as in (C), but anti-CD19 CAR T cells were used instead of anti-EGFR CAR T cells. \*\*\* $p = 0.0002$  for CD19 GTN GO versus CD19 GTN at a 1:1 E:T ratio; \* $p = 0.0108$  for CD19 GTN GO versus CD19 GTN at a 1:3 E:T ratio. (E) CAR T cells, coexpressing either GFP or CpNA were treated with exogenous galactose oxidase for 24 h. Cellular supernatants were collected and IFN $\gamma$  levels were detected by ELISA. (F) IL-2 levels in 24 h supernatants as detected by ELISA.

With light microscopy, we observed that the presence of CpNA led to greater cell-cell association between T cells and tumor cells in co-cultures (Figures S3A and S3B). While co-cultures without NA had many T cells that were not engaged in clusters with tumor targets, the cultures with CpNA had comparatively few unengaged T cells (Figures S3A and S3B). The ability of NA to promote cell-cell adhesion has been previously demonstrated

and has been hypothesized by others to explain its pro-immunogenic effect.<sup>10</sup>

**CpNA and GO-mediated T cell activation depends on the CD2:CD58 signaling axis**

The mechanism by which the CpNA and GO combination acts as T cell mitogens remains incompletely described. Novogrodsky

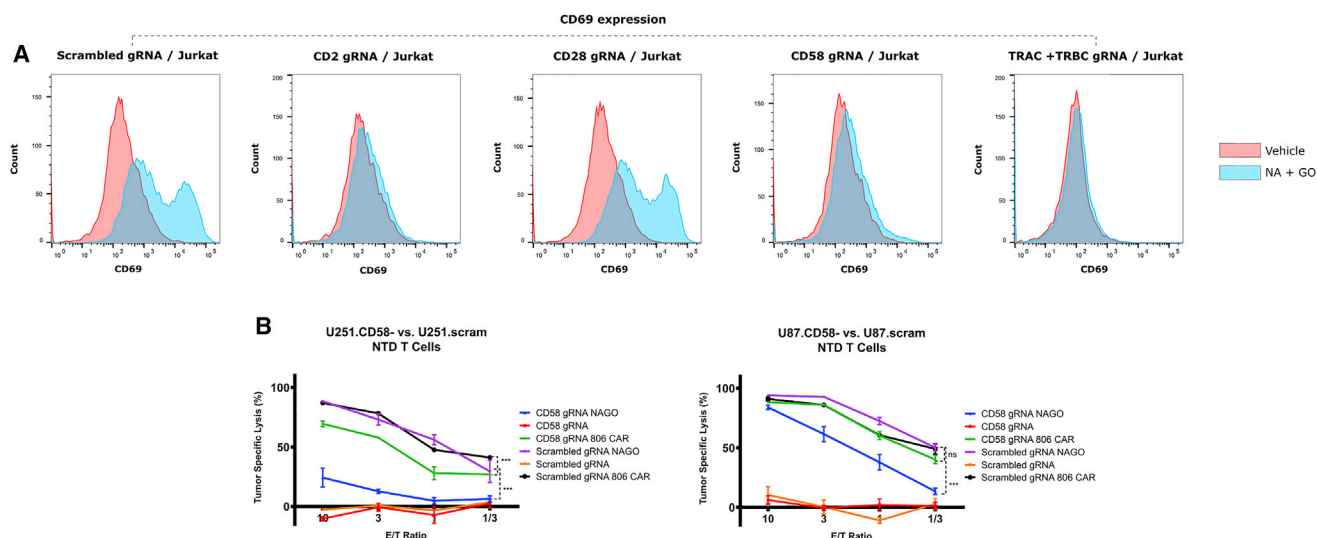


**Figure 3. The combination of CpNA and GO activate T cells and promote tumor lysis in a CD2:CD58-dependent manner**

(A) Jurkat cells were infected with the lentiCRISPR-v2 system adapted with gRNAs for *CD2*, *CD28*, *CD58*, the T cell receptor alpha and beta chains (*TRAC* and *TRBC*), and a scrambled nontargeting control. The cells were selected with puromycin and knockout confirmed by flow cytometry 5 days after transduction. After an overnight incubation with NA and GO, the cells were stained with APC-conjugated anti-CD69 antibody and assessed by flow cytometry. (B) Luciferase expressing U87 and U251 cells were infected with the lentiCRISPR-v2 system encoding gRNAs against CD58 or a scrambled sequence. Knockout was confirmed after 5 days. The target cells were plated at  $20 \times 10^3$  per well and co-incubated with nontransduced or 806 CAR T cells at E:T ratios of 10:1, 3:1, 1:1, or 1:3. Wells with nontransduced T cells were treated with NA and GO (50  $\mu$ M and 375  $\mu$ M, respectively) or PBS vehicle. Tumor lysis was determined by bioluminescence assessment after 24 h. Data are means  $\pm$  SEM, showing a representative experiment from three replicates with separate donors.

hypothesized that free amines may attack the GO-generated reactive aldehydes in a Schiff base reaction, leading to covalent cross linking of cell-surface receptors and transmission of activating signals.<sup>27</sup> However, the precise receptors involved in transmitting the activating signals are unknown. A report by Ocklind et al. demonstrated that anti-CD2 or CD58 monoclonal antibodies could block the formation of rosettes between human T cells and sheep erythrocytes in the presence of CpNA and GO.<sup>34</sup> We hypothesized that eliminating CD2 or CD58 expression would abrogate the effects of CpNA and GO on T cell activation and tumor cell lysis.

We adapted the lentiCRISPR-v2 system of Sanjana et al. with guide RNAs (gRNAs) for *CD2*, *CD28*, *CD58*, *TRAC*, *TRBC*, and a scrambled control.<sup>35</sup> After producing lentiviral particles, we transduced Jurkat cells, a T cell leukemic line commonly used in investigations of TCR and CD2 signaling. We confirmed gene knockout by flow cytometry 5 days later (Figure S4). To assess activation of the cells after overnight CpNA and GO stimulation, we measured expression of CD69, a marker of T cell activation.<sup>36</sup> These data show that Jurkat cells deficient in CD2, CD58, or the TRC chains TRAC and TRBC are not activated by CpNA and GO treatment (Figure 3A).

Conversely, the loss of CD28 or expression of a nontargeting gRNA did not affect the response to the enzymes (Figure 3A). Therefore, CD2, its ligand CD58, and the TCR are required for CpNA and GO in combination to activate Jurkat cells.

Based on the CRISPR knockout data, we suggest that Jurkat cells are activated in the presence of CpNA and GO through complementation of CD2 and its ligand CD58 expressed on neighboring cells. The requirement for the TCR is due to its role in transmitting signals from the CD2 axis.<sup>37</sup> If the enzymes do act through CD2-CD58 complementation, then CD58 expression on tumor cells may contribute to their CpNA and GO-mediated lysis. Using the lentiCRISPR-v2 constructs, we transduced luciferase-expressing U87 and U251 tumor cells with CD58 or scrambled gRNAs and confirmed knockout 5 days later (Figure S4). We co-cultured these cells with nontransduced T cells at various E:T ratios, with and without exogenous CpNA and GO, for 24 h and determined cell lysis with bioluminescence assay. These data show that CD58-deficient tumor cells are resistant to NA- and GO-stimulated T cell cytotoxicity, with tumor-specific lysis decreasing 47.8% ( $p = 0.0081$ ) and 91.7% ( $p = 0.00053$ ) for U87 and U251 cells, respectively, when CD58 is knocked out (Figure 3B, values for ET = 1). In parallel experiments, we included EGFR-directed CAR T cells to examine whether CD58 knockout confers resistance to CAR-stimulated lysis. We found that CAR T cell-mediated lysis was not significantly inhibited in CD58 deficient tumor cells, with reductions of 0.06% ( $p = 0.92$ ) and 41.3% ( $p = 0.092$ ) compared with scrambled gRNA transduced cells (Figure 3B, values for ET = 1), suggesting that loss of CD58 confers resistance to NA and GO-mediated lysis specifically instead of only providing a general resistance to T cell cytotoxicity.

### **CpNA secretion confers naïve-like differentiation to T cell cultures *in vitro***

Differentiation status is an important determinant of CAR T cell efficacy. Therefore, we performed a comprehensive assessment of differentiation using well-established surface markers. We show that CpNA-expressing T cells possess significantly higher levels of naïve-like subsets at the end of the *ex vivo* culture process (Figures S5A and S5B). Importantly, levels of naïve-like cells provide the most meaningful predictors of efficacy in CAR T cell trials, with superior engraftment, proliferation, and persistence following infusion. These differentiation data suggest that one mechanism for enhanced CpNA-expressing CAR T performance *in vivo* may be enhanced durability and long-term immunosurveillance.

### **CpNA secretion enhances CAR T activity against U87 solid tumors and Nalm6 leukemia *in vivo*.**

Based on the *in vitro* findings, we hypothesized that CAR T cells secreting CpNA would better eradicate xenografted solid tumors in mice compared with CAR T cells alone, and that exogenous GO may further augment this benefit. We generated anti-EGFR and anti-CD19 CAR T cells as previously described, co-transduced with either the GTN (CpNA secreting) or GFP constructs. Each mouse received  $250 \times 10^3$  luciferase-expressing U87 tumor cells via subcutaneous injection in the flank (Figure 4A). On day 7, the tumors were palpable, and the mice received  $500 \times 10^3$  CAR T cells in PBS each by tail vein injection. On days 8 and 21, the mice received 30  $\mu$ L of GO (37,500 mU/mL in PBS) or vehicle by intra-tumoral injection. On a weekly basis, the tumor volume and bioluminescence were assessed with caliper measurements and the IVIS Spectrum imaging system, respectively. In animals receiving the irrelevant CD19-directed CAR T cells, the best tumor control occurred with CpNA secreting CAR T cells plus GO injections, which produced a 42.7% ( $p = 0.0474$ ) and 66.3% ( $p = 0.0069$ ) reduction in tumor bioluminescent imaging (BLI) at days 21 and 28, respectively, compared with the next best treatment (Figure 4B). This suggests NA and GO may have stimulated T cell activation and lysis of the tumor. However, by day 35, 2 weeks after the last injection of GO, the CpNA secreting CAR T plus GO arm was no longer significantly better than other conditions (Figure 4B,  $p = 0.9800$ ). In 806 CAR T treated animals, the CpNA secreting T cells controlled the tumor significantly better than all other conditions, with an 85.9% lower tumor BLI compared with the next best treatment at the final time point (Figure 4D,  $p = 0.0005$ ). However, 806 GTN CAR T-treated animals that received injected intra-tumoral GO did worse than those receiving PBS (Figure 4D,  $p = 0.0005$ ). The mice showed no evidence of accelerated graft versus host effect either by physical inspection or serial weights. Overall, the secretion of CpNA by EGFR-targeting CAR T cells led to enhanced tumor control, while producing no adverse effects in the mice (as assessed by weight, blood counts, and serum chemistries). The addition of GO, however, did not further benefit animals receiving CpNA secreting EGFR-targeting CAR T cells.

Mechanistically, our *in vitro* assays had revealed that CpNA secreting CAR T cells possessed a more naïve-like

(CCR7<sup>+</sup>CD45RO<sup>-</sup> with slower expansion) phenotype. As naïve-like T cells have been demonstrated to confer superior persistence and longer-lasting immunosurveillance against hematologic malignancies, we used an NSG mouse/Nalm6 tumor rechallenge model to test the hypothesis that CpNA secreting CAR T cells would produce more durable tumor control. Each mouse (five per cohort) received  $1 \times 10^6$  luciferase-expressing Nalm6 tumor cells by tail vein injection (Figure 5A). On day 5, we infused CpNA secreting versus GFP control CD19-directed CAR T cells. On day 33, mice received an additional  $1 \times 10^6$  Nalm6.GFP/Luc cells by tail vein injection. By day 50, mice treated with the CpNA secreting CAR T cells had a greater than 1,000-fold lower tumor burden than those treated with control CAR T cells ( $*p = 0.0163$ , Figure 5B). Concordantly, 80% of mice in the CpNA CAR T group survived until the end of the experiment versus 0% survival in the GFP control group ( $*p = 0.0210$ , Figure 5C). Blood was collected on day 44, and while the CpNA CAR T group did demonstrate 350-fold higher levels of human CD45 + engrafted lymphocytes, this result was not significant perhaps due to low sample size secondary to mortality in the GFP group ( $p = 0.3372$ , Figure 5D). Two weeks after tumor rechallenge, the BLI of the CpNA CAR T group started to decrease, indicating tumor regression, and by the last measurement on day 50 the tumor burden in that group was barely detectable (Figure 5E).

### **CpNA secretion enhances CAR T activity against B16 melanoma but not the SY5Y neuroblastoma model**

As *in vitro* studies suggest that GO adds to the effect of NA by facilitating activation of *in situ* T cells through CD2:CD58, we hypothesized that the absence of an endogenous immune system in NSG mice might account for the lack of enhancement of CpNA CAR T-mediated lysis after addition of GO. To test the system in an immune-competent model, we implanted C57BL/6 mice with syngeneic B16F10 tumor cells expressing human CD19. Mice were randomized to treatment on days 5 and 12 with CD19-directed CAR T cells, co-transduced with GTN or GFP constructs, or NTD controls (Figure S6A). Mice also received intra-tumoral injections of NA and GO, GO, or PBS vehicle on days 6 and 13 as indicated in figures. Similar to the NSG experiment, we saw the best tumor control in the CpNA CAR T plus PBS injection treatment arm, with a 42.8% reduction in tumor volume by day 21 compared with NTD- and PBS-treated animals ( $p = 0.0126$ ) and 33.3% reduction compared with the CpNA CAR T plus GO treatment arm (Figure S6B), although the latter was not significant ( $p = 0.0667$ ). Analyzing blood collected on day 21, we saw engraftment of CD45.1+ adoptively transferred T cells in all treatment arms, although as assessed by one-way ANOVA with corrections for multiple comparisons, there were no significant differences between arms (Figure S6C,  $p = 0.0642$ ). Assessment of weights by two-way ANOVA (mixed effects model) showed no significant treatment or time-treatment interaction effects (Figure S6D,  $p = 0.2635$  and  $0.0598$ , respectively). Overall, in this syngeneic solid tumor model, we observed superiority of CpNA secreting CAR T cells but an absence of improvement with additional exogenous GO.

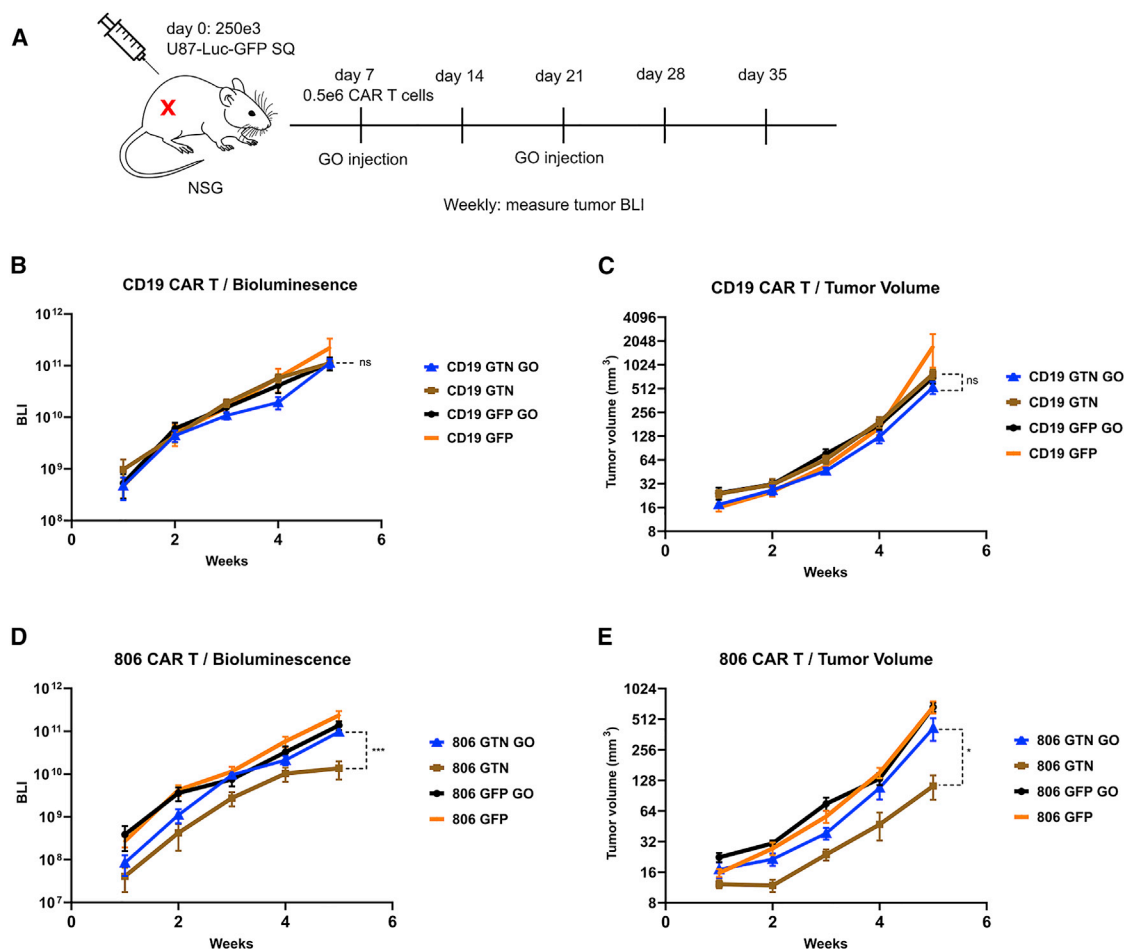


**Figure 4. Tumor bioluminescence in NSG mice after implantation with U87 tumor cells and treatment with *CpNA* secreting CAR T cells**

(A) NSG mice were implanted by subcutaneous flank injection with  $250 \times 10^3$  luciferase-expressing U87 tumor cells. On day 7, the mice received  $500 \times 10^3$  CAR T cells in PBS injected by tail vein. The CAR T cells expressed 806 (EGFR-targeting) or anti-CD19 CARs plus co-transduced GTN (*CpNA* secreting) or GFP constructs. On days 8 and 21, the mice received 30 mL of GO (37,500 mU/mL in PBS) or vehicle by intra-tumoral injection. Every seventh day, the tumor bioluminescence was assessed with the IVIS Spectrum imaging system. (B) Bioluminescence measurements in mice treated with CD19 CAR T cells. Data are means  $\pm$  SEM from seven replicate mice per cohort. By T test statistics, \* $p = 0.0474$  for CD19 GTN GO versus CD19 GTN PBS at 21 days; \*\* $p = 0.0069$  for CD19 GTN GO versus CD19 GTN PBS at 28 days;  $p = 0.9800$  for CD19 GTN GO versus CD19 GTN PBS at 35 days. (C) Tumor volume measurements in mice treated with CD19 CAR T cells. Data are means  $\pm$  SEM from seven replicate mice per cohort. By T test statistics,  $p = 0.1013$  for CD19 GTN GO versus CD19 GTN PBS at 35 days. (D) Bioluminescence measurements in mice treated with anti-EGFR (806) CAR T cells. Data are means  $\pm$  SEM from seven replicate mice per cohort. \*\* $p = 0.0040$  for 806 GTN GO versus 806 GTN PBS at 21 days;  $p = 0.1131$  for 806 GTN GO versus 806 GTN PBS at 28 days; \*\*\* $p = 0.0005$  for 806 GTN GO versus 806 GTN PBS at 35 days. (E) Tumor volume measurements in mice treated with anti-EGFR (806) CAR T cells. Data are means  $\pm$  SEM from seven replicate mice per cohort. \* $p = 0.0240$  for 806 GTN GO versus 806 GTN PBS at 35 days.

We next evaluated the antitumor function of *CpNA*-expressing CAR T-cells, using our well-established human xenograft model of neuroblastoma. SY5Y xenografts establish an immune-suppressive tumor environment enriched with immune and metabolic checkpoints. Infused CAR T cells effectively traffic to SY5Y tumors.<sup>38</sup> Despite undergoing robust proliferation, their antitumor function is limited.<sup>39</sup> The experimental layout for testing the efficacy of anti-GD-2 CAR T cells in this model is illustrated in Figure S7A. *CpNA*-expressing, anti-GD-2 4-1BBsCAR-T cells were expanded over 9 days until rested. To establish xenografts, immunodeficient mice were intravenously (i.v.) injected with  $0.5 \times 10^6$

Click Beetle Green Luciferase-expressing SY5Y tumor cells. To determine the influence of *CpNA* on CAR T cell potency, we infused,  $0.75 \times 10^6$  GFP or *CpNA*-expressing CAR T cells and measured tumor size at regular intervals by bioluminescence imaging. As expected, SY5Y xenografts grew exponentially over time. Control T cells (no CAR) had minimal impact on tumor cell growth (Figure S7C). Overall tumor volume was significantly reduced in tumor-bearing mice infused with CAR infected T cells. However, overall tumor burden remained high in *CpNA*-expressing CARTs. The levels of circulating T cells were significantly less in the *CpNA* CAR group, suggesting that proliferation

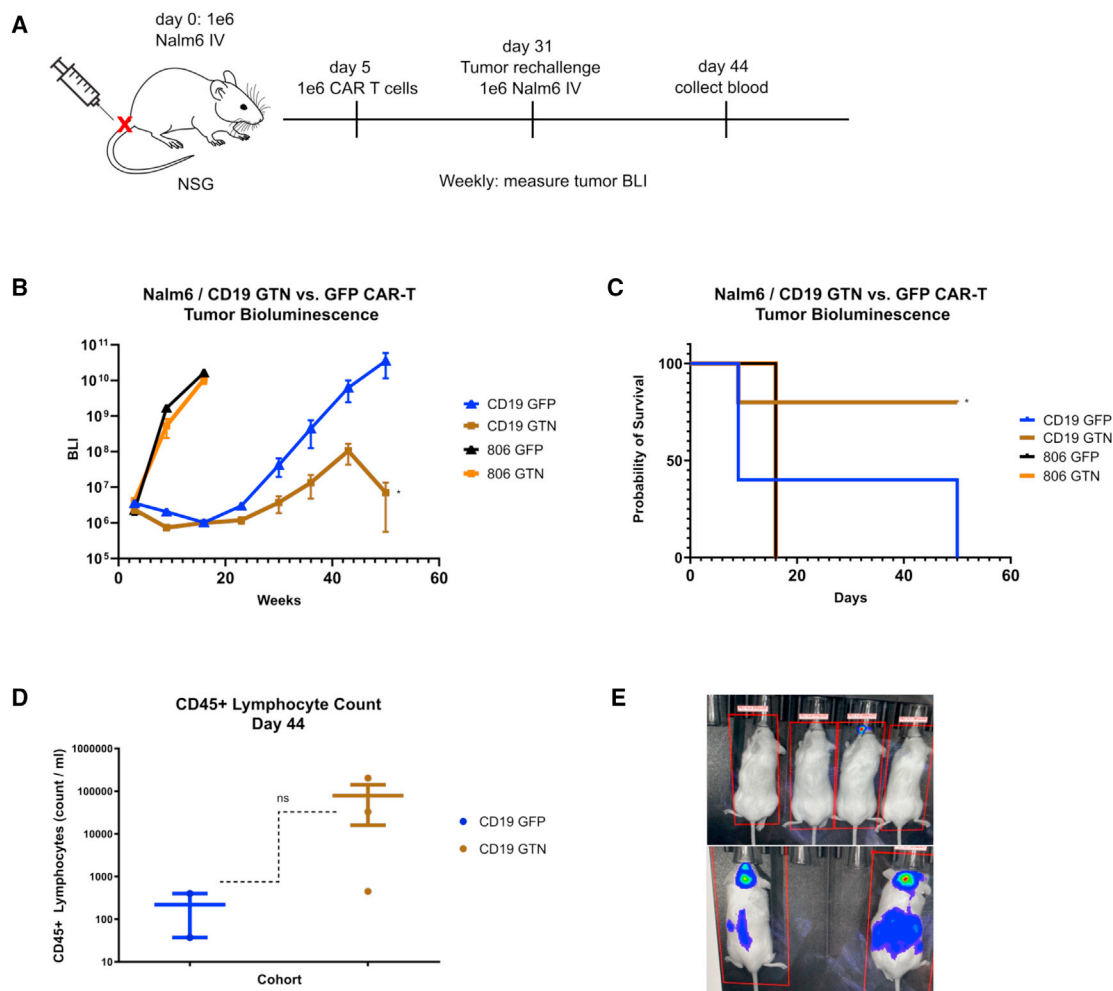


**Figure 5. Targeting sialic acids with NA enhances CAR T cell antitumor function in the Nalm-6 xenograft model of leukemia**

(A) NSG mice were infused by tail vein injection with  $1 \times 10^6$  luciferase-expressing Nalm tumor cells (day 0). On day 5, the mice received  $1 \times 10^6$  CAR T cells in PBS injected by tail vein. The CAR T cells expressed either tumor-targeting anti-CD19 CARs or irrelevant control 806 (EGFR-targeting) CARs, plus co-transduced GTN (CpNA secreting) or GFP constructs. Every week, the tumor bioluminescence was assessed with the IVIS Spectrum imaging system. (B) Bioluminescence measurements in Nalm6 tumor-bearing mice treated with anti-CD19 or 806 CAR T cells either secreting CpNA (GTN construct) or expressing GFP. Data are means  $\pm$  SEM from starting cohorts of five mice per treatment arm. By two-way ANOVA, including all treatment arms, both time effect ( $*p = 0.0485$ ) and treatment cohort effect ( $*p = 0.0226$ ) were significant. A two-way ANOVA including only CD19 GTN and CD19 GFP arms showed significant time ( $*p = 0.0446$ ), treatment ( $*p = 0.0163$ ), and time  $\times$  treatment interaction ( $***p < 0.0001$ ) effects. (C) Survival proportions of Nalm6 tumor-bearing mice in each treatment cohort. Mice were killed if found to have BLI measurements over  $1 \times 10^{10}$  photon flux (p/s). Analysis with log rank (Mantel-Cox) testing demonstrated that the CD19 GTN and CD19 GFP survival curves are significantly different ( $*p = 0.0210$ ). (D) Blood harvested on day 44 by retro-orbital puncture was stained with anti-human CD45 antibody in Truecount tubes (BD Biosciences) to detect adoptively transferred T cells. Data are CD45 + cells per mL of blood for individual mice plus cohort means  $\pm$  SEM. By T test statistics with Welch's correction for unequal variances, the differences between CD19 GTN and CD19 GFP were not significant ( $p = 0.3372$ ). (E) Images from final weekly measurement demonstrating BLI (photon flux intensity) of surviving mice, treated with either CpNA secreting (top) or control GFP-expressing (bottom) CD19-directed CAR T cells.

was diminished following antigen exposure in this distinct micro-environment (Figure S7D). Overall effector function was compromised due to significantly lower CD8+ T cell numbers in the CAR CpNA group. SY5Y is a rapidly growing tumor and the aggressive nature of this malignancy limits the *in vivo* study to approximately 2 weeks. This is unsuited to approaches that offer therapeutic potential via enhanced persistence.

**Conclusions**

In this study, we engineered CAR T cells to secrete *C. perfringens* NA, hypothesizing that NA-expressing CAR Ts would have enhanced antitumor function by counteracting sialoglycan-mediated checkpoint pathways. We found that, *in vitro*, CAR T-secreted NA alone does enhance cytotoxicity against certain tumor lines during short-term co-culture assays. Moreover, *ex vivo* expanded T cells exposed

to NA activity have a more naïve-like (CCR7<sup>+</sup>; CD45RO<sup>-</sup>) differentiation profile. Less-differentiated CAR T products such as naïve (Tn), stem cell memory (Tscm), and central memory T cells (Tcm) have more potent antitumor activity compared with effector or effector-memory differentiated T cells.<sup>30–32</sup> Correspondingly, the NA-secreting CAR T cells had enhanced persistence and more durable immunosurveillance within a tumor rechallenge model. One compelling model for T cell differentiation is that of “quorum sensing,” in which interactions between clustering, primed T cells during a critical period determine their effector versus memory differentiation fate. Surface intercellular receptors including the integrin LFA-1 have been demonstrated to transmit differentiating signals between T cells.<sup>40</sup> Treatment with NA has been used for decades in research to promote rosette formation and contact between immune cells and targets.<sup>41,42</sup> On microscopy, there is generally a relative absence of unengaged, bystander T cells when NA is included in the media; virtually all T cells are involved in rosettes. These results suggest a model in which sialic acid removal influences T cell intercellular contact and therefore differentiation fate. Therapeutic strategies that target the immunomodulatory functions of sialic acids may also benefit from polarizing adoptive T cell products to a naïve-like phenotype.

Our findings regarding the CD2:CD58 axis are intriguing, because recent research has demonstrated the importance of the CD58 ligand in tumor immunosurveillance. Diverse tumor types can gain resistance to T and natural killer cell-mediated cytotoxicity through loss of CD58 expression.<sup>43–45</sup> Majzner et al. demonstrated that large B cell lymphomas (LBLCs) with aberration of CD58 had only a 25% rate of complete response with CAR T therapy compared with 82% for CD58-intact tumors.<sup>44</sup> The finding that the NA and GO combination requires CD58 for mitogenic signaling could provide a non-genetic approach to assay for the functional expression of this ligand on tumor cells. Importantly, our findings regarding the CD2:CD58 axis do not extend the known immune potentiating mechanisms of NA alone, as the presence of GO is required in addition to NA for this phenomenon.

We sought to boost the effect of NA by testing it in combination with a second glyco-active enzyme, GO, which can oxidize galactose residues exposed by NA. The combination of secreted NA and exogenous GO does enhance T cell polyfunctionality and nonspecific cytotoxicity *in vitro*. Mechanistically, the enzyme combination relies on the CD2:CD58 signaling axis to induce stimulatory effects. Results from our xenograft models of GBM, as well as our syngeneic model of B16 melanoma, however, show that NA alone enhances CAR T cell antitumor function *in vivo*, but when combined with GO, the subset of CAR Ts secreting NA demonstrates inferior tumor control. By distinguishing the relative importance of NA versus GO as adjuvants for CAR T cell therapies, we provide novel evidence that arming CAR T cells with NA enhances immunotherapeutic activity.

Our findings suggest possible mechanisms for the failure of injected GO to further enhance the performance of CAR T cells secreting NA *in vivo*. In the presence of both enzymes, T cells broadly react

to targets expressing CD58. When applied to a co-culture assay, the effect of the enzyme combination leads to greater engagement of effectors (particularly nontransduced T cells) with tumor targets. Within the animal models, however, the enzyme combination may misdirect CAR T cells toward antigen-negative but CD58-positive bystander cells, effectively reducing the effector to tumor target ratio. Therefore, the success of the combination in co-culture assays may be an artifact of the lack of cellular diversity *in vitro*, with absent stromal and benign host cells that one would find in the tumor microenvironment. An alternative but not mutually exclusive hypothesis is that the stimulatory signal of the enzyme combination may be supraphysiologic and facilitate T cell exhaustion, an effect that may not be apparent in short-term co-culture assays but would be revealed in longer term animal studies. The calcium-calcineurin-NFAT signaling axis in T cells provides a link between excessive activation signals and an exhausted phenotype, and this effect could be at work in our *in vivo* findings of the NA and GO combination.<sup>46</sup>

In the design of combination immunotherapies, proteins that act on immune cell and tumor glycoproteins have been underexplored. Here, we use a nonnative enzyme, *CpNA*, to directly target surface glycans that suppress T cell function. Arming CAR T cells with *CpNA* confers superior efficacy and durability across a wide range of tumor models. Interestingly, we observed a striking T cell intrinsic benefit of *CpNA*. We show that NA shifts the differentiation of T cells into a naïve-like state, culminating in increased persistence and sustained tumor control *in vivo*. Our work addresses an immediate challenge and important priority for the clinical domain. Future work will be directed toward defining the role of *CpNA* in T cell differentiation. Such studies will shed light on sialic acids as a regulatory parameter influencing T cell fate.

## MATERIALS AND METHODS

### Tumor cell lines and culture

The human GB cell lines U87 and U251 and human B cell leukemia cell line Nalm6 were acquired from the American Type Culture Collection (ATCC). The tumor cell lines were transduced to stably express the CBG and eGFP under control of the EF-1 $\alpha$  promoter. The cells were sorted on an Influx cell sorter (BD Biosciences) 3 days after transduction to be 100% GFP positive. The GB cell lines were maintained in Improved MEM Zinc Option (Gibco) with 10% fetal bovine serum (FBS) and 1% each of penicillin-streptomycin, GlutaMAX, HEPES, and sodium pyruvate. The Nalm6 cells were maintained in RPMI (Corning) with 10% FBS and 1% each of penicillin-streptomycin and HEPES.

### Lentiviral production

The lentiviral vector pELNS-GFP\_T2A\_NA (GTN) encodes eGFP and *C. perfringens* NA separated by a T2A self-cleaving peptide and under the transcriptional control of EF-1  $\alpha$ . Lentiviral supernatants were generated by transient transfection of 293-T cells with pELNS-GFP\_T2A\_NA. 293-T cells were initially seeded in T150 flasks and grown to 80% confluence in 25 mL of culture medium (RPMI1640); 90  $\mu$ L Lipofectamine 2000 DNA transfection reagent was combined with 7  $\mu$ g pCL-VSVG, 18  $\mu$ g pRSV-REV, and 18  $\mu$ g

of pGAG-POL (Nature Technology) as well as 15  $\mu\text{g}$  of pELNS-GFP\_T2A\_NA. This mixture was incubated at room temperature for 15 min. DNA-Lipofectamine complexes were then added to the 293-T cells.

After 24 h, infectious supernatants were sterile filtered through a 0.45- $\mu\text{m}$  syringe tip cellulose acetate filter and collected in a 50-mL conical tube. To pellet the lentivirus, the supernatant was spun in a Thermo Fisher Scientific Centrifuge (LYNX 4000) at 18,000 RCF, overnight, at 4°C. The supernatant was removed, and the lentiviral pellet was resuspended in 1.6 mL of culture medium, aliquoted, and stored at  $-80^{\circ}\text{C}$ . Generation of the 806 CAR, CD19 CAR, and eGFP encoding lentiviral particles followed the same procedure.

#### **In vitro T cell transduction and expansion**

Primary human leukocytes (PBLs) from healthy male and female volunteers were collected at the University of Pennsylvania's Apheresis Unit. Informed consent was obtained from all participants before collection. All experimental procedures and methods were approved by the University of Pennsylvania Institutional Review Board. T cells were purified at the University's Human Immunology Core by negative selection using the RosetteSep T cell enrichment cocktail (Stemcell). The T cells were activated overnight with anti-CD3/CD28 beads (Thermo Fisher Scientific). Populations of the cells were then transduced with lentiviral vectors for 806 CAR, CD19 CAR, GFP, or GTN constructs. The cells were expanded in complete RPMI Media (Corning), and after 10 days were frozen in aliquots and thawed as needed for experiments.

#### **Cytotoxicity assay**

The ability of CAR T cells co-transduced with GTN or GFP to kill tumor targets was tested in a luciferase-based cytotoxicity assay. CBG-expressing U87 cells ( $20 \times 10^3$ ) were cultured overnight in a 96-well microplate (Corning). The following day, CAR+ T cells were added to each well at E:T ratios of 10:1, 3:1, 1:1, and 1:3. Recombinant NA and GO (Millipore Sigma) were added in PBS to certain wells to final concentrations of 50 mU/mL and 375 mU/mL, respectively, while other wells received vehicle. Each condition was repeated in triplicate. After 24 h, luciferin in PBS was added to each well for a final concentration of 150  $\mu\text{g}/\text{mL}$ . Bioluminescence was recorded with a Synergy HTX plate reader (BioTek).

#### **Flow cytometry**

For knockout studies, cell-surface protein expression was assessed using the following antibodies: anti-CD2-APC [RPA-2.10], anti-CD28-APC [CD28.2], anti-CD58-APC [TS2/9], anti-TRAC/TRBC-APC [IP26] (BioLegend). For anti-EGFR CAR expression, cells were incubated with recombinant EGFRvIII-Fc (Novus Biologicals) followed by polyclonal APC-conjugated anti-Fc secondary (Jackson ImmunoResearch). The anti-CAR19 idiotype for surface expression of CAR19 was provided by Novartis. The expression of murine CD45.1 was assessed with anti-mCD45.1-APC [A20] (BioLegend). In all cases, cells were washed with PBS, incubated with antibodies at room temperature for 30 min in buffer consisting of PBS, 1% BSA, and 5 mM EDTA,

washed twice in PBS (or stained with secondary if indicated and washed), and evaluated on a BD LSR Fortessa. Analysis was performed using FlowJo software (Tree Star Inc. version 10.1).

#### **Enzyme-linked immunosorbent assay**

Target-expressing cells ( $20 \times 10^3$  U87 per well) were cultured overnight in a 96-well V-bottom plate. Thawed and rested CAR T cells were added at an E:T ratio of 1:1. The conditions included the following: CAR T cells, CAR T cells with NA secretion and GFP expression, and CAR T cells with GFP expression alone. The enzymes NA and GO were added at final concentrations of 50 mU/mL and 375 mU/mL, respectively, to appropriate wells as indicated in figure legends. All conditions were performed in triplicate. After 20 h, supernatants were removed, and the cytokines IFN- $\gamma$  and IL-2 were quantified by DuoSet ELISA (R&D Systems).

#### **Neuraminidase activity assay**

U87 and Nalm6 target cells ( $20 \times 10^3$  per well) were cultured overnight in a 96-well V-bottom plate. Thawed and rested CAR T cells co-transduced with GTN or GFP were washed once in fresh media and then added at a 10:1 ratio of GFP+ cells to target cells. After 24 h, the plate was centrifuged at  $500 \times g$  for 3 min, and supernatants were tested for NA activity using the Fluorometric - Blue Neuraminidase Assay Kit (Abcam) per the manufacturer's protocol.

#### **In vivo models**

All mouse experiments were conducted in according to IACUC-approved protocols. Using NSG mice,  $250 \times 10^3$  U87-luc-eGFP cells were injected subcutaneously in the right flank, with seven mice per group. For each injection, the tumor cells were suspended in 100  $\mu\text{L}$  of 20% Matrigel in PBS. One week after tumor implantation, the animals were injected i.v. via tail vein with  $0.5 \times 10^6$  EGFR or CD19-directed CAR T cells, either secreting CpNA or not as indicated in the figures. On a weekly basis, anesthetized mice were imaged using a Xenogen IVIS Spectrum system (Caliper Life Science) to assess tumor bioluminescence. Total bioluminescent flux was quantified using Living Image 4.4 (PerkinElmer). Tumor volumes were assessed via caliper measurement.

In the Nalm6 leukemia model, NSG mice were infused with  $1 \times 10^6$  Nalm6-luc-eGFP tumor cells on day 0. On day 5, the mice received either CpNA secreting or GFP-expressing CAR T infusions by tail vein injection, with five mice per cohort. Bioluminescence was evaluated weekly with the IVIS Spectrum imager as in the U87 experiment. On day 31, mice were re-challenged with an additional  $1 \times 10^6$  tumor cells. Bloods were collected into Trucount tubes by cheek bleed procedure on day 44, stained for human CD45, and evaluated by flow cytometry to quantify the engrafted adoptive cells in the peripheral blood.

For the syngeneic mouse melanoma model,  $50 \times 10^3$  B16F10.CD19 melanoma cells expressing human CD19 were implanted subcutaneously on the right flank in CD45.2 + C57BL/6 mice (The Jackson Laboratory), with seven mice per treatment arm. To generate CAR T cells, splenocytes were harvested from CD45.1 + congenic donor mice, from which T cells were isolated using the EasySep Mouse T cell

Isolation Kit (Stemcell Technologies), activated with Dynabeads Mouse T-Activator CD3/CD28 beads, and transduced by spinfection with ecotropic retrovirus encoding the CD19-directed CAR, GTN, or GFP constructs. Prior to use of mouse CAR T cells, the expression of CAR, GFP, and functional NA were confirmed by flow cytometry or enzyme activity assay as previously described for human cells. Mice with evidence of tumor engraftment (tumor volume  $>50 \text{ mm}^3$ ) on day 5 were randomized to either CD19-directed CAR T (co-expressing CpNA or GFP) or NTD cell infusions, which occurred on days 5 and 12, as well as intra-tumoral injections of NA and GO, GO, or PBS as described in the figures. Tumor volumes were measured weekly beginning on day 5 as well as at the end of the experiment on day 21. To assess CAR T engraftment, blood was collected on day 21 by cardiac puncture, stained with APC-conjugated anti-CD45.1 antibody (Biolegend, clone A20) in TruCount tubes (BD Biosciences), and evaluated with flow cytometry. Animals were euthanized at the end of the experiment or when they met prespecified endpoints according to the protocols.

For the GD-2 xenograft model, animals were injected via tail vein with  $0.5 \times 10^6$  SY5Y- CBG tumor cells (ATCC) in 0.1 mL sterile PBS. On day 4, tumor engraftment was confirmed;  $0.75 \times 10^6$  anti-GD2 CAR T cells or nontransduced NTD human T cells were injected i.v. in 100  $\mu\text{L}$  of sterile PBS, 5 days after injection of SY5Y-CBG tumor cells. Anesthetized mice were imaged using a Xenogen IVIS Spectrum system (Caliper Life Science) twice a week. Mice were given an intraperitoneal injection of D-luciferin (150 mg/kg; Caliper Life Sciences). Total flux was quantified using Living Image 4.4 (PerkinElmer) by drawing rectangles of identical area around mice, reaching from head to 50% of the tail length. Peripheral blood was obtained by retro-orbital bleeding in an EDTA-coated tube, and blood was examined fresh for evidence of T cell engraftment, and differentiation, by flow cytometry using BD TruCount (BD Biosciences).

Animals were euthanized at the end of the experiment before showing signs of toxicity and before reaching signals higher than  $1 \times 10^{11}$  p/s total flux per mouse (in accordance with our Institutional Animal Care and Use Committee [IACUC] protocols).

#### T cell differentiation assay

Activated CAR T cells were expanded for 9 to 11 days and subsequently stained with a panel of monoclonal antibodies to assess differentiation. The following pre-titrated antibodies were used: anti-CCR7-FITC (clone 150,503; BD PharMingen); anti-CD45RO-PE (clone UCHL1), anti-CD8-H7APC (clone SK1; BD Biosciences); anti-CD4-BV605 (clone OKT4).  $1 \times 10^6$  cells were immunostained as follows: cells were washed with PBS and stained for viability using LIVE/DEAD Fixable aqua (Molecular Probes) for 15 min, washed once, and resuspended in fluorescence-activated cell sorting (FACS) buffer consisting of PBS, 1% BSA, and 5 mM EDTA. Cells were then incubated with the above indicated antibodies for 30 min at room temperature. Samples were then washed three times with FACS buffer and fixed in 1% paraformaldehyde. Positively stained cells were differentiated from background using fluorescence-minus-one controls. Flow

cytometry was performed on BD LSR Fortessa. Analysis was performed using FlowJo software (Tree Star version 10.1).

#### SUPPLEMENTAL INFORMATION

Supplemental information can be found online at <https://doi.org/10.1016/j.ymthe.2021.11.014>.

#### ACKNOWLEDGMENTS

We thank Drs. Carl June, Elizabeth Hexner, Gerald Linette, Don Siegel, and Stephen Bagley at the University of Pennsylvania, as well as Dr. Michael Dustin at the University of Oxford, for their helpful discussions. We also thank the Human Immunology, Flow Cytometry, and Stem Cell and Xenograft cores at the University of Pennsylvania. R.S.O. is supported by the NIH grant RO1CA226983-04. Research reported in this publication was also supported by the National Center for Advancing Translational Sciences of the National Institutes of Health under award number TL1TR001880 (J.S.D.), as well as a St. Baldrick's Foundation Scholar Award, National Blood Foundation Scientific Research Grant Award, and Office of the Assistant Secretary of Defense for Health Affairs through the Peer Reviewed Cancer Research Program under Award No. W81XWH-20-1-0417 (S.G.). The content is solely the responsibility of the authors and does not necessarily represent the official views of the National Institutes of Health. This study was also funded, in part, by the Glioblastoma Translational Center of Excellence within The Abramson Cancer Center at the University of Pennsylvania.

#### AUTHOR CONTRIBUTIONS

J.S.D., Z.B., D.M.O., M.M., and R.S.O. designed the study. J.S.D., S.G., V.B., Z.B., D.M.O., M.M., and R.S.O. provided conceptual guidance. J.S.D., S.G., E.S., L.J., J.L., Z.B., and R.S.O. performed the experiments. J.S.D., Z.B., and R.S.O. analyzed the data. J.S.D. and R.S.O. wrote the manuscript. Z.B., S.G., and D.M.O. read and made comments on the manuscript.

#### DECLARATION OF INTERESTS

M.C.M. is an inventor on patent applications related to CAR technology and has received licensing royalties from Novartis corporation; S.G. and M.C.M. are inventors on patent applications related to methods of manufacturing CAR T cells. D.M.O., Z.B., L.J., R.T., and V.B. are inventors on patents related to CAR T cells that have been filed by the University of Pennsylvania. The other authors declare no financial or other conflicts of interest.

#### REFERENCES

- Majzner, R.G., and Mackall, C.L. (2019). Clinical lessons learned from the first leg of the CAR T cell journey. *Nat. Med.* 25, 1341–1355.
- Murciano-Goroff, Y.R., Warner, A.B., and Wolchok, J.D. (2020). The future of cancer immunotherapy: microenvironment-targeting combinations. *Cell Res.* 30, 507–519.
- De Sousa Linares, A., Leitner, J., Grabmeier-Pfistershammer, K., and Steinberger, P. (2018). Not all immune checkpoints are created equal. *Front. Immunol.* 9, 1909.
- Agrawal, B. (2019). New therapeutic targets for cancer: the interplay between immune and metabolic checkpoints and gut microbiota. *Clin. Transl. Med.* 8, 1–13.
- Dusoswa, S.A., Verhoeff, J., Abels, E., Méndez-Huergo, S.P., Croci, D.O., Kuijper, L.H., de Miguel, E., Wouters, V.M.C.J., Best, M.G., Rodriguez, E., et al. (2020).

- Glioblastomas exploit truncated O-linked glycans for local and distant immune modulation via the macrophage galactose-type lectin. *Proc. Natl. Acad. Sci. U S A* *117*, 3693–3703.
6. Rodriguez, E., Boelaars, K., Brown, K., Eveline Li, R.J., Kruijssen, L., Bruijns, S.C.M., van Ee, T., Schetters, S.T.T., Crommentuijn, M.H.W., van der Horst, J.C., et al. (2021). Sialic acids in pancreatic cancer cells drive tumour-associated macrophage differentiation via the siglec receptors siglec-7 and siglec-9. *Nat. Commun.* *12*, 1–14.
  7. Rodriguez, E., Schetters, S.T., and van Kooyk, Y. (2018). The tumour glyco-code as a novel immune checkpoint for immunotherapy. *Nat. Rev. Immunol.* *18*, 204–211.
  8. Stanczak, M.A., Siddiqui, S.S., Trefny, M.P., Thommen, D.S., Boligan, K.F., von Gunten, S., Tzankov, A., Tietze, L., Lardinois, D., Heinzlmann-Schwarz, V., et al. (2018). Self-associated molecular patterns mediate cancer immune evasion by engaging siglecs on T cells. *J. Clin. Invest.* *128*, 4912–4923.
  9. Ikehara, Y., Ikehara, S.K., and Paulson, J.C. (2004). Negative regulation of T cell receptor signaling by siglec-7 (p70/AIRM) and siglec-9. *J. Biol. Chem.* *279*, 43117–43125.
  10. Büll, C., den Brok, M.H., and Adema, G.J. (2014). Sweet escape: sialic acids in tumor immune evasion. *Biochim. Biophys. Acta* *1846*, 238–246.
  11. Cohnen, A., Chiang, S.C., Stojanovic, A., Schmidt, H., Claus, M., Saftig, P., Janßen, O., Cerwenka, A., Bryceson, Y.T., and Watzl, C. (2013). Surface CD107a/LAMP-1 protects natural killer cells from degranulation-associated damage. *Blood* *122*, 1411–1418. <https://doi.org/10.1182/blood-2012-07-441832>, <https://www.ncbi.nlm.nih.gov/pubmed/23847195>.
  12. Khazen, R., Müller, S., Gaudenzio, N., Espinosa, E., Marie-pierre, P., and Valitutti, S. (2016). Melanoma cell lysosome secretory burst neutralizes the CTL-mediated cytotoxicity at the lytic synapse. *Nat. Commun.* *7*, 10823. <https://doi.org/10.1038/ncomms10823>, <https://www.ncbi.nlm.nih.gov/pubmed/26940455>.
  13. Santegeerts, K.C.M., Gielen, P.R., Büll, C., Schulte, B.M., Kers-Rebel, E.D., Küsters, B., Bossman, S.A.J.F.H., Ter Laan, M., Wesseling, P., and Adema, G.J. (2019). Expression profiling of immune inhibitory siglecs and their ligands in patients with glioma. *Cancer Immunol. Immunother.* *68*, 937–949.
  14. Büll, C., Boltje, T.J., van Dinther, E.A., Peters, T., de Graaf, A.M., Leusen, J.H., Kreutz, M., Figdor, C.G., den Brok, M.H., and Adema, G.J. (2015). Targeted delivery of a sialic acid-blocking glycomimetic to cancer cells inhibits metastatic spread. *ACS Nano* *9*, 733–745.
  15. Bekesi, J.G., Arneault, G.S., Walter, L., and Holland, J.F. (1972). Immunogenicity of leukemia L1210 cells after neuraminidase treatment. *J. Natl. Cancer Inst.* *49*, 107–118.
  16. Bekesi, J.G., Roboz, J.P., and Holland, J.F. (1976). Therapeutic effectiveness of neuraminidase-treated tumor cells as an immunogen in man and experimental animals with leukemia. *Ann. N. Y. Acad. Sci.* *277*, 313–331.
  17. Sedlacek, H.H., Hagmayer, G., and Seiler, F.R. (1986). Tumor therapy of neoplastic diseases with tumor cells and neuraminidase. *Cancer Immunol. Immunother.* *23*, 192–199.
  18. Miyagi, T., Wada, T., Yamaguchi, K., and Hata, K. (2003). Sialidase and malignancy: a minireview. *Glycoconj. J.* *20*, 189–198.
  19. Gray, B.N., Walker, C., Andrewartha, L., Freeman, S., and Bennett, R.C. (1989). Controlled clinical trial of adjuvant immunotherapy with BCG and neuraminidase-treated autologous tumour cells in large bowel cancer. *J. Surg. Oncol.* *40*, 34–37.
  20. He, D., Sun, L., Li, C., Hu, N., Sheng, Y., Chen, Z., Li, X., Chi, B., and Jin, N. (2014). Anti-tumor effects of an oncolytic adenovirus expressing hemagglutinin-neuraminidase of newcastle disease virus in vitro and in vivo. *Viruses* *6*, 856–874.
  21. Zhou, Z., Wang, X., Jiang, L., Li, D., and Qian, R. (2021). Sialidase-conjugated “NanoNiche” for efficient immune checkpoint blockade therapy. *ACS Appl. Bio. Mater.* *4*, 5735–5741.
  22. Hsieh, H., Calcutt, M.J., Chapman, L.F., Mitra, M., and Smith, D.S. (2003). Purification and characterization of a recombinant  $\alpha$ -N-acetylgalactosaminidase from *Clostridium perfringens*. *Protein Expr. Purif.* *32*, 309–316.
  23. Moustafa, I., Connaris, H., Taylor, M., Zaitsev, V., Wilson, J.C., Kiefel, M.J., von Itzstein, M., and Taylor, G. (2004). Sialic acid recognition by vibrio cholerae neuraminidase. *J. Biol. Chem.* *279*, 40819–40826.
  24. Seyrantepe, V., Landry, K., Trudel, S., Hassan, J.A., Morales, C.R., and Pshzhetsky, A.V. (2004). Neu4, a novel human lysosomal lumen sialidase, confers normal phenotype to sialidosis and galactosialidosis cells. *J. Biol. Chem.* *279*, 37021–37029.
  25. Rajendran, M., Nachbagauer, R., Ermler, M.E., Bunduc, P., Amanat, F., Izikson, R., Cox, M., Palese, P., Eichelberger, M., and Krammer, F. (2017). Analysis of anti-influenza virus neuraminidase antibodies in children, adults, and the elderly by ELISA and enzyme inhibition: evidence for original antigenic sin. *MBio* *8*, 2281.
  26. Novogrodsky, A., and Katchalski, E. (1973). Induction of lymphocyte transformation by sequential treatment with neuraminidase and galactose oxidase. *Proc. Natl. Acad. Sci. U S A* *70*, 1824–1827.
  27. Novogrodsky, A. (1975). Induction of lymphocyte cytotoxicity by modification of the effector or target cells with periodate or with neuraminidase and galactose oxidase. *J. Immunol.* *114*, 1089–1093. <http://www.jimmunol.org/cgi/content/abstract/114/3/1089>.
  28. Rhodes, J., Zheng, B., and Morrison, C.A. (1995). Galactose oxidation as a potent vaccine adjuvant strategy. efficacy in murine models and in protection against a bovine parasitic infection. *Ann. N. Y. Acad. Sci.* *754*, 169.
  29. Reinhard, K., Rengstl, B., Oehm, P., Michel, K., Billmeier, A., Hayduk, N., Klein, O., Kuna, K., Ouchan, Y., Wöll, S., et al. (2020). An RNA vaccine drives expansion and efficacy of claudin-CAR-T cells against solid tumors. *Science* *367*, 446–453.
  30. Gattinoni, L., Klebanoff, C.A., Palmer, D.C., Wrzesinski, C., Kerstann, K., Yu, Z., Finkelstein, S.E., Theoret, M.R., Rosenberg, S.A., and Restifo, N.P. (2005). Acquisition of full effector function in vitro paradoxically impairs the in vivo anti-tumor efficacy of adoptively transferred CD8 T cells. *J. Clin. Invest.* *115*, 1616–1626.
  31. Berger, C., Jensen, M.C., Lansdorp, P.M., Gough, M., Elliott, C., and Riddell, S.R. (2008). Adoptive transfer of effector CD8 T cells derived from central memory cells establishes persistent T cell memory in primates. *J. Clin. Invest.* *118*, 294–305.
  32. Alizadeh, D., Wong, R.A., Yang, X., Wang, D., Pecoraro, J.R., Kuo, C.F., Aguilar, B., Qi, Y., Ann, D.K., Starr, R., et al. (2019). IL15 enhances CAR-T cell antitumor activity by reducing mTORC1 activity and preserving their stem cell memory phenotype. *Cancer Immunol. Res.* *7*, 759–772.
  33. O'Rourke, D.M., Nasrallah, M.P., Desai, A., Melenhorst, J.J., Mansfield, K., Morrisette, J.J.D., Martinez-Lage, M., Brem, S., Maloney, E., Shen, A., et al. (2017). A single dose of peripherally infused EGFRvIII-directed CAR T cells mediates antigen loss and induces adaptive resistance in patients with recurrent glioblastoma. *Sci. Transl. Med.* *9*, eaaa0984. <https://doi.org/10.1126/scitranslmed.aaa0984>, <https://www.ncbi.nlm.nih.gov/pubmed/28724573>.
  34. Ocklind, G., Talts, J., and Lindahl-Kiessling, K. (1988). Activation of human T cells by neuraminidase-galactose oxidase-treated erythrocytes involving CD2 (T11) and its complementary structure. *Scand. J. Immunol.* *27*, 697–704.
  35. Sanjana, N.E., Shalem, O., and Zhang, F. (2014). Improved vectors and genome-wide libraries for CRISPR screening. *Nat. Methods* *11*, 783–784.
  36. Bajnok, A., Ivanova, M., Rigó, J., and Toldi, G. (2017). The distribution of activation markers and selectins on peripheral T lymphocytes in preeclampsia. *Mediators Inflamm.* *2017*, 8045161.
  37. Kaizuka, Y., Douglass, A.D., Vardhana, S., Dustin, M.L., and Vale, R.D. (2009). The coreceptor CD2 uses plasma membrane microdomains to transduce signals in T cells. *J. Cell Biol.* *185*, 521–534.
  38. Sellmyer, M., Richman, S., Lohith, K., Hou, C., Lieberman, B., Mankoff, D., Mach, R., Milone, M., and Farwell, M. (2018;59:122). In vivo monitoring of CAR T cells using [18F] fluoropropyl-trimethoprim. *Mol. Ther.*
  39. Ghassemi, S., Martinez-Becerra, F.J., Master, A.M., Richman, S.A., Heo, D., Leferovich, J., Tu, Y., García-Cañaveras, J.C., Ayari, A., et al. (2020). Enhancing chimeric antigen receptor T cell anti-tumor function through advanced media design. *Mol. Ther. Methods Clin. Dev.* *18*, 595–606.
  40. Gérard, A., Khan, O., Beemiller, P., Oswald, E., Hu, J., Matloubian, M., and Krummel, M.F. (2013). Secondary T cell-T cell synaptic interactions drive the differentiation of protective CD8 T cells. *Nat. Immunol.* *14* (4), 356–363.
  41. Galili, U., and Schlesinger, M. (1974). The formation of stable E rosettes after neuraminidase treatment of either human peripheral blood lymphocytes or of sheep red blood cells. *J. Immunol.* *112*, 1628–1634.

42. Weiner, M.S., Bianco, C., and Nussenzweig, V. (1973). Enhanced binding of neuraminidase-treated sheep erythrocytes to human T lymphocytes. *Blood* 42, 939–946.
43. Challa-Malladi, M., Lieu, Y.K., Califano, O., Holmes, A.B., Bhagat, G., Murty, V.V., Dominguez-Sola, D., Pasqualucci, L., and Dalla-Favera, R. (2011). Combined genetic inactivation of  $\beta$ 2-microglobulin and CD58 reveals frequent escape from immune recognition in diffuse large B cell lymphoma. *Cancer Cell* 20, 728–740.
44. Majzner, R.G., Frank, M.J., Mount, C., Tousley, A., Kurtz, D.M., Sworder, B., Murphy, K.A., Manousopoulou, A., Kohler, K., Rotiroti, M.C., et al. (2020). CD58 aberrations limit durable responses to CD19 CAR in large B cell lymphoma patients treated with axicabtagene ciloleucel but can be overcome through novel CAR engineering. *Blood* 136, 53–54.
45. Frangieh, C.J., Melms, J.C., Thakore, P.I., Geiger-Schuller, K.R., Ho, P., Luoma, A.M., Cleary, B., Jerby-Arnon, L., Malu, S., Cuoco, M.S., et al. (2021). Multi-modal pooled perturb-CITE-seq screens in patient models define novel mechanisms of cancer immune evasion. *Nat. Genet.* 53, 332–341.
46. Hogan, P.G. (2017). Calcium–NFAT transcriptional signalling in T cell activation and T cell exhaustion. *Cell Calcium* 63, 66–69.

# Epigenetic strategies to boost CAR T cell therapy

Behnia Akbari,<sup>1</sup> Navid Ghahri-Saremi,<sup>1</sup> Tahereh Soltantoyeh,<sup>1</sup> Jamshid Hadjati,<sup>1</sup> Saba Ghassemi,<sup>2</sup> and Hamid Reza Mirzaei<sup>1</sup>

<sup>1</sup>Department of Medical Immunology, School of Medicine, Tehran University of Medical Sciences, Tehran 1417613151, Iran; <sup>2</sup>Center for Cellular Immunotherapies, Perelman School of Medicine, University of Pennsylvania, Philadelphia, PA 19104, USA

**Chimeric antigen receptor (CAR) T cell therapy has led to a paradigm shift in cancer immunotherapy, but still several obstacles limit CAR T cell efficacy in cancers. Advances in high-throughput technologies revealed new insights into the role that epigenetic reprogramming plays in T cells. Mechanistic studies as well as comprehensive epigenome maps revealed an important role for epigenetic remodeling in T cell differentiation. These modifications shape the overall immune response through alterations in T cell phenotype and function. Here, we outline how epigenetic modifications in CAR T cells can overcome barriers limiting CAR T cell effectiveness, particularly in immunosuppressive tumor microenvironments. We also offer our perspective on how selected epigenetic modifications can boost CAR T cells to ultimately improve the efficacy of CAR T cell therapy.**

## INTRODUCTION

For years, the cornerstone of cancer therapy has been surgery, chemotherapy, and radiation therapy.<sup>1</sup> More recently, targeted therapies, in particular cell-based therapies such as adoptive T cell and chimeric antigen receptor (CAR) T cell therapies, have led to tremendous successes against cancer.<sup>1,2</sup> Although CAR T cell therapy has been approved by the US Food and Drug Administration (FDA) in several hematological malignancies, its success in solid tumors has been limited. There are several roadblocks impeding CAR T cell therapy in solid tumors, including (1) antigen heterogeneity/loss that renders the CAR obsolete, (2) the presence of immunosuppressive cells and molecules within the tumor microenvironment (TME), (3) poor persistence of *ex vivo* expanded CAR T cells, and (4) impaired penetration and trafficking of CAR T cells to tumor sites.<sup>3</sup>

Despite efforts to overcome these barriers, there still is no approved CAR T cell therapy for solid tumors. Combining CAR T cells with immune checkpoint blockades, oncolytic viruses, bispecific T cell engagers, and cytokines has increased the efficacy of adoptively transferred cells in preclinical models. There are still some unaddressed aspects of CAR T cell biology and functionality, such as understanding how epigenetic reprogramming and gene regulation enhance CAR T cell antitumor function.<sup>4–6</sup> The central dogma of molecular biology has come under scrutiny by the emerging field of epigenetics. In recent years epigenetic studies on cancer as well as immune cells have gener-

ated plenty of useful data. The current challenge is to translate this knowledge to a favorable clinical outcome. In this review, we discuss how epigenetic modifications of CAR T cells and tumor cells can boost the efficacy of CAR T cell therapy. Table 1 lists some challenges to CAR T cell therapy and summarizes some epigenetic modification-based overcoming solutions.

## EPIGENETIC MECHANISMS

The term “epigenetic,” defined as “on top of” genetic, describes changes in gene expression independent of the genetic code itself. Epigenetic modifications can be divided into four main areas: (1) genomic or DNA modifications that are a result of cytosine methylation or hydroxymethylation, (2) histone modifications that are a result of acetylation, methylation, phosphorylation, and other processes, (3) non-coding RNA (ncRNA)-associated modifications that are responsible for microRNA (miRNA) (and other ncRNA)-associated gene expression, and (4) higher order-associated modifications.<sup>22,23</sup> The placement, turnover, and activity of DNA or histone modifications can be conducted by “writers,” “erasers,” and “readers,” respectively. While writers and erasers are responsible for DNA and histone epigenetic modifications, reader proteins translate these modifications to cell behaviors, including gene expression, DNA repair, and replication, through employing their specific domains that recognize certain epigenetic modifications.<sup>24,25</sup>

### DNA-associated modifications

DNA can be modified by several mechanisms, and direct nucleotide methylation is the most common of these modifications. CpG islands involved cytosine base methylation at carbon 5. DNA can be marked by *de novo* mechanisms (catalyzed via DNA methyltransferase [DNMT] 3A/B/L) and once stabilized can be inherited through sequential cell divisions and maintained by the activity of DNMT1.<sup>26</sup> Another family of proteins, named ten-eleven translocation (TET), is responsible for demethylation events.<sup>27</sup> Methylation at promoters often causes a decrease in gene expression and suppression of gene transcription. In contrast,

<https://doi.org/10.1016/j.ymthe.2021.08.003>

**Correspondence:** Hamid R. Mirzaei, PhD, Department of Medical Immunology, School of Medicine, Tehran University of Medical Sciences, Tehran 1417613151, Iran.

**E-mail:** [h-mirzaei@tums.ac.ir](mailto:h-mirzaei@tums.ac.ir)

**Table 1. Challenges to CAR T cell therapy in solid tumors and epigenetic solutions**

Challenges		Overcoming strategies based on epigenetic modifications	Refs.	
Antigen heterogeneity	heterogeneous expression of antigens in the tumors	using DNMTis and HDACis to induce expression of CTAs and HERVs	3,7-9	
Impaired trafficking	mismatched chemokines and their receptors	using histone, DNA, and miRNA modifications to overexpress chemokines and their receptors	3,10-12	
Hostile tumor microenvironment	physical barriers	extracellular matrix, stromal cells, vasculature		
	immunosuppressive cells	Tregs, MDSCs, iDCs, M2 macrophages		
	soluble immunosuppressive molecules	inhibitory enzymes (arginase, IDO1), ligands (PDL-1/2, FasL), others (IL-10, TGF- $\beta$ )	using histone, DNA, and miRNAs modifications to repress immunomodulatory molecules	3,11,13-15
	immunosuppressive condition	low PH, hypoxia		
T cell-intrinsic regulation	PD1, TGIT, A2ar, CTLA-4, TIM3, LAG3	using histone, DNA, and miRNA modifications to downregulate inhibitory molecules	3,16-21	

DNMTi, DNA methyltransferase inhibitor; HDACi, histone deacetylase inhibitor; HERV, human endogenous retroviruses; iDCs, immature dendritic cells; MDSC, myeloid-derived suppressor cell.

highly expressed genes show high levels of methylation inside the genes (i.e., introns); however, a low degree of methylation at promoter or regulatory sites of the genes is observed.<sup>26,28</sup>

### Histone-associated modifications

At the next level, DNA is wrapped around core proteins called histones. These cationic proteins can be posttranslationally modified by acetylation, methylation, phosphorylation, ubiquitination, SUMOylation (small ubiquitin-related modifier), and lactylation.<sup>29-31</sup> Histone modifications can be permissive, poised, and repressing, depending on which histone tail residue is modified. For example, histone acetylation (histone 3 of lysine 27 [H3K27]) is an activating or permissive histone modification by increasing chromatin accessibility at promoter or enhancer sites of genes. Another well-studied histone modification is methylation. In contrast to histone acetylation, histone methylation is more complicated. For instance, lysine 4 of histone 3 trimethylation (H3K4me3) is associated with permissive promoters or enhancers and euchromatin structure of the genome, but mono-methylation of H3K4 (H3K4me1) is associated with poised enhancer sites.<sup>32</sup> In contrast, trimethylation of H3K27 (H3K27me3) gives rise to heterochromatin and repression of gene transcription.<sup>32</sup> Other modifications including histone ubiquitination, SUMOylation, and lactylation can also occur. These modifications are essential for maintaining gene expression and overall chromatin structure in cells. It has been shown that mono-ubiquitination is associated with transcriptional activation while de-ubiquitination suppresses transcription. Consistently, histone SUMOylation is associated with transcription repression.<sup>33</sup>

### ncRNA-associated modifications

ncRNAs provide another level to epigenetic regulation. Interestingly, most human transcripts do not encode for proteins but play important roles in cell differentiation and function. Regulatory ncRNAs can be divided in two subgroups based on their size: short chain ncRNAs (including miRNAs, small interfering RNAs

[siRNAs], and PIWI-interacting RNAs [piRNAs]) and long ncRNAs (lncRNAs).<sup>34</sup> Recent studies have shown that ncRNAs and more specifically miRNAs and siRNAs can effectively silence genes by altering histone deacetylation, methylation, and DNA methylation.<sup>35-37</sup> In the following sections we discuss the how modulation of miRNAs either through their repression or overexpression (restoring) can alter the function of (CAR) T cells. There are many tools to inhibit miRNAs, including antisense anti-miRNA oligonucleotides (AMOs), locked nucleic acid (LNA) anti-miRNAs, antagomirs, miRNA sponges, miRNA masks, and miRNA-targeting small molecule inhibitors.<sup>38</sup> Nearly all of these tools use complementary single-strand oligonucleotides to sequester the targeted miRNA. Other tools that can be used to enhance miRNA expression include miRNA mimics and miRNA expression vectors.<sup>38</sup>

### Higher order-associated modifications

Eukaryotic DNA wraps around core histone proteins to form a nucleosome. The dynamics of higher order chromatin organization and condensation plays a major role in the regulation of replication, DNA repair, and recombination and, more importantly, acts as an epigenetic modifier in gene transcription and expression.<sup>39</sup> Importantly, chromatin accessibility changes in line with T cell differentiation.<sup>40</sup> Chromosomes are separated into discrete topologically associating domains (TADs). TADs are highly self-interacting regions in the DNA molecule. This means that DNA sequences within a TAD interact with each other more frequently than other DNA sequences.<sup>41-43</sup> Each TAD restricts the spread of heterochromatin or euchromatin by boundaries. These boundaries are enriched with a transcriptional repressor known as CCCTC-binding factor (CTCF), a protein that acts as an insulating factor. TADs are mainly conserved throughout development across species; however, the dynamics of their intra interactions occur in a tissue- and cell-specific manner.<sup>43,44</sup> Figure 1 illustrates the various epigenetic levels in the eukaryotic cells.

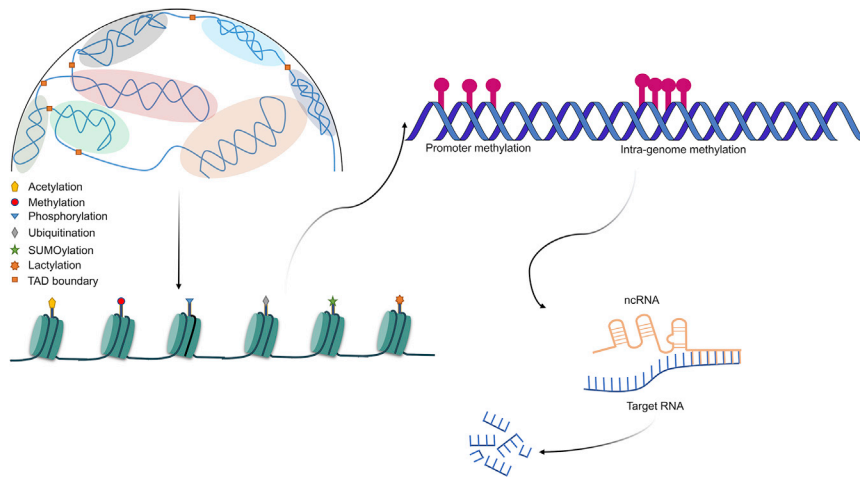


**Figure 1. Epigenetic levels in the eukaryotic cells**

Four levels of epigenetic mechanisms exist in the eukaryotic cells. Higher order epigenetic modifications can alter gene expression by chromatin remodeling. Histone modifications can shape euchromatin or heterochromatin formation and regulate gene expression. DNA methylation can both induce and repress gene expression based on methylation position in the genome. Lastly, ncRNAs can both induce and repress gene expression by targeting RNAs. These mechanisms, all together, shape cell behavior and fate in humans.

## EPIGENETIC MECHANISMS IN T CELLS

In recent years, epigenetic studies demonstrated how epigenetic mechanisms regulate T cell activation, maturation, and exhaustion.<sup>23,45</sup> Epigenetic mechanisms important for T cell differentiation are discussed below.

### DNA-associated mechanisms in T cells

In naive T cells, effector genes are generally methylated; however, naive/memory-associated genes exist in an unmethylated form. In contrast, effector T cells are characterized by methylated naive/memory-associated genes and unmethylated effector genes. As T cells transition into central and/or stem cell memory subsets, their effector genes can be remethylated.<sup>23,46,47</sup> Histone methyltransferases and DNMTs (DNMT1, DNMT3A) are highly active in exhausted T cells. Inhibiting DNMT3A can prevent terminal exhaustion of T cells and increase the development of less differentiated T cells in chronic inflammations such as chronic viral diseases or cancers.<sup>48</sup> Also, inhibition of DNMT3A at early stages of T cell differentiation into effector cells leads to the development of central memory T cells.<sup>49,50</sup> These studies indicate that upon T cell activation and differentiation, based on the cell fate, several genes are required to be methylated and demethylated to form effector or memory cells.<sup>23</sup> Indeed, inhibiting *de novo* methylation of effector-related genes in naive T cells upon activation can reduce the effector cell population and increase the memory-like cell population.<sup>50</sup> Moreover, inhibition of *de novo* methylation of genes in effector or memory T cells can prevent formation of terminally exhausted T cells upon chronic antigen exposure.<sup>51</sup> In another interesting study, it was demonstrated that decreased methylation at the CX3CR1 locus in effector memory T cells promotes their migratory activities.<sup>52</sup> Taken together, these findings show that DNA methylation is a critical epigenetic mechanism underlying T cell fate and behavior. Figure 2 illustrates epigenetic alterations in T cells during their differentiation program.

### Histone-associated mechanisms in T cells

As we mentioned above, histone methylations can be divided into three groups, that is, permissive histone modifications such as

H3K4me3, repressive histone modifications such as H3K27me3, and poised histone modifications such as H3K4me1 and H3K27me3 at enhancer sites or H3K27me3 and H3K4me3 at promoter sites.<sup>32</sup> Several studies have shown the importance of histone methylation in T cells. In naive T cells H3K4me3 and H3K27me3 modifications are frequently observed. H3K4me3 modifications are also commonly found in memory T cells.<sup>53</sup> For example, H3K4me3 modification at a number of loci, including TCF7, LEF1, and KLF2, supports the formation of central memory T ( $T_{CM}$ ) cells and stem cell memory T ( $T_{SCM}$ ) cells. An increase in H3K27me3 at memory-related genes induces the differentiation of effector memory T ( $T_{EM}$ ) cells.<sup>54</sup> Interestingly, increases in H3K4me3 and decreases in H3K27me3 at the *Gcnt1* locus enhance the trafficking of memory T cells to tumor sites in an interleukin (IL)-15-dependent manner.<sup>55</sup> Moreover, while acetylation and phosphorylation of histones H3 and H4 are decreased upon T cell activation (in proximal regions of the IL-2 promoter),<sup>56</sup> downregulation of diacetylated histone H3 in T cells in chronic viral infection led to development of exhausted T cells. These findings suggest that inhibition of histone H3 deacetylase may enhance the function of T cells.<sup>57</sup> Histone acetyltransferase binding to ORC1 (HBO1)-mediated acetylation of histones H3 and H4 promotes the development of exhausted T cells. This might be explained by the role of the TOX transcription factor (TF).<sup>16</sup> TOX interacts with acetyltransferase in the HBO1 complex (KAT7) and enhances the gene expression of inhibitory receptors in T cells. More specifically, H3K27 acetylation at intronic and intergenic regions is shown to be associated with T cell exhaustion.<sup>58</sup> In aggregate, it seems that inhibition of H3K27 acetylation and/or using histone acetyltransferase inhibitors (HATis) can reverse T cell exhaustion. Increasing evidence supports a role for HATis and histone deacetylase inhibitors (HDACis) in modulating T cell fate and function. For instance, adding HDACis and IL-21 to cultures of differentiated CD8<sup>+</sup> T cells led to enhanced central memory T cell development.<sup>59</sup> Another study showed that HDAC1 and HDAC2 inhibitors promote differentiation of CD4<sup>+</sup> T cells to cytotoxic CD4<sup>+</sup> T cells, which are enriched for gene signatures characteristic of cytotoxic CD8<sup>+</sup> T cells.<sup>60</sup> In line with this finding, treating mice with an HDAC1 inhibitor results in an upregulation of pathways and genes responsible for CD8<sup>+</sup> T cell cytotoxic activity.<sup>61</sup> Altogether, it seems that application of HATis or HDACis

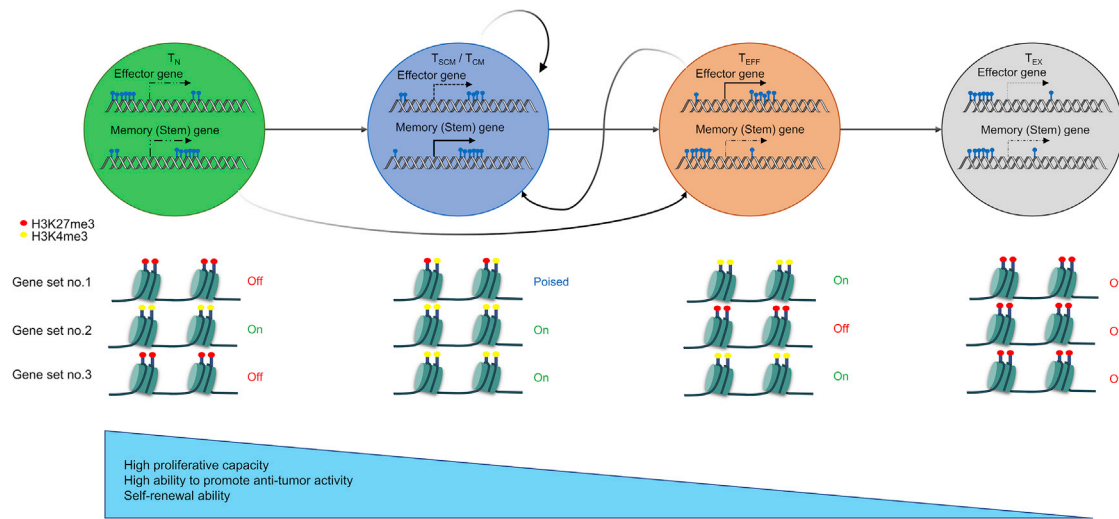


**Figure 2. Epigenetic alterations in T cells during their differentiation**

Each phenotype of T cells has a distinct epigenetic phenotype. In the naive T cells, gene expression for both effector and stem genes is at minimal levels; however, memory T cells show upregulation in gene expression by alteration in DNA methylation and histone modifications. Effector T cells show repression of stem-related genes, while exhausted or dysfunctional T cells are characterized by low gene expression levels in both effector and stem genes. T<sub>N</sub>, naive T cell; T<sub>SCM</sub>, stem cell memory T cell; T<sub>CM</sub>, central memory T cell; T<sub>EX</sub>, exhausted T cell.

can be useful for the generation of more functional CAR T cells. Still, current HDACis and HATis are mainly pan-HDAC inhibitors or pan-HAT inhibitors. These findings highlight a need for the development of new epidrugs targeting specific HDACs and HATs. Also, more studies are needed to evaluate the effects of HATis and HDACis on T cell differentiation and function. Besides the methylation and acetylation of histones, SUMOylation is important for regulatory T cell (Treg) differentiation, and its loss maintains repressive histone remodeling at the FOXP3 promoter.<sup>62</sup> Recent studies have also shown that lactylation of histones is associated with metabolic changes in M1-polarizing macrophages differentiating in response to lipopolysaccharide (LPS) treatment.<sup>63</sup> In agreement with this notion, a study has reported that inhibition of lactate dehydrogenase (LDHi) combined with IL-21 can induce stem cell memory phenotype in the treated T cells.<sup>64</sup> Although speculative, the authors suggest that LDHi may affect H3K79 methylation and histone lactylation.<sup>63</sup> The biological role of histone ubiquitination, SUMOylation, and lactylation remains to be fully elucidated, and further research is required to address the exact function of these modifications in T cells.

#### ncRNA-mediated mechanisms in T cells

ncRNAs and transcription factors also regulate gene expression and chromatin remodeling. Intuitively, silencing “non-T cell genes” via posttranscriptional gene suppression is a viable means to direct T cell differentiation during development. Similarly, miRNAs modulate T cell activation, proliferation, and transition to central memory versus effector differentiated subsets by silencing or inducing target genes. Silencing inhibitory receptor transcripts by miRNAs (e.g., miR-138) can overcome T cell-intrinsic dysregulations (e.g., T cell exhaustion) and promote tumor regression in the context of cancer immunotherapy.<sup>65</sup> It is increasingly accepted that activated T cells

undergo transcriptional changes as well as miRNAome modifications to support cell proliferation and effector functions.<sup>66</sup> The miRNAome repertoire continuously adapts during the ordered T cell differentiation process.<sup>67,68</sup> Furthermore, several miRNAs involved in silencing essential transcripts for T cell effector function can be repressed by miRNA inhibitors in the context of cancer immunotherapy. For instance, the miR-17-92 cluster is highly active during T cell proliferation and differentiation. miR-17-92 promotes mammalian target of rapamycin (mTOR) signaling by targeting mTOR inhibitory molecules such as PTEN and PHLPP2. Notably, miR-17-92 overexpression promotes T cell differentiation and survival. In addition, miR-17-92-deficient T cells are impaired in proliferation and differentiation.<sup>69</sup> miR-17-92 manipulation has resulted in changes in Id3 expression, a DNA-binding inhibitor that is a key regulator in memory differentiation, and thus miR-17-92 levels can balance the effector/memory ratio in T cells.<sup>70–73</sup> Consistently, miR-15/16 clusters have been shown to restrain memory T cell formation and differentiation by targeting several memory- and survival-associated mRNAs.<sup>17</sup> Several other miRNAs influence T cell activation, expansion, survival, and antitumor response, including miR-155, by targeting SHIP-1 and promoting phosphatidylinositol 3-kinase (PI3K)-AKT and STAT signaling;<sup>74,75</sup> miR-146a, which targets nuclear factor  $\kappa$ B (NF- $\kappa$ B) and interrupts T cell effector function;<sup>76–78</sup> and miR-23a, which is upregulated in cytotoxic T lymphocytes (CTLs) in response to TME-secreted transforming growth factor  $\beta$  (TGF- $\beta$ ) and can target the transcription factor Blimp-1, which is required for T cell differentiation and cytotoxicity. Therefore, targeting miR-23a and maintaining desired levels of Blimp-1 can prevent tumor-dependent immunosuppression.<sup>79</sup> miR-139, miR-150, and miR-342 have also been shown to target eomesodermin (EOMES), CD25, and perforin.<sup>80</sup> Additionally, miR-150 can target c-Myb and

its downregulation leads to memory T cell development,<sup>80,81</sup> while its overexpression has been shown to reduce T cell proliferation.<sup>82</sup> miR-214 enhances T cell proliferation upon activation by targeting PTEN,<sup>83</sup> and miR-181a is a tolerogenic miRNA and targets serine/threonine phosphatases in T cells.<sup>84,85</sup> Other forms of ncRNAs, including siRNAs, have also been studied in T cells. For instance, siRNA-mediated depletion of EOMES, which is enriched in terminally exhausted T cells,<sup>86</sup> results in enhanced killing capacity and cytokine production in CD8<sup>+</sup> T cells.<sup>87</sup> Altogether, there are plenty of ncRNAs that can shape T cell phenotype and function. Several studies have demonstrated that ncRNAs, including miRNAs, can regulate other epigenetic mechanisms (DNA and histone modification). For instance, it has been shown that miR-29 can inhibit the activity of *de novo* DNA methylation,<sup>88,89</sup> while miR-17-5p and miR-20a can induce heterochromatin formation.<sup>90</sup> Other types of ncRNAs such as piRNAs and lncRNAs also have been shown to regulate gene expression by DNA and histone modifications.<sup>65</sup>

#### Higher order mechanisms in T cells

Often viewed as “higher order levels of epigenetic remodeling,” cell type-specific DNA remodeling in TADs can bring distal enhancer regions near a promoter to further regulate gene expression. This type of epi-reprogramming regulates cytokine expression in CD4<sup>+</sup> T cells and CD8 expression in CD8<sup>+</sup> T cells.<sup>91–93</sup> Chromatin remodeling factors, including CTCF, and cohesion complexes play pivotal roles in the regulation of chromatin interactions, accessibility, nucleosomal sliding, and ultimately gene expression. Loss of these proteins can disrupt chromatin interactions, resulting in aberrant gene expression.<sup>94,95</sup> For instance, CTCF and cohesion ablation in thymocytes impairs T cell differentiation.<sup>96,97</sup> Interaction of epigenetic readers, writers, and erasers with chromatin remodeling proteins can facilitate and regulate gene expression. In a study, it has been demonstrated that following T cell receptor (TCR) stimulation of CD8<sup>+</sup> T cells, chromatin remodeling by STAB1 results in recruitment of a histone deacetylase complex at enhancer sites of *pdccl1*. This complex downregulates PD-1 expression. Interestingly, tumor-derived TGF- $\beta$  downregulates STAB1 expression through binding of SMAD proteins to the STAB1 promoter. It also releases the *pdccl1* promoter from STAB1 repression by competing with STAB1 for binding to the enhancer of *pdccl1*. This competition results in increased PD-1 expression.<sup>98</sup> Additionally, recent studies have found that the HMG-box transcription factor TOX is a central regulator of T cell exhaustion.<sup>16,18,58</sup> In the absence of TOX, the development and formation of exhausted T cells is blunted.<sup>18</sup> These findings suggest that TOX can promote chromatin remodeling and alter genomic architecture to govern the epigenetic development of exhausted T cells.<sup>16,18</sup> Table 2 summarizes various epigenetic mechanisms in T cells.

Taken together, these studies shed light on the several layers of epigenetic reprogramming in T cell immunobiology. As these layers converge on T cell differentiation, it is likely that epigenetic modifications can be increasingly employed in the context of cancer immunotherapy. In theory, epigenetic remodeling of (CAR) T cells can over-

come several challenges to CAR T cell therapy through increasing the persistence and survival of T cells, diminishing the exhaustion of T cells, improving their infiltration, and promoting memory phenotype formation.

#### EPIGENETIC REPROGRAMMING OF CAR T CELL DIFFERENTIATION TO PRODUCE LESS DIFFERENTIATED CAR T CELLS

Human and murine studies have shown that less differentiated CD8<sup>+</sup> T cells exhibit superior antitumor function.<sup>99–101</sup> As the general CAR T expansion protocol gives rise to terminally differentiated cells, optimizing the CAR T cell manufacturing process to produce less differentiated cells is greatly needed. Almost all CAR T cell production protocols need *ex vivo* expansion that result in the generation of more differentiated T cells with low proliferative capacity *in vivo*.<sup>102</sup> Manipulation and modification of T cell-specific signaling pathways (following stimulation) can uncouple expansion from differentiation. In support of this principle, disruption of TET2 (a chromatin modifier that encodes methyl cytosine dioxygenase enzyme that facilitates DNA demethylation to activate gene expression) in a T cell clone resulted in potent antitumor activity and proliferation of anti-CD19 CAR T cells in a patient.<sup>103</sup> Interestingly, a metabolic byproduct, S-2-hydroxyglutarate (S-2HG), limits effector differentiation and supports increased memory formation and prolonged persistence of CAR T cells.<sup>104,105</sup> This byproduct competitively inhibits  $\alpha$ -ketoglutarate-dependent proteins such as TET family proteins.<sup>23</sup> Thus, inhibition of *ex vivo* CAR T cell differentiation by TET2 elimination or inhibition can lead to enhanced CAR T cell durability. Furthermore, inhibition of the histone acetylation reader BRD4, a member of the bromodomain and extra-terminal domain (BET) protein family, by JQ-1 shows similar results with S-2HG treatment.<sup>106</sup> In general, during T cell differentiation into effector phenotype, several “memory” genes, including FOXO1, KLF2, LEF1, TCF7, IL2RA, CD27, TNF, CCR7, and SELL, are repressed. This repression is mediated by repressive DNA methylation and repressive histone modifications (H3K27me3). Conversely, effector-related transcription factors and genes (e.g., EOMES, TBX21, PRDM1, GZMA, GZMB, PRF1, IFNG, and KLRG1) are upregulated by downregulating repressive modifications at genic and intragenic regions.<sup>46,52,107–110</sup> Reversing these alterations via miRNAs (specific) or pharmacologic treatments may give rise to less differentiated CAR T cells with enhanced potential.

#### EPIGENETIC REPROGRAMMING TO PROMOTE CENTRAL MEMORY AND STEM CELL MEMORY PHENOTYPES IN CAR T CELLS

Memory cells, and more specifically central and stem cell memory CAR T cells, are the preferred subset in the context of cancer immunotherapy. Central memory as well as stem-like T cells have higher persistence and superior antitumor activity compared to effector memory cells. Epigenetic reprogramming of CAR T cells to promote central memory, and retain stem cell, differentiated progeny will improve the efficacy of CAR T cell therapy.

**Table 2. Summary of various epigenetic mechanisms in T cells**

Epigenetic level	Mechanism	Effect on T cells	Refs.
DNA-associated mechanisms	methylation, hydroxymethylation	<i>de novo</i> DNA methylation can induce exhaustion	48
		methylation can induce differentiation of CD8 <sup>+</sup> cells to effector cells upon stimulation	46
		methylation and remethylation of the <i>pdc1</i> locus are associated with naive and memory phenotypes, respectively, while exhausted T cells showed a fully unmethylated <i>pdc1</i> locus genotype	47
		inhibition of <i>de novo</i> DNA methylation (DNMT3a) at early stages of effector memory differentiation accelerate central memory T cell development	49
		reduced methylation of CX3CR1 chemokine leads to effector memory T cell differentiation	52
Histone-associated mechanisms	methylation, acetylation, phosphorylation, and other processes	trimethylation of both H3K4 and H3K27 is associated with a naive phenotype, and trimethylation of H3K4 is associated with a memory/effector phenotype	53
		trimethylation of H3K27 is upregulated in effector T cells whereas trimethylation of H3K4 is shown to be upregulated in memory T cells (T <sub>SCM</sub> , T <sub>CM</sub> )	54
		inhibition of H3 histone deacetylation results in development of memory cells from an exhausted phenotype	57
		acetylation of H3 and H4 histones by HBO1 complex leads to exhaustion	16
		inhibition of histone lactylation might induce stem cell memory development	63,64
		H3 and H4 histone acetylation and phosphorylation decrease in the proximal promoter region of IL-2 upon T cell activation	56
		enrichment for H3K4me3 and a decrease of H3K27me3 at the <i>Gcnt1</i> gene result in enhanced trafficking of memory cells	55
Non-coding RNA-mediated mechanisms	miRNAs, lncRNAs, siRNAs	H3K27 acetylation at intronic and intergenic regions is concomitant with an exhausted phenotype	58
		miR-17-92 levels are associated with T cell differentiation and phenotype status	69,72
		miR-15/16 clusters can target memory-related genes, and their overexpression can induce apoptosis and terminally effector T cell development	17
		miR-150 reduces proliferation of CD4 <sup>+</sup> cells	82
		repression of PD-1 and CTLA-4 by miR-138 induces tumor regression	65
		a group of miRNAs downregulated/upregulated in effector T cells compared to memory and naive T cells	67,68
Higher order mechanisms	genomic architecture	miR-146a downregulation results in less apoptosis, increased proliferation, and enhanced effector function	76,77
		TOX family transcription factors interplay with exhaustion	16,18,58

Transcription factors play an important role in T cell differentiation. In the context of chronic infections, Blimp-1 drives the differentiation of short-lived T cells with an effector phenotype. Interestingly, Blimp-1 co-localizes with two epigenetic modifiers (G9a and HDAC2) at the loci for IL-2 and CD27.<sup>19</sup> Blimp-1 promotes effector cell differentiation through epigenetic repression of memory-associated genes similar to other repressive epigenetic modulators.<sup>50,111–113</sup> Genetically disabling Blimp-1 in CD8<sup>+</sup> T cells promoted memory cell formation and more importantly enhanced the proliferative capacity of CD8<sup>+</sup> cells in response to IL-2.<sup>19</sup> Therefore, genetic or epigenetic disruption of Blimp-1 in CAR T cells by CRISPR-Cas-9, miRNAs (e.g., miR-23a), or siRNAs may also improve cell proliferation, memory cell formation, and antitumor activity. As discussed above, inhibition of DNMT3A at early stages of T cell differentiation leads to memory T cell development.<sup>49,50</sup> Potentially, DNMT3A inhibitors might become useful in the manufacturing of CAR T cells. As mentioned before, miR-15/16 can target several memory-associated

mRNAs, including Bcl-2, CD28, and IL-7R transcripts, and attenuate memory T cell formation and differentiation as well as effector functions in CD8<sup>+</sup> T cells.<sup>17</sup> In addition, miR-150 targets c-Myb. c-Myb regulates anti-apoptotic pathways and promotes CD8<sup>+</sup> T cell memory differentiation.<sup>81</sup> Since miRNAs are involved in T cell differentiation, they can influence memory/effector formation. Thus, overexpression of some miRNAs as well as downregulation of memory restraining miRNAs such as miR-15/16 clusters and/or miR-150 may become an important strategy for restoring function in CAR T cells and the development of memory CAR T cells. Inducing central memory CAR T cells by miRNA has been examined by Zhang et al.<sup>20</sup> They have shown that miR-143 can regulate memory T cell differentiation through metabolic changes (glucose restriction) in CD8<sup>+</sup> T cells. They also showed that overexpression of miR-143 leads to reduced expression of exhaustion marker KLRG1 and increased expression of memory-related marker CD127 in T cells. To show the advantages of overexpression of miR-143, they transfected miR-143 mimics in

anti-HER2 CAR T cells. They observed that tumor cell lysis was increased in miR-143 overexpressed group. Complementary loss-of-function approaches showed that antagomirs to miR-143 decreased T cell-mediated cytotoxicity. Mechanistically, miR-143 regulates the expression of glucose transporter 1 (Glut-1) by binding to its 3' UTR transcript. The same results were also observed where Glut-1 was targeted by siRNA in the T cells. Additionally, their data showed that miR-143 can promote central memory T cell formation and induce a higher antitumor response by inhibiting glucose metabolism.<sup>20</sup> Although epigenetic manipulation of genetically engineered tumor-specific T cells by miRNAs holds great promise, caution should be taken particularly in case of adoptive transfer to patients. In addition, further studies are required to assess differentiation and effector function of CD4<sup>+</sup> cells. Future studies will reveal whether epidrugs that repress terminal effector-related genes as well as miRNAs or DNA/histone modifiers that induce memory-related genes can be used in CAR T cell therapy aiming to promote and maintain CAR T cells with memory phenotype.

#### EPIGENETIC REPROGRAMMING TO ENHANCE CAR T CELL INFILTRATION

Tumor cells use several mechanisms to escape from CAR T cell surveillance. Insufficient trafficking of CAR T cells to the tumor site is one barrier to adoptive immunotherapies. Indeed, enhancing CAR T cell infiltration to the tumor site can overcome this immune evasion tactic. Several factors contribute to insufficient trafficking of CAR T cells to the tumor site such as mismatched chemokine receptor with secreted chemokine in tumor bed, downregulation of adhesion molecules, and physical barriers at tumor site.<sup>114</sup> Also, overexpression of chemokine receptors in CAR T cells can enhance infiltration capacity of CAR T cells into tumor bed. Zou et al.<sup>115</sup> demonstrated that the concurrent downregulation of PD-1, TIM3, and LAG3 in anti-Her2 CAR T cells increases their infiltration to tumor sites. Increased chromatin accessibility at the CD56 locus as well as upregulation of chemokines CXCL9, CXCL10, and CXCL12 enhanced the ability of PD-1/TIM3/LAG3-modified CAR T cells to infiltrate tumors. CA-STAT5 (a constitutively active form of STAT5) expression can also enhance infiltration and trafficking of CD4<sup>+</sup> T cells to the tumor site by epigenetic remodeling,<sup>116</sup> indicating the importance of STAT proteins in higher order epigenetic modifications. In several cancers, increased expression of CXCR3 observed in tumor-infiltrating lymphocytes (TILs) was correlated with more infiltration. Therefore, inducing CXCR3 in CAR T cells by epigenetic mechanisms can be useful in cancers expressing CXCL9, CXCL10, and CXCL11 chemokines. Consistently, it has been shown that miR-155-deficient T cells have impaired function as well as trafficking,<sup>10</sup> as miR-155 targets suppressor of cytokine signaling 1 (SOCS-1) in T cells.<sup>75</sup> It seems that miR-155 upregulation in CAR T cells might be an interesting strategy to promote trafficking and the effective antitumor response of CAR T cells. Forced expression of CCR2 has been shown to enhance trafficking and survival of CAR T cells in cancer.<sup>117,118</sup> Interestingly, let-7 miRNAs target and inhibit CCR2 as well as CCR5 expression in T cells.<sup>119</sup> Targeting let-7 might therefore be a possible option for improving CAR T cell infiltration. CX3CR1 enhances im-

mune cell infiltration and tumor regression in CX3CL1<sup>+</sup> tumors.<sup>120</sup> T cells genetically engineered to overexpress CX3CR1 have significantly enhanced infiltration.<sup>121</sup> However, until now, no experimentally approved miRNAs that can target CX3CR1 in T cells have been reported. miR-27a-5p targets and inhibits expression of this chemokine receptor in NK cells.<sup>122</sup> Thus, targeting miRNAs that inhibit CX3CR1 expression can be an attractive approach for enhancing the infiltration of CAR T cells. Another chemokine receptor supporting infiltration is CXCR6. This chemokine receptor is expressed on naive T cells at low levels. Murine T cells deficient for CXCR6 are unable to properly infiltrate into mammary tumors.<sup>123</sup> Another interesting strategy would be to selectively modify tumor cells (epigenetically) to release chemokines that enhance CAR T cell infiltration. [Table 3](#) highlights important T cell miRNAs that can be potentially modulated for effective CARs.

#### EPIGENETIC REPROGRAMMING TO IMPROVE CAR T CELL PERSISTENCE

Among several barriers in CAR T cell therapy, poor persistence of infused CAR T cells is a critical challenge. In general, suboptimal persistence is correlated with poor clinical remission in the cancer.<sup>127</sup> Moreover, CAR T cells with impaired persistence show limited antitumor efficacy. One factor that limits persistence is replicative senescence, which can lead to reduced proliferative capacity and counter long-term therapeutic efficacy.<sup>128</sup> Telomere shortening, damage, and erosion contribute to senescence.<sup>129</sup> Similar to other cells, after each replication cycle the length of telomere is shortened in CAR T cells. In this regard, Bai et al.<sup>130</sup> demonstrated that increasing telomere abundance in anti-CD19 CAR T cells is associated with prolonged persistence and efficient antitumor response. Several studies have discussed STAT signaling as a key pathway in the promotion of cell persistence.<sup>4</sup> CAR T cells expressing CA-STAT5 show higher persistence and expansion rates as well as superior antitumor function. The authors demonstrated that these responses are a consequence of chromatin and epigenetic remodeling in the T cells as most non-coding genomic regions become highly accessible. Furthermore, the expression levels of various genes associated with T cell dysfunction such as Runx2, Id2, Nr4a2, and TOX were reduced, while several other genes such as Gata1, Jun, Junb, Fos, Fosl2, and EZH2 were upregulated and activated.<sup>116</sup> Therefore, epigenetic modification of the STAT5 pathway may be a promising strategy to promote the generation of highly persistent and poly-functional CAR T cells. Bcl-2 proteins can be divided into two groups based on inducing (pro-apoptotic) or inhibiting (anti-apoptotic) apoptosis in the cells. Indeed, anti-apoptotic members such as Bcl-2 can enhance CAR T cell persistence.<sup>131</sup> Another approach to enhance CAR T cell persistence is by downregulating pro-apoptotic proteins such as Bad and/or Bax. Altogether, it seems that targeting Bcl-2 family proteins by siRNA or other epigenetic mechanisms (e.g., miRNAs) can modulate CAR T cells persistence. However, possible adverse effects related to hyperactivation of CAR T cells must be assessed in the future studies. Since persistence is related to several other mechanisms in (CAR) T cells such as memory cell formation, other transcription factors influencing effector/

**Table 3. Selected T cell miRNAs that can be potentially modulated in CAR T cells**

Source	miRNA	Target	Mechanism of action	CAR T study	Refs.
T cells	miR-214	PTEN	enhances proliferation upon stimulation	no	83
	miR-143	Glut-1	promotes memory development	yes	20
	miR-146a	NF-κB	regulates and reduces effector function	no	76,77
	miR-23a	Blimp-1	reduces T cell differentiation and effector function	no	79
	miR-150	IL-2R $\alpha$ , ARR2	reduces effector function and proliferation	no	80,82
	miR-155	SHIP-1, SOCS-1	enhances proliferation, persistence, trafficking, and function of CD8 <sup>+</sup> T cells	no	10,74,75,124
	miR-17-92	PHLPP2, PTEN	enhances cell proliferation, persistence, and differentiation	yes	125
	miR-15/16	several	inhibits memory T cell formation and differentiation	no	17
	miR-181a	DUSP5, DUSP6, PTPN11, PTPN22	induces tolerance	no	84
	miR-139	EOMES, perforin	reduce effector function	no	80
	miR-342				
	miR-28	CTLA-4, PD-1	decrease immune checkpoint expression	no	65,126
	miR-138				
	Let-7	CCR2, CCR5	impairs trafficking	no	119

memory formation can also regulate CAR T cells persistence. Kagoya et al.<sup>106</sup> demonstrated that inhibition of histone acetyltransferase p300 (writer) and BET protein BRD4 (reader) not only leads to downregulation of BATF transcription factor and induces prolonged persistence, but it also promotes expression of memory associated markers and genes in T cells. Moreover, upon TCR or CAR stimulation of naive or memory precursor cells, BMI1 expression is induced in (CAR) T cells. In contrast, BMI1 expression is lost in terminally differentiated T cells. BMI1 is a member of the Polycomb repressive complex 1 (PRC1) family that reads H3K27me3 histone tails. This protein represses expression of genes that promote senescence and apoptosis (p16INK4A and p14ARF) in many cells, such as T cells.<sup>132,133</sup> Reduced levels of BMI1 lead to defects in T cell expansion.<sup>134</sup> Therefore, maintaining BMI1 expression at balanced levels or its overexpression in CAR T cells can be an ideal approach to enhance persistence and function in CAR T cells. Besides epigenetic modifications of DNA and histones, miRNAs can affect (CAR) T cell function and persistence. Forced expression of miR-155 in CD8<sup>+</sup> T cells enhances their antitumor activity, persistence, and proliferation.<sup>124</sup> Sasaki et al.<sup>135</sup> demonstrated that miR-17-92 is downregulated in T cells from glioblastoma patients, conferring a lower persistence rate of tumor-specific T cells and thereby diminishing tumor control. Thus, re-expressing this miRNA cluster in T cells from cancer patients might promote T cell persistence. In line with this notion, Ohno et al.<sup>125</sup> demonstrated that miR-17-92 overexpression in anti-EGFRvIII CAR T cells improves their persistence, proliferation, and antitumor function in a glioblastoma xenograft model. Epigenetically reprogramming patient-derived T cells may be an innovative strategy to generate more functionally effective CAR T cells. Mechanistically, miR-17 and miR-19b are parts of the miR-17-92 cluster and are shown to be critical for the T help-

er (Th)1 response by targeting TGF- $\beta$ R2 and PTEN, respectively. These miRNAs not only promote T cell proliferation and interferon (IFN)- $\gamma$  production, but they also protect T cells from activation-induced cell death (AICD).<sup>69,136</sup> Future studies will likely reveal the impact of miRNA-mediated posttranscriptional gene silencing as well as epigenetic modifications to Bcl-2 on CAR T cell persistence and effector function in clinical settings.

#### EPIGENETIC REPROGRAMMING TO OVERCOME CAR T CELL EXHAUSTION

Due to the immunosuppressive TME and prolonged antigen exposure, infused CAR T cells can become progressively dysfunctional. The ability of “exhausted” T cells to eliminate cancer cells wanes; hence, prevention from exhaustion will greatly enhance the rate of tumor regression and remission.<sup>137</sup> Until now, one of the main strategies to overcome exhaustion was immune checkpoint blockade. Recent work published by Beltra et al.<sup>138</sup> reported that exhausted T cells have four distinct developmental stages: the two first subsets are TCF1<sup>+</sup>, the next is an intermediate subset that is TCF1<sup>-</sup> and shows higher levels of effector function compared to other subsets, and the fourth is composed of terminally exhausted T cells. Following PD-1 therapy, the intermediate subset expands more than other subsets. While the cells can regain some elements of functional competence, they never regain their central memory status. Therefore, more effective tools to revert exhaustion in T cells is needed. As T cells undergo differentiation, their DNA methylation status is modified by DNMTs.<sup>23</sup> Also, data have shown that T cells from cancer patients are largely dysfunctional,<sup>139</sup> and this arises from dysregulation in the methylation status of its epigenome.<sup>140</sup> DNA methylation can lead to exhaustion and limit T cell-based immunotherapy.<sup>51</sup> T cells from cancer

patients are largely dysfunctional due to dysregulation in the methylation status of their epigenome.<sup>139,140</sup> In line with these notions, targeting a major component of the *de novo* DNA methylation program, DNMT3A, either pharmacologically (decitabine, a DNMT inhibitor [DNMTi]) or genetically, preserves the proliferation of these functionally incompetent T cells. Treated T cells express naive and memory-related genes at higher levels and downregulate exhaustion-related genes despite prolonged antigen exposure.<sup>141–143</sup> During exhaustion, an increase in the expression of exhaustion-related transcription factors such as the bZIP-IFN regulatory factor (IRF) family with or without an increase in the expression of JunB or BATF is a consequence of dysregulation of the AP-1 transcription factor binding motif. In exhausted cells, AP-1/IRF complexes limit the formation of the AP-1/Fos-Jun heterodimer. Consistent with this, a recent study showed that overexpression of c-Jun led to the formation of exhaustion-resistant CAR T cells with an increase in antitumor function and decreased expression of PD-1 and CD39. This finding reveals that c-Jun overexpression can activate AP-1 and prevent the formation of exhaustion-related complexes in chromatin.<sup>144</sup> Several studies have demonstrated that NR4A and the TOX family of proteins are upregulated in T cell exhaustion.<sup>16,40,145–149</sup> Therefore, targeting NR4A family proteins and TOX family transcription factors can lead to reduced expression of inhibitory receptors and the promotion of effector function in CAR T cells.<sup>18</sup> Mechanistically, TOX is induced by nuclear factor of activated T cells (NFAT)2 in a calcineurin-dependent manner. At later phases of the differentiation program, TOX operates in a feed-forward loop and becomes calcineurin-independent. Therefore, sustained levels of TOX are associated with exhaustion.<sup>16</sup> Also, persistent levels of TOX and NR4A interfere with NFAT. “Partnerless” NFAT or NFAT that does not cooperate with AP-1 at its cognate response elements in genetic loci induces the expression of inhibitory genes in T cells to promote exhaustion.<sup>18</sup> Moreover, since T cell studies have shown the importance of the TOX transcription factor and the acetyltransferase HBO1 complex in chromatin remodeling and in promoting T cell exhaustion, targeting the HBO1 complex in CAR T cells by specific miRNAs or CRISPR-Cas-9 may become a beneficial strategy to revert exhaustion and enhance antitumor efficacy of CAR T cells in clinical practice. Indeed, expression of memory-related or effector-related transcription factors leads to an epigenetic rewiring of T cells. Importantly, miR-28 and miR-138 can target immune checkpoints such as PD-1 and CTLA-4 and revert an exhausted phenotype.<sup>126,150</sup> miR-28 has been identified as a key miRNA in rescuing IL-2 and tumor necrosis factor (TNF)- $\alpha$  secretion in the TME.<sup>126</sup>

#### INTERPLAY BETWEEN EPIGENETIC MODIFICATIONS AND CAR T CELL METABOLISM

Metabolic fitness is an important determinant of efficacy in CAR T cells.<sup>151</sup> It is well established that T cells alter their metabolic activity to support their growth and differentiation. Naive and early memory T cells rely on oxidative phosphorylation (OXPHOS) and mitochondrial metabolism.<sup>152,153</sup> Following TCR stimulation, activated T cells

rapidly shift their metabolism from OXPHOS to glycolysis. Restricting glucose metabolism to the cytoplasm (aerobic glycolysis) channels metabolites into anabolic reactions supporting macromolecular biosynthesis.<sup>153,154</sup> Primary human T cells also rely on glutamine metabolism, both oxidative and reductive, to support acetyl-coenzyme A (CoA) synthesis.<sup>155</sup> Acetyl-CoA provides the functional acetyl group for histone acetylation, providing a means to control gene expression at the IFN- $\gamma$  locus in activated T cells.<sup>156,157</sup> Understanding which substrates fuel the tricarboxylic acid (TCA) cycle and hence short chain CoA replenishment is important, as mitochondrial function is compromised in T cells traversing solid tumor environments.<sup>158</sup> Intrinsic deficits in mitochondrial function that occur in terminally differentiated T cells, exhausted T cells, and T cells traversing hypoxic tumors will undoubtedly impact epigenetic reprogramming and gene expression. Deficits in mitochondrial function and energy-generating capacity also occur following chemotherapy treatment.<sup>159</sup>

Competition for nutrients in solid tumors has important implications for T cell function. Extracellular glucose levels diminish in tumors, and interstitial lactate levels increase in a reciprocal manner.<sup>160</sup> Histone lactylation is an under-studied epigenetic remodeling event with important implications for T cell function. To date, 28 lactylation sites on histone proteins have been identified. A recent study provided evidence that lysine lactylation regulates ARG1 expression in differentiating macrophages.<sup>63</sup> Histone lactylation regulates cancer-associated fibroblast differentiation in the context of pancreatic ductal adenocarcinoma.<sup>161</sup> With the development and increased use of small molecules targeting lactate production (LDHi) and lactate secretion (inhibitors to monocarboxylate transporters), additional studies are needed to understand their impact on epigenetic remodeling on adoptively transferred T cells in solid tumors.

Restricting epigenetic remodeling events (via metabolic regulation) to distinct T cell subsets may give rise to metabolically fitter (CAR) T cell progeny with superior antitumor activity. Metabolites other than acetyl-CoA influence epigenetic regulation in T cells. *S*-adenosylmethionine (SAM) regulates DNA and histone methylation in T cells by providing methyl groups, whereas the TCA cycle intermediate, and glutamine derivative,  $\alpha$ -ketoglutarate regulates DNA and histone demethylation in an oxygen-dependent manner.<sup>162,163</sup> Suppressing  $\alpha$ -ketoglutarate-mediated demethylation of DNA using S-2HG increases the formation of CD8<sup>+</sup> central memory CAR T cells.<sup>105</sup> Glycolysis replenishes nicotinamide adenine dinucleotide (NAD<sup>+</sup>), a fundamental metabolite regulating histone deacetylation.<sup>164</sup> NAD<sup>+</sup> is an important cofactor for sirtuins, a family of enzymes that regulate gene expression in a redox-sensitive manner.<sup>105</sup> MicroRNAs also regulate CAR T cell metabolism by epigenetic effects. miR-143 overexpression in CAR T cells decreases glucose uptake and induces expression of carnitine palmitoyl transferase 1a (CPT1A). CPT1A is a rate-limiting enzyme in fatty acid oxidation (FAO). In line with energy partitioning principles, increasing FAO leads to a corresponding decreased reliance on glucose and glycolysis. Of note, FAO is a metabolic pathway previously implicated in the

production of memory CAR T cells.<sup>20,165</sup> However, the role of FAO in memory differentiation is controversial, as it is largely based on studies using nonspecific doses of etomoxir. Some tumors such as renal cell carcinoma display a unique preference for glutamine over glucose.<sup>166</sup> Thus, future studies are necessary to uncover what fuels mitochondrial function during memory T cell differentiation *in situ*, and how the resultant metabolic pathways converge on epigenetic reprogramming. Taken together, reprogramming CAR T cell metabolism through the use of epidrugs is an interesting strategy for the generation of metabolically fitter CAR T cells with superior antitumor activity. However, more studies are needed to fully elucidate possible crosstalk between epigenetics and metabolism in (CAR) T cells.

### EPIGENETIC STRATEGIES IN CAR T CELL COMBINATION THERAPY

To overcome hostile conditions found within tumors, combining CAR T cell therapies with various cancer treatment modalities has gained increasing attention. With the renewed interest in combinatorial approaches, the role of both tumor cell immunobiology and the status of the endogenous immune system must be considered. In the following sections we discuss how such combination therapies, in particular epigenetic modifiers, can significantly improve the efficacy of CAR T cell therapy.

#### Epigenetic strategies to upregulate desirable antigens in tumors

Antigen loss and antigen heterogeneity are important barriers impeding efficacy in CAR T cell therapy. Upregulation or induction of tumor-associated antigens (TAAs) or cancer testis antigens (CTAs) can overcome antigen heterogeneity and prevent antigen loss in the tumors. Epigenetic drugs, especially those that can facilitate DNA demethylation and/or histone acetylation, have the potential to upregulate all antigen-processing machinery components, thereby increasing TAA abundance, as well as costimulatory molecule expression such as CD40 and CD80 and major histocompatibility complex (MHC) classes I and II,<sup>167–169</sup> and stress and death-induced ligands, including DR5 and TRAIL.<sup>170,171</sup> DNMTis and HDACis enhance cancer cell recognition by increasing the expression of CTAs, which are expressed in embryonic and germ cells, whereas in somatic cells their promoters are methylated. DNMTis promote DNA demethylation, permitting the re-expression of CTAs in cancer cells in several solid tumors.<sup>7–9,79</sup> HDACis also induce the expression of CTAs at lower levels compared to DNMTis.<sup>172</sup> As we discussed previously, inhibition of DNMT3a in T cells can reduce the abundance of exhausted T cells and promote the generation of central memory cells.<sup>48,49</sup> Following treatment with decitabine, CAR T cells showed superior antitumor activity.<sup>142</sup> A recent study demonstrated that pretreatment of lymphoma cells with decitabine leads to CD19 overexpression and enhanced CAR T cell function. The authors also reported that two patients who received decitabine before CAR T cell therapy achieved complete responses.<sup>173</sup> Viral tumor antigens can also be expressed following DNMTis.<sup>174</sup> Over time, and consequent to viral infection, human endogenous retroviruses (HERVs) are integrated into the genome of germ cells. While most HERVs are non-coding, several

HERVs encode functional proteins such as HERV-K HML-2 isoforms.<sup>175</sup> HERVs are expressed followed by DNMTis and HDACis.<sup>176</sup> Anti-HERV-K CAR T cells have shown antitumor promise in xenograft models of melanoma.<sup>177</sup> Ewing sarcoma (EwS) is a solid tumor characterized by low antigen expression and high antigen heterogeneity. Expression of enhancer of zeste homolog 2 (EZH2; an enzyme that contributes to the histone methylation) in Ewing sarcoma cells is associated with reduced antigen presentation and decreased immunogenicity.<sup>178</sup> Pharmacological targeting of EZH2 at doses reducing H3K27me3 could selectively and reversibly induce GD2 surface expression in tumor cells. They concluded that combination therapy with CAR T cells plus EZH2 inhibitors may significantly enhance antitumor activity of CAR T cells.<sup>179</sup>

Similarly, Kunert et al.<sup>180</sup> reported that DNMTi and HDACi treatment led to CTA MAGE-C2 overexpression in breast cancer cells. CTA MAGE-C2 antigen is a corresponding target for genetically engineered T cell expressing MAGE-C2-TCR. Taken together, epigenetic modification-based combination strategies such as using a DNMTi and CAR T cells can make tumor cells more immunogenic, probably through overexpression of MHC class I and MHC class II on the tumor cell surface as well as increasing expression of costimulatory molecules including CD40 and CD80. Therefore, these combination therapies not only can synergistically activate the endogenous immune system but they also can prevent and/or revert antigen loss. Moreover, CAR T cell qualities in terms of functionality and longevity can be improved through inducing memory phenotypes and repressing exhaustion by application of epidrugs.

#### Epigenetic strategies to overcome hostile TME features

In addition to the role of HERVs as target antigens, epigenetic modulation of HERVs can promote a type I and III IFN response, which can boost the overall antitumor immune response. DNMTis and HDACis promote the transcription of HERVs in a bidirectional manner, leading to formation of double-stranded RNAs (dsRNAs) in the cells. dsRNAs can activate RIG-I and MDA5 receptors. Together with IRF3, IRF7, and NF- $\kappa$ B, dsRNA/RIG-I and dsRNA MDA5 complexes can activate transcription of IFNs and IFN receptor interaction. These processes lead to the induction of IFN-stimulated genes (ISGs) through JAK/STAT signaling pathways. Furthermore, ISGs can induce various immunomodulatory genes and increase expression of chemokines and cytokines to attract and activate immune cells. A recent study demonstrated that low doses of a DNMTi can increase the expression of ISGs, chemokines and cytokines, antigen processing and presentation, and CTAs.<sup>79</sup> Different investigations have reported that cancer cells treated with DNMTis and HDACis can increase the infiltration of CD8<sup>+</sup> T cells to tumor sites through activation of the IFN type I response<sup>11</sup> and overexpression of CXCL9 and CXCL10 in breast cancer tissue.<sup>12</sup> Moreover, lysine-specific histone demethylase 1A (LSD1) ablation in cancer cells was shown to induce IFN type I responses as well as HERV expression and, more interestingly, enhance CD8<sup>+</sup> T cell infiltration in tumors.<sup>181</sup> Moreover, inactivation of nuclear receptor binding SET domain protein 1 (NSD1), a histone methyltransferase catalyzer, can reduce CD8<sup>+</sup>

T cell infiltration in several cancers. In line with this finding, inactivating mutations in NSD1 mimics the characteristics of cold tumors.<sup>182</sup> Thus, modifying LSD1 as well as NSD1 is interesting to pursue in the context of CAR T cell cancer therapy.

The epigenetic status of the PD-L2 locus in tumor cells is another relevant candidate to investigate. Methylation of several CpG sites in the PD-L2 locus correlates with CD8<sup>+</sup> T cells infiltration in tumor sites.<sup>183</sup> CCL5 and CXCL9 were previously shown to play a pivotal role in T cell infiltration, whereas CCL5 is often epigenetically silenced in cancer cells. A recent study revealed that decitabine stimulates CCL5 re-expression in tumor cells and enhances T cell infiltration to tumor tissues.<sup>184</sup> Various studies have demonstrated that DNMTis could enhance the antitumor function of T cells by modulating the immunosuppressive activity of myeloid-derived suppressor cells (MDSCs) and macrophages within the TME.<sup>11,13-15</sup> Treating B16 melanoma-bearing mice with HDACis revealed that the epigenetic modification of tumor cells not only enhances the efficacy of adoptively transferred cells but also promotes the infiltration of anti-gp-100 T cells following the increased expression of gp-100 and MHC molecules.<sup>185</sup> In addition to inhibiting histone writers, disrupting histone readers can also be a good therapeutic option in several cancers. For example, in an ovarian cancer model and squamous cell carcinoma, treatment with JQ-1, a BET inhibitor, could remarkably decrease PD-L1 expression on tumor cells and tumor-associated immune cells.<sup>186,187</sup> It is well documented that the TME contains several suppressive cells, including Tregs, M2 macrophages, MDSCs, tumor-associated neutrophils, as well as cancer-associated fibroblasts.<sup>188</sup> These cells exploit several mechanisms to hinder the effective immune response in the TME. These mechanisms include the secretion of immunosuppressive molecules (IL-10, TGF- $\beta$ , arginase, IDO, prostaglandin E<sub>2</sub> [PGE<sub>2</sub>], adenosine) and increased surface expression of inhibitory molecules. These soluble and insoluble molecules can inhibit antitumor function of CAR T cells in various ways. For example, tryptophan is an essential amino acid for the activation, proliferation, and survival of CAR T cells.<sup>189</sup> Indoleamine 2,3-dioxygenase 1 (IDO) is a rate-limiting enzyme that catabolizes tryptophan to kynurenine.<sup>190</sup> The production of kynurenine and catabolization of tryptophan limit the function of CAR T cells and their antitumor activity.<sup>191,192</sup> IDO is expressed in several cancers, and its expression is correlated with poor T cell infiltration and clinical outcome.<sup>193</sup> Various studies have documented that IFN- $\gamma$  can induce IDO expression as well as PD-L1.<sup>194</sup> In recent studies, miR-153 and miR-448 were shown to suppress IDO1 expression effectively in colorectal xenograft models.<sup>195,196</sup> Furthermore, miR-153 overexpression in cancer cells could enhance CAR T cell killing capacity *in vitro* and suppress tumor growth in a murine colorectal cancer xenograft model through suppression of IDO1 expression.<sup>196</sup> PGE<sub>2</sub> is an immunosuppressive component of the TME. This soluble eicosanoid can increase cancer cell proliferation and inhibit an effective antitumor T cell response. miR-21 and miR-155 have been shown to stimulate PGE<sub>2</sub>-dependent signaling in tumor cells through

augmentation of the active form of PGE<sub>2</sub>.<sup>197,198</sup> In contrast, miR-708 and miR-137 can inhibit PGE<sub>2</sub> production and decrease the levels of this molecule in tumors.<sup>199,200</sup> There are several other miRNAs such as miR-126 and miR-503-5p that can target tumorigenic molecules such as VEGF and inhibit angiogenesis.<sup>201-204</sup> miR-30a-5p and miR-422a target CD73,<sup>205,206</sup> an ecto-5'-nucleotidase that can generate adenosine from AMP. Extracellular adenosine is a key immunosuppressive metabolite that restricts activation of CAR T cells and impairs their antitumor responses. In line with these findings, it has been reported that genetic and pharmacological targeting of the adenosine A<sub>2</sub> receptor could significantly improve antitumor function of CAR T cells.<sup>207</sup> It has also been shown that miR-22 targets galectin-9, a ligand of the inhibitory receptor TIM-3 on T cells.<sup>208</sup> There many other miRNAs that can target TGF- $\beta$  and their receptors,<sup>209-211</sup> reactive oxygen species (ROS), and HIF1- $\alpha$  signaling pathways,<sup>212,213</sup> as well as other immune checkpoint ligands such as PD-L1.<sup>214,215</sup> In an interesting study, it has been demonstrated that miR-141 can inhibit the recruitment of immunoregulatory cells to tumor sites.<sup>216</sup> Altogether, these exciting findings highlight the potential of combining miRNAs and CAR T cells to elicit favorable immune responses and, thereby, better clinical outcomes.

Both cancerous and healthy cells are able to secrete extracellular vesicles containing lipids, proteins, RNAs, and DNAs, which are called exosomes. These extracellular vesicles facilitate crosstalk between cancer cells and immune cells. This crosstalk has been implicated in the tumorigenesis process and response to therapy.<sup>217</sup> Cancer cells can secrete and transport immunosuppressive molecules (e.g., miRNAs) to immune cells and, as a consequence, disarm these antitumor cells. In line with this concept, a recent study revealed that miRNAs in melanoma-derived exosomes can alter cytokine secretion and TCR signaling in CD8<sup>+</sup> T cells. Some of these exosomal miRNAs (e.g., miR-181a/b and miR-498) were able to directly bind to the 3' UTR of TNF and decrease TNF- $\alpha$  secretion. Exosomal miR-3187-3p inhibits the expression of CD45, which is known as a signaling gatekeeper in TCR signaling.<sup>218</sup> In addition to direct control of the T cell response in the TME, exosomes can indirectly alter T cell antitumor response. It has been shown that exosomal miR-23a-3p can target PTEN in macrophages and reduce the expression of PTEN and phosphorylation of AKT. It can also increase PD-L1 expression on macrophages in hepatocellular carcinoma.<sup>219</sup> Moreover, TAM-derived exosomes containing miR-29a-3p and miR-21-5p have been shown to inhibit the antitumor response and enhance tumor growth by targeting the 3' UTR of STAT3 in T cells.<sup>220</sup> STAT3 is crucial transcription factor in Th17 differentiation. Thus, STAT3 targeting by miRNAs secreted from TAMs can increase the Treg/Th17 ratio and promote immunosuppression.<sup>220</sup> In contrast, it has been discovered that activated T cells can secrete cytotoxic extracellular vesicles containing miR-298-5p. This miRNA can inhibit metastasis and tumor invasion through activation of caspase-3 and induction of apoptosis in mesenchymal tumor stromal cells.<sup>221</sup> In aggregate, blocking the secretion or

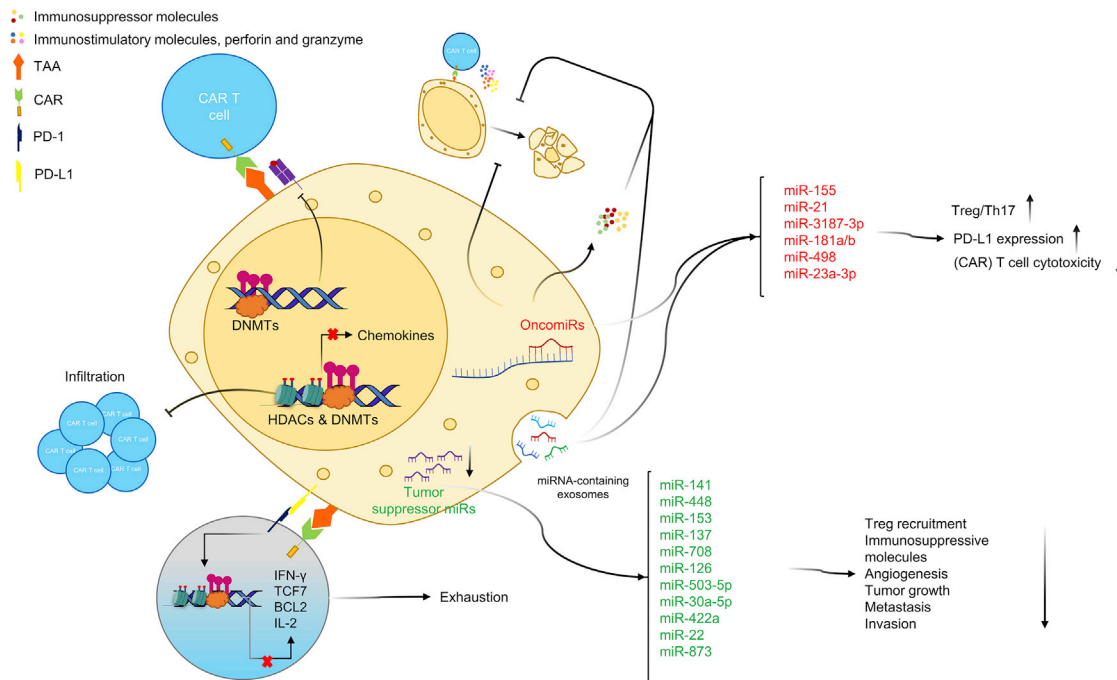


**Figure 3. CAR T cells in TME**

DNMTs and HDACs in tumor cells can suppress TAA and MHC expression as well as suppress transcription of Th1-associated cytokines and chemokines necessary for T cell infiltration. PD-1/PD-L1 interaction can induce CAR T cell exhaustion by epigenetic remodeling. Tumor-derived exosomes inhibit TCR signaling and cytokine production in (CAR) T cells, leading to impaired tumor killing ability of these cells. Alternatively, tumor suppressor miRNAs can promote immune cell functions and inhibit tumor cell invasion and angiogenesis. Tumor suppressor miRNAs can also inhibit Treg recruitment to the tumor site. These miRNAs are mainly downregulated in several tumors.

generation of cancer-derived exosomes or more specifically inhibiting the expression of oncomiRs, including miR-23a-3p, miR-29a-3p, miR-21-5p, miR-181a/b, miR-498 and miR-3187-3p, and/or promoting immunostimulatory miRNAs, including miR-298-5p, may be an important therapeutic strategy in the context of CAR T cell therapy. Figure 3 illustrates different layers of epigenetics on the CAR T cells within the TME. Altogether, understanding the mechanisms of immune evasion and epigenetic alterations in tumor cells can provide an important rationale for using epidrugs in combination with adoptive cell therapies. However, further investigations are needed to elucidate the molecular epigenetic mechanisms responsible for immune evasion mechanisms and genetic alterations in tumor and immune cells. Table 4 represents a list of miRNAs that can be potentially targeted in tumors in the context of CAR T cell therapy.

### Conclusions

Although CAR T cells have shown remarkable strides in the treatment of patients with advanced cancers, there are still challenges limiting their overall efficacy in solid tumors. In this review we discuss how utilizing epigenetic mechanisms and modifications can overcome these challenges (Figure 4). For example, overexpression or restoration of memory-related genes as well as the downregulation or suppression of exhaustion-related genes may

enhance CAR T cell persistence and long-lasting immune surveillance.

The epigenome of patient-derived T cells is also a critical factor for generation of fully functional CAR T cells with superior antitumor activity. As accumulating data suggest, T cells derived from cancer patients may be epigenetically dysregulated compared to T cells derived from healthy individuals.<sup>222–224</sup> Therefore, caution should be taken in translation of *in vitro* and *in vivo* studies to clinical trials. It seems that epigenome mapping of T cells isolated from patients might be a solution to overcome this challenge. With the help of epigenome data extracted from patient T cells, it would be possible to reprogram epigenetically dysregulated T cells into fully functional and epigenetically fit CAR T cells. Moreover, the use of allogeneic CAR T cells from healthy donors might be another alternative strategy to overcome this limitation.

Epigenetically modulating CAR T cells or cells in their surrounding microenvironment might also help prevent antigen loss and heterogeneity and also make CAR T cell therapy more effective in the context of a harsh TME. However, note that our knowledge in this field is still poor and many details are unknown.

It is now well established that epigenetic modifications are major players in the progression of cancer and pivotal regulators of

**Table 4. List of miRNAs that can be potentially targeted in the context of CAR T cell therapy**

Source	miRNAs	Target	Mechanism of action	Cancer	CAR T cell study	Refs.
Tumor-derived exosomes	miR-3187-3p	CD45 (PTPRC)	TCR signaling alteration	melanoma	no	218
	miR-181a/b	TNF- $\alpha$	cytotoxicity reduction	melanoma	no	218
	miR-498					
	miR-23a-3p	PTEN	PD-L1 expression in macrophages	HCC	no	219
	miR-29a-3p	STAT3	secreted from TAMs; upregulation of Treg/Th17 ratio	several	no	220
	miR-21-5p					
	miR-298-5p	N/D; caspase-3	secreted from T cells, induces apoptosis via caspase-3 activation on MSCs	fibrosarcoma	no	221
Tumor cells	miR-141	CXCL1	inhibits Treg recruitment	NSCLC	no	216
	miR-448	IDO1	enhance proliferation and antitumor function of CD8 <sup>+</sup> T cells	CC	no	195
	miR-153				yes	196
	miR-155	PTGES/PTGES2	increases PGE2 production and cell proliferation	breast	no	198
	miR-137	COX-2	inhibits COX-2 and PGE2 production	retinoblastoma	no	199
	miR-21	HPGD	promotes expression of active PGE2	OTSCC	no	197
	miR-708	COX-2 and mPGES-1	inhibits PGE2 production	NSCLC	no	200
	miR-126	VEGF-A	reduces cell proliferation, inhibits angiogenesis	several cancers	no	201,203,204
	miR-503-5p	VEGF-A	inhibits angiogenesis	CC	no	202
	miR-30a-5p	CD73	inhibits adenosine production	NSCLC	no	205
	miR-422a	CD73	inhibits adenosine production	HNSCC	no	206
	miR-22	galectin-9	suppresses cell growth, invasion, and metastasis	HCC	no	208
	miR-873	PD-L1	attenuates stemness and resistance of tumor cells	breast	no	214

HCC, hepatocellular carcinoma; N/D, no data; NSCLC, non-small cell lung carcinoma; CC, colon cancer; OTSCC, oral tongue squamous cell carcinoma; HNSCC, head and neck squamous cell carcinoma; TAM, tumor-associated macrophage; MSC, mesenchymal stromal cell.

(CAR) T cell functionality, which altogether are determinative factors in the clinical outcome of adoptive (CAR) T cell therapy. An ever-growing understanding of epigenetic processes will bring us closer to the prospect of safer and more effective T cell-based therapies. Epigenetic modifications with DNMTis and HDACis may lead to more efficient clinical outcomes. For example, by using DNMTis in CAR T cell production protocol, it is possible to achieve a higher level of central memory CAR T cells. Another attractive epigenetic-based approach involves the use of CAR T cells in combination with DNMTis. This strategy may prevent antigen loss or heterogeneity

and simultaneously promote an endogenous antitumor immune response. In line with this strategy, using ncRNAs such as miRNAs is also promising and shows multiple advantages compared to other gene engineering strategies. As miRNAs can target multiple molecules at the same time, and also target DNMTs (e.g., miR-29), the manipulation of a single ncRNA might entirely alter CAR T cell function. Indeed, due to their small size they can be readily used in multicistronic CAR platforms. However, note that as epigenetic regulators such epidrugs can affect multiple pathways within the cells, safety cautions should be considered. In summary, it can be concluded

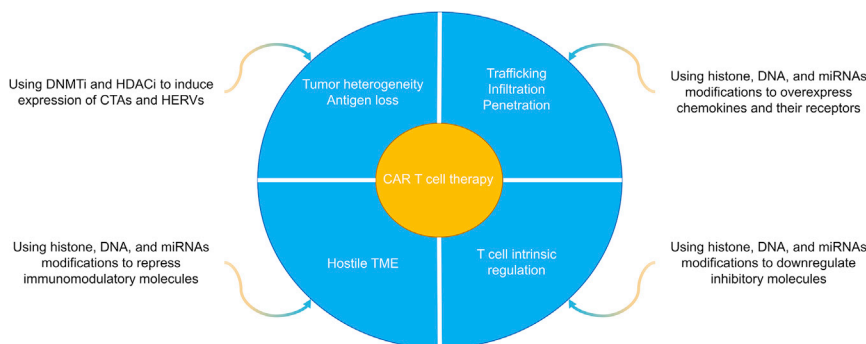


**Figure 4. Epigenetic modifications that can be done to overcome roadblocks in CAR T cell therapy**

DNA and histone modifications as well as miRNAs can be modified by epidrugs and other tools such as antagomiRs to increase expression and presentation of tumor antigens, enhance trafficking of CAR T cells and other immune cells, modify the immunosuppressive tumor microenvironment, and modulate T cell-intrinsic features, including promoting memory phenotype development, reverting exhaustion, and enhancing persistence of CAR T cells.

that epigenetic modifications have the potential to revolutionize CAR T cell therapy and present the next, and more effective, generation of T cell-based cancer immunotherapies.

## ACKNOWLEDGMENTS

This work was supported in part through funding provided by Tehran University of Medical Sciences (grants nos. 50756 and 50760, awarded to H.R.M.), National Institute for Medical Research Development (NIMAD) of Iran (grant no. 996475, awarded to H.R.M.), a St. Baldrick's Foundation Scholar Award (to S.G.), a National Blood Foundation Scientific Research Grant Award (to S.G.), as well as by the Office of the Assistant Secretary of Defense for Health Affairs through the Peer-Reviewed Cancer Research Program under award no. W81XWH-20-1-0417 (to S.G.).

## AUTHOR CONTRIBUTIONS

The conception and design of the paper were done by H.R.M., J.H., and S.G. The initial draft was completed by B.A., N.G.-S., and T.S. Editing and further drafts were done by H.R.M. and S.G. All authors reviewed the final version of the paper.

## DECLARATION OF INTERESTS

The authors declare no competing interests.

## REFERENCES

- Birdi, H.K., Jirovec, A., Cortés-Kaplan, S., Werier, J., Nessim, C., Diallo, J.S., and Ardolino, M. (2021). Immunotherapy for sarcomas: New frontiers and unveiled opportunities. *J. Immunother. Cancer* 9, e001580.
- Kruger, S., Ilmer, M., Kobold, S., Cadilha, B.L., Endres, S., Ormanns, S., Schuebbe, G., Renz, B.W., D'Haese, J.G., Schloesser, H., et al. (2019). Advances in cancer immunotherapy 2019—Latest trends. *J. Exp. Clin. Cancer Res.* 38, 268.
- Mirzaei, H.R., Rodriguez, A., Shepphird, J., Brown, C.E., and Badie, B. (2017). Chimeric antigen receptors T cell therapy in solid tumor: Challenges and clinical applications. *Front. Immunol.* 8, 1850.
- Tian, Y., Li, Y., Shao, Y., and Zhang, Y. (2020). Gene modification strategies for next-generation CAR T cells against solid cancers. *J. Hematol. Oncol.* 13, 54.
- Bansal, R., and Reshef, R. (2021). Revving the CAR—Combination strategies to enhance CAR T cell effectiveness. *Blood Rev.* 45, 100695.
- Watanabe, N., McKenna, M.K., Rosewell Shaw, A., and Suzuki, M. (2021). Clinical CAR-T cell and oncolytic virotherapy for cancer treatment. *Mol. Ther.* 29, 505–520.
- James, S.R., Link, P.A., and Karpf, A.R. (2006). Epigenetic regulation of X-linked cancer/germline antigen genes by DNMT1 and DNMT3b. *Oncogene* 25, 6975–6985.
- Weber, J., Salgaller, M., Samid, D., Johnson, B., Herlyn, M., Lassam, N., Treisman, J., and Rosenberg, S.A. (1994). Expression of the MAGE-1 tumor antigen is up-regulated by the demethylating agent 5-aza-2'-deoxycytidine. *Cancer Res.* 54, 1766–1771.
- Coral, S., Sigalotti, L., Altomonte, M., Engelsberg, A., Colizzi, F., Cattarossi, L., Maraskovsky, E., Jager, E., Seliger, B., and Maio, M. (2002). 5-Aza-2'-deoxycytidine-induced expression of functional cancer testis antigens in human renal cell carcinoma: Immunotherapeutic implications. *Clin. Cancer Res.* 8, 2690–2695.
- Dickey, L.L., Worme, C.L., Glover, J.L., Lane, T.E., and O'Connell, R.M. (2016). MicroRNA-155 enhances T cell trafficking and antiviral effector function in a model of coronavirus-induced neurologic disease. *J. Neuroinflammation* 13, 240.
- Stone, M.L., Chiappinelli, K.B., Li, H., Murphy, L.M., Travers, M.E., Topper, M.J., Mathios, D., Lim, M., Shih, I.M., Wang, T.L., et al. (2017). Epigenetic therapy activates type I interferon signaling in murine ovarian cancer to reduce immunosuppression and tumor burden. *Proc. Natl. Acad. Sci. USA* 114, E10981–E10990.
- Peng, D., Kryczek, I., Nagarsheth, N., Zhao, L., Wei, S., Wang, W., Sun, Y., Zhao, E., Vatan, L., Szeliga, W., et al. (2015). Epigenetic silencing of T<sub>H</sub>1-type chemokines shapes tumour immunity and immunotherapy. *Nature* 527, 249–253.
- Luo, N., Nixon, M.J., Gonzalez-Ericsson, P.L., Sanchez, V., Opalenik, S.R., Li, H., Zahnaw, C.A., Nickels, M.L., Liu, F., Tantawy, M.N., et al. (2018). DNA methyltransferase inhibition upregulates MHC-I to potentiate cytotoxic T lymphocyte responses in breast cancer. *Nat. Commun.* 9, 248.
- Zhou, J., Yao, Y., Shen, Q., Li, G., Hu, L., and Zhang, X. (2017). Demethylating agent decitabine disrupts tumor-induced immune tolerance by depleting myeloid-derived suppressor cells. *J. Cancer Res. Clin. Oncol.* 143, 1371–1380.
- Terracina, K.P., Graham, L.J., Payne, K.K., Manjili, M.H., Baek, A., Damle, S.R., and Bear, H.D. (2016). DNA methyltransferase inhibition increases efficacy of adoptive cellular immunotherapy of murine breast cancer. *Cancer Immunol. Immunother.* 65, 1061–1073.
- Khan, O., Giles, J.R., McDonald, S., Manne, S., Ngiow, S.F., Patel, K.P., Werner, M.T., Huang, A.C., Alexander, K.A., Wu, J.E., et al. (2019). TOX transcriptionally and epigenetically programs CD8<sup>+</sup> T cell exhaustion. *Nature* 571, 211–218.
- Gagnon, J.D., Kageyama, R., Shehata, H.M., Fassett, M.S., Mar, D.J., Wigton, E.J., Johansson, K., Litterman, A.J., Odorizzi, P., Simeonov, D., et al. (2019). miR-15/16 restrain memory T cell differentiation, cell cycle, and survival. *Cell Rep.* 28, 2169–2181.e4.
- Seo, H., Chen, J., González-Avalos, E., Samaniego-Castruita, D., Das, A., Wang, Y.H., López-Moyado, I.F., Georges, R.O., Zhang, W., Onodera, A., et al. (2019). TOX and TOX2 transcription factors cooperate with NR4A transcription factors to impose CD8<sup>+</sup> T cell exhaustion. *Proc. Natl. Acad. Sci. USA* 116, 12410–12415.
- Shin, H.M., Kapoor, V., Guan, T., Kaech, S.M., Welsh, R.M., and Berg, L.J. (2013). Epigenetic modifications induced by Blimp-1 regulate CD8<sup>+</sup> T cell memory progression during acute virus infection. *Immunity* 39, 661–675.
- Zhang, T., Zhang, Z., Li, F., Ping, Y., Qin, G., Zhang, C., and Zhang, Y. (2018). miR-143 regulates memory T cell differentiation by reprogramming T cell metabolism. *J. Immunol.* 201, 2165–2175.
- He, S., Liu, Y., Meng, L., Sun, H., Wang, Y., Ji, Y., Purushe, J., Chen, P., Li, C., Madzo, J., et al. (2017). Ezh2 phosphorylation state determines its capacity to maintain CD8<sup>+</sup> T memory precursors for antitumor immunity. *Nat. Commun.* 8, 2125.
- Linnér, A., and Almgren, M. (2020). Epigenetic programming—The important first 1000 days. *Acta Paediatr.* 109, 443–452.
- Henning, A.N., Roychoudhuri, R., and Restifo, N.P. (2018). Epigenetic control of CD8<sup>+</sup> T cell differentiation. *Nat. Rev. Immunol.* 18, 340–356.
- Strahl, B.D., and Allis, C.D. (2000). The language of covalent histone modifications. *Nature* 403, 41–45.
- Musselman, C.A., Lalonde, M.E., Côté, J., and Kutateladze, T.G. (2012). Perceiving the epigenetic landscape through histone readers. *Nat. Struct. Mol. Biol.* 19, 1218–1227.
- Jones, P.A. (2012). Functions of DNA methylation: Islands, start sites, gene bodies and beyond. *Nat. Rev. Genet.* 13, 484–492.
- Pastor, W.A., Aravind, L., and Rao, A. (2013). TETonic shift: Biological roles of TET proteins in DNA demethylation and transcription. *Nat. Rev. Mol. Cell Biol.* 14, 341–356.
- Ball, M.P., Li, J.B., Gao, Y., Lee, J.H., LeProust, E.M., Park, I.H., Xie, B., Daley, G.Q., and Church, G.M. (2009). Targeted and genome-scale strategies reveal gene-body methylation signatures in human cells. *Nat. Biotechnol.* 27, 361–368.
- Kouzarides, T. (2007). Chromatin modifications and their function. *Cell* 128, 693–705.
- Martin, C., and Zhang, Y. (2005). The diverse functions of histone lysine methylation. *Nat. Rev. Mol. Cell Biol.* 6, 838–849.
- Liberti, M.V., and Locasale, J.W. (2020). Histone lactylation: A new role for glucose metabolism. *Trends Biochem. Sci.* 45, 179–182.
- Kimura, H. (2013). Histone modifications for human epigenome analysis. *J. Hum. Genet.* 58, 439–445.
- Shiio, Y., and Eisenman, R.N. (2003). Histone sumoylation is associated with transcriptional repression. *Proc. Natl. Acad. Sci. USA* 100, 13225–13230.

34. Sana, J., Faltejskova, P., Svoboda, M., and Slaby, O. (2012). Novel classes of non-coding RNAs and cancer. *J. Transl. Med.* *10*, 103.
35. Kim, D.H., Villeneuve, L.M., Morris, K.V., and Rossi, J.J. (2006). Argonaute-1 directs siRNA-mediated transcriptional gene silencing in human cells. *Nat. Struct. Mol. Biol.* *13*, 793–797.
36. Hawkins, P.G., Santos, S., Adams, C., Anest, V., and Morris, K.V. (2009). Promoter targeted small RNAs induce long-term transcriptional gene silencing in human cells. *Nucleic Acids Res.* *37*, 2984–2995.
37. Kim, D.H., Saetrom, P., Snøve, O., Jr., and Rossi, J.J. (2008). MicroRNA-directed transcriptional gene silencing in mammalian cells. *Proc. Natl. Acad. Sci. USA* *105*, 16230–16235.
38. Shah, M.Y., Ferrajoli, A., Sood, A.K., Lopez-Berestein, G., and Calin, G.A. (2016). microRNA therapeutics in cancer—An emerging concept. *EBioMedicine* *12*, 34–42.
39. Li, G., and Reinberg, D. (2011). Chromatin higher-order structures and gene regulation. *Curr. Opin. Genet. Dev.* *21*, 175–186.
40. Scott-Browne, J.P., López-Moyado, I.F., Trifari, S., Wong, V., Chavez, L., Rao, A., and Pereira, R.M. (2016). Dynamic changes in chromatin accessibility occur in CD8<sup>+</sup> T cells responding to viral infection. *Immunity* *45*, 1327–1340.
41. Nora, E.P., Lajoie, B.R., Schulz, E.G., Giorgetti, L., Okamoto, I., Servant, N., Piolot, T., van Berkum, N.L., Meisig, J., Sedat, J., et al. (2012). Spatial partitioning of the regulatory landscape of the X-inactivation centre. *Nature* *485*, 381–385.
42. Dixon, J.R., Selvaraj, S., Yue, F., Kim, A., Li, Y., Shen, Y., Hu, M., Liu, J.S., and Ren, B. (2012). Topological domains in mammalian genomes identified by analysis of chromatin interactions. *Nature* *485*, 376–380.
43. Pombo, A., and Dillon, N. (2015). Three-dimensional genome architecture: Players and mechanisms. *Nat. Rev. Mol. Cell Biol.* *16*, 245–257.
44. Yu, M., and Ren, B. (2017). The three-dimensional organization of mammalian genomes. *Annu. Rev. Cell Dev. Biol.* *33*, 265–289.
45. Zebly, C.C., Gottschalk, S., and Youngblood, B. (2020). Rewriting history: Epigenetic reprogramming of CD8<sup>+</sup> T cell differentiation to enhance immunotherapy. *Trends Immunol.* *41*, 665–675.
46. Scharer, C.D., Barwick, B.G., Youngblood, B.A., Ahmed, R., and Boss, J.M. (2013). Global DNA methylation remodeling accompanies CD8 T cell effector function. *J. Immunol.* *191*, 3419–3429.
47. Youngblood, B., Oestreich, K.J., Ha, S.J., Duraiswamy, J., Akondy, R.S., West, E.E., Wei, Z., Lu, P., Austin, J.W., Riley, J.L., et al. (2011). Chronic virus infection enforces demethylation of the locus that encodes PD-1 in antigen-specific CD8<sup>+</sup> T cells. *Immunity* *35*, 400–412.
48. Ghoneim, H.E., Fan, Y., Moustaki, A., Abdelsamed, H.A., Dash, P., Dogra, P., Carter, R., Awad, W., Neale, G., Thomas, P.G., and Youngblood, B. (2017). De novo epigenetic programs inhibit PD-1 blockade-mediated T cell rejuvenation. *Cell* *170*, 142–157.e19.
49. Youngblood, B., Hale, J.S., Kissick, H.T., Ahn, E., Xu, X., Wieland, A., Araki, K., West, E.E., Ghoneim, H.E., Fan, Y., et al. (2017). Effector CD8 T cells dedifferentiate into long-lived memory cells. *Nature* *552*, 404–409.
50. Ladle, B.H., Li, K.P., Phillips, M.J., Pucsek, A.B., Haile, A., Powell, J.D., Jaffee, E.M., Hildeman, D.A., and Gamper, C.J. (2016). De novo DNA methylation by DNA methyltransferase 3a controls early effector CD8<sup>+</sup> T-cell fate decisions following activation. *Proc. Natl. Acad. Sci. USA* *113*, 10631–10636.
51. Youngblood, B.A., Ghoneim, H.E., Abdelsamed, H.A., Moustaki, A., Fan, Y., Crawford, J., Thomas, P.G., Stewart, E., and Federico, S. (2019). De novo DNA methylation programs regulate T cell exhaustion and limit T cell-based immunotherapies. *J. Immunol.* *202* (1 Suppl), 134.114.
52. Shin, M.S., You, S., Kang, Y., Lee, N., Yoo, S.A., Park, K., Kang, K.S., Kim, S.H., Mohanty, S., Shaw, A.C., et al. (2015). DNA methylation regulates the differential expression of CX3CR1 on human IL-7R $\alpha$ <sup>low</sup> and IL-7R $\alpha$ <sup>high</sup> effector memory CD8<sup>+</sup> T cells with distinct migratory capacities to the fractalkine. *J. Immunol.* *195*, 2861–2869.
53. Russ, B.E., Olshanksy, M., Smallwood, H.S., Li, J., Denton, A.E., Prier, J.E., Stock, A.T., Croom, H.A., Cullen, J.G., Nguyen, M.L., et al. (2014). Distinct epigenetic signatures delineate transcriptional programs during virus-specific CD8<sup>+</sup> T cell differentiation. *Immunity* *41*, 853–865.
54. Crompton, J.G., Narayanan, M., Cuddapah, S., Roychowdhuri, R., Ji, Y., Yang, W., Patel, S.J., Sukumar, M., Palmer, D.C., Peng, W., et al. (2016). Lineage relationship of CD8<sup>+</sup> T cell subsets is revealed by progressive changes in the epigenetic landscape. *Cell. Mol. Immunol.* *13*, 502–513.
55. Nolz, J.C., and Harty, J.T. (2014). IL-15 regulates memory CD8<sup>+</sup> T cell O-glycan synthesis and affects trafficking. *J. Clin. Invest.* *124*, 1013–1026.
56. Chen, X., Wang, J., Woltring, D., Gerondakis, S., and Shannon, M.F. (2005). Histone dynamics on the interleukin-2 gene in response to T-cell activation. *Mol. Cell. Biol.* *25*, 3209–3219.
57. Zhang, F., Zhou, X., DiSpirito, J.R., Wang, C., Wang, Y., and Shen, H. (2014). Epigenetic manipulation restores functions of defective CD8<sup>+</sup> T cells from chronic viral infection. *Mol. Ther.* *22*, 1698–1706.
58. Kim, C.G., Jang, M., Kim, Y., Leem, G., Kim, K.H., Lee, H., Kim, T.S., Choi, S.J., Kim, H.D., Han, J.W., et al. (2019). VEGF-A drives TOX-dependent T cell exhaustion in anti-PD-1-resistant microsatellite stable colorectal cancers. *Sci. Immunol.* *4*, eaay0555.
59. Wang, J., Hasan, F., Frey, A.C., Li, H.S., Park, J., Pan, K., Haymaker, C., Bernatchez, C., Lee, D.A., Watowich, S.S., and Yee, C. (2020). Histone deacetylase inhibitors and IL21 cooperate to reprogram human effector CD8<sup>+</sup> T cells to memory T cells. *Cancer Immunol. Res.* *8*, 794–805.
60. Preglej, T., Hamminger, P., Luu, M., Bulat, T., Andersen, L., Göschl, L., Stolz, V., Rica, R., Sandner, L., Waltenberger, D., et al. (2020). Histone deacetylases 1 and 2 restrain CD4<sup>+</sup> cytotoxic T lymphocyte differentiation. *JCI Insight* *5*, 133393.
61. McCaw, T.R., Goel, N., Brooke, D.J., Katre, A.A., Londoño, A.I., Smith, H.J., Randall, T.D., and Arend, R.C. (2021). Class I histone deacetylase inhibition promotes CD8 T cell activation in ovarian cancer. *Cancer Med.* *10*, 709–717.
62. Ding, X., Wang, A., Ma, X., Demarque, M., Jin, W., Xin, H., Dejean, A., and Dong, C. (2016). Protein SUMOylation is required for regulatory T cell expansion and function. *Cell Rep.* *16*, 1055–1066.
63. Zhang, D., Tang, Z., Huang, H., Zhou, G., Cui, C., Weng, Y., Liu, W., Kim, S., Lee, S., Perez-Neut, M., et al. (2019). Metabolic regulation of gene expression by histone lactylation. *Nature* *574*, 575–580.
64. Hermans, D., Gautam, S., García-Cañaveras, J.C., Gromer, D., Mitra, S., Spolski, R., Li, P., Christensen, S., Nguyen, R., Lin, J.X., et al. (2020). Lactate dehydrogenase inhibition synergizes with IL-21 to promote CD8<sup>+</sup> T cell stemness and antitumor immunity. *Proc. Natl. Acad. Sci. USA* *117*, 6047–6055.
65. Wei, J.W., Huang, K., Yang, C., and Kang, C.S. (2017). Non-coding RNAs as regulators in epigenetics (Review). *Oncol. Rep.* *37*, 3–9.
66. Bronevetsky, Y., and Ansel, K.M. (2013). Regulation of miRNA biogenesis and turnover in the immune system. *Immunol. Rev.* *253*, 304–316.
67. Wu, H., Neilson, J.R., Kumar, P., Manocha, M., Shankar, P., Sharp, P.A., and Manjunath, N. (2007). miRNA profiling of naïve, effector and memory CD8 T cells. *PLoS ONE* *2*, e1020.
68. Salaun, B., Yamamoto, T., Badran, B., Tsunetsugu-Yokota, Y., Roux, A., Baitsch, L., Rouas, R., Fayyad-Kazan, H., Baumgaertner, P., Devevre, E., et al. (2011). Differentiation associated regulation of microRNA expression in vivo in human CD8<sup>+</sup> T cell subsets. *J. Transl. Med.* *9*, 44.
69. Jiang, S., Li, C., Olive, V., Lykken, E., Feng, F., Sevilla, J., Wan, Y., He, L., and Li, Q.J. (2011). Molecular dissection of the miR-17-92 cluster's critical dual roles in promoting Th1 responses and preventing inducible Treg differentiation. *Blood* *118*, 5487–5497.
70. Wu, T., Wieland, A., Araki, K., Davis, C.W., Ye, L., Hale, J.S., and Ahmed, R. (2012). Temporal expression of microRNA cluster miR-17-92 regulates effector and memory CD8<sup>+</sup> T-cell differentiation. *Proc. Natl. Acad. Sci. USA* *109*, 9965–9970.
71. Ji, Y., Pos, Z., Rao, M., Klebanoff, C.A., Yu, Z., Sukumar, M., Reger, R.N., Palmer, D.C., Borman, Z.A., Muranski, P., et al. (2011). Repression of the DNA-binding inhibitor Id3 by Blimp-1 limits the formation of memory CD8<sup>+</sup> T cells. *Nat. Immunol.* *12*, 1230–1237.
72. Khan, A.A., Penny, L.A., Yuzefpolskiy, Y., Sarkar, S., and Kalia, V. (2013). MicroRNA-17~92 regulates effector and memory CD8 T-cell fates by modulating proliferation in response to infections. *Blood* *121*, 4473–4483.

73. Yang, C.Y., Best, J.A., Knell, J., Yang, E., Sheridan, A.D., Jesionek, A.K., Li, H.S., Rivera, R.R., Lind, K.C., D'Cruz, L.M., et al. (2011). The transcriptional regulators Id2 and Id3 control the formation of distinct memory CD8<sup>+</sup> T cell subsets. *Nat. Immunol.* *12*, 1221–1229.
74. Lind, E.F., Elford, A.R., and Ohashi, P.S. (2013). Micro-RNA 155 is required for optimal CD8<sup>+</sup> T cell responses to acute viral and intracellular bacterial challenges. *J. Immunol.* *190*, 1210–1216.
75. Dudda, J.C., Salaun, B., Ji, Y., Palmer, D.C., Monnot, G.C., Merck, E., Boudousquie, C., Utschneider, D.T., Escobar, T.M., Perret, R., et al. (2013). MicroRNA-155 is required for effector CD8<sup>+</sup> T cell responses to virus infection and cancer. *Immunity* *38*, 742–753.
76. Yang, L., Boldin, M.P., Yu, Y., Liu, C.S., Ea, C.K., Ramakrishnan, P., Taganov, K.D., Zhao, J.L., and Baltimore, D. (2012). miR-146a controls the resolution of T cell responses in mice. *J. Exp. Med.* *209*, 1655–1670.
77. Boldin, M.P., Taganov, K.D., Rao, D.S., Yang, L., Zhao, J.L., Kalwani, M., Garcia-Flores, Y., Luong, M., Devrekanli, A., Xu, J., et al. (2011). miR-146a is a significant brake on autoimmunity, myeloproliferation, and cancer in mice. *J. Exp. Med.* *208*, 1189–1201.
78. Yu, T., Ju, Z., Luo, M., Hu, R., Teng, Y., Xie, L., Zhong, C., Chen, L., Hou, W., Xiong, Y., and Feng, Y. (2019). Elevated expression of miR-146a correlates with high levels of immune cell exhaustion markers and suppresses cellular immune function in chronic HIV-1-infected patients. *Sci. Rep.* *9*, 18829.
79. Li, H., Chiappinelli, K.B., Guzzetta, A.A., Easwaran, H., Yen, R.W., Vataapalli, R., Topper, M.J., Luo, J., Connolly, R.M., Azad, N.S., et al. (2014). Immune regulation by low doses of the DNA methyltransferase inhibitor 5-azacitidine in common human epithelial cancers. *Oncotarget* *5*, 587–598.
80. Trifari, S., Pipkin, M.E., Bandukwala, H.S., Ajjō, T., Bassein, J., Chen, R., Martinez, G.J., and Rao, A. (2013). MicroRNA-directed program of cytotoxic CD8<sup>+</sup> T-cell differentiation. *Proc. Natl. Acad. Sci. USA* *110*, 18608–18613.
81. Chen, Z., Stelekati, E., Kurachi, M., Yu, S., Cai, Z., Manne, S., Khan, O., Yang, X., and Wherry, E.J. (2017). miR-150 regulates memory CD8 T cell differentiation via c-Myb. *Cell Rep.* *20*, 2584–2597.
82. Sang, W., Sun, C., Zhang, C., Zhang, D., Wang, Y., Xu, L., Zhang, Z., Wei, X., Pan, B., Yan, D., et al. (2016). MicroRNA-150 negatively regulates the function of CD4<sup>+</sup> T cells through AKT3/Bim signaling pathway. *Cell. Immunol.* *306*–*307*, 35–40.
83. Jindra, P.T., Bagley, J., Godwin, J.G., and Iacomini, J. (2010). Costimulation-dependent expression of microRNA-214 increases the ability of T cells to proliferate by targeting Pten. *J. Immunol.* *185*, 990–997.
84. Li, Q.J., Chau, J., Ebert, P.J., Sylvester, G., Min, H., Liu, G., Braich, R., Manoharan, M., Soutschek, J., Skare, P., et al. (2007). miR-181a is an intrinsic modulator of T cell sensitivity and selection. *Cell* *129*, 147–161.
85. Schietinger, A., Delrow, J.J., Basom, R.S., Blattman, J.N., and Greenberg, P.D. (2012). Rescued tolerant CD8 T cells are preprogrammed to reestablish the tolerant state. *Science* *335*, 723–727.
86. Li, J., He, Y., Hao, J., Ni, L., and Dong, C. (2018). High levels of Eomes promote exhaustion of anti-tumor CD8<sup>+</sup> T cells. *Front. Immunol.* *9*, 2981.
87. Jia, B., Zhao, C., Rakszawski, K.L., Claxton, D.F., Ehmann, W.C., Rybka, W.B., Mineishi, S., Wang, M., Shike, H., Bayerl, M.G., et al. (2019). Eomes<sup>+</sup>T-bet<sup>low</sup> CD8<sup>+</sup> T cells are functionally impaired and are associated with poor clinical outcome in patients with acute myeloid leukemia. *Cancer Res.* *79*, 1635–1645.
88. Benetti, R., Gonzalo, S., Jaco, I., Muñoz, P., Gonzalez, S., Schoeftner, S., Murchison, E., Ancl, T., Chen, T., Klatt, P., et al. (2008). A mammalian microRNA cluster controls DNA methylation and telomere recombination via Rbl2-dependent regulation of DNA methyltransferases. *Nat. Struct. Mol. Biol.* *15*, 268–279.
89. Sinkkonen, L., Hugenschmidt, T., Berninger, P., Gaidatzis, D., Mohn, F., Artus-Revel, C.G., Zavolan, M., Svoboda, P., and Filipowicz, W. (2008). MicroRNAs control de novo DNA methylation through regulation of transcriptional repressors in mouse embryonic stem cells. *Nat. Struct. Mol. Biol.* *15*, 259–267.
90. Gonzalez, S., Pisano, D.G., and Serrano, M. (2008). Mechanistic principles of chromatin remodeling guided by siRNAs and miRNAs. *Cell Cycle* *7*, 2601–2608.
91. Tsytzykova, A.V., Rajsbaum, R., Falvo, J.V., Ligeiro, F., Neely, S.R., and Goldfeld, A.E. (2007). Activation-dependent intrachromosomal interactions formed by the TNF gene promoter and two distal enhancers. *Proc. Natl. Acad. Sci. USA* *104*, 16850–16855.
92. Spilianakis, C.G., and Flavell, R.A. (2004). Long-range intrachromosomal interactions in the T helper type 2 cytokine locus. *Nat. Immunol.* *5*, 1017–1027.
93. Ktistaki, E., Garefalaki, A., Williams, A., Andrews, S.R., Bell, D.M., Foster, K.E., Spilianakis, C.G., Flavell, R.A., Kosyakova, N., Trifonov, V., et al. (2010). CD8 locus nuclear dynamics during thymocyte development. *J. Immunol.* *184*, 5686–5695.
94. Phillips-Cremins, J.E., Sauria, M.E., Sanyal, A., Gerasimova, T.I., Lajoie, B.R., Bell, J.S., Ong, C.T., Hookway, T.A., Guo, C., Sun, Y., et al. (2013). Architectural protein subclasses shape 3D organization of genomes during lineage commitment. *Cell* *153*, 1281–1295.
95. Watson, L.A., Wang, X., Elbert, A., Kernohan, K.D., Galjart, N., and Bérubé, N.G. (2014). Dual effect of CTCF loss on neuroprogenitor differentiation and survival. *J. Neurosci.* *34*, 2860–2870.
96. Shih, H.Y., Verma-Gaur, J., Torkamani, A., Feeney, A.J., Galjart, N., and Krangel, M.S. (2012). *Tcr* gene recombination is supported by a *Tcr* enhancer- and CTCF-dependent chromatin hub. *Proc. Natl. Acad. Sci. USA* *109*, E3493–E3502.
97. Heath, H., Ribeiro de Almeida, C., Sleutels, F., Dingjan, G., van de Nobelen, S., Jonkers, I., Ling, K.W., Gribnau, J., Renkawitz, R., Grosveld, F., et al. (2008). CTCF regulates cell cycle progression of  $\alpha\beta$  T cells in the thymus. *EMBO J.* *27*, 2839–2850.
98. Stephen, T.L., Payne, K.K., Chaurio, R.A., Allegrezza, M.J., Zhu, H., Perez-Sanz, J., Perales-Puchalt, A., Nguyen, J.M., Vara-Ailor, A.E., Eruslanov, E.B., et al. (2017). SATB1 expression governs epigenetic repression of PD-1 in tumor-reactive T cells. *Immunity* *46*, 51–64.
99. Sommermeier, D., Hudecek, M., Kosasih, P.L., Gogishvili, T., Maloney, D.G., Turtle, C.J., and Riddell, S.R. (2016). Chimeric antigen receptor-modified T cells derived from defined CD8<sup>+</sup> and CD4<sup>+</sup> subsets confer superior antitumor reactivity in vivo. *Leukemia* *30*, 492–500.
100. Rosenberg, S.A., Yang, J.C., Sherry, R.M., Kammula, U.S., Hughes, M.S., Phan, G.Q., Citrin, D.E., Restifo, N.P., Robbins, P.F., Wunderlich, J.R., et al. (2011). Durable complete responses in heavily pretreated patients with metastatic melanoma using T-cell transfer immunotherapy. *Clin. Cancer Res.* *17*, 4550–4557.
101. Gattinoni, L., Klebanoff, C.A., Palmer, D.C., Wrzesinski, C., Kerstann, K., Yu, Z., Finkelstein, S.E., Theoret, M.R., Rosenberg, S.A., and Restifo, N.P. (2005). Acquisition of full effector function in vitro paradoxically impairs the in vivo antitumor efficacy of adoptively transferred CD8<sup>+</sup> T cells. *J. Clin. Invest.* *115*, 1616–1626.
102. Ghassemi, S., Nunez-Cruz, S., O'Connor, R.S., Fraietta, J.A., Patel, P.R., Scholler, J., Barrett, D.M., Lundh, S.M., Davis, M.M., Bedoya, F., et al. (2018). Reducing *ex vivo* culture improves the antileukemic activity of chimeric antigen receptor (CAR) T cells. *Cancer Immunol. Res.* *6*, 1100–1109.
103. Fraietta, J.A., Nobles, C.L., Sammons, M.A., Lundh, S., Carty, S.A., Reich, T.J., Cogdill, A.P., Morrisette, J.J.D., DeNizio, J.E., Reddy, S., et al. (2018). Disruption of *TET2* promotes the therapeutic efficacy of CD19-targeted T cells. *Nature* *558*, 307–312.
104. Tyrakis, P.A., Palazon, A., Macias, D., Lee, K.L., Phan, A.T., Veliça, P., You, J., Chia, G.S., Sim, J., Doedens, A., et al. (2016). S-2-hydroxyglutarate regulates CD8<sup>+</sup> T lymphocyte fate. *Nature* *540*, 236–241.
105. Foskolou, I.P., Barbieri, L., Vernet, A., Bargiela, D., Cunha, P.P., Velica, P., Suh, E., Pietsch, S., Matuleviciute, R., Rundqvist, H., et al. (2020). The S enantiomer of 2-hydroxyglutarate increases central memory CD8 populations and improves CAR-T therapy outcome. *Blood Adv.* *4*, 4483–4493.
106. Kagoya, Y., Nakatsugawa, M., Yamashita, Y., Ochi, T., Guo, T., Anczurowski, M., Saso, K., Butler, M.O., Arrowsmith, C.H., and Hirano, N. (2016). BET bromodomain inhibition enhances T cell persistence and function in adoptive immunotherapy models. *J. Clin. Invest.* *126*, 3479–3494.
107. He, B., Xing, S., Chen, C., Gao, P., Teng, L., Shan, Q., Gullicksruud, J.A., Martin, M.D., Yu, S., Harty, J.T., et al. (2016). CD8<sup>+</sup> T cells utilize highly dynamic enhancer repertoires and regulatory circuitry in response to infections. *Immunity* *45*, 1341–1354.
108. Rodriguez, R.M., Suarez-Alvarez, B., Lavín, J.L., Mosén-Ansorena, D., Baragaño Raneros, A., Márquez-Kisinosky, L., Aransay, A.M., and Lopez-Larrea, C.

- (2017). Epigenetic networks regulate the transcriptional program in memory and terminally differentiated CD8<sup>+</sup> T cells. *J. Immunol.* *198*, 937–949.
109. Abdelsamed, H.A., Moustaki, A., Fan, Y., Dogra, P., Ghoneim, H.E., Zebley, C.C., Triplett, B.M., Sekaly, R.P., and Youngblood, B. (2017). Human memory CD8 T cell effector potential is epigenetically preserved during in vivo homeostasis. *J. Exp. Med.* *214*, 1593–1606.
  110. Araki, Y., Fann, M., Wersto, R., and Weng, N.P. (2008). Histone acetylation facilitates rapid and robust memory CD8 T cell response through differential expression of effector molecules (eomesodermin and its targets: Perforin and granzyme B). *J. Immunol.* *180*, 8102–8108.
  111. Henning, A.N., Klebanoff, C.A., and Restifo, N.P. (2018). Silencing stemness in T cell differentiation. *Science* *359*, 163–164.
  112. Kakaradov, B., Arsenio, J., Widjaja, C.E., He, Z., Aigner, S., Metz, P.J., Yu, B., Wehrens, E.J., Lopez, J., Kim, S.H., et al. (2017). Early transcriptional and epigenetic regulation of CD8<sup>+</sup> T cell differentiation revealed by single-cell RNA sequencing. *Nat. Immunol.* *18*, 422–432.
  113. Pace, L., Goudot, C., Zueva, E., Gueguen, P., Burgdorf, N., Waterfall, J.J., Quivy, J.P., Almouzni, G., and Amigorena, S. (2018). The epigenetic control of stemness in CD8<sup>+</sup> T cell fate commitment. *Science* *359*, 177–186.
  114. Jo, Y., Ali, L.A., Shim, J.A., Lee, B.H., and Hong, C. (2020). Innovative CAR-T cell therapy for solid tumor; current duel between CAR-T spear and tumor shield. *Cancers (Basel)* *12*, E2087.
  115. Zou, F., Lu, L., Liu, J., Xia, B., Zhang, W., Hu, Q., Liu, W., Zhang, Y., Lin, Y., Jing, S., et al. (2019). Engineered triple inhibitory receptor resistance improves anti-tumor CAR-T cell performance via CD56. *Nat. Commun.* *10*, 4109.
  116. Ding, Z.C., Shi, H., Aboelella, N.S., Fesenkova, K., Park, E.J., Liu, Z., Pei, L., Li, J., McIndoe, R.A., Xu, H., et al. (2020). Persistent STAT5 activation reprograms the epigenetic landscape in CD4<sup>+</sup> T cells to drive polyfunctionality and antitumor immunity. *Sci. Immunol.* *5*, eaba5962.
  117. Craddock, J.A., Lu, A., Bear, A., Pule, M., Brenner, M.K., Rooney, C.M., and Foster, A.E. (2010). Enhanced tumor trafficking of GD2 chimeric antigen receptor T cells by expression of the chemokine receptor CCR2b. *J. Immunother.* *33*, 780–788.
  118. Moon, E.K., Carpenito, C., Sun, J., Wang, L.C., Kapoor, V., Predina, J., Powell, D.J., Jr., Riley, J.L., June, C.H., and Albelda, S.M. (2011). Expression of a functional CCR2 receptor enhances tumor localization and tumor eradication by retargeted human T cells expressing a mesothelin-specific chimeric antibody receptor. *Clin. Cancer Res.* *17*, 4719–4730.
  119. Angelou, C.C., Wells, A.C., Vijayaraghavan, J., Dougan, C.E., Lawlor, R., Iverson, E., Lazarevic, V., Kimura, M.Y., Peyton, S.R., Minter, L.M., et al. (2020). Differentiation of pathogenic Th17 cells is negatively regulated by let-7 microRNAs in a mouse model of multiple sclerosis. *Front. Immunol.* *10*, 3125.
  120. Zhang, J., Endres, S., and Kobold, S. (2019). Enhancing tumor T cell infiltration to enable cancer immunotherapy. *Immunotherapy* *11*, 201–213.
  121. Siddiqui, I., Erreni, M., van Brakel, M., Debets, R., and Allavena, P. (2016). Enhanced recruitment of genetically modified CX3CR1-positive human T cells into Fractalkine/CX3CL1 expressing tumors: Importance of the chemokine gradient. *J. Immunother. Cancer* *4*, 21.
  122. Regis, S., Caliendo, F., Dondero, A., Casu, B., Romano, F., Loiacono, F., Moretta, A., Bottino, C., and Castriconi, R. (2017). TGF- $\beta$ 1 downregulates the expression of CX<sub>3</sub>CR1 by inducing miR-27a-5p in primary human NK cells. *Front. Immunol.* *8*, 868.
  123. Matsumura, S., Wang, B., Kawashima, N., Braunstein, S., Badura, M., Cameron, T.O., Babb, J.S., Schneider, R.J., Formenti, S.C., Dustin, M.L., and Demaria, S. (2008). Radiation-induced CXCL16 release by breast cancer cells attracts effector T cells. *J. Immunol.* *181*, 3099–3107.
  124. Monnot, G.C., Martinez-Usatorre, A., Lanitis, E., Lopes, S.F., Cheng, W.C., Ho, P.C., Irving, M., Coukos, G., Donda, A., and Romero, P. (2019). miR-155 overexpression in OT-1 CD8<sup>+</sup> T cells improves anti-tumor activity against low-affinity tumor antigen. *Mol. Ther. Oncolytics* *16*, 111–123.
  125. Ohno, M., Ohkuri, T., Kosaka, A., Tanahashi, K., June, C.H., Natsume, A., and Okada, H. (2013). Expression of miR-17-92 enhances anti-tumor activity of T-cells transduced with the anti-EGFRvIII chimeric antigen receptor in mice bearing human GBM xenografts. *J. Immunother. Cancer* *1*, 21.
  126. Li, Q., Johnston, N., Zheng, X., Wang, H., Zhang, X., Gao, D., and Min, W. (2016). miR-28 modulates exhaustive differentiation of T cells through silencing programmed cell death-1 and regulating cytokine secretion. *Oncotarget* *7*, 53735–53750.
  127. Jafarzadeh, L., Masoumi, E., Fallah-Mehrdadi, K., Mirzaei, H.R., and Hadjati, J. (2020). Prolonged persistence of chimeric antigen receptor (CAR) T cell in adoptive cancer immunotherapy: Challenges and ways forward. *Front. Immunol.* *11*, 702.
  128. Rufer, N., Migliaccio, M., Antonchuk, J., Humphries, R.K., Roosnek, E., and Lansdorf, P.M. (2001). Transfer of the human telomerase reverse transcriptase (*TERT*) gene into T lymphocytes results in extension of replicative potential. *Blood* *98*, 597–603.
  129. Migliaccio, M., Amacker, M., Just, T., Reichenbach, P., Valmori, D., Cerottini, J.C., Romero, P., and Nabholz, M. (2000). Ectopic human telomerase catalytic subunit expression maintains telomere length but is not sufficient for CD8<sup>+</sup> T lymphocyte immortalization. *J. Immunol.* *165*, 4978–4984.
  130. Bai, Y., Kan, S., Zhou, S., Wang, Y., Xu, J., Cooke, J.P., Wen, J., and Deng, H. (2015). Enhancement of the in vivo persistence and antitumor efficacy of CD19 chimeric antigen receptor T cells through the delivery of modified TERT mRNA. *Cell Discov.* *1*, 15040.
  131. Wang, H., Han, P., Qi, X., Li, F., Li, M., Fan, L., Zhang, H., Zhang, X., and Yang, X. (2021). Bcl-2 enhances chimeric antigen receptor T cell persistence by reducing activation-induced apoptosis. *Cancers (Basel)* *13*, 197.
  132. Jacobs, J.J., Kieboom, K., Marino, S., DePinho, R.A., and van Lohuizen, M. (1999). The oncogene and Polycomb-group gene *bmi-1* regulates cell proliferation and senescence through the *ink4a* locus. *Nature* *397*, 164–168.
  133. Sherr, C.J. (2004). Principles of tumor suppression. *Cell* *116*, 235–246.
  134. Heffner, M., and Fearon, D.T. (2007). Loss of T cell receptor-induced Bmi-1 in the KLRG1<sup>+</sup> senescent CD8<sup>+</sup> T lymphocyte. *Proc. Natl. Acad. Sci. USA* *104*, 13414–13419.
  135. Sasaki, K., Kohanbash, G., Hoji, A., Ueda, R., McDonald, H.A., Reinhart, T.A., Martinson, J., Lotze, M.T., Marincola, F.M., Wang, E., et al. (2010). miR-17-92 expression in differentiated T cells—Implications for cancer immunotherapy. *J. Transl. Med.* *8*, 17.
  136. Olive, V., Li, Q., and He, L. (2013). miR-17-92: A polycistronic oncomir with pleiotropic functions. *Immunol. Rev.* *253*, 158–166.
  137. Poorebrahim, M., Melief, J., Pico de Coaña, Y., L Wickström, S., Cid-Arregui, A., and Kiessling, R. (2021). Counteracting CAR T cell dysfunction. *Oncogene* *40*, 421–435.
  138. Beltra, J.C., Manne, S., Abdel-Hakeem, M.S., Kurachi, M., Giles, J.R., Chen, Z., Casella, V., Ngiow, S.F., Khan, O., Huang, Y.J., et al. (2020). Developmental relationships of four exhausted CD8<sup>+</sup> T cell subsets reveals underlying transcriptional and epigenetic landscape control mechanisms. *Immunity* *52*, 825–841.e8.
  139. Thommen, D.S., and Schumacher, T.N. (2018). T cell dysfunction in cancer. *Cancer Cell* *33*, 547–562.
  140. Schietinger, A., Philip, M., Krisnawan, V.E., Chiu, E.Y., Delrow, J.J., Basom, R.S., Lauer, P., Brockstedt, D.G., Knoblaugh, S.E., Hämmerling, G.J., et al. (2016). Tumor-specific T cell dysfunction is a dynamic antigen-driven differentiation program initiated early during tumorigenesis. *Immunity* *45*, 389–401.
  141. Zebley, C.C., Petersen, C.T., Prinzing, B., Bell, M., Fan, Y., Crawford, J.C., Houke, H., Haydar, D., Yi, Z., Nguyen, P., DeRenzo, C., et al. (2020). De novo DNA methylation programs regulate CAR T-cell exhaustion. *J. Immunol.* *204* (1 Suppl), 246.245.
  142. You, L., Han, Q., Zhu, L., Zhu, Y., Bao, C., Yang, C., Lei, W., and Qian, W. (2020). Decitabine-mediated epigenetic reprogramming enhances anti-leukemia efficacy of CD123-targeted chimeric antigen receptor T-cells. *Front. Immunol.* *11*, 1787.
  143. Wang, Y., Tong, C., Dai, H., Wu, Z., Han, X., Guo, Y., Chen, D., Wei, J., Ti, D., Liu, Z., et al. (2021). Low-dose decitabine priming endows CAR T cells with enhanced and persistent antitumor potential via epigenetic reprogramming. *Nat. Commun.* *12*, 409.
  144. Lynn, R.C., Weber, E.W., Sotillo, E., Gennert, D., Xu, P., Good, Z., Anbunathan, H., Lattin, J., Jones, R., Tieu, V., et al. (2019). c-Jun overexpression in CAR T cells induces exhaustion resistance. *Nature* *576*, 293–300.
  145. Mognol, G.P., Spreafico, R., Wong, V., Scott-Browne, J.P., Togher, S., Hoffmann, A., Hogan, P.G., Rao, A., and Trifari, S. (2017). Exhaustion-associated regulatory

- regions in CD8<sup>+</sup> tumor-infiltrating T cells. *Proc. Natl. Acad. Sci. USA* 114, E2776–E2785.
146. Pauken, K.E., Sammons, M.A., Odorizzi, P.M., Manne, S., Godec, J., Khan, O., Drake, A.M., Chen, Z., Sen, D.R., Kurachi, M., et al. (2016). Epigenetic stability of exhausted T cells limits durability of reinvigoration by PD-1 blockade. *Science* 354, 1160–1165.
  147. Philip, M., Fairchild, L., Sun, L., Horste, E.L., Camara, S., Shakiba, M., Scott, A.C., Viale, A., Lauer, P., Merghoub, T., et al. (2017). Chromatin states define tumour-specific T cell dysfunction and reprogramming. *Nature* 545, 452–456.
  148. Chen, J., López-Moyado, I.F., Seo, H., Lio, C.J., Hempleman, L.J., Sekiya, T., Yoshimura, A., Scott-Brownie, J.P., and Rao, A. (2019). NR4A transcription factors limit CAR T cell function in solid tumours. *Nature* 567, 530–534.
  149. Martinez, G.J., Pereira, R.M., Äijö, T., Kim, E.Y., Marangoni, F., Pipkin, M.E., Togher, S., Heissmeyer, V., Zhang, Y.C., Crotty, S., et al. (2015). The transcription factor NFAT promotes exhaustion of activated CD8<sup>+</sup> T cells. *Immunity* 42, 265–278.
  150. Wei, J., Nduom, E.K., Kong, L.Y., Hashimoto, Y., Xu, S., Gabrusiewicz, K., Ling, X., Huang, N., Qiao, W., Zhou, S., et al. (2016). miR-138 exerts anti-glioma efficacy by targeting immune checkpoints. *Neuro-oncol.* 18, 639–648.
  151. Pellegrino, M., Del Bufalo, F., De Angelis, B., Quintarelli, C., Caruana, I., and de Billy, E. (2020). Manipulating the metabolism to improve the efficacy of CAR T-cell immunotherapy. *Cells* 10, E14.
  152. Geltink, R.I.K., Kyle, R.L., and Pearce, E.L. (2018). Unraveling the complex interplay between T cell metabolism and function. *Annu. Rev. Immunol.* 36, 461–488.
  153. O'Sullivan, D. (2019). The metabolic spectrum of memory T cells. *Immunol. Cell Biol.* 97, 636–646.
  154. Menk, A.V., Scharping, N.E., Moreci, R.S., Zeng, X., Guy, C., Salvatore, S., Bae, H., Xie, J., Young, H.A., Wendell, S.G., and Delgoffe, G.M. (2018). Early TCR signaling induces rapid aerobic glycolysis enabling distinct acute T cell effector functions. *Cell Rep.* 22, 1509–1521.
  155. O'Connor, R.S., Guo, L., Ghassemi, S., Snyder, N.W., Worth, A.J., Weng, L., Kam, Y., Philipson, B., Trefely, S., Nunez-Cruz, S., et al. (2018). The CPT1a inhibitor, etomoxir induces severe oxidative stress at commonly used concentrations. *Sci. Rep.* 8, 6289.
  156. Peng, M., Yin, N., Chhangawala, S., Xu, K., Leslie, C.S., and Li, M.O. (2016). Aerobic glycolysis promotes T helper 1 cell differentiation through an epigenetic mechanism. *Science* 354, 481–484.
  157. Qiu, J., Villa, M., Sanin, D.E., Buck, M.D., O'Sullivan, D., Ching, R., Matsushita, M., Grzes, K.M., Winkler, F., Chang, C.H., et al. (2019). Acetate promotes T cell effector function during glucose restriction. *Cell Rep.* 27, 2063–2074.e5.
  158. Scharping, N.E., Menk, A.V., Moreci, R.S., Whetstone, R.D., Dadey, R.E., Watkins, S.C., Ferris, R.L., and Delgoffe, G.M. (2016). The tumor microenvironment represses T cell mitochondrial biogenesis to drive intratumoral T cell metabolic insufficiency and dysfunction. *Immunity* 45, 374–388.
  159. Das, R.K., O'Connor, R.S., Grupp, S.A., and Barrett, D.M. (2020). Lingering effects of chemotherapy on mature T cells impair proliferation. *Blood Adv.* 4, 4653–4664.
  160. Ho, P.C., Bihuniak, J.D., Macintyre, A.N., Staron, M., Liu, X., Amezquita, R., Tsui, Y.C., Cui, G., Micevic, G., Perales, J.C., et al. (2015). Phosphoenolpyruvate is a metabolic checkpoint of anti-tumor T cell responses. *Cell* 162, 1217–1228.
  161. Bhagat, T.D., Von Ahrens, D., Dawlaty, M., Zou, Y., Baddour, J., Achreja, A., Zhao, H., Yang, L., Patel, B., Kwak, C., et al. (2019). Lactate-mediated epigenetic reprogramming regulates formation of human pancreatic cancer-associated fibroblasts. *eLife* 8, e50663.
  162. Roy, D.G., Chen, J., Mamane, V., Ma, E.H., Muhire, B.M., Sheldon, R.D., Shorstova, T., Koning, R., Johnson, R.M., Esaulova, E., et al. (2020). Methionine metabolism shapes T helper cell responses through regulation of epigenetic reprogramming. *Cell Metab.* 31, 250–266.e9.
  163. Schwartzman, J.M., Thompson, C.B., and Finley, L.W.S. (2018). Metabolic regulation of chromatin modifications and gene expression. *J. Cell Biol.* 217, 2247–2259.
  164. Navas, L.E., and Carnero, A. (2021). NAD<sup>+</sup> metabolism, stemness, the immune response, and cancer. *Signal Transduct. Target. Ther.* 6, 2.
  165. van der Windt, G.J., O'Sullivan, D., Everts, B., Huang, S.C., Buck, M.D., Curtis, J.D., Chang, C.H., Smith, A.M., Ai, T., Faubert, B., et al. (2013). CD8 memory T cells have a bioenergetic advantage that underlies their rapid recall ability. *Proc. Natl. Acad. Sci. USA* 110, 14336–14341.
  166. Reinfeld, B.I., Madden, M.Z., Wolf, M.M., Chytil, A., Bader, J.E., Patterson, A.R., Sugiura, A., Cohen, A.S., Ali, A., Do, B.T., et al. (2021). Cell-programmed nutrient partitioning in the tumour microenvironment. *Nature* 593, 282–288.
  167. Maeda, T., Towatari, M., Kosugi, H., and Saito, H. (2000). Up-regulation of costimulatory/adhesion molecules by histone deacetylase inhibitors in acute myeloid leukemia cells. *Blood* 96, 3847–3856.
  168. Wang, L.X., Mei, Z.Y., Zhou, J.H., Yao, Y.S., Li, Y.H., Xu, Y.H., Li, J.X., Gao, X.N., Zhou, M.H., Jiang, M.M., et al. (2013). Low dose decitabine treatment induces CD80 expression in cancer cells and stimulates tumor specific cytotoxic T lymphocyte responses. *PLoS ONE* 8, e62924.
  169. Magner, W.J., Kazim, A.L., Stewart, C., Romano, M.A., Catalano, G., Grande, C., Keiser, N., Santaniello, F., and Tomasi, T.B. (2000). Activation of MHC class I, II, and CD40 gene expression by histone deacetylase inhibitors. *J. Immunol.* 165, 7017–7024.
  170. Nakata, S., Yoshida, T., Horinaka, M., Shiraishi, T., Wakada, M., and Sakai, T. (2004). Histone deacetylase inhibitors upregulate death receptor 5/TRAIL-R2 and sensitize apoptosis induced by TRAIL/APO2-L in human malignant tumor cells. *Oncogene* 23, 6261–6271.
  171. Insinga, A., Monestiroli, S., Ronzoni, S., Gelmetti, V., Marchesi, F., Viale, A., Altucci, L., Nervi, C., Minucci, S., and Pelicci, P.G. (2005). Inhibitors of histone deacetylases induce tumor-selective apoptosis through activation of the death receptor pathway. *Nat. Med.* 11, 71–76.
  172. Wischnewski, F., Pantel, K., and Schwarzenbach, H. (2006). Promoter demethylation and histone acetylation mediate gene expression of MAGE-A1, -A2, -A3, and -A12 in human cancer cells. *Mol. Cancer Res.* 4, 339–349.
  173. Li, S., Xue, L., Wang, M., Qiang, P., Xu, H., Zhang, X., Kang, W., You, F., Xu, H., Wang, Y., et al. (2019). Decitabine enhances cytotoxic effect of T cells with an anti-CD19 chimeric antigen receptor in treatment of lymphoma. *OncoTargets Ther.* 12, 5627–5638.
  174. Fratta, E., Coral, S., Covre, A., Parisi, G., Colizzi, F., Danielli, R., Nicolay, H.J., Sigalotti, L., and Maio, M. (2011). The biology of cancer testis antigens: Putative function, regulation and therapeutic potential. *Mol. Oncol.* 5, 164–182.
  175. Zhang, M., Liang, J.Q., and Zheng, S. (2019). Expressional activation and functional roles of human endogenous retroviruses in cancers. *Rev. Med. Virol.* 29, e2025.
  176. Daskalakis, M., Brocks, D., Sheng, Y.H., Islam, M.S., Ressenrova, A., Assenov, Y., Milde, T., Oehme, I., Witt, O., Goyal, A., et al. (2018). Reactivation of endogenous retroviral elements via treatment with DNMT- and HDAC-inhibitors. *Cell Cycle* 17, 811–822.
  177. Krishnamurthy, J., Rabinovich, B.A., Mi, T., Switzer, K.C., Olivares, S., Maiti, S.N., Plummer, J.B., Singh, H., Kumaresan, P.R., Huls, H.M., et al. (2015). Genetic engineering of T cells to target HERV-K, an ancient retrovirus on melanoma. *Clin. Cancer Res.* 21, 3241–3251.
  178. Zingg, D., Arenas-Ramirez, N., Sahin, D., Rosalia, R.A., Antunes, A.T., Haeusel, J., Sommer, L., and Boyman, O. (2017). The histone methyltransferase Ezh2 controls mechanisms of adaptive resistance to tumor immunotherapy. *Cell Rep.* 20, 854–867.
  179. Kailayangiri, S., Altwater, B., Lesch, S., Balbach, S., Göttlich, C., Kühnemundt, J., Mikesch, J.H., Schelhaas, S., Jamitzky, S., Meltzer, J., et al. (2019). EZH2 inhibition in Ewing sarcoma upregulates G<sub>D2</sub> expression for targeting with gene-modified T cells. *Mol. Ther.* 27, 933–946.
  180. Kunert, A., van Brakel, M., van Steenberghe-Langeveld, S., da Silva, M., Coulie, P.G., Lamers, C., Sleijfer, S., and Debets, R. (2016). MAGE-C2-specific TCRs combined with epigenetic drug-enhanced antigenicity yield robust and tumor-selective T cell responses. *J. Immunol.* 197, 2541–2552.
  181. Sheng, W., LaFleur, M.W., Nguyen, T.H., Chen, S., Chakravarthy, A., Conway, J.R., Li, Y., Chen, H., Yang, H., Hsu, P.H., et al. (2018). LSD1 ablation stimulates anti-tumor immunity and enables checkpoint blockade. *Cell* 174, 549–563.e19.
  182. Brennan, K., Shin, J.H., Tay, J.K., Prunello, M., Gentles, A.J., Sunwoo, J.B., and Gevaert, O. (2017). NSD1 inactivation defines an immune cold, DNA hypomethylated subtype in squamous cell carcinoma. *Sci. Rep.* 7, 17064.

183. Lingohr, P., Dohmen, J., Semaan, A., Branchi, V., Dietrich, J., Bootz, F., Kalff, J.C., Matthaei, H., and Dietrich, D. (2019). Clinicopathological, immune and molecular correlates of *PD-L2* methylation in gastric adenocarcinomas. *Epigenomics* *11*, 639–653.
184. Dangaj, D., Bruand, M., Grimm, A.J., Ronet, C., Barras, D., Duttagupta, P.A., Lanitis, E., Duraiswamy, J., Tanyi, J.L., Benencia, F., et al. (2019). Cooperation between constitutive and inducible chemokines enables T cell engraftment and immune attack in solid tumors. *Cancer Cell* *35*, 885–900.e10.
185. Vo, D.D., Prins, R.M., Begley, J.L., Donahue, T.R., Morris, L.F., Bruhn, K.W., de la Rocha, P., Yang, M.Y., Mok, S., Garban, H.J., et al. (2009). Enhanced antitumor activity induced by adoptive T-cell transfer and adjunctive use of the histone deacetylase inhibitor LAQ824. *Cancer Res.* *69*, 8693–8699.
186. Zhu, H., Bengsch, F., Svoronos, N., Rutkowski, M.R., Bitler, B.G., Allegranza, M.J., Yokoyama, Y., Kossenkov, A.V., Bradner, J.E., Conejo-Garcia, J.R., and Zhang, R. (2016). BET bromodomain inhibition promotes anti-tumor immunity by suppressing PD-L1 expression. *Cell Rep.* *16*, 2829–2837.
187. Wang, W., and Tan, J. (2019). Co-inhibition of BET proteins and PD-L1 as a potential therapy for OSCC through synergistic inhibition of FOXM1 and PD-L1 expressions. *J. Oral Pathol. Med.* *48*, 817–825.
188. Labani-Motlagh, A., Ashja-Mahdavi, M., and Loskog, A. (2020). The tumor microenvironment: A milieu hindering and obstructing antitumor immune responses. *Front. Immunol.* *11*, 940.
189. Ninomiya, S., Narala, N., Huye, L., Yagyu, S., Savoldo, B., Dotti, G., Heslop, H.E., Brenner, M.K., Rooney, C.M., and Ramos, C.A. (2015). Tumor indoleamine 2,3-dioxygenase (IDO) inhibits CD19-CAR T cells and is downregulated by lymphodepleting drugs. *Blood* *125*, 3905–3916.
190. Hennequart, M., Pilote, L., Cane, S., Hoffmann, D., Stroobant, V., Plaen, E., and Van den Eynde, B.J. (2017). Constitutive IDO1 expression in human tumors is driven by cyclooxygenase-2 and mediates intrinsic immune resistance. *Cancer Immunol. Res.* *5*, 695–709.
191. Routy, J.P., Routy, B., Graziani, G.M., and Mehraj, V. (2016). The kynurenine pathway is a double-edged sword in immune-privileged sites and in cancer: Implications for immunotherapy. *Int. J. Tryptophan Res.* *9*, 67–77.
192. Terness, P., Bauer, T.M., Röse, L., Dufter, C., Watzlik, A., Simon, H., and Opelz, G. (2002). Inhibition of allogeneic T cell proliferation by indoleamine 2,3-dioxygenase-expressing dendritic cells: Mediation of suppression by tryptophan metabolites. *J. Exp. Med.* *196*, 447–457.
193. Godin-Ethier, J., Hanafi, L.A., Piccirillo, C.A., and Lapointe, R. (2011). Indoleamine 2,3-dioxygenase expression in human cancers: Clinical and immunologic perspectives. *Clin. Cancer Res.* *17*, 6985–6991.
194. Spranger, S., Spaepen, R.M., Zha, Y., Williams, J., Meng, Y., Ha, T.T., and Gajewski, T.F. (2013). Up-regulation of PD-L1, IDO, and T<sub>regs</sub> in the melanoma tumor microenvironment is driven by CD8<sup>+</sup> T cells. *Sci. Transl. Med.* *5*, 200ra116.
195. Lou, Q., Liu, R., Yang, X., Li, W., Huang, L., Wei, L., Tan, H., Xiang, N., Chan, K., Chen, J., and Liu, H. (2019). miR-448 targets IDO1 and regulates CD8<sup>+</sup> T cell response in human colon cancer. *J. Immunother. Cancer* *7*, 210.
196. Huang, Q., Xia, J., Wang, L., Wang, X., Ma, X., Deng, Q., Lu, Y., Kumar, M., Zhou, Z., Li, L., et al. (2018). miR-153 suppresses IDO1 expression and enhances CAR T cell immunotherapy. *J. Hematol. Oncol.* *11*, 58.
197. He, Q., Chen, Z., Dong, Q., Zhang, L., Chen, D., Patel, A., Koya, A., Luan, X., Cabay, R.J., Dai, Y., et al. (2016). MicroRNA-21 regulates prostaglandin E2 signaling pathway by targeting 15-hydroxyprostaglandin dehydrogenase in tongue squamous cell carcinoma. *BMC Cancer* *16*, 685.
198. Kim, S., Lee, E.S., Lee, E.J., Jung, J.Y., Lee, S.B., Lee, H.J., et al. (2020). Targeted eicosanoid profiling reveals microRNA-155 shifts PGE2/PGD2 balance towards oncogenic state. *bioRxiv*. <https://doi.org/10.1101/2020.04.08.032136>.
199. Zhang, J., He, J., and Zhang, L. (2018). The down-regulation of microRNA-137 contributes to the up-regulation of retinoblastoma cell proliferation and invasion by regulating COX-2/PGE2 signaling. *Biomed. Pharmacother.* *106*, 35–42.
200. Monteleone, N.J., and Lutz, C.S. (2020). miR-708-5p targets oncogenic prostaglandin E2 production to suppress a pro-tumorigenic phenotype in lung cancer cells. *Oncotarget* *11*, 2464–2483.
201. Liu, B., Peng, X.C., Zheng, X.L., Wang, J., and Qin, Y.W. (2009). miR-126 restoration down-regulate VEGF and inhibit the growth of lung cancer cell lines in vitro and in vivo. *Lung Cancer* *66*, 169–175.
202. Wei, L., Sun, C., Zhang, Y., Han, N., and Sun, S. (2020). miR-503-5p inhibits colon cancer tumorigenesis, angiogenesis, and lymphangiogenesis by directly downregulating VEGF-A. *Gene Ther.*, Published online June 12, 2020. <https://doi.org/10.1038/s41434-020-0167-3>.
203. Yang, J., Lan, H., Huang, X., Liu, B., and Tong, Y. (2012). MicroRNA-126 inhibits tumor cell growth and its expression level correlates with poor survival in non-small cell lung cancer patients. *PLoS ONE* *7*, e42978.
204. Kong, R., Ma, Y., Feng, J., Li, S., Zhang, W., Jiang, J., Zhang, J., Qiao, Z., Yang, X., and Zhou, B. (2016). The crucial role of miR-126 on suppressing progression of esophageal cancer by targeting VEGF-A. *Cell. Mol. Biol. Lett.* *21*, 3.
205. Zhu, J., Zeng, Y., Li, W., Qin, H., Lei, Z., Shen, D., Gu, D., Huang, J.A., and Liu, Z. (2017). CD73/NT5E is a target of miR-30a-5p and plays an important role in the pathogenesis of non-small cell lung cancer. *Mol. Cancer* *16*, 34.
206. Bonnin, N., Armandy, E., Carras, J., Ferrandon, S., Battiston-Montagne, P., Aubry, M., Guihard, S., Meyronet, D., Foy, J.P., Saintigny, P., et al. (2016). miR-422a promotes loco-regional recurrence by targeting NT5E/CD73 in head and neck squamous cell carcinoma. *Oncotarget* *7*, 44023–44038.
207. Masoumi, E., Jafarzadeh, L., Mirzaei, H.R., Alishah, K., Fallah-Mehrjardi, K., Rostamian, H., Khakpoor-Koosheh, M., Meshkani, R., Noorbakhsh, F., and Hadjati, J. (2020). Genetic and pharmacological targeting of A2a receptor improves function of anti-mesothelin CAR T cells. *J. Exp. Clin. Cancer Res.* *39*, 49.
208. Chen, S., Pu, J., Bai, J., Yin, Y., Wu, K., Wang, J., Shuai, X., Gao, J., Tao, K., Wang, G., and Li, H. (2018). EZH2 promotes hepatocellular carcinoma progression through modulating miR-22/galectin-9 axis. *J. Exp. Clin. Cancer Res.* *37*, 3.
209. Boguslawska, J., Kryst, P., Poletajew, S., and Piekielek-Witkowska, A. (2019). TGF- $\beta$  and microRNA interplay in genitourinary cancers. *Cells* *8*, E1619.
210. Yu, Y., Luo, W., Yang, Z.J., Chi, J.R., Li, Y.R., Ding, Y., Ge, J., Wang, X., and Cao, X.C. (2018). miR-190 suppresses breast cancer metastasis by regulation of TGF- $\beta$ -induced epithelial-mesenchymal transition. *Mol. Cancer* *17*, 70.
211. Zhang, C., Chen, B., Jiao, A., Li, F., Sun, N., Zhang, G., and Zhang, J. (2018). miR-663a inhibits tumor growth and invasion by regulating TGF- $\beta$ 1 in hepatocellular carcinoma. *BMC Cancer* *18*, 1179.
212. Lu, C., Zhou, D., Wang, Q., Liu, W., Yu, F., Wu, F., and Chen, C. (2020). Crosstalk of microRNAs and oxidative stress in the pathogenesis of cancer. *Oxid. Med. Cell. Longev.* *2020*, 2415324.
213. Peng, X., Gao, H., Xu, R., Wang, H., Mei, J., and Liu, C. (2020). The interplay between HIF-1 $\alpha$  and noncoding RNAs in cancer. *J. Exp. Clin. Cancer Res.* *39*, 27.
214. Gao, L., Guo, Q., Li, X., Yang, X., Ni, H., Wang, T., Zhao, Q., Liu, H., Xing, Y., Xi, T., and Zheng, L. (2019). miR-873/PD-L1 axis regulates the stemness of breast cancer cells. *EBioMedicine* *41*, 395–407.
215. Grenda, A., and Krawczyk, P. (2017). New dancing couple: PD-L1 and microRNA. *Scand. J. Immunol.* *86*, 130–134.
216. Lv, M., Xu, Y., Tang, R., Ren, J., Shen, S., Chen, Y., Liu, B., Hou, Y., and Wang, T. (2014). miR141-CXCL1-CXCR2 signaling-induced Treg recruitment regulates metastases and survival of non-small cell lung cancer. *Mol. Cancer Ther.* *13*, 3152–3162.
217. Dai, J., Su, Y., Zhong, S., Cong, L., Liu, B., Yang, J., Tao, Y., He, Z., Chen, C., and Jiang, Y. (2020). Exosomes: Key players in cancer and potential therapeutic strategy. *Signal Transduct. Target. Ther.* *5*, 145.
218. Vignard, V., Labbé, M., Marec, N., André-Grégoire, G., Jouand, N., Fonteneau, J.F., Labarrière, N., and Fradin, D. (2020). MicroRNAs in tumor exosomes drive immune escape in melanoma. *Cancer Immunol. Res.* *8*, 255–267.
219. Liu, J., Fan, L., Yu, H., Zhang, J., He, Y., Feng, D., Wang, F., Li, X., Liu, Q., Li, Y., et al. (2019). Endoplasmic reticulum stress causes liver cancer cells to release exosomal miR-23a-3p and up-regulate programmed death ligand 1 expression in macrophages. *Hepatology* *70*, 241–258.
220. Zhou, J., Li, X., Wu, X., Zhang, T., Zhu, Q., Wang, X., Wang, H., Wang, K., Lin, Y., and Wang, X. (2018). Exosomes released from tumor-associated macrophages transfer miRNAs that induce a Treg/Th17 cell imbalance in epithelial ovarian cancer. *Cancer Immunol. Res.* *6*, 1578–1592.

## Review

221. Seo, N., Shirakura, Y., Tahara, Y., Momose, F., Harada, N., Ikeda, H., Akiyoshi, K., and Shiku, H. (2018). Activated CD8<sup>+</sup> T cell extracellular vesicles prevent tumour progression by targeting of lesional mesenchymal cells. *Nat. Commun.* *9*, 435.
222. Fraietta, J.A., Lacey, S.F., Orlando, E.J., Pruteanu-Malinici, I., Gohil, M., Lundh, S., Boesteanu, A.C., Wang, Y., O'Connor, R.S., Hwang, W.T., et al. (2018). Determinants of response and resistance to CD19 chimeric antigen receptor (CAR) T cell therapy of chronic lymphocytic leukemia. *Nat. Med.* *24*, 563–571.
223. Arcangeli, S., Falcone, L., Camisa, B., De Girardi, F., Biondi, M., Giglio, F., Ciceri, F., Bonini, C., Bondanza, A., and Casucci, M. (2020). Next-generation manufacturing protocols enriching T<sub>SCM</sub> CAR T cells can overcome disease-specific T cell defects in cancer patients. *Front. Immunol.* *11*, 1217.
224. Das, R.K., Vernau, L., Grupp, S.A., and Barrett, D.M. (2019). Naïve T-cell deficits at diagnosis and after chemotherapy impair cell therapy potential in pediatric cancers. *Cancer Discov.* *9*, 492–499.